City Research Online

City St George's, University of London

Citation: Vafaei Shalmani, M. (2022). Seismic fragility assessment of high-rise steel buildings strengthened with moment resisting and bracing frames and under various soil conditions to the ASCE and Eurocodes regulations. (Unpublished Doctoral thesis, City, University of London)

This is the accepted version of the paper.

This version of the publication may differ from the final published version. To cite this item please consult the publisher's version.

Permanent repository link: https://openaccess.city.ac.uk/id/eprint/28394/

Copyright and Reuse: Copyright and Moral Rights remain with the author(s) and/or copyright holders. Copies of full items can be used for personal research or study, educational, or not-for-profit purposes without prior permission or charge, unless otherwise indicated, provided that the authors, title and full bibliographic details are credited, a hyperlink and/or URL is given for the original metadata page and the content is not changed in any way. For full details of reuse please refer to City Research Online policy.

City Research Online: http://openaccess.city.ac.uk/ publications@citystgeorges.ac.uk

Seismic Fragility Assessment of High-Rise Steel Buildings Strengthened with Moment Resisting and Bracing Frames and under Various Soil Conditions to the ASCE and Eurocodes Regulations

By

Mehran Vafaei Shalmani

A thesis submitted for the Partial Fulfilment of the Requirements for the Degree Doctor of Philosophy in the School of Mathematics, Computer Science and Engineering

February 2022

Acknowledgement

I would like to express my appreciation to the people who helped me throughout this long journey, scientifically and mentally. This research has seen so many days of disappointment and hard work from very first stages that was started by literature review towards all the end, which was simulations and calculations.

I hope, this research can make a significant impact on the world's structural engineering community theoretically, analytically and scientifically. Indeed, this research could not be accomplished without the help and support of my supervisor Dr. Feng Fu and Prof. Ashraf Ayoub.

I would like to thank the love of my life who shared all her supports and love during all the hard times and made me believe in myself.

I would like to thank the love of my life who shared all her supports and love during all the hard times and made me believe in myself.In the end, I would like to thank my best friends, who were being more than just a friend. Ardavan Farjad Moghaddam, Shahbaz Kakavand and Soheil Soltanieh thank you for being supportive and helpful.

Abstract

This study aims to focus on finding out some effective methods to assess possibility of collapse and behaviour of high-rise steel structure with different lateral stability systems under seismic loadings. Seismic Fragility functions are a powerful method to characterize the probabilistic vulnerability of buildings under earthquake. Therefore, the aim of this research is to develop fragility curves for moment resisting and braced steel framed buildings (V and X-bracing system) with slim deck flooring system.

This thesis investigated the probability of the failure of high-rise steel buildings under seismic loads. There are several experimental and numerical researches implemented in this subject area which have guided other researchers to understand better the failure mechanism and likelihood of buildings under seismic activities. However, due to the lack of research and data with regard to high-rise structures, the main aim of the research is to develop high resolution fragility curve of high-rise buildings and to find out the roles of the different lateral stability systems in resisting earthquake load. Furthermore, the new flooring system,i.e. slim deck flooring system, has been considered in the present research. In addition, the effect of slab steel reinforcement in energy dissipation for the structure is also studied in this research.

For this PhD research project, 3D numerical models of buildings have been built. Over two hundred time-history analyses have been made for different types of steel frames with various stability systems in the process to generate the fragility curves. The soil types, peak ground acceleration of earthquake and the connection of structural elements and different design guidelines used in the analysis have been taken into the account. During the analysis, three dimensional components of ground motion acceleration have been applied to the foundation of the structure. The method of generating fragility curves is analytical. This method is beneficial regarding construction cost and accuracy. However, its drawback is that it is time consuming. In addition, the energy dissipation and collapse mechanism of structure are the key aspects that have been take into the account alongside of the study.

This study aims at using a time-history analysis to simulate the possibility of failure in high-rise braced structures under seismic activities and to develop the fragility curve.

In addition, the analysis will be carried out based on the Eurocode and ASCE and there will be a comparison of Eurocode's results versus ASCE's outcomes.

Table of Contents

Abstract II

Chapter 1: Introduction and Objectives 1

1.1. Introduction 1

1.2. Project Background 2

1.3. Problem statement and motivation 4

1.4. Research objective and scope of work 5

1.5. Thesis Structure 7

Chapter 2: Literature Review, Case Studies and Approaching Method 8

2.1. Literature Review 8

2.1.1. Steel Frames 9

2.1.2 Braced frame 9

2.1.3. Moment resisting frame 11

2.1.4. Slim deck floor slab 12

2.1.5. Collapse mechanism 14

2.2. Fragility Curve 18

2.3. Economic Losses 27

2.4. Existing studies related to developing fragility curve 28

2.4.1. Effectiveness of bracing system on high-rise steel structure 29

2.4.2. Developing of fragility curve for low and mid-rise steel structures with X-bracing and by using non-linear time history analyses 32

2.4.3. Seismic Fragility Curve of Steel and Reinforced concrete frames based in the near and far field ground motion record 35

2.4.4. Summary of Case Studies 39

2.5. Approaching method 40

Chapter 3: Methodology and Approach 43
3.1. Research methodology and procedure 43
3.2. Theoretical – Fragility Curves 45
3.3. Damage state 47
3.3.1. ASCE 47
3.3.2. Eurocode 48
3.4. Database Generation Using ETABS 49
3.4.1. Loads combination definitions in ETABS 53
3.4.2. How the load combinations combined 54
Chapter 4: Developing Numerical Result of Fragility Curves of the Moment Resisting Frame, V-Bracing and X-Bracing 60
4.1. Dataset Generation using Numerical Analysis and Simulation 60
4.2. Prototype building 61
4.2.1. Sizes and Dimensions of Elements 63
4.2.2. The limitation and boundary condition of the model 66
4.3. Types of frames 68
4.3.1. Moment Resisting Frame 68
4.3.2. X-Bracing Frame 74
4.3.3. V-Bracing Frame 80
4.4. Discussion 86
4.4.1. Vibrational modes 90
Chapter 5: The Effect of the Soil Conditions on Developing Fragility Curves 91
5.1. Detailed statistical analysis of the database 91
5.2. Moment Resisting Frame 92
5.3. X-Bracing Frame 99

5.4. V-Bracing Frame 107

5.5. Discussion 115

Chapter 6: The effect of Slimdeck on the performance of the structures against seismic activities 119

Chapter 7: Conclusion, Recommendation, and the Future Works 122

7.1. Conclusion and future work 122

7.2. Future works and Recommendation 124

References 126

Additional references 130

Other language 131

Appendix 132

A1. List of the earthquakes 132

A2. Summary of results in MR 153

A3. Summary of results in XB 171

A4. Summary of the VB results 192

Table of Figures

Figure 1. Three basic vertical seismic system [10] 9

Figure 2. Types of steel bracing. (a to c) x-bracing frame; (d to e) inverted V-brace and V-brace frame; (f tog) K-brace and double K-braced frame; (h to i) single diagonal braced frames; (j) Knee bracing [17] 10

Figure 3. (a) Collapse fragility based on ASCE 7-05 ignoring the uncertainty in collapse capacity; (b) Modified collapse fragility based on ASCE 7-10. [23] 19

Figure 4. Example of fragility curve [48] 22

Figure 5. Classification of fragility curves [49] 23

Figure 6. General approach of calculating the fragility curve (these numbers are for example only) by Prof. Jack Baker [59] 23

Figure 7.Building Performance levels [28, 29] 24

Figure 8. Comparison of performance of existing and new buildings [28] 25

Figure 9.comparison of the displacement of steel structure with different steel bracing [18] 29

Figure 10. Comparison of maximum shear forces in steel structures occurred [18] 30

Figure 11.Maximum bending moments [18] 30

Figure 12.plan view of the structures [36] 32

Figure 13. Fragility cures for 3-story frames F32 (2-bay frame), FO34 (4-bay) and FO36 (6-bay) [36] 33

Figure 14. Fragility cures for 5-story frames F52 (2-bay frame), FO54 (4-bay) and FO356 (6-bay) [36] 33

Figure 15. Fragility cures for 7-story frames F72 (2-bay frame), FO74 (4-bay) and FO76 (6-bay) [36] 34

Figure 16.Fragility curves of three and six storey structure in concrete and steel frame [38] .37

Figure 17. Sample of Acceleration time history in horizontal direction (ETABS) 49

Figure 18. Sample of Acceleration time history in vertical direction (ETABS) 50

Figure 19. Example of time history index (PEER) 50

Figure 20. List of time history functions (ETABS) 51

Figure 21. Available actions for time history of the structure (ETABS) 52

Figure 22. Example of Load case's tree in ETABS 54

Figure 23. Sample of seismic loading (ETABS) 57

Figure 24. Plan view of the structure (AutoCAD Drawing) – measures are in meter.....61
Figure 25. Elevation view of Structure with dimensions (AutoCAD Drawing) – Measure is in meter.....62
Figure 26.overview of the Section Property of the structure (each colour belongs to specific types of material).....64
Figure 27.Example of the slim deck design in ETABs.....65
Figure 28. Example of the Slim Deck on secondary beam (credited by TATA Steel).....65
Figure 29. Detail of the ComFlor 100 Deck (by TATA Steel) 66
Figure 30. Fragility curve of Moment Resisting frame - ASCE Regulation.....69
Figure 31. Fragility curve of Moment Resisting frame - Eurocode Regulation.....72
Figure 32. Overall View of the Structure in ETABS 75
Figure 33. Fragility curve of X-Bracing frame - ASCE Regulation.....76
Figure 34.Fragility curve of X-Bracing frame - Eurocode Regulation.....78
Figure 35. Overall View of V-Bracing in ETABS 81
Figure 36. Fragility curve of V-Bracing frame - ASCE Regulation.....81
Figure 37.Fragility curve of V-Bracing frame - Eurocode Regulation 83
Figure 38.Comparison of fragility curves of all frames on Eurocode 87
Figure 39.Comparison of fragility curves of all frames on ASCE.....87
Figure 40. Median of the Simulations.....89
Figure 41. Variance of the Simulations.....90
Figure 42. MR Frame - Type C soil - ASCE Regulation.....94
Figure 43. MR Frame - Soil Type C – Eurocode Regulation 95
Figure 44. MR-Type D-ASCE Regulation.....97
Figure 45. MR Frame - Type D soil- Eurocode Regulation 98
Figure 46. Fragility Curve of Moment Resisting Frame for soil type C & D in Eurocode and ASCE 99
Figure 47. XB Frame - Soil Type C –ASCE Regulation.....101
Figure 48. XB Frame - Soil Type C - Eurocode Regulation.....103
Figure 49.Fragility Curve - XB Frame - Soil Type D –ASCE Regulation 105
Figure 50. Fragility Curve - XB Frame - Soil Type D - Eurocode Regulation.....106
Figure 51. Fragility Curve of X-Bracing Frame for soil type C & D in Eurocode and ASCE.....107

Figure 52.Fragility Curve - VB Frame - Soil Type C - ASCE Regulation 109
Figure 53. Fragility Curve - VB Frame - Soil Type C - Eurocode Regulation 110
Figure 54. Fragility Curve - VB Frame - Soil Type C - Eurocode Regulation 112
Figure 55. Fragility Curve - V-Bracing - Soil Type D – Eurocode Regulation 113
Figure 56.Fragility Curve of V-Bracing Frame for soil type C & D in Eurocode and ASCE.....114
Figure 57. Example of the Time history - Sudden Shock - High PGA 116
Figure 58. Example of the Time history - Few Shocks - Low PGA.....116
Figure 59. Comparison of the normal deck and slim deck in fragility curve 120

List of Tables:

Table 1. Possibility of failures in different structure frames 14

Table 2. Building Performance targets in old and new structures [28] 26

Table 3.Beam and column size of Steel frame [38] 35

Table 4.Beam cross section, Concrete frame [38] 35

Table 5. Column section, Concrete Frame [38] 35

Table 6. Selective ground motion records for NF [38] 36

Table 7. Selective ground motion records for FF [38] 36

Table 8.Categorization of vulnerability curve [45, 46 and 47] 42

Table 9. Allowable Story Drift (table 12.12.1 ASCE) 47

Table 10. Short-Period Site Coefficient (Soil Type A to E) - ASCE 7-16 Table 11.4-1 56

Table 11. Short-Period Site Coefficient (Soil Type A to E) - ASCE 7-16 Table 11.4-2 58

Table 12. Recommended Value for φ 58

Table 13. Suitable value for the ψ 59

Table 14. Internal and External Column Sizes of the Building 63

Table 15. Data of Moment Resisting frame of Failure according to ASCE and Eurocode 68

Table 16. Details of the Moment resisting frame - Generating Fitted Fragility Curve and Fraction of Analysis Causing Collapse - ASCE 70

Table 17. Data of Moment Resisting frame of Failure according to Eurocode 72

Table 18. Details of the Moment resisting frame - Generating Fitted Fragility Curve and Fraction of Analysis Causing Collapse –Eurocode regulation 73

Table 19. Data of X-Bracing frame of Failure according to ASCE 76

Table 20.Details of the X-Bracing frame - Generating Fitted Fragility Curve and Fraction of Analysis Causing Collapse - ASCE 77

Table 21. Data of X-Bracing frame of Failure according to Eurocode 78

Table 22.Details of the X-Bracing frame - Generating Fitted Fragility Curve and Fraction of Analysis Causing Collapse - Eurocode 79

Table 23. Data of V-Bracing frame of Failure according to ASCE 82

Table 24.Details of the V-Bracing frame - Generating Fitted Fragility Curve and Fraction of Analysis Causing Collapse - ASCE 82

Table 25.Data of V-Bracing frame of Failure according to Eurocode 84

Table 26.Details of the V-Bracing frame - Generating Fitted Fragility Curve and Fraction of Analysis Causing Collapse - Eurocode 84
Table 27. MR-Type C 92
Table 28. MR-Type C-ASCE 93
Table 29. MR -Type C- Eurocode 94
Table 30. MR-Type D 96
Table 31. MR-Type D- ASCE 96
Table 32. MR- Type D- Eurocode 98
Table 33. XB Frame - Soil Type C - Overall Results 99
Table 34. XB Frame - Soil Type C - ASCE regulation 100
Table 35. XB Frame - Type Soil C - Eurocode Regulation 101
Table 36. XB Frame - Type Soil D - Overall Results 103
Table 37. XB Frame - Type Soil D - ASCE Regulation 104
Table 38. XB Frame - Type Soil D - Eurocode Regulation 105
Table 39. VB Frame - Type Soil C - Overall Result 107
Table 40. VB Frame - Type Soil C - ASCE Regulation 108
Table 41. VB Frame - Soil Type C - Eurocode Regulation 109
Table 42. VB Frame - Soil Type D - Overall Results 111
Table 43.XB Frame - Soil Type D - ASCE Regulation 111
Table 44. VB Frame - Soil Type D - Eurocode Regulation 113
Table 45. The number of time history in each range of peak ground acceleration 117
Table 46.list of the earthquakes selected in the analysis to develop the fragility curves 132
Table 47. Summary of results in MR 153
Table 48. Summary of results in XB 171
Table 49. VB Summary of the results 192

Chapter 1: Introduction and Objectives

1.1. Introduction

For many years, dealing with natural disasters has been an important fact for designing structures in seismic zones. Alongside natural disasters, the demand for places to live and work in has been increasing. As a result, and due to the fact that the population has been growing as well (14.07% increase from 2006 to 2019) [8], high-rise structure is the most convenient option to accommodate people in a less consumed area. Data shows that the number of these buildings is increasing due to the facts. Therefore, more research is required in order to understand the behaviour of tall buildings better.

This study aims to focus on the possibility of collapse mechanism and non-linear behaviour of high-rise steel structure under seismic loadings. Due to the lack of post-earthquake research and data concerning of these type of structures, this research aims to provide a preliminary data in this area as much as possible. The best method to find the probability of failure of the structure against seismic activity is an analytical method aided by finite element programs to simulate the situation. Developing fragility curves for moment resistant as well as V and X-bracing system with slim deck flooring system are the two main aims of the research. The fragility results obtained from the existing research efforts with those obtained from the current study are compared to verify the simulation process and the accuracy of the methodology.

In addition, another goal of this research is to add the slim deck slab to the flooring system, providing a better understanding of the behaviour of this new flooring system under seismic loading. Lack of research in the context of slim deck flooring system is another motivation of this study. Therefore, this research aims to gain the knowledge in this area.

The main aim of this research is to carry out a three-dimensional time history analysis to simulate the possibility of failures in high-rise braced and non-braced composite frame structures under earthquake ground motions and to develop the fragility curve.

1.2. Project Background

The disasters such as earthquake, flood and many other natural catastrophes will put human's life in danger. Coping and dealing with natural disasters is one of the main important factors in earthquake engineering. Engineers and researchers endeavour to improve the impact, resistance and durability of structures against these disasters by using different techniques and methods.

The factors that lead to research into earthquake for modern cities to become the priority, are:

1. Increase in the number of cities and infrastructures in seismic zone
2. Expanded and developed cities that are located in seismic zone
3. Rise in the number of facilities and amenities which leads to the requirement of more human resources

Meanwhile, as the population is increasing, the need for space to live and work is rising. These facts lead the demand for of high-rise structures for official and residential use to increase. In fact, to understand the behaviour of high-rise structures, more research is required to be conducted in areas such as collapse mechanism, connection behaviour, energy dissipation, etc. The following facts are the reasons why high-rise buildings are more prominent: [1] [2]

- Shortage of the land and increasing demand for business and residential space
- Technological advancement, innovation in structural system and economic growth
- Human aspiration to build higher and desire for aesthetics in urban settings

In this thesis, the focus is to develop fragility curves for high-rise steel composite frame using slim deck flooring system with different lateral stability system, hence, providing an effective design method for this type of buildings under seismic loads. There are some existing researches in this area mainly for reinforced concrete structures, highway bridges and few for steel structures (majority of existing research is limited to low and mid-rise buildings in steel structures). Furthermore, to obtain a better accuracy and realistic resolution of fragility curves

are the main aim and objective of this research. The main reason for using accurate analytical method in the derivation of fragility curve is the lack of post-earthquake damage data. [3]

Post-earthquake operations are increasing concerns not only to essential facilities such as police and fire stations and hospitals, but also to manufacturing facilities, banks, and many other businesses concerned with the loss of revenue or loss of market share that would result from a lengthy outage following an earthquake. Organizations and owners who wish to reduce their seismic exposure will need to address the non-structural hazards in their facilities.

Generally, an appropriate procedure to define the expected damage is a mechanics-based approach. On the basis of deformation demands, the result of the procedure should be physical damage to the structure. Damage levels could also be defined based on repair costs. In general, these methods should be applicable only when using a significant amount of data related to their characterisation, which can be obtained by historic failures, expert evaluation [4] and field survey or investigation [5-7].

The derivation of non-linear FCs (fragility curves) from post-earthquake or expertise data (e.g., empirical data) cannot be sufficient for the realisation of a reliable risk assessment tool. On the contrary, this approach needs to be supplemented by numerical analysis. The main reason for using accurate analytical methods in the derivation of FCs is the lack of post-earthquake damage data.

A series of recorded accelerograms, with various peak ground acceleration values and different frequency contents, were used for each building to create a relatively large statistical data for developing reliable fragility curves. Two damage indices, including the “inter-story drifts” and the “axial plastic deformation of bracing elements”, were used.

In addition, the risk assessment is an important fact that needs to be considered. There are many facts that lead to the importance of risk assessment:

- Increasing the number of cities that were on seismic faults
- Growth in population density

- Increase in quality and quantity of the urban facilities in cities which rises the probability of damages after seismic activity
- Improvement in the quality of seismic analysis (such as the data recording of the earthquake, the science and understanding of structure and soil)

1.3. Problem statement and motivation

The purpose and motivation of the research are to gain knowledge in the behaviour of tall buildings against seismic activities. To be more specific, the aim is set to find the probability of failure of high-rise un-braced and braced steel frame structures under seismic activities. Many studies have been conducted regarding the probability of failure in the tall buildings.

However, most existing fragility curves are developed for high-rise concrete structures and bridges. On the other hand, there are very limited studies for steel structure. There is no accurate numerical analysis for this type of steel structure (V / X - bracing system high-rise structure) yet.

Slim deck flooring system is a conventional technology that reduces overall floor height, using fewer steel beams. Due to inadequate research on this subject, the slim deck will be added to flooring system models simulated.

Another challenge of this research is to develop a comparison between the current studies related to the probability of the failure of the moment resisting frame, eccentric and concentric bracing system.

To summarize, there is limited and not accurate data and research in the area that is related to the probability of the failure of steel structure and braced structure in building. There are few researches and lab experiments which are only limited to low and mid-rise structure. There are no reliable results, proper comparison and insufficient investigations about the effect of bracing in fragility and energy dissipation of structure.

1.4. Research objective and scope of work

Nowadays, the assessment of the functionality of the structure against seismic activity has become one of the important topics for civil engineers and researchers. On the other hand, the knowledge and detail in this area is limited, therefore further investigation will lead the engineers and researchers to a better understanding about the non-linear behaviour of high-rise steel structure under seismic load.

According to the published researches and data, there are a significant number of researches that have been done in concrete design for bridges, residential, official buildings, and tall structures. Also, the number of experiments and relative number analysis and simulations with regard to the behaviour of high-rise steel structure under seismic loading and developing fragility curves has been mentioned. Meanwhile, the studies in steel structures are very restricted to limited numerical analysis and mainly focused on low and mid-rise buildings. The main aim of this study is to focus on the probability of collapse mechanism and fragility curves of high-rise steel structures by using a slim deck flooring system. According to Eurocode EN 1991-1-7 (Annex A- Categorisation of building types) [11], the structure with 15 or more storeys is called high-rise structure. For the time history analysis, non-linear material behaviour has been considered.

This study investigates the methodology for the development of analytical seismic fragility curves for high-rise steel structure under seismic loads (Time-history analysis). Different bracing methods tested (V and X-bracing), which then compared with moment resisting frames and the behaviour of them analysed. The main objectives can be summarised by the following points:

- Identifying a suite of realistic ground motions being representative of the seismic hazard for the specific region
- Identifying the appropriate capacities and limit states for the components of the bracing steel structure with slim deck floor slab and comparing them with those of normal slim deck

- Exploring the impact of using various earthquake intensity measures on the probabilistic seismic demand models (in moment resisting frame for slim deck and normal deck, X-bracing and V-bracing)
- Identifying the appropriate capacities and limit states for the components of each steel frame building
- Generating seismic fragility curve for each of the bracing type (Moment resistance frame, X-Bracing and V-Bracing) through time history analysis
- Generating and simulating the fragility curve (probability of failure) on the prototype/ pre-designed high rise steel structure by Eurocode and ASCE codes

Using slim deck flooring system on moment resisting and bracing frame as a lateral stability. Furthermore, a comparison of the performance of the different structural analysis under seismic loads, will be taken into account.

In addition, the purpose of this research is to increase the knowledge of engineers on the behaviour of high-rise reinforced steel structures under seismic loading, as well as the probability of the failure of the structures under earthquake.

A comparison of the European and American regulations is taken into account. Also, the details of the simulation of the analysis in every aspect such as the direction of deflection and the type of assumed soil for time-history, have been considered.

1.5. Thesis Structure

This chapter presents the context of the research that will be addressed in the chapters that follow.

Chapter 2 provides the literature review and the case studies of the possible causes to the structural failure. Afterwards, the alternative options to withstand seismic loads will be explained. In addition, a number of papers which are related to this research will be studied in detail, in order to provide a better understanding of the subject and to gain an approachable method to develop fragility curve. In addition, several case studies are to be reviewed to support the concepts and the result.

Chapter 3 explains briefly the methodology and the procedure of approaching to the results that this study focuses on. In this section, the step-by-step scientific method on how this investigation will proceed will be explained in detail. Mainly, this section has been divided into two main parts which consist of theoretical and analytical process.

There is a discussion about the different approaches of developing analytical method for fragility curve.

Chapter 4 goes through the steps and calculation on how to model the porotype of the structure. The limitations and circumstances are also discussed. Generating fragility curve on each type of frame is illustrated. There is a comparison between Eurocode's and ASCE's results. Also, the general discussion and comparison will be taken into the account.

Chapter 5 consists of comments on analysis and comparisons in more depth. The different type of soils and their effect on different frames will be discussed. Next, the fragility curves of each soil for each frame will be generated.

Chapter 6 provides the conclusion and gives some suggestions and implications for future research.

Chapter 2: Literature Review, Case Studies and Approaching Method

2.1. Literature Review

In this section of the thesis, an investigation about the following factors will be reviewed. This would provide the understanding of the seismic activities, their problems, and possible solutions.

In the methodology section, more details about the simulation, modelling and fragility curve (definition and calculation of FC) will be discussed.

General discussion of literature review consists of:

- Introduction of steel frames, bracing system and types of bracing ; and elaboration on how lateral stability gains structural performance
- Review and discuss of the causes of collapses and also damages to the buildings that earthquake could bring ; and types of failure
- Introducing fragility curve method

2.1.1. Steel Frames

Seismic engineers can opt for three basic alternative types of vertical-lateral load resisting systems (moment resisting frame, braced frame, and shear walls) for steel structures, which has been demonstrated in Figure 1. These basic systems have a number of variations, mainly related to the structural materials used and the ways in which the members are connected. [10]

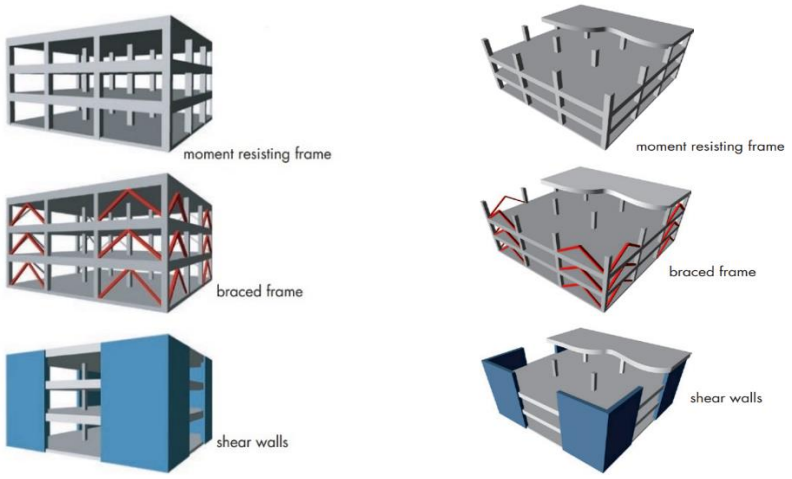

Figure 1. Three basic vertical seismic system [10]

There are multiple forms of frames that, being designed based on different types of earthquakes are braced frame and moment resisting frame. The brace frames section is categorised into single diagonal, cross bracing, K bracing, V and Inverted V bracing.

2.1.2 Braced frame

The braced frame is the reinforcement of the steel structure for tall buildings that requires extra strength and stiffness in order to deal with sudden shocks and forces.

Braced frames act in the same way as shear walls; however, they generally provide less resistance but better ductility depending on their detailed design. They provide more architectural design freedom than shear walls. There are two general types of braced frames: conventional concentric and eccentric. In the concentric frame, the centre lines of the bracing members meet the horizontal beam at a single point. In the eccentric braced frame, the braces are deliberately designed to meet the beam some distance apart from one another: the short piece of the beam between the ends of the braces is called a link beam. The purpose

of the link beam is to provide ductility to the system: under heavy seismic forces, the link beam will distort and dissipate the energy of the earthquake in a controlled way, thus protecting the remainder of the structure. [11-16]

Figure 2 shows different types of steel bracing system. In general, bracing systems are divided into X-bracing, V-bracing, inverted V-bracing , K-bracing, Single diagonal and Knee bracing. However, in this research only V-bracing and inverted V-bracing in eccentric and concetric mode will be modelled, which consist of two types: Concentric bracing System and eccentric bracing system. [11-16]

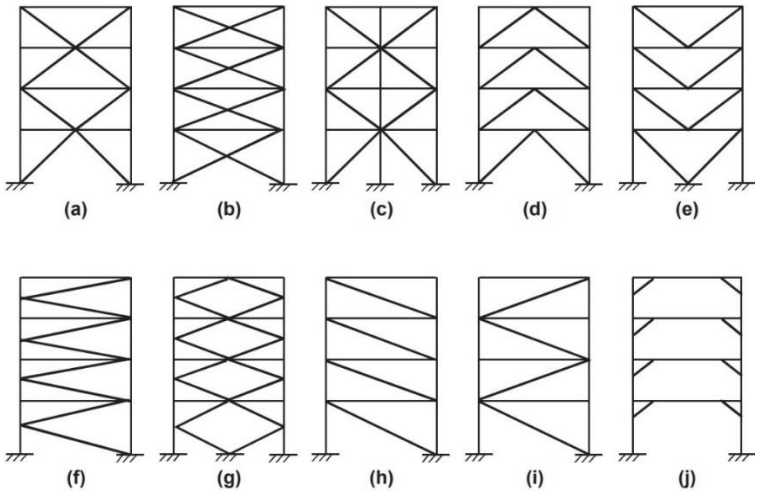

Figure 2. Types of steel bracing. (a to c) x-bracing frame; (d to e) inverted V-brace and V-brace frame; (f tog) K-brace and double K-braced frame; (h to i) single diagonal braced frames; (j) Knee bracing [17]

2.1.2.1. Concentric Lateral Stability

Concentric bracings increase the lateral stiffness of the frame, which accordingly increases the natural frequency and usually decreases the lateral storey drift. On the other hand, an increase in the stiffness may attract a larger inertia force due to the earthquake. Further, while the bracings decrease the bending moments and shear forces in columns, they increase the axial compression in the columns to which they are connected. [18]

2.1.2.2. Eccentric Lateral Stability

Eccentric bracings reduce the lateral stiffness of the system and improve the energy dissipation capacity. The lateral stiffness of the system depends upon the flexural stiffness property of the beams and columns, thereby reducing the lateral stiffness of the frame. The

vertical component of the bracing forces due to earthquake causes lateral concentrated load on the beams at the point of connection of the eccentric bracings. [18]

2.1.3. Moment resisting frame

A moment resisting frame is the engineering term for a frame structure with no diagonal bracing in which the lateral forces are resisted primarily by bending in the beams and columns mobilized by strong joints between them. Moment-resistant frames provide the most architectural design freedom. [17]

Moment-resisting frames (also called moment frames) are, in their simplest form, rectilinear assemblages of beams and columns, with the beams rigidly connected to the columns. Resistance to lateral forces is provided primarily by rigid frame action that is, by the development of bending moments and shear forces in the frame members and joints. By virtue of the rigid beam-to-column connections, a moment frame cannot displace laterally without bending the beams and columns. The bending rigidity and strength of the frame members is, therefore, the primary source of lateral stiffness and strength for the entire frame. [19, 20]

2.1.4. Slim deck floor slab

This type of flooring system is very recent and a relatively new system to replace the composite downstand beam. According to TATA floor design manual slimdek has many advantages such as: [34, 35]

- A shallow composite slab, which provides excellent load resistance, diaphragm action and robustness.
- An Asymmetric Slimflor® Beam (ASB), which achieves efficient composite action without the need for shear studs.
- An inherent fire resistance of up to 60 minutes with ASB fire-engineered (ASB (FE)) sections.
- Lighter, thinner web ASBs, which can be used unprotected in buildings requiring up to 30 minutes fire resistance or in fireprotected applications

This flooring system has been widely employed in the commercial sector. Also, its advantages are now being realised in residential applications. It has been used in major residential projects in Glasgow, Manchester, Cardiff, Portsmouth, Bristol and London. Another advantage of this flooring system is that it can be combined with other components, such as rectangular hollow sections (RHS) for columns and edge beams, light steel infill walls and separating walls that are directly supported by the composite floor, as well as roof-top penthouses and mansard roofs using light steel framing. [34, 35]

Indeed, several studies have been done regarding the slim deck behaviour under seismic activities. However, there is a lack of data and research on this subject. To be more specific, this research also aims to simulate the behaviour of this types of the slab in high-rise structure when subjected to earthquakes. The validating and comparison of results with current studies is the next step of this study.

The advantages of slimdek usage

This slab flooring system brings many advantages such as the significant reduction in floor to floor depth. That reduction will lead to asignificant reduction in sacing cladding cost, the total height of the building and the dead load. [61,62]

In general, this type of flooring system is more beneficail in terms of cost and construction time. On the other hand, it makes the structure lighter and the constructability easier. Also, researches and tests show that by using this system,the energy dissipation would slightly have better performance against seismic activity. [61,62]

2.1.5. Collapse mechanism

Engineers always design structures with an extra safety in the calculation. However, in some cases due to the large external loads, undetermined force or unpredicted live loads might cause the structure to fail in an unexpected situation. In general, steel is a ductile and strong material. [21]

Table 1, demonstrates the possible failures of each type of framework in structure. [21]

Table 1. Possibility of failures in different structure frames

Steelwork	Reinforced or pre-stressed concrete	Brickwork or masonry
Yielding	Crushing	Crushing
Brittle fracture	Chemical deterioration	Cracking
Shear fracture	Steel deterioration	Mortar joints
Fatigue	Bond failure	Frost damage
Buckling	Shear failure	Chemical deterioration
Corrosion	Frost damage	
Creep		
Welded/ bolted joints		

Damages, causes and failures

The damages and losses which an earthquake brings can be summerised in the following points: [21]

- Structural damages
- Putting human lives in danger
- Economical losses (can be calculated and predicted as non-structural component)

The factors which lead the structures to damage are: [21]

- The usage and types of the building (residential, official or bussiness)
- How crowded the structure might be inside
- Effects and damages the structure absorbs during the earthquake
- External forces

- Ground movement
- Type and the specification of the structure (having anti-seismic system, heavy/light buildings)

Causes of failure

There are a number of reasons that lead a structure to fail. Although in most cases, the failure can be related to more than one aspect. In general, the causes of failure can be summarised in the following points [21]:

- Material
- Design
- Inadequate erection
- Foundation failure
- Workmanship
- Overload
- Failure to use or communicate existing building information
- Lack of knowledge
- Deterioration in service

Types of failures

There are several types of damages that could occur locally and globally on the structures.

2.1.5.1. Yielding

Yielding failure occurs when there is local / global stretching and thinning of the steel. This type of failure is happening due to overloading or miscalculation in design. Yielding failure generally is a product of: [21]

- Inadequate erection procedures
- Incorrect assumption of loads such as impact loads, earthquakes or explosions

2.1.5.2. Brittle

This type of failure occurs under normal design loading condition. It requires a combination of circumstances such as tension stresses, an initial defect or sever stress concentration.

2.1.5.3. Fatigue

Fatigue failure happens when an element is subjected to the fluctuated forces (or stress) which cause slow growth in the following element. Final failure or damage occurs when a crack grows to a sufficient size, causing the structure to fail under the loads. This unstable situation can cause a shear fracture. [21]

2.1.5.4. Buckling

An element can be subjected to buckling failure when it is overloaded, therefore, it will buckle. Buckling in steel structure will be in different forms such as: [2]

- Overall buckling of complete compression member
- Lateral buckling of bending member
- Torsional buckling
- Stiffener buckling
- Local plate panel buckling
- Torsion

2.1.5.5. Connection failure

There are many possibilities that lead the joints or connection sections to failure. According to the researches in 1981 on the probability of structural failure in steel buildings, the reasons can be summarised as: [21]

- Reduction in weld-ability of steel causing a crack, which leads the load bearing capacity of the structure to decrease
- Incorrect design in joints. This possibility occurs when the combination of forces and loads has been underestimated. Another possibility is that the joints might be made incorrectly.
- Misreading of drawings and welding of the wrong size can cause another possibility that leads the connection to fail

2.1.5.6. Soft Story (Weak Story)

In this type of failure, the building will decrease its strength to overcome the loads and fail from the lower floors. The main reasons of this type of failure would be miscalculation or underestimating of the loads that should be taken by lower height of the structure.

2.1.5.7. Resonance

This phenomenon happens when the live loads such as wind and seismic activity hit the structure and cause the structure to oscillate two times faster than its normal natural frequency of its own. This only happens when the additional force harmonically acts with the same cycle of oscillation of the structure therefore, the building will be taking two times more than its normal force when subjected to maximum deflection.

2.2. Fragility Curve

One of the most important tools in evaluating the seismic damage to structures is the so-called fragility curve. The fragility curve for certain types of building structures is used to represent the probabilities that the structural damages, under various levels of seismic excitation, exceed specified damage states. According to Clotaire Michel [24], Fragility curves is a statistical tool representing the probability of exceeding a given damage state (or performance) as a function of an engineering demand parameter that represents the ground motion (preferably spectral displacement at a given frequency). [3]

In ASCE 7 (2010 edition) [26] utilized hazard-based S_a values corresponding to a 2% probability of exceedance in 50 years as the basis for seismic design such as MCE, which stands for Maximum Considered Earthquake. However, designs based on these S_a values did not provide a uniform probability of collapse for structures located in different regions of the United States, as the seismic collapse risk was inconsistent and region-dependent. Conceptually, a uniform probability of collapse would be obtained if one assumed that the variability in the collapse capacity and the uncertainty in the site-specific ground motion hazard curve were negligible. The term collapse capacity refers to the ground motion intensity (i.e., spectral acceleration at the fundamental period of the structure) at which the system approaches the limit state of collapse. The collapse capacity will normally depend on other characteristics of the entire waveform of the ground motion (the acceleration time history) too. The fact that the waveform is uncertain means the corresponding spectral acceleration that the structure can resist without collapsing is also uncertain. This variability is referred to as aleatory. [27]

There are several approaches to select the time histories for the simulations. Among these, two methods are mainly used in many research studies into seismic activity. The first one is Cornel which introduces the probability analysis and is aimed at generating a time history that will have a response spectrum as close as desired to the target spectrum [64]. The second method is Incremental dynamic analysis (IDA) is a parametric analysis method , which has recently emerged in several different forms to estimate more thoroughly structural performance under seismic loads. More thoroughly It involves subjecting a structural model to one (or more) ground motion record(s), each scaled to multiple levels of intensity, thus producing one (or more) curve(s) of response parameterized versus intensity level [65].

However, a more randomly wide range of selected time history was decided to be used, following the Backer's works for fragility as including more random data makes the result more unbiased. Moreover, Prof. Kappos has suggested using this method of approaching as well. [66,67].

Furthermore, the collapse capacity will also depend on the level of conservatism of the design, the construction details of the structure, and other structural characteristics that are influenced by subjective design decisions. This uncertainty is referred to as epistemic uncertainty. If the variability in collapse capacity is ignored, the collapse capacity becomes equal to the hazard-based Sa for which the structure is designed. Therefore, the collapse fragility of the structure would resemble a step function of the type shown in Figure 3. The term "collapse fragility" refers to the probability of collapse conditioned on Sa at the fundamental period of the structure. This approach implies that when a structure is designed based on the MCE ground motion and the uncertainty in the site-specific ground motion hazard is ignored, the structure would be expected to have a 2% probability of collapse in 50 years, which is identical to the hazard associated with the MCE ground motion. It is evident that designing for uniform-hazard ground motions does not result in structures with uniform collapse probability when it is recognized that there is uncertainty in collapse capacity. [15]

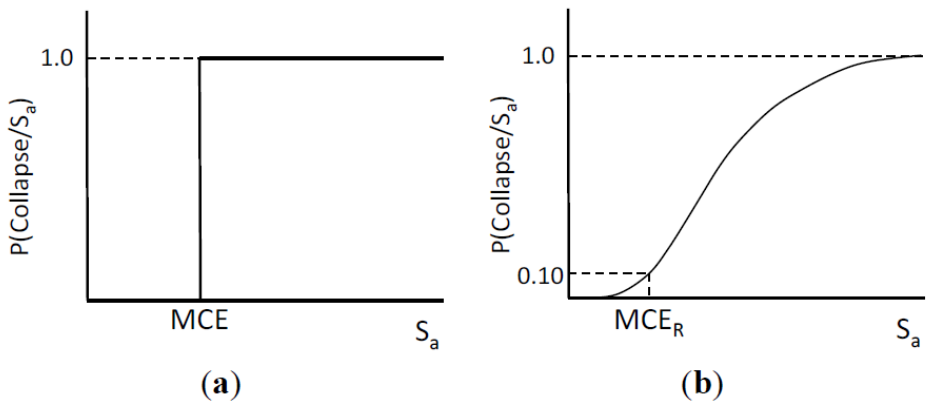

Figure 3. (a) Collapse fragility based on ASCE 7-05 ignoring the uncertainty in collapse capacity; (b) Modified collapse fragility based on ASCE 7-10. [23]

The drift performance level varies depending on the guidelines that result from intensive research. For example, FEMA- 273 [16] classifies the performance level into four categories, namely operational phase (OP) with 0.5% drift, immediate occupancy (IO) with 1.0% drift, life safety (LS) with less than 2.5% drift, and collapse prevention (CP) with more than 2.5% drift.

The performance based seismic design is incorporated with incremental dynamic analysis (IDA) to determine the structure drift and develop the structure fragility curve. The fragility curve is a log-normal function that expresses the probability of reaching or exceeding a specific damage state. The fragility curve is a highly useful method in predicting the extent of probable damage. It can describe the probability of a structure being damaged beyond a specific state when subjected to different levels of ground shaking. [24, 25]

Fragility functions enable the analyst to have control over the data collected, by means of choosing the IM (intensity measure) levels at which analysis is performed and the number of analysis performed at each level. This motivates the investigation below into effective ways to perform that data collection.

$$P(C|IM = x) = \phi \frac{\ln\left(x/\phi\right)}{\beta} \quad (1)$$

$$P(C|IM = x_j)_{observed} = \frac{number\ of\ collapseswhen\ IM{=}x_j}{number\ of\ ground\ motions}$$

Where $P(C|IM = x)$ is the probability that a ground motion with IM = x will cause the structure to collapse, Φ( ) is the standard normal cumulative distribution function (CDF), θ is the median of the fragility function (the IM level with 50% probability of collapse) and β is the standard deviation of ln IM (sometimes referred to the dispersion of IM). Equation 1 implies that the IM values of ground motions causing collapse of a given structure are lognormally distributed; this is a common assumption that has been confirmed as reasonable in a number of cases.

IM can be known as the intensity of the seismic activity. [51 – 54]

$$P(z_j\ collapses\ in\ n_j\ ground\ motions) = \binom{n_j}{z_j} P_j^{z_j} (1 - P_j)^{n_j - z_j}$$

Where

z_j = number of collapses

n_j = ground motions

$P_j^{z_j}$ = Probability of collapses

$(1 - P_j)^{n_j - z_j}$ = probability of non collapses

$$P_j = \phi\left(\frac{\ln\left(x/\phi\right)}{\beta}\right)^{z_j}$$

P_j = True probability of collapse (does not happen a lot)

$$ln\theta' = \frac{1}{n}\sum_{i=1}^{n} \ln IM_i$$

$$\beta' = \sqrt{\frac{1}{n-1}\sum_{i=1}^{n}\left(\ln\left(IM_i/\theta'\right)\right)}$$

Where n is the number of ground motions considered or independent number of observed data, and IM_i is the IM value associated with onset of collapse for the *i*th ground motion. This is a method of moments estimator, as lnθ and β are the mean and standard deviation, respectively, of the normal distribution representing the ln(IM)values. Note that the mean of ln(IM) is equal to the median of IM in the case that IM is lognormally distributed, which is why using the sample mean in this manner produces an estimate of θ . The mean and standard deviation, or moments, of the distribution are estimated using the sample moments from a set of data.

$$Likelihood = \phi\left(\frac{\ln\left(IM_i/\theta\right)}{\beta}\right)$$

Where ϕ ( ) denotes the standard normal distribution PDF. The (n-m) is ground motions that did not cause collapse at IM_{max} are called censored data, as we only know that IM_i is greater than IM_{max} (e.g., Klugman et al. 2012, section 15.2.4). The likelihood that a given ground motion can be scaled to IM_{max} without causing collapse is the probability that IM_i is greater than IM_{max}

$$Likelihood = 1 - \phi\left(\frac{\ln\left(IM_{max}/\theta\right)}{\beta}\right)$$

Making the reasonable assumption that the IM_i value for each ground motion is independent, the likelihood of the entire data set being observed is the product of the individual likelihoods

$$Likelihood = (\prod_{i=1}^{m} \phi\left(\frac{\ln\left({IM_i}/{\theta}\right)}{\beta}\right))\left(1-\phi\left(\frac{\ln\left({IM_{max}}/{\theta}\right)}{\beta}\right)\right)^{n-m}$$

Where Π denotes a product over i values from 1 to m (corresponding to the m ground motions that caused collapse at IM levels less than IM_{max}). Using this equation, the fragility function parameters are then obtained by varying the parameters until the likelihood function is maximized. It is mathematically equivalent and numerically easier to maximize the logarithm of the likelihood function, so in general we do that

$$\{\theta', \beta'\} = arg_{\theta,\beta} \max \sum_{j=1}^{m} \{\ln \phi\left(\frac{\ln\left({IM_i}/{\theta}\right)}{\beta}\right)\} + (n-m)\left(1-\phi\left(\frac{\ln\left({IM_{max}}/{\theta}\right)}{\beta}\right)\right)$$

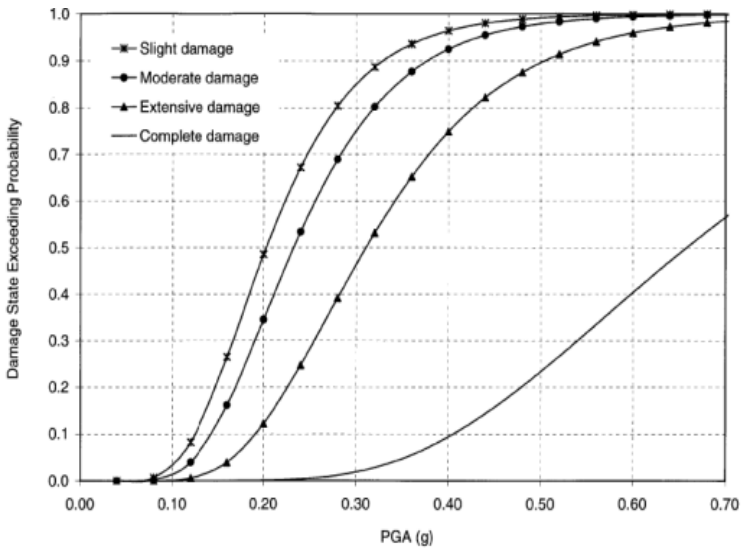

Figure 4. Example of fragility curve [48]

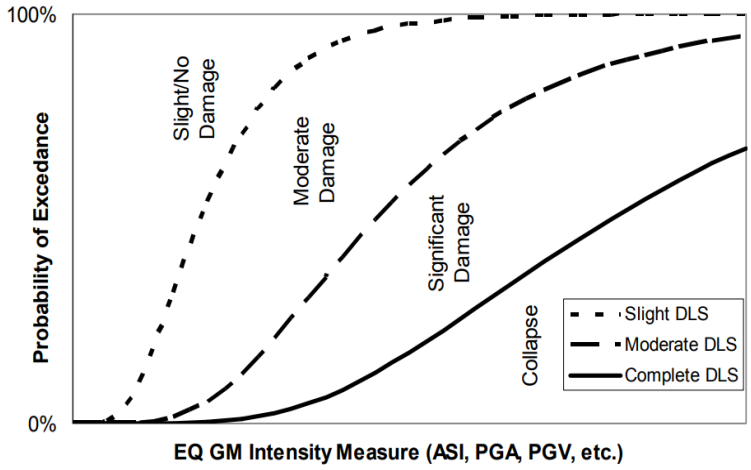

Figure 5. Classification of fragility curves [49]

Figures 23 and 24 illustrate the general fragility curves with different damage limit states. Fragility curves can be divided into 4 categories of slight, moderate, extensive (or significant) and complete damage (or collapse). [51 – 55]

All these formula's have been generated in Excel in order to calculate the fragility curves easily.

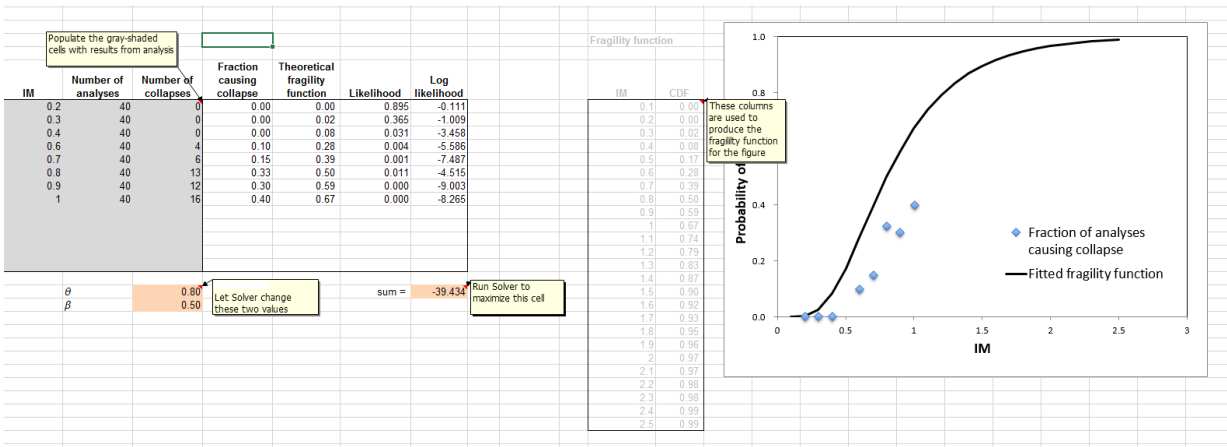

Figure 6. General approach of calculating the fragility curve (these numbers are for example only) by Prof. Jack Baker [59]

Rehabilitation Objectives

		Building Performance Levels			
		Operational Performance Level (1-A)	Immediate Occupancy Performance Level (1-B)	Life Safety Performance Level (3-C)	Collapse Prevention Performance Level (5-E)
Earthquake Hazard Level	50%/50 year	a	b	c	d
	20%/50 year	e	f	g	h
	BSE-1 (~10%/50 year)	i	j	k	l
	BSE-2 (~2%/50 year)	m	n	o	p

k + p = BSO
k + p + any of a, e, i, m; or b, f, j, or n = Enhanced Objectives
o = Enhanced Objective
k alone or p alone = Limited Objectives
c, g, d, h = Limited Objectives

Figure 7.Building Performance levels [28, 29]

The Rehabilitation Objective selected as a basis for design will determine, to a great extent, the cost and feasibility of any rehabilitation project, as well as the benefit to be obtained in terms of improved safety, reduction in property damage, and interruption of use in the event of future earthquakes. Figure 4, presents a matrix indicating the broad range of Rehabilitation Objectives that may be used in these Guidelines. [30]

The Following figures explain the performance level of the building under old and new codes. Seismic provision in the modern building code was adopted after 1973 caused a considerable increase in the performance of the structure. As a result, most of the old buildings (structures built before 1979) had less resistance against seismic load. Detailed description of performance category of structure, their limitation, and the design of the structure in new and old structure will be explained briefly. [28]

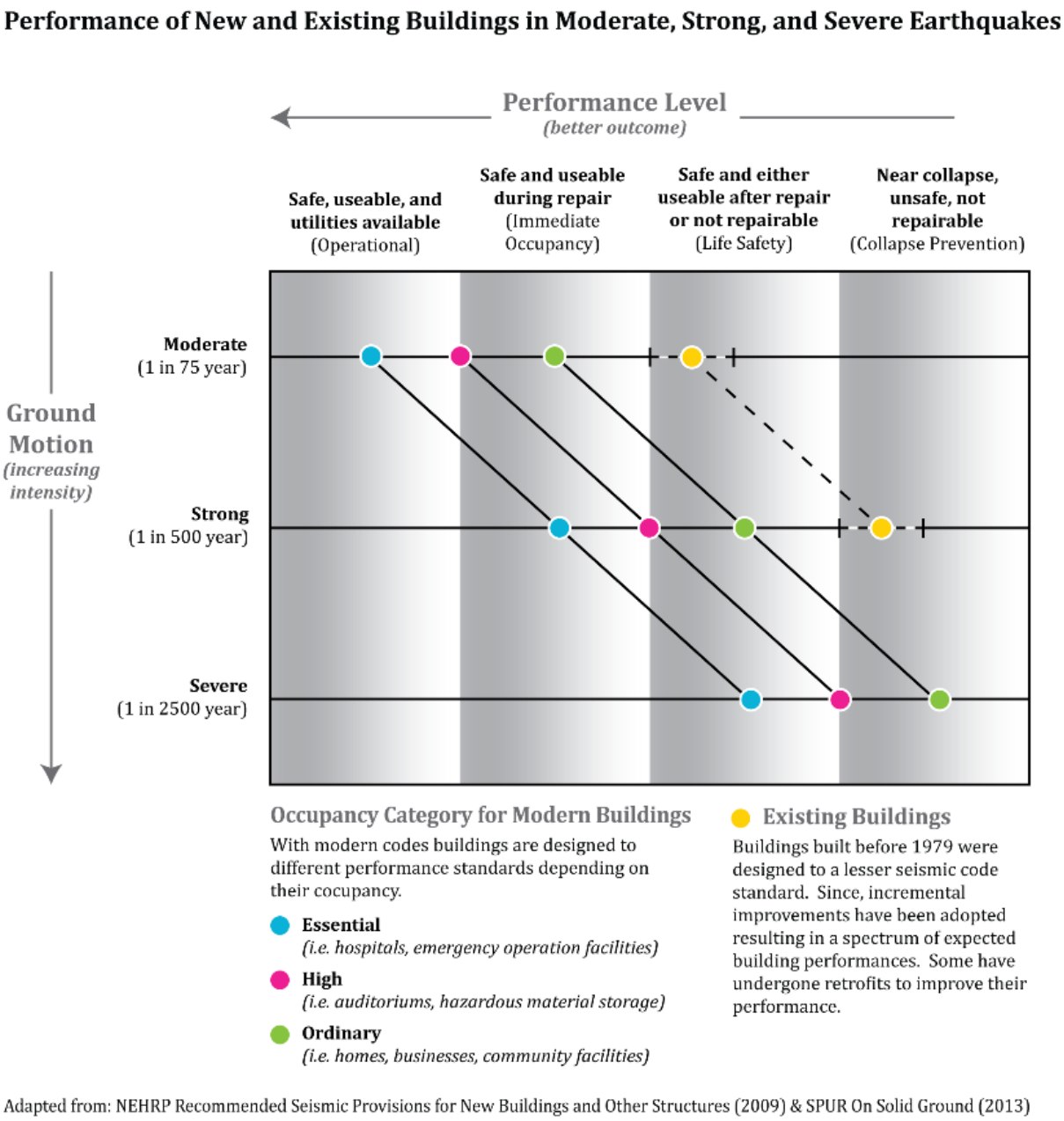

Figure 8. Comparison of performance of existing and new buildings [28]

More detail regarding the different types of building performance, along with an explanation of some additional circumstances have been demonstrated in Table 2. In addition, this table will review the new building's limitations and old building's regulations in each level of building performance.

Table 2. Building Performance targets in old and new structures [28]

Performance Category	Description	Newer buildings (using Current building code)	Older buildings
Safe and Operational	Building will experience only very minor damage and has energy, water, wastewater and telecommunications systems to back up any disruption to the normal utility services.	Performance expected of new essential facilities such as emergency operation centres, facility hazardous materials, hospitals and large gathering places.	Most older buildings are not expected to meet this level performance
Safe and usable during repair	Building will experience damage and disruption to their utility services, but no significant damage to the structural system. They may be occupied without restriction	A few non-essential buildings will meet this performance target. Recommended performance for new non-essential buildings	
Safe and usable after repair	Building may experience significant structural damage that will require repairs prior to resuming unrestricted occupancy. These buildings will likely to receive a yellow tag after the expected earthquake. Time required for repair will vary from months to years.	This is the current expectation for new and non-essential buildings	This is the high end of performance recommended for existing buildings undergoing rehabilitation
Safe but not Repairable	Building may experience extensive structural damage and may nearly collapse. Even if repair is technically feasible, it might not be financially justifiable. Many buildings performing at this level are expected to receive red tag after the expected earthquake	This is the low end of acceptability for new and no-essential buildings	This is often the performance goal used for existing buildings undergoing rehabilitation. This is the low end of performance recommended for existing buildings that are undergoing rehabilitation

Unsafe	Partial or complete collapse. Damage will likely lead to significant casualties in the event of an expected earthquake	No new building is expected to have this level of performance target	Some existing building types are known to be unsafe and need to be addressed most urgently in new mitigation policies. These include unreinforced masonry, non-ductile concrete and soft story buildings

2.3. Economic Losses

In order to calculate the economic losses, many facts need to be taken into account. Each region and country, etc, due to the different method of construction and the limit states applied on the buildings (soil conditions, material usage and etc), it may incur various construction costs. The construction cost can be also considered as a main factor, as the labour and material cost in each country is different. However, since the project is mainly focusing on the whole effect of the bracing system in high rise steel structure on fragility curve, therefore, construction cost is not going be the aim of this project.

Thus, an estimation of construction costs can be suggested as a future research study as the focus and the aim of the present research is to find the effect of fragility curve by adding bracing system into high rise steel structures.

2.4. Existing studies related to developing fragility curve

In this section, different papers related to fragility curve will be reviewed and summarised. The literature review will aid this study to gain an accurate and better understanding of the mentioned subject.

These investigations direct the study in the right make us have clear the subject better and make us have clear expectations related to the simulation's outcome.

The first case study is about the effect of using bracing system in high-rise steel structures, the results of which can be used for the validation of this study.

The second case study is about the effect of X-bracing in low and mid-rise structures under seismic loading by developing fragility curves. This research is a great example of how to develop fragility curve. In the same way, the result in this research shows that the number of the stories are not directly related to the probability of failure in X-bracing steel structure in low and mid-rise structures.

The third paper is about the effectiveness of the location of ground motions (far field or near field) which can affect the behaviour of the structure. Also this paper, compares the concrete frame structure with moment resisting steel structure.

Last study, explains the behaviour of the slim deck under seismic loading which is very useful and relevant to the aim of this research, as the data from the experiment can be related to the future work of this study.

2.4.1. Effectiveness of bracing system on high-rise steel structure

As previously mentioned, there are very few researches in this area. On one of the studies which is about the effect of bracing system on high-rise structures, the focus is on the performance of the structure against lateral loads (wind and earthquake). Five models have been introduced in this study: moment resisting frame, X-brace model, single diagonal, V-brace, and inverted V-brace model. All models have been simulated in ETABs. The live and dead loads, layout of the structure and all other aspects are similar in all 5 models.

Results show that a twenty-storey building (G+19) can have reduction of displacement up to 68.43% by using bracing system. In this study, also the bending moments and the shear force have been monitored. [18]

Maximum lateral displacements

Types of models	Displacements	% Reduction in Displacement
unbraced model	44.69	
X- Brace	26.4	28.82
Single diagonal	15.2	68.43
V- Brace	28.9	32.64
Inverted V	27.1	34.75

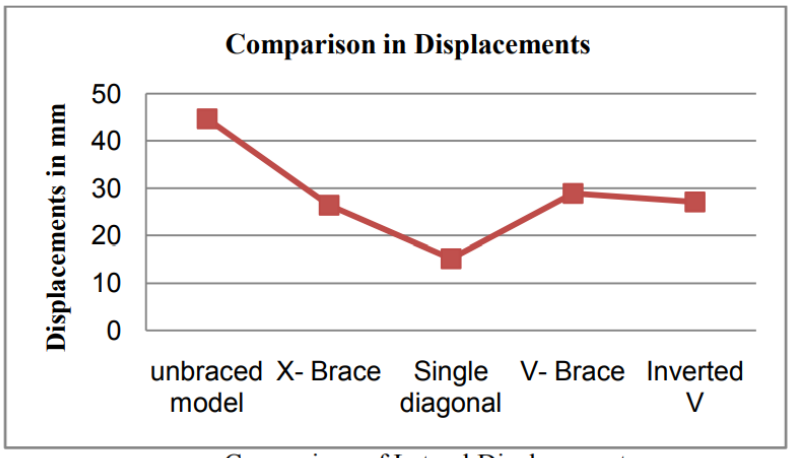

Comparison of Lateral Displacements

Figure 9.comparison of the displacement of steel structure with different steel bracing [18]

Maximum Shear Force

Models	Shear Force in KN
Without braces	302.60
X-Braces	881.27
Single diagonal braces	1030.51
V-Braces	872.54
Inverted V Brces	872.547

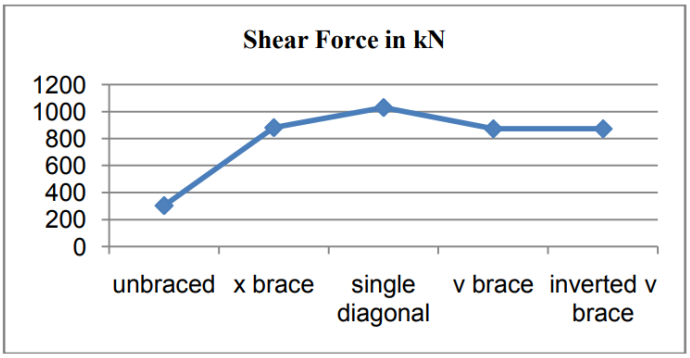

Comparison in Shear Force

Figure 10. Comparison of maximum shear forces in steel structures occurred [18]

Bending Moments

Models	Bending moments in KN-m
Without braces	883435.53
X-Braces	1114999
Single diagonal braces	907647.44
V-Braces	1110893.37
Inverted V Brces	1112013

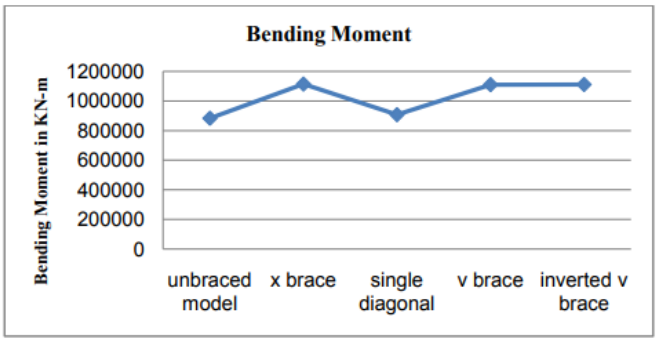

comparison in Bending moments

Figure 11.Maximum bending moments [18]

The following conclusions have been drawn based on the results obtained from present study: [18]

- The concept of using steel bracing is one of the advantageous concepts which can be used to strengthen or retrofit the existing structures.

- The lateral storey displacements of the building are greatly reduced by the use of single diagonal bracings arranged as diamond shape in 3rd and 4th bay in comparison to concentric (X) bracing and eccentric (V) bracing system.

2.4.2. Developing of fragility curve for low and mid-rise steel structures with X-bracing and by using non-linear time history analyses

In this paper, the investigation was about developing fragility curves for low and mid-rise structures that have X-bracing. The nonlinear time history analysis provided to develop fragility curves for these buildings. The aim of this investigation is to find the difference between the behaviour of these structures as well as to assess also the effectiveness of height, number of bays and the X-bracing on the probability of these structure's failure. The failure of them. Three types of steel structures have been analysed. The difference between these analyses is the height (or number of the floors). The three, five and seven story structures have structure has been selected. The bracing type, plan and other specification of the structures are similar to each other. The fragility curves have been developed into three performance level of minor, moderate and extensive level of damages. These categorization s can be divided into immediate occupancy (IO), Life safety (LS) and collapse prevention (CP). [36, 37]

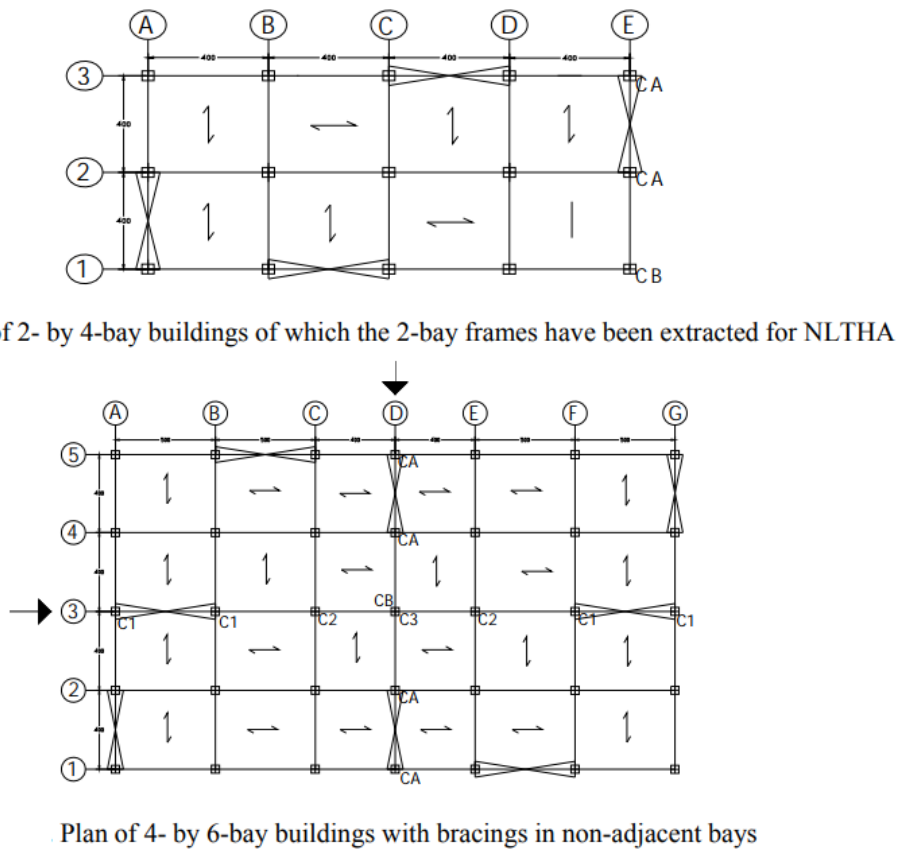

Figure 12.plan view of the structures [36]

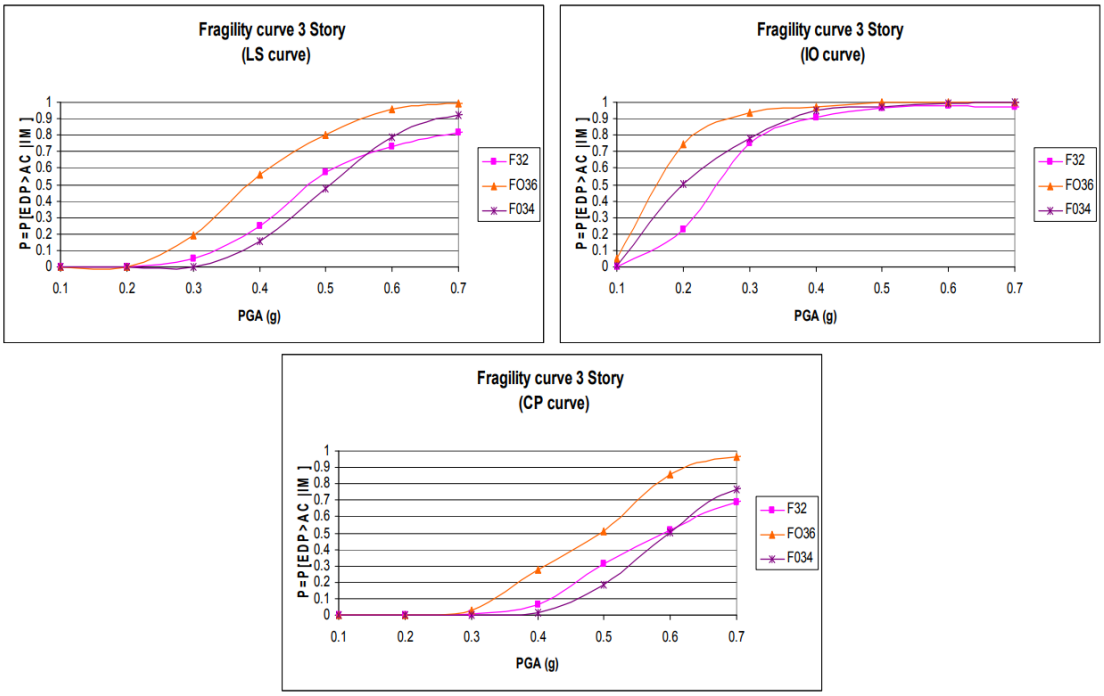

Figure 13. Fragility cures for 3-story frames F32 (2-bay frame), FO34 (4-bay) and FO36 (6-bay) [36]

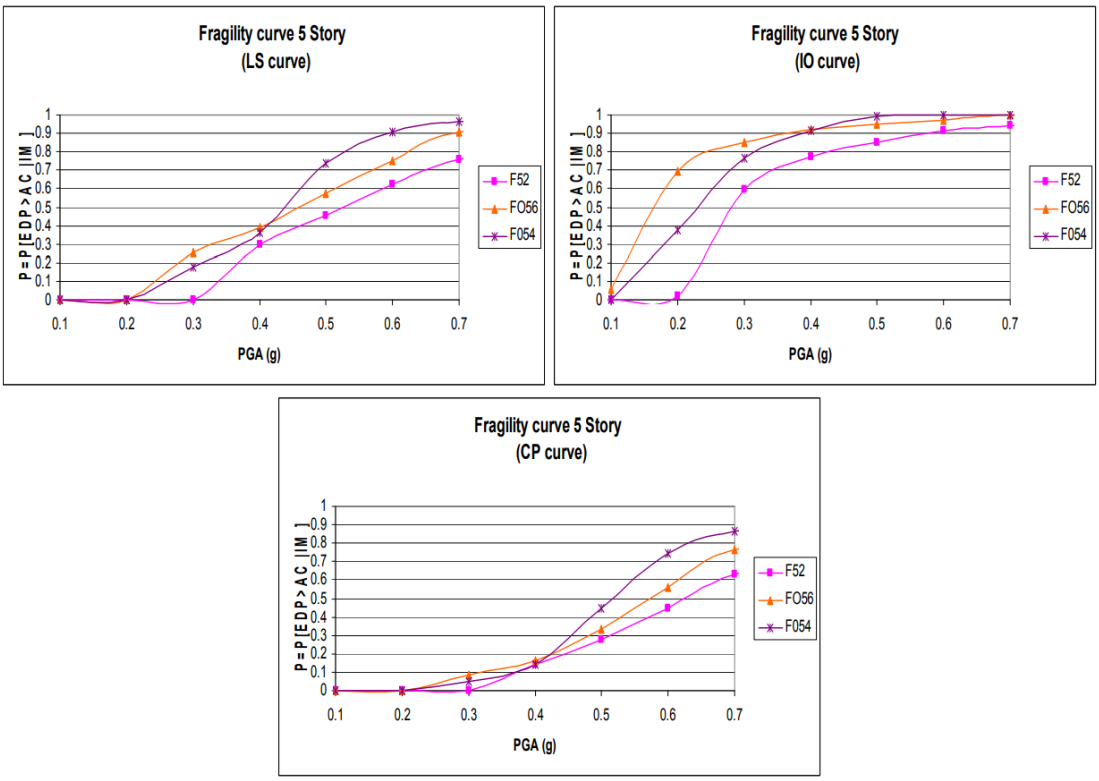

Figure 14. Fragility cures for 5-story frames F52 (2-bay frame), FO54 (4-bay) and FO356 (6-bay) [36]

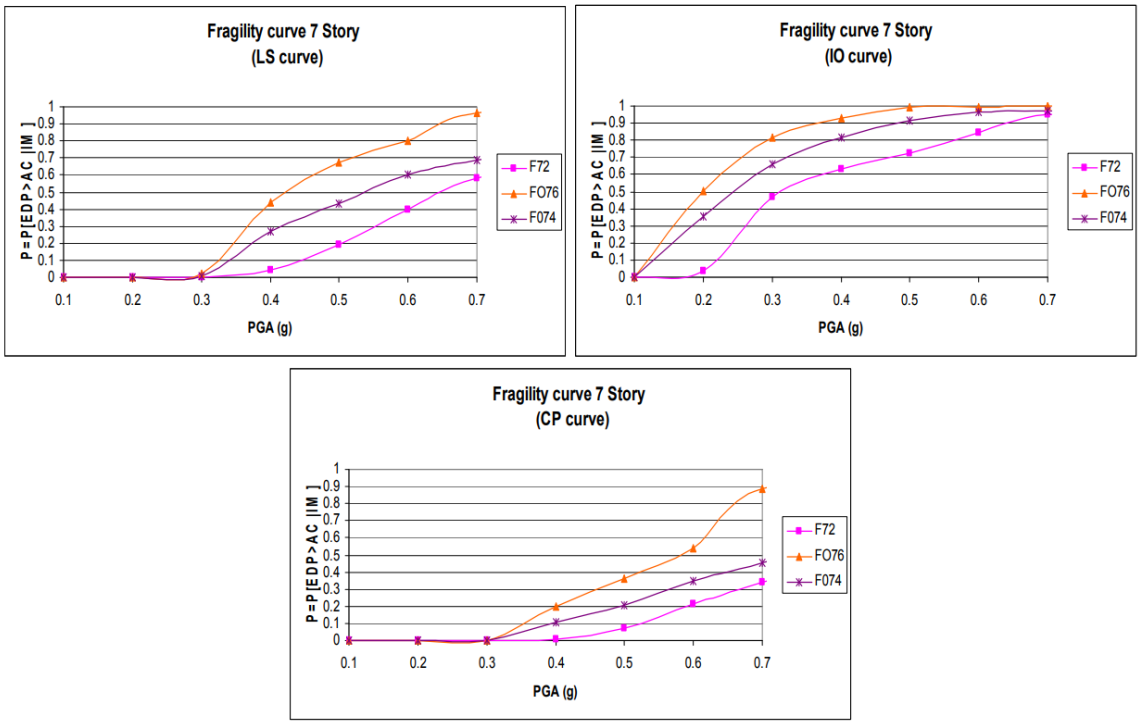

Figure 15. Fragility cures for 7-story frames F72 (2-bay frame), FO74 (4-bay) and FO76 (6-bay) [36]

To summarise the results, based on the figures and fragility curves, in for three different level s of the overall damage, fragility curves were developed for steel buildings with various numbers of stories and X-bracings. By using nonlinear time history analysis, and considering once the "inter-story drift" and once more for the "axial plastic deformation of bracing elements" as the damage index, the following conclusions can be stated: [24]

- The number of stories of frames does not have a remarkable effect on their fragility values in various performance levels (for low and mid-rise steel structures).
- The number of bays is an important factor in the fragility values of frames, and as this number increases the fragility values (probability of failure) proportionally increases.
- In general, for PGA values of 0.5g or more, the variation of fragility values is less than the variation corresponding to PGA values below 0.5g.

2.4.3. Seismic Fragility Curve of Steel and Reinforced concrete frames based in the near and far field ground motion record

This case study, consists of analysis and research about the behaviour of steel and concrete low and mid-rise structures. Both type of structures (concrete and steel) have been tested under seismic loading based on two categories of Near field (NF) and Far field (FF) ground motions. The fragility curve is calibrated to the Incremental Dynamic Analysis (IDA) curve based on building materials and frame heights. The frames have been designed by using Eurocode. Table s 3, 4 and 5 are shows a detailed summary of the structure element's sizes.

Table 3.Beam and column size of Steel frame [38]

No. of storey	Beam Size (mm)	Column size (mm)
3	533 x 210 x 109	305 x 305 x 198
6	533 x 210 x 82	305 x 305 x 198

Table 4.Beam cross section, Concrete frame [38]

No. of storey	Beam Size (mm)	reinforcement (mm)	Shear Link
3	300 x 700	6T25	8 mm link @ 150 mm c/c
6	300 x 700	4T32	8 mm link @ 150 mm c/c

Table 5. Column section, Concrete Frame [38]

No. of storey	Column Size (mm)	Reinforcement (mm)
3	500 x 500	6T32
6	500 x 500	6T32

Near field ground motion which has been studied in this research is define as all the seismic activities that occur within the 20km of the surface of the ground. The far field ground motions are the activities that happen in a depth of more than 20km. Tables 6 and 7 summarise the ground motion that has been used in this research.

Table 6. Selective ground motion records for NF [38]

Name record	Earthquake Location	Year
NGA 0146	Coyote Lake	1979
NGA 0235	Mammoth lake	1980
NGA 0318	Westmorland	1981
NGA 0545	Chalfant Valley-02	1986
NGA 0680	Whitter Narrows	1987
NGA 1646	Sierra Madre	1991
NGA 1740	Litte Skull Mountain	1992

Table 7. Selective ground motion records for FF [38]

Name record	Earthquake Location	Year
NGA 0101	Northern California-07	1975
NGA 0106	Oroville-01	1975
NGA 0206	Imperial Valley-07	1979
NGA 0221	Livemore-02	1980
NGA 0225	Anza (Horse Canyon)-01	1980
NGA 0389	Coalinga-02	1983
NGA 1990	Gulf of California	2001

The earthquake magnitude is within the range of 5 – 6 M_W. These ground motions were scaled to match the elastic response spectra. The elastic response spectra generated ranged from 0.05 to 0.6 g in increments of 0.05 g. The fragility curve is calibrated to the incremental dynamic analysis (IDA) curve based on building materials and frame heights. The five performance levels and two types of ground motions prescribed by FEMA-273 are used as structure performance benchmarks in generating the IDA curve. [38, 39]

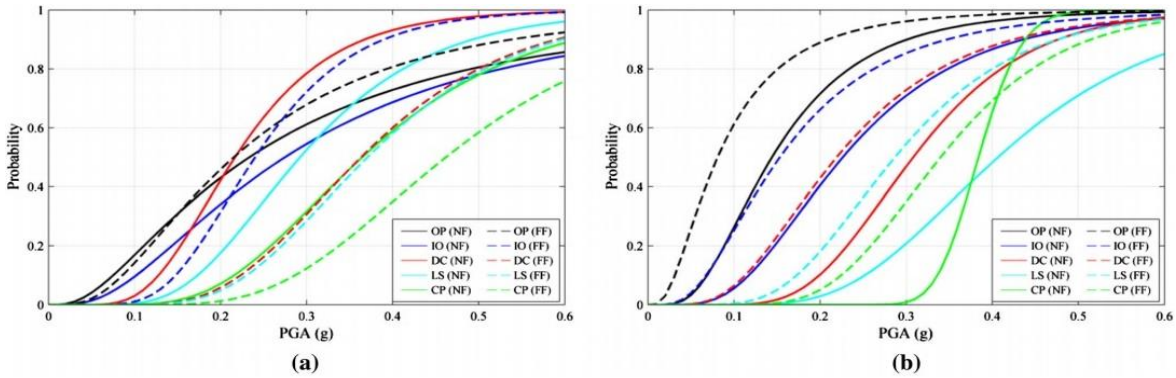

Fragility curve for a three-storey frame. **a** Fragility curve for a steel frame. **b** Fragility curve for a concrete frame

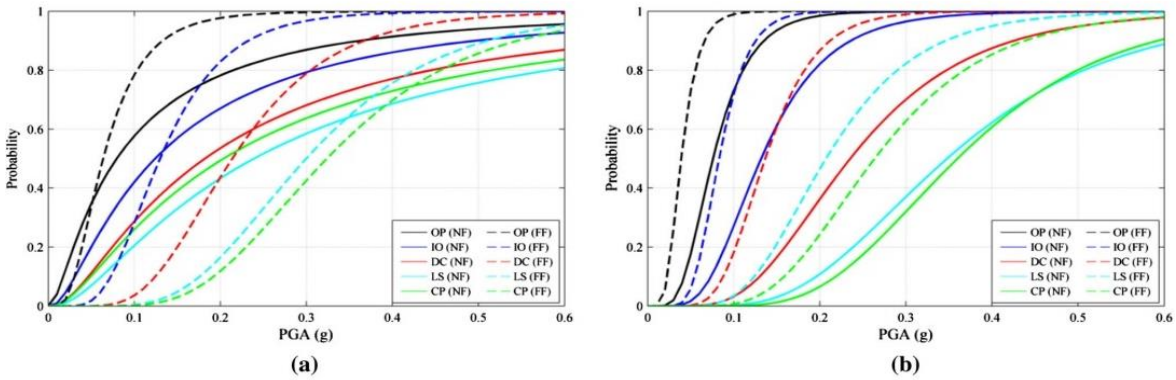

Fragility curve for a six-storey structure. **a** Fragility curve for a steel frame. **b** Fragility curve for a concrete frame

Figure 16.Fragility curves of three and six storey structure in concrete and steel frame [38]

The fragility curve for two types of structures (concrete and steel frame) has been generated. The structures have been designed by Eurocode and simulated in SAP2000. The summery of the graph can by illustrated be the following facts: [38]

- The drift profiles of the three- and six-storey structures under the NF records are almost similar. However, they have different drift percentages. Similar findings are obtained from the structures under the FF records. The drift profiles indicate that the steel frame is stiffer than the concrete frame for the three-storey structures under the NF and FF records. However, the concrete frame is stiffer than the steel frames for six storey structures under the NF and FF records.
- The fragility curves are developed based on the type of material used, as well as the height and under different ground motion records. The fragility curve or damage probability curve is based on the limit states of five performance levels, which are OP (Operational Phase), IO (Immediate Occupancy), DC (Damage Control), LS (Life Safety), and CP (Collapse Prevention). The three-storey steel frame demonstrates the highest

probability of reaching or exceeding the OP (72%) and CP (7%) levels based on the ground motion records for NF. The concrete frame has the highest probability of reaching or exceeding the OP level at 98% for the six-storey structures. The steel frame has the highest probability of damage at the CP level (50%). The concrete frame has the highest probability of reaching or exceeding the OP level based on the FF records, which registers 89% for the three-storey structures and 100% for the six-storey structures. The concrete frame also records the highest probability for both storeys at the CP level, which registers 5% for the three-storey structures and 24% for the six-storey structures.

- The higher probability of reaching the OP level occurred at the FF records as shown in a comparison of the fragility curves between NF and FF records. Concrete material exhibited a higher probability of OP for both NF and FF records. However, NF records produced the maximum probability of damage for the steel frame structure at the CP level stage. Meanwhile, a concrete frame has the highest probability of damage for the frame structure exposed to the FF records.

2.4.4. Summary of Case Studies

This research overviewed the concept of fragility curve by using the slim deck flooring system and gathered the relative investigation that lead the study to a better understanding of the expected outcome, and the reasons for structure failure during simulation.

In the literature review, there were several case studies and experimental research were reviewed.

1. Effect of bracing on lateral load (wind and seismic): the results of these simulations and analysis help to understand better the effect of bracing system on possible reduction that might appear in bending moment, shear force in compression and displacement.

2. Fragility curve in different levels of damages for mid- and low-rise steel structures: the provided data was very helpful. One of the outcomes of this research was, the number of storeys is not causing a remarkable effect on the characteristics of the structure such as bending, deflection and their fragility. Another fact that has been observed was the variation of the fragility after 0.5g, becoming more evident in the results.

3. Near field and far field seismic activity in 3 and 6 storey structures for steel and concrete frames. This review and research represented that steel would be stiffer in low rise building compared to concrete which showed a better performance in 6 storeys (as a matter of stiffness). On the other hand, results revealed that concrete reaches the higher probability of failure earlier than steel in most of the cases.

2.5. Approaching method

Seismic risk describes the potential for damage or losses that a region is prone to experience following a seismic event. This contrasts with seismic hazard, which quantifies the recurrence rates of different ground motions. Seismic risk can also be defined as the spatially and temporally integrated product of the seismic hazard, the value of assets and the fragility of assets. [41]

In order to do a fragility analysis of the structure, some parameters are required in order to simulate and predict the behaviour of the failure modes of the structures when subjected to seismic forces. The intensity and the magnitude of the earthquake are one of those parameters that are related to the behaviour of the structure. These factors are found by PGA, PGV, PGD, S_a , S_d and Mercalli intensity scale.

An emerging tool in seismic risk assessment (SRA) is the use of fragility curves. A fragility curve is a conditional probability that gives the likelihood that a structure will meet or exceed a certain level of damage for a given ground motion intensity. Currently, fragility curves are derived by using empirical data from previous earthquake's expert opinions or via analytical methods. Empirical fragility curves often lack adequate data and are only applicable to limited regions. Fragility curves based on expert opinion are also very subjective in that they rely heavily on the experts' seismic experience with the steel structure under consideration. Previously, developed analytical fragility curves were based on simplified models and simplified methodologies, which by their very nature include a significant amount of epistemic uncertainty, and therefore do not completely represent the performance of most structures. To adequately represent the fragility of a structure and to improve the reliability and effectiveness of seismic risk assessment tools, improved fragility curves for buildings are needed. [41]

Design Deficiencies can be another fact that may lead the structure to failure. To be more specific, in rural and urban areas, it is sometimes challenging to encounter engineered structures. Unfortunately, some of the engineers and architects are not familiar with earthquake resistant design. The lacks of appropriate design in terms of architecture and structure as a matter of architectural and structural can be listed as follows: [43, 44]

- Low lateral resistance and redundancy
- Irregularities in plan and elevation
- Soft storey, weak story
- Short Column, Long and short column and improper width of columns
- Overhangs
- Strong beam–weak column joints, etc.

Detailing deficiencies is another reason that will cause structure to collapse. The basic principle of detailing is to provide the necessary strength and ductility at critical sections of structural members and at beam-column joints. [49]

Detailing deficiencies occur mostly due to the tendency to violate the code provisions about detailing of members or to disregard the detailing in the design drawings both intentionally and due to ignorance. These deficiencies can be listed as follows:

- Insufficient transverse reinforcement
- Insufficient spliced length of bars
- Insufficient beam to column joint reinforcement
- Constructional deficiencies: Incorrect site applications due to the lack of supervision and careless contractors result in structures different than initial architectural and engineering design.

Fragility curve can be derived by four different methods. Empirical, judgment, analytical and hybrid methods are used to estimate the probability of the failure of any element and structure. These methods can be summarised in Table 8.

Table 8.Categorization of vulnerability curve [45, 46 and 47]

Category		
Empirical	Benefits	Based on post-earthquake survey or on expert opinion Most realistic method
	Drawbacks	Highly specific to a particular seismo-tectonic, geotechnical and built environment The observation data used tend to be scarce and highly clustered in the low-damage, low ground motion severity range There are errors in building damage classifications Damage due to multiple earthquakes maybe aggregated
Judgement	Benefits	Based on expert opinion and experience Curves can be easily made to include all the factors
	Drawbacks	The reliability of the curves depends on the individual experience of the experts consulted
Analytical	Benefits	Based on the damage distributions simulated from analysis Reduced bias Increase reliability of vulnerability estimate for different structure
	Drawbacks	Considerable time consuming on computational analysis, the limitation and modelling capacity The number of choices of analytical method, idealisation, seismic hazard and damage model influence the derived curves and have been seen to cause significant discrepancies in seismic risk assessment
Hybrid	Benefits	Compensates for the scarcity of the observation data, subjectivity of the judgmental data and modelling deficiencies of analytical procedures Modification of analytical or judgment-based relationships with observational data and experimental results
	Drawbacks	The consideration of multiple data sources is necessary for the correct determination of vulnerability curve reliability

According to the investigations and the high demand on this subject, there are several ways to achieve the fragility curves of structures. Due to the lack of post-earthquake data in high-rise structures, empirical methods would not be suitable. Due to the lack of research in this section, it would not be logical and reasonable to use judgmental method. For hybrid method, there are not sufficient data available. Therefore, the best solution is to do an analytical method.

Chapter 3: Methodology and Approach

3.1. Research methodology and procedure

According to the literature review and the case studies, there has not been adequate research in developing the fragility function for high-rise steel structure with slim deck flooring system. This research aims to investigate the probability of the steel structure failure under seismic load by using analytical method. This method has some advantages and disadvantages which have been summarised previously. (Table 8)

There will be three different types of framing system s. Moment resisting frame that has been selected from designed structure in Century City in the United States. The other two framing s are X and V bracing that are the popular and common reinforcements for composite structures. In order to monitor and analyse the results and database, it requires to be modelled and analysed, in order to review the effect of bracing on fragility curve.

In order to fully understand the behaviour of the collapse mechanism and the probability of failure in high-rise steel structures, moment resisting frame will model and analyse alongside of the V and X-bracing models.

Another reason to pursue this aim is to have more detailed analysis regarding the effect of additional lateral stability and the behaviour of structure under same conditions of simulation.

The methodology of the research can be divided mainly into two parts.

1) Theoretical derivation:

Mainly, it is focusing on the methodology of how to gain analytical results. In this research, theoretical aspect would be the step-by-step method to derive the fragility functions. Alongside with the derivation of the fragility function the approach is to develop the analytical results and to revise the regulation of seismic calculation in ASCE and Eurocode.

The structure has been designed under ASCE codes therefore, it will be logical and convenient to set the simulation conditions under ASCE code. Alongside with that Eurocode circumstances and limitations of designs, load combination and calculation have been taken into account to overview the results and outcomes.

2) Modelling and simulation

The restrictions and limitations that might be added to the model needs to be considered. In this research:

- The frames of structures are moment resisting, V bracing and X-bracing.
- The definition of high-rise structure is the structure with 15 or more storeys
- Layout of structures are the same
- Soil categories of time history of earthquake are considered

3.2. Theoretical – Fragility Curves

It is necessary to develop fragility curves for high rise steel frame structure to help the risk evaluation and collapse mitigation design for various seismic zones. As previously stated in the report, the fragility curve is probabilities that the structural damages, under various levels of seismic excitation, exceed specified damage states. In this part of the report the derivation to find the fragility curve of structure is demonstrated. [50]

In this chapter, the fundamentals and the approach of the design will be discussed. To summarise the methodology of the output, it can be said that the time history analysis has been selected to proceed with. The ground motion details have been collected carefully, in order to be same location to have / experience the same type of the soil. The time histories are mainly from Pasadena, Cape Town, Golden Gate Park, El Centro Array, Holister City hall, Parkfield Cholame station. With total number of 236-time histories. The data collected by using the 5% damping ratio. Each time history has the three-dimensional data that relates to the ground motion in each direction (X, Y and Z). The Data was implemented into the model by using ETABs. The mainly preferred NEHRP Based on Vs,30 of the data are in type C and D.

The reason for selecting type C and D, is the variety (number of time-history records) in this classification was higher. As it requires large number of time-history record to have a better resolution for the fragility curve. In order to cope with the non-linearity of the results plastic hinges were introduced. However, since the loads are not exceeding the limits (life-time and safety limits), therefore in most of the cases the plastic hinge does not contribute to the simulations. Since, given the lack of computational power and hardware availability in this research, it has been decided to minimise or not include some factors. One of which is soil interaction. Therefore, realistic time history data was applied into foundation of structure with pre-design damping ratio.

By the details provided in each time history, it is possible to calculate the spectural acceleration of each seismic activity over time, automatically in Etabs, which saves time significantly. However, each spectra from time history has its own Sa (0.2s) and S1 and long period transition. Therefore, each time needs the review and change of the data required to

add to the seismic loading. For further detail related to the time history analysis in ETABs, information has been provided in. [63]

In ETABs plastic hinges can be added the to avoid the plastic deformation and failure in the beams. It is noteworthy that, the simulation with plastic hinges increases the time and power of computational calculations significantly. In the early stage, several worst-case scenarios with the highest PGA have been examined and none of the results appear to have any deformation and force on plastic hinges, therefore following the result. For most part of the simulation plastic hinges have been removed since the outcome represented that the limitation and applied forces does not have any impact on the failure of the beams. In addition, since the earthquake design level of the structure is in Immediate Occupancy (IO) therefore the structure does not attend the non-linearity significantly at all.

In order to judge the level of the failure in the result of FE simulations, the story drift of the structure has been selected as an Engineering Demand Parameter (EDP) to judge the theoretical failure of the structure.

The simulation mainly divided the intensity of the ground motion of the seismic activity into two directions of X and Y direction. In X-direction, the combination of the X and Z directions are included in the input of the model. However, in the load combination the seismic load divided into two directions X and Y, while calculation of the seismic activity in horizontal direction is also combined with two magnitude and direction.

3.3. Damage state

Fragility functions are the statistical destitution of how structure is behaving under seismic load. In this research, it can be defined by the probabilities at which building might fail under specific damage state. These facts are pertained to engineering demand parameters and are theoretical. In order to derive the fragility function, the damage state should be first determined in analysis and then stated in detail.

There are several methods for failure judgement of a building. The best option to reduce the time of judgement and improve the quality of the analysis, is to judge the structure by its deflection or displacement. In this case, it would be monitoring the storey drift of the building in each case after the simulation.

3.3.1. ASCE

According to the table of 12.12.1 in ASCE code, the limitaion for storey drift on the prototype selected for simulation could be acceptable up to 1.5% of the total height or 0.015h. (All other structures – Category III)

Table 9. Allowable Story Drift (table 12.12.1 ASCE)

Structure	Risk Category		
	I or II	III	IV
Structures, other than masonry shear wall structures, four stories or less above the base as defined in Section 11.2, with interior walls, partitions, ceilings, and exterior wall systems that have been designed to accommodate the storey drifts	0.025h	0.020h	0.015h
Masonry cantilever shear wall structures	0.010h	0.010h	0.010h
Other masonry shear wall structures	0.007h	0.007h	0.007h
All other structures	0.020h	0.015h	0.010h

Category III is stating that Buildings and other structures, the failure of which could pose a substantial risk to human life III Buildings and other structures, not included in Risk Category IV, with potential to cause a substantial economic impact and/or mass disruption of day-to

day civilian life in the event of failure in buildings and other structures not included in Risk Category IV (including, but not limited to, facilities that manufacture, process, handle, store, use, or dispose of such substances as hazardous fuels, hazardous chemicals, hazardous waste, or explosives) containing toxic or explosive substances where the quantity of the material exceeds a threshold quantity established by the Authority Having Jurisdiction and is sufficient to pose a threat to the public if released.

In this research category III will be the point of the judgement of structure that it would fail if exceeded.

3.3.2. Eurocode

According to Cl. 4.4.3.2(1) in Eurocode for the damage limitation (serviceability) limit state:

$$d_r \, v \leq 0.01 \, h$$

Where d_r is the design inter-storey drift, v is a reduction factor that takes into account the lower return period of the frequent earthquake and is assumed as 0.5, and h is the storey height. The limit of maximum storey drift is 1% of total height or 0.01 h, is applicable to cases where the non-structural components are fixed to the structure in a way that does not interfere with structural deformation. For cases with non-ductile or brittle non-structural elements, this limit is reduced to 0.75% and 0.5%, respectively.

For all the simulations that have been designed under Eurocode regulation, if the storey drift exceeds above 1% of the total height of the structure, it can be counted as a global failure theoretically.

3.4. Database Generation Using ETABS

In order to apply the non-linear time history analysis to the model, it required to download the data of the earthquakes. In appendix section, the details of the selected earthquake have been mentioned. (Appendix A1)

The First step is to define the non-linear time history to the structure. Defining time history in ETABs requires the details of the acceleration time history for each earthquake in X and Y directions. In order to create more realistic data outcome, in X-direction ,2 directions of X and Z were applied as a time history to the foundation of the building. Therefore, a 3-dimensional force was applied to the foundation.

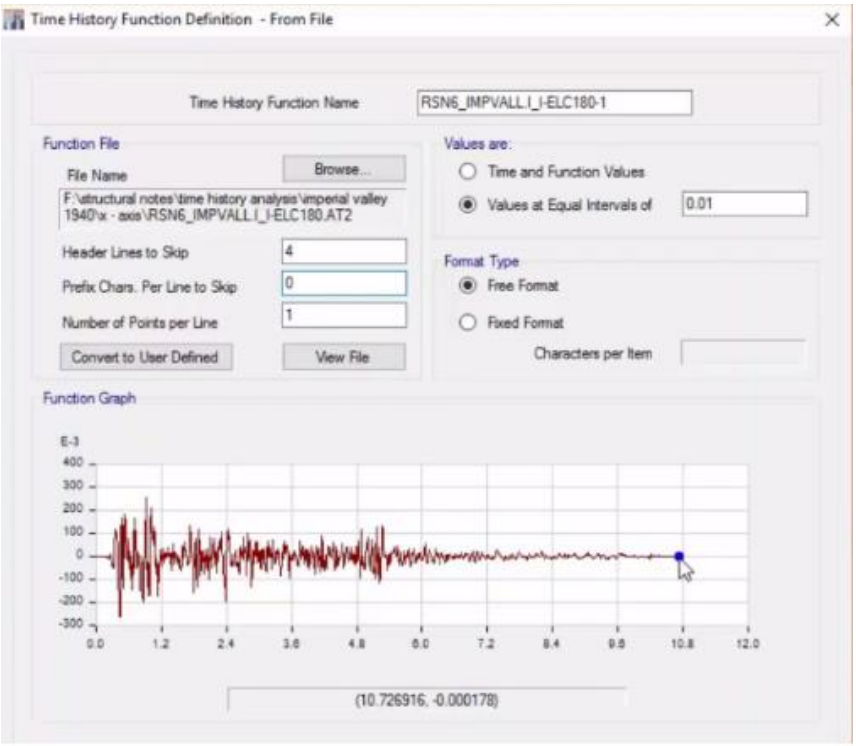

Figure 17. Sample of Acceleration time history in horizontal direction (ETABS)

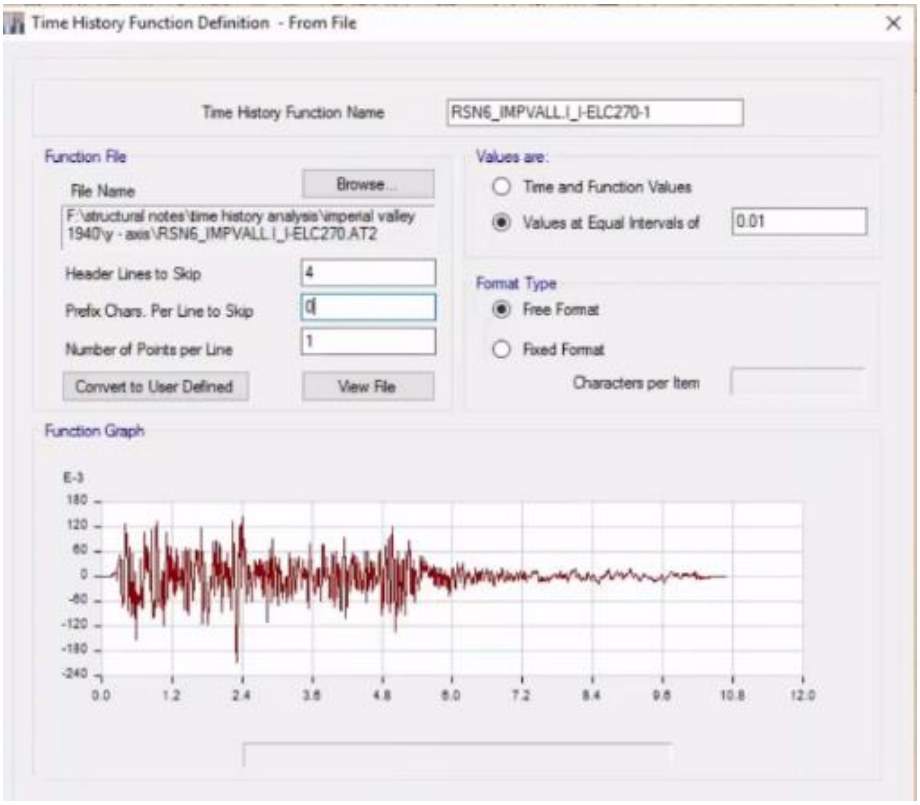

Figure 18. Sample of Acceleration time history in vertical direction (ETABS)

Figure 18 and 19 are the example of one of the time histories. There are two horizontal ground accelerations in X and Z directions. Also, there is a vertical ground acceleration in Y direction. Each time history has a series of data being in recorded in its unique equal intervals. Therefore, the total amount of seismic activity is the multiply of total number of recorded activities and the value intervals.

```
PEER NGA STRONG MOTION DATABASE RECORD
Northridge-01, 1/17/1994, Sylmar - Olive View Med FF, 90
ACCELERATION TIME SERIES IN UNITS OF G
NPTS=   2000, DT=   .0200 SEC
```

Figure 19. Example of time history index (PEER)

NPTS: total number of recorded points (acceleration data)

DT: time interval of recorded points

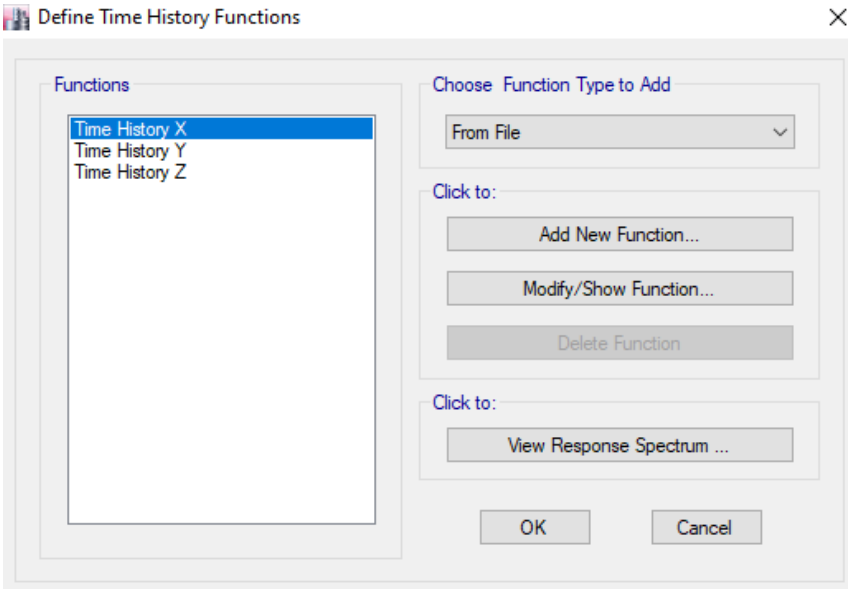

Figure 20. List of time history functions (ETABS)

Next step, depending on the aim of the research, is to target the spectrum which will be created and then will be matched to the frequency and time history with target response spectrum. Therefore, in order to select the time history as a load case which will be non-linear, the time histories in both directions (X and Y) will be added to the model.

Value of the intervals in each time-history will depend on the interval of recorded data. And in each case, they should be checked and modified.

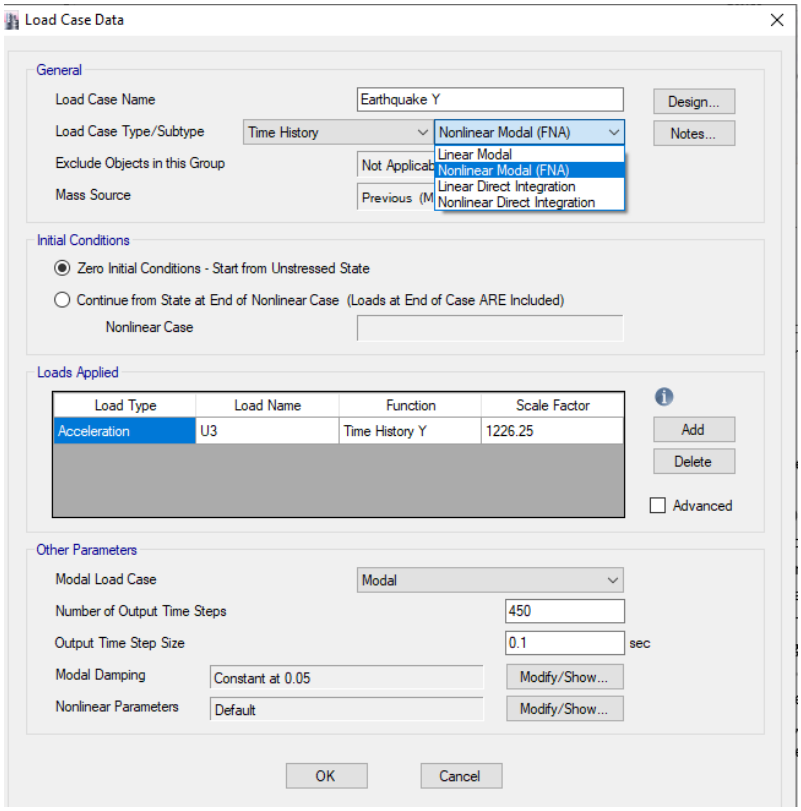

Figure 21. Available actions for time history of the structure (ETABS)

Load case type, in this research, will be non-linear Modal (FNA – fast non-linear analysis). The time steps of each scenario will be depending on the duration of the seismic activities and the intervals.

Note that the scale factor formula is

$$Scale\ \ Factor = I.\frac{g}{R}$$

Where I is impotence factor, g is acceleration due to gravity (9.81 m/s2) and R is response reduction factor.

According to the CSI manual of the program:

If dynamic base shear is less than 85% of the static base shear, then the scale factor should be adjusted such that the response-spectrum base shear matches 85% of the static base shear. In this case, the new scale factor would be (I g / R) * (0.85 * static base shear / response-spectrum base shear). Analysis should then be rerun with this scale factor specified in the response-spectrum case.

For defining the load cases, it is necessary to define all the coefficients and the relationships between each load to the structures.

3.4.1. Loads combination definitions in ETABS

To summarise, all the factors acting on the structure that have influence on the behaviour of the structure have been listed below:

- Dead loads
- Live loads

The dead and live loads are designed for office use and according to ASCE live loads is 2.4 kN/m2.

It is noteworthy that in load combination, the total dead load would equal to the assumed dead load for the office plus the pre-existing dead load in the building itself.

- Time history

Time history analysis is a step-by- step analysis of the dynamic response of a structure to a specified loading that may vary with time. Time history analysis is used to determine the seismic response of a structure under dynamic loading of representative earthquake. [60]

Each seismic activity has its specific characteristic in terms of the period, peak point and the violation.

- Spectral acceleration

Each earthquake depending on the soil condition, PGA and the period, has its own spectral

- Soil condition

Soil condition can be classified from A to E (soft to hard)

- Loads combinations

Each simulation calculated the different loads combinations for structure and the shear wall.

After applying all factors required to evaluate the seismic activity, dead and live loads should be applied to the load case. Then different scenarios will be added to the load cases which will be called load combinations. The following load cases are explained in section 3.4.2.

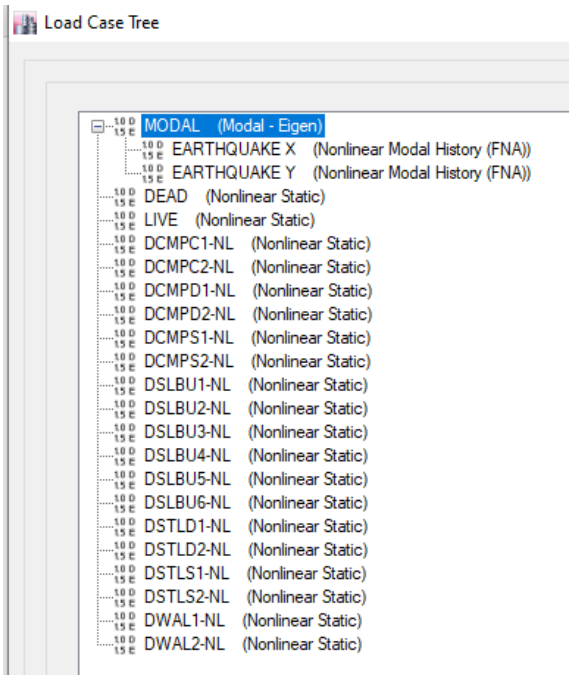

Figure 22. Example of Load case's tree in ETABS

The figure above is demonstrating the load cases that have been set to simulate and analyse for each time-history. The greatest reactions out of these combinations will be taken into the account and note for making final decision regarding the theoretical failure on the building by the help of the limit states.

3.4.2. How the load combinations combined

The first stage is to clarify the loads which need to be concerned (such as dead loads, live loads, and seismic loads). Since the seismic loads would be in form of time history analysis, the data from time history should be applied. Next the combination of horizontal seismic activity would be E_h and vertical seismic activity would be E_v as the formulas stated in section 3.4.2.

The dead load and live load are added into the load combination separately. There will be the option to add the load of the elements (such as beam, column, and slabs).

The last step is to define the ratio of each load that will contribute to simulation. The worst-case scenario with highest deflection would be taken into account as a judgment of the result. The inter storey drift calculated and the models that have over the limitation of the inter storey drift, will be count as a failure occurred in the building.

3.4.2.1. Load combinations in ASCE

Basic combination loads for strength design of structures, in ASCE are as follows:

1. $1.4\ (Dead\ Load)$
2. $1.2\ (Dead\ Laod) + 1.6\ (Live\ Loads + Loads\ due\ to\ lateral\ earth\ pressure) + 0.5(Roof\ live\ load\ or\ snow\ load\ or\ rain\ loads)$
3. $1.2\ (Dead\ Loads) + 1.6\ (Roof\ Live\ Loads\ or\ Snow\ Load\ orRain\ load) + (\ live\ loads\ or\ 0.5\ wind\ load)$
4. $1.2\ (\ Dead\ Laods) + 1.0\ (wind\ loads) + Live\ Loads + 0.5\ (Roof\ live\ load\ or\ snow\ load\ or\ rain\ loads)$
5. $0.9\ (Dead\ Load) + 1.0\ (Wind\ Loads)$

In addition, there are several load combinations for seismic effects which should take into the account:

6. $1.2\ (Dead\ Loads) +\ E_v +\ E_h + Live\ loads + 0.2\ (Snow\ Loads)$
7. $0.9\ (Dead\ Load) -\ E_v +\ E_h$

Where E_v and E_h are the vertical and horizontal earthquake loads. Each seismic activity, depending on their directions has different aspects and factors that can affect on the structure.

On equation (6) E (seismic load effects) will be the addition of E_v and E_h. On the other hand, the E for equation (7) is the subtraction of horizontal seismic load effects against its vertical load.

Horizontal seismic load can be defined by the following formula:

$$E_h = \rho\ Q_E$$

Where Q_E is defined as effects of horizontal seismic forces from V or F_P, such effects shall result from application of horizontal forces simultaneously in two directions at right angles to each other) and

ρ is redundancy factor and shall be assigned to the seismic force-resisting system in each of two orthogonal directions for all structures.

Vertical seismic load can be defined by the following formula:

$$E_v = 0.2\, S_{DS}\, D$$

Where S_{DS} is the design spectral response acceleration parameter at short periods obtained and D is the effect of dead load.

Design spectral response acceleration can be calculated by the following method and use of table of the short period site coefficient:

$$S_{DS} = \frac{2}{3}\, S_{MS}$$

Where S_{MS} is the MCE_R (risk-targeted maximum considered earthquake) at the rate of 5% damped and spectral response acceleration parameter at short periods adjusted for site class effects.

Spectrum response acceleration parameter can be calculated by the following method:

$$S_{MS} = F_a\, S_s$$

Where S_s is the mapped MCER spectral response acceleration parameter at short periods and F_a is the short period site coefficient which depends on the classification of the site (soil type can be different).

Table 10. Short-Period Site Coefficient (Soil Type A to E) - ASCE 7-16 Table 11.4-1

Short-Period Site Coefficient, F_a						
Mapped risk-targeted maximum considered earthquake (MCE_R) spectral response acceleration parameter at short period						
Site Class	$S_S \leq 0.25$	$S_S = 0.5$	$S_S = 0.75$	$S_S = 1.0$	$S_S = 1.25$	$S_S \geq 1.5$
A	0.8	0.8	0.8	0.8	0.8	0.8
B	0.9	0.9	0.9	0.9	0.9	0.9
C	1.3	1.3	1.2	1.2	1.2	1.2
D	1.6	1.4	1.2	1.1	1.0	1.0
E	2.4	1.7	1.3	---	---	---

In ETABS, each time history has its own characteristics, which are the site class the spectral acceleration at 0.2s and 1.0s. Then, by providing the mentioned details, it calculates the design earthquake spectral response acceleration parameter at short period, S_{DS}, and at 1 s period, S_{D1}.

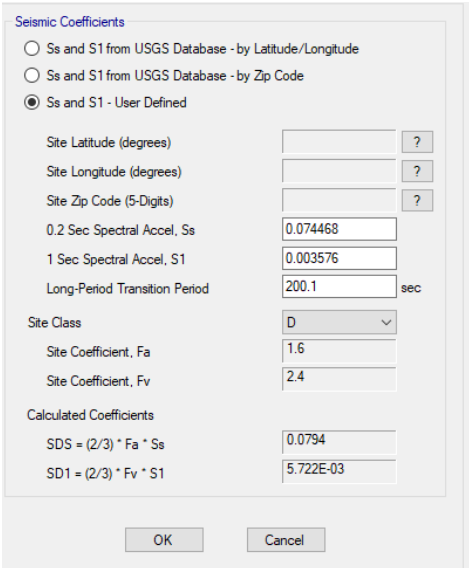

Figure 23. Sample of seismic loading (ETABS)

$$S_{D1} = \frac{2}{3} S_{M1}$$

Where S_{M1} is The MCER spectral response acceleration parameters at 1 second and can be calculated by $S_{M1} = F_v S_1$

S_1 is the mapped MCE_R spectral response acceleration parameter at a period of 1 second.

Table 11. Short-Period Site Coefficient (Soil Type A to E) - ASCE 7-16 Table 11.4-2

Short-Period Site Coefficient, F_V						
Mapped risk-targeted maximum considered earthquake (MCE_R) spectral response acceleration parameter at short period						
Site Class	$S_1 \leq 0.1$	$S_1 = 0.2$	$S_1 = 0.3$	$S_1 = 0.4$	$S_1 = 0.5$	$S_1 \geq 0.6$
A	0.8	0.8	0.8	0.8	0.8	0.8
B	0.8	0.8	0.8	0.8	0.8	0.8
C	1.5	1.5	1.5	1.5	1.5	1.4
D	2.4	2.2	2.0	1.9	1.8	1.7
E	4.2	---	---	---	---	---

3.4.2.2. Load combination in Eurocode

The basic load combination for this design according to the EN1990 and the seismic load combination is $E_d = \sum_{Permanent} G_{kj} + A_{Ed} + \sum_{Reduced\ Variable} \psi_{2i}\, \varrho_{ki}$

Where:

E_d is the design action effect, A_{Ed} is earthquake action, ψ_{2i} is quasi permanent factor and the range is between 0.0 – 0.8, ϱ_{ki} is variable (live load) and G_{kj} is permanent dead load

Seismic mass can be followed by: $\psi_{Ei} = \psi_{2i}\, \varphi$

φ is in the range of 0.5 – 1.0 depending on the loading type

Table 12. Recommended Value for φ

Type of variable action	Storey	φ
Categories A–C[a]	• Roof	1.0
	• Stories with correlated occupancies	0.8
	• Independently occupied storeys	0.5
Categories D–F[a] and Archives		1.0

[a] Categories as defined in BS EN 1991-1-1: 2002

Table 13. Suitable value for the ψ

Actions	ψ_0	ψ_1	ψ_2
Imposed loads in buildings, category (see EN 1991-1-1)			
Category A: domestic residential areas	0.7	0.5	0.3
Category B: office areas	0.7	0.5	0.3
Category C: congregation areas	0.7	0.7	0.6
Category D: shopping areas	0.7	0.7	0.6
Category E: storage areas	1.0	0.9	0.8
Category F: traffic area, vehicle weight ≤ 30 kN	0.7	0.7	0.6
Category G: traffic area, 30 kN < vehicle weight ≤ 160 kN	0.7	0.5	0.3
Category H: roofs	0.0	0.0	0.0
Snow loads on buildings (see EN 1991-1-3)			
Finland, Iceland, Norway, Sweden	0.7	0.5	0.2
Remainder of CEN Member states, for sites located at altitude H > 1000 m a.s.l.	0.7	0.5	0.2
Remainder of CEN Members states, for sites located at altitude H ≤ 1000 m a.s.l.	0.5	0.2	0.0
Wind loads on buildings (see EN 1991-1-4)	0.6	0.2	0.0
Temperature (non-fire) in buildings (see EN 1991-1-5)	0.6	0.5	0.0

Chapter 4: Developing Numerical Result of Fragility Curves of the Moment Resisting Frame, V-Bracing and X-Bracing

4.1. Dataset Generation using Numerical Analysis and Simulation

In this Chapter, the datasets and the numerical results will be summarised and compared in each structural frame separately. In addition, the results have been summarised in the form of tables and figures along with the additional information provided.

The focus of this chapter is to overview the extracted data from simulation and compare the Moment Resisting (MR), V-Bracing (VB) and X-Bracing (XB) frames in Eurocode and ASCE code.

Mainly this chapter will be focus on the results by itself and the comparison of the frames. In the next chapter, all the possible reasons of the behaviour and more details regarding the aspects will be discussed.

The main important aspect of this research is to find out the fragility curve of high-rise steel structures with concrete shell and slim deck flooring system under seismic activities. In addition to the main purpose, the energy dissipation throughout the elements of the structure was put into investigation to understand better the behaviour of the building in this situation.

In addition to the main aims and objective of the research, the relationship between the effects of lateral stability on steel structure subjected to the fragility function of structure will be taken into the account.

The building is a prototype of the designed building located in Century City, CA, the USA, designed based on ASCE 7-10. For further investigation additional lateral stabilities and new flooring system have been implemented into the design.

236-time histories in three type of frames and two types of designed regulations have been simulated in a three-dimensional simulating program called ETABS.

The details of the earthquakes and the required outcome of the three composite frames are available in the appendix.

4.2. Prototype building

The structure has been designed following the real design of buildings in Century City in the USA. It has been designed by ASCE 7-10 (American Society of Civil Engineering) and target design collapse level of 1% probability in 50 years. These numbers have been calculated and simulated by numbers of recorded ground motions.

The details of the modelling of the structure are briefly explained by following figures and tables:

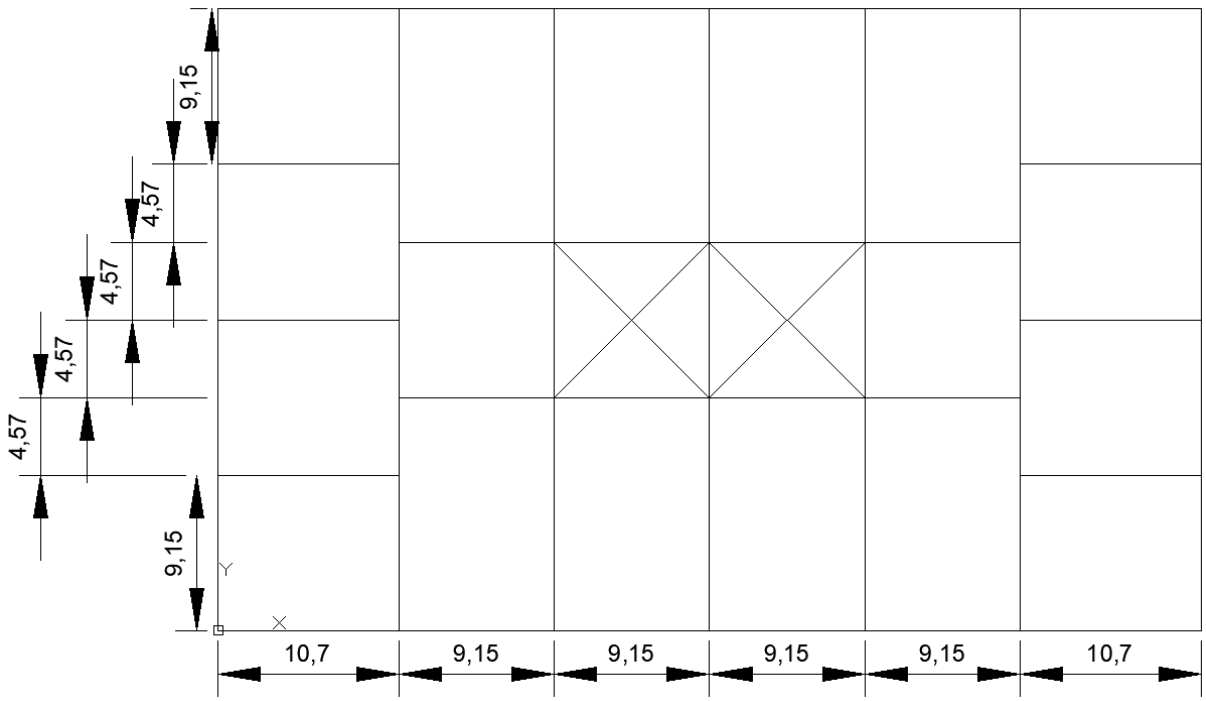

Figure 24. Plan view of the structure (AutoCAD Drawing) – measures are in meter

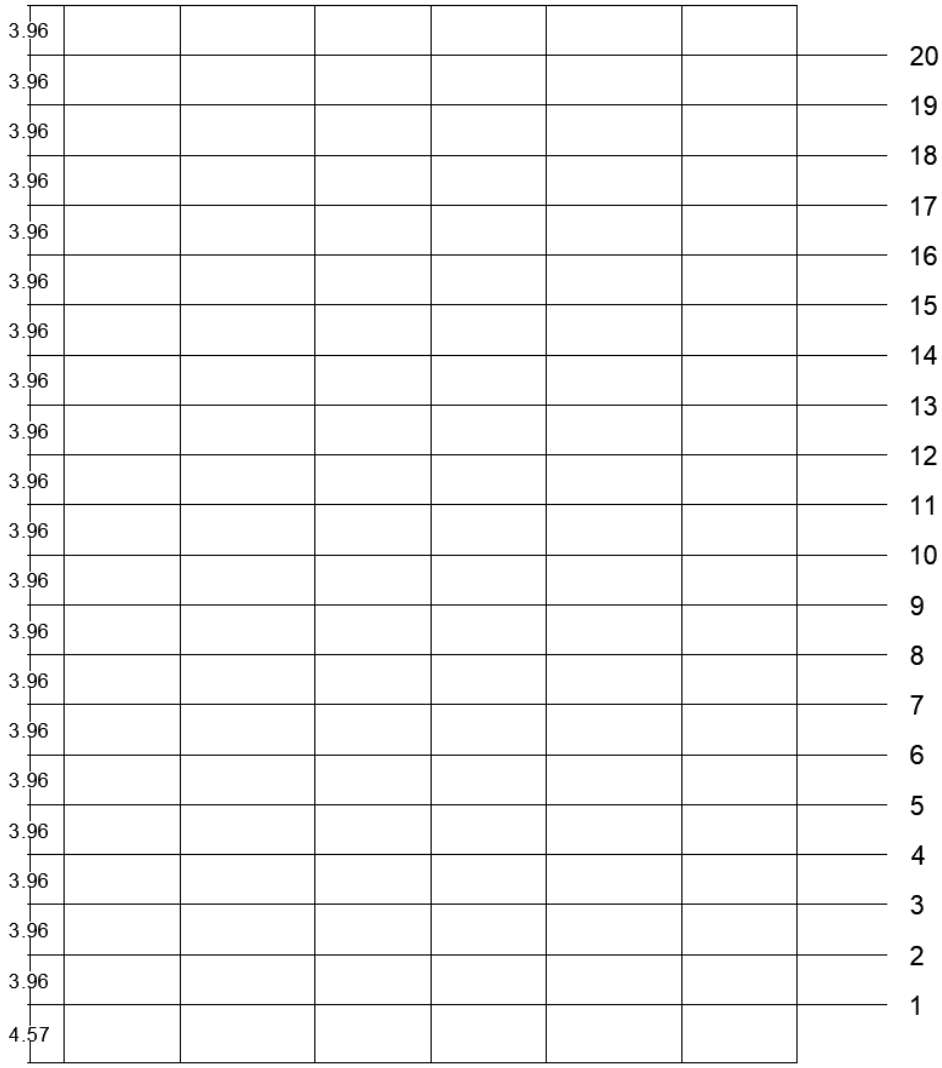

Figure 25. Elevation view of Structure with dimensions (AutoCAD Drawing) – Measure is in meter

T he load combinations of the building would be, the load of structure by itself (has been added into the ETABS) and thedead and live loads will be assumed for office use.

The size of the columns has been summarised by the Table 14. These sizes have been verified by the conditions that explained before and the structure is approved by ASCE regulation.

Typical live loads for the floors are 2.39 KN/m^2, the roof live loads designed are 0.96KN/m^2 and for the partitions are 0.72 KN/m^2. The rest of slabs designed are for the live load of 4.79 KN/m^2.

4.2.1. Sizes and Dimensions of Elements

The height of the first floor is 4.57m and the rest of floors have the height of 3.96m. As a result, the total height of the structure is 79.8m.

The distance between internal columns are 9.15 (length and width) and the distance of internal columns to external column in length and width is 10.7m and 9.15m respectively. Also, the column are spliced at 3rd, 5th,7th,9th,11th,13th, 15th, 17th and 19th as in detailed is explained in the following table. (Table 14)

There are two boxes in the middle, which are the lift shafts and are made from concrete reinforcement.

Table 14. Internal and External Column Sizes of the Building

FLOOR	SIZE OF THE BEAMS	SIZE OF INTERIOR COLUMNS	SIZE OF EXTERIOR COLUMNS
GROUND	W 36 x 282	W 36 x 487	W 36 x 652
1	W 36 x 282	W 36 x 487	W 36 x 652
2	W 36 x 282	W 36 x 487	W 36 x 529
3	W 36 x 282	W 36 x 487	W 36 x 529
4	W 36 x 262	W 36 x 411	W 36 x 487
5	W 36 x 262	W 36 x 411	W 36 x 487
6	W 36 x 256	W 36 x 395	W 36 x 395
7	W 36 x 256	W 36 x 395	W 36 x 395
8	W 36 x 256	W 36 x 395	W 36 x 361
9	W 36 x 256	W 36 x 395	W 36 x 361
10	W 36 x 232	W 36 x 330	W 36 x 302
11	W 36 x 232	W 36 x 330	W 36 x 302
12	W 36 x 194	W 36 x 302	W 36 x 262
13	W 36 x 194	W 36 x 302	W 36 x 262
14	W 36 x 182	W 36 x 247	W 36 x 231
15	W 36 x 182	W 36 x 247	W 36 x 231
16	W 36 x 148	W 36 x 231	W 36 x 231
17	W 36 x 148	W 36 x 231	W 36 x 231
18	W 36 x 103	W 36 x 231	W 36 x 231
19	W 24 x 94	W 36 x 231	W 36 x 231

In total, there are 1406 models simulated by ETABS in three dimensions. There are three types of lateral stabilities, five types of soils and 236 different time histories applied to the designed structure.

In this chapter, the results will be divided into two main groups of the frames of the structures and types of regulations applied to analyse the structure.

Slim deck is placed inside the primary beam and supported by secondary beams. The figure below explains the arrangement of the columns, beams (secondary and primary) and slabs.

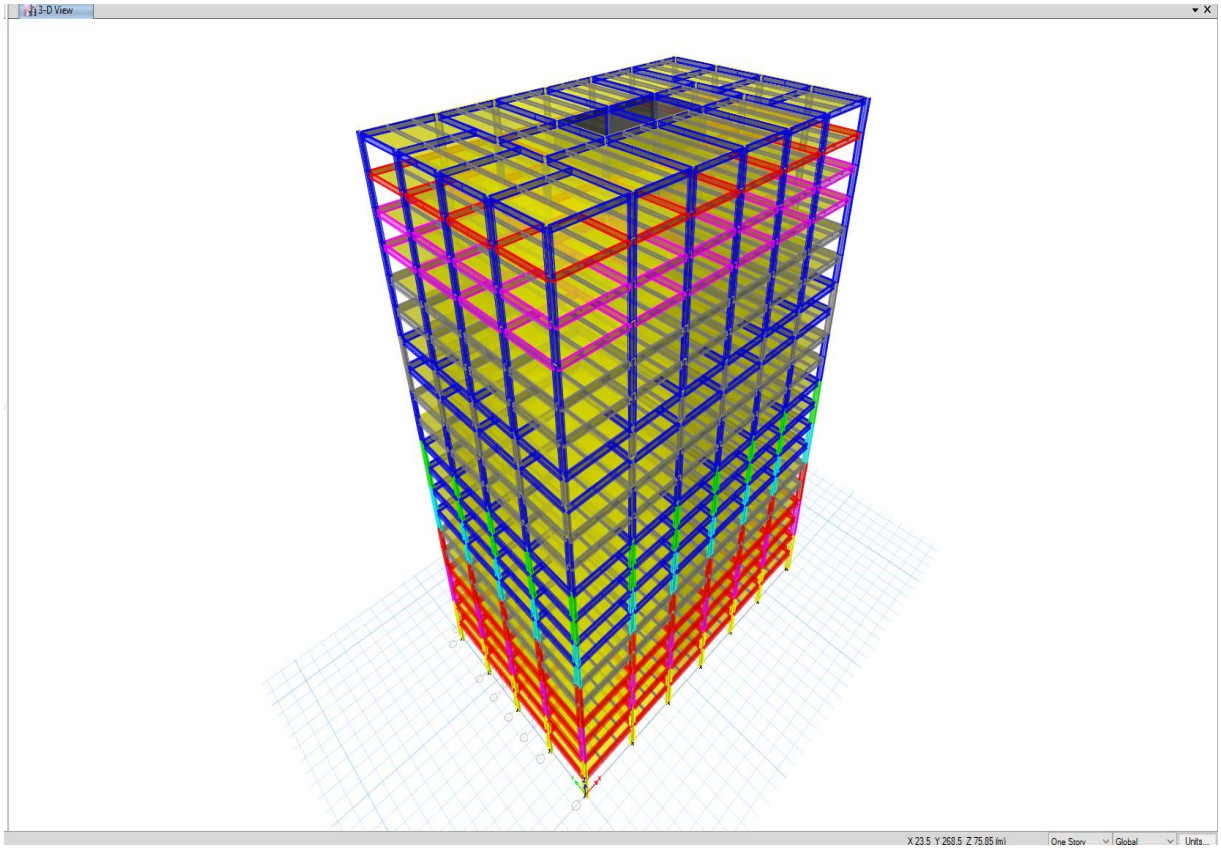

Figure 26.overview of the Section Property of the structure (each colour belongs to specific types of material)

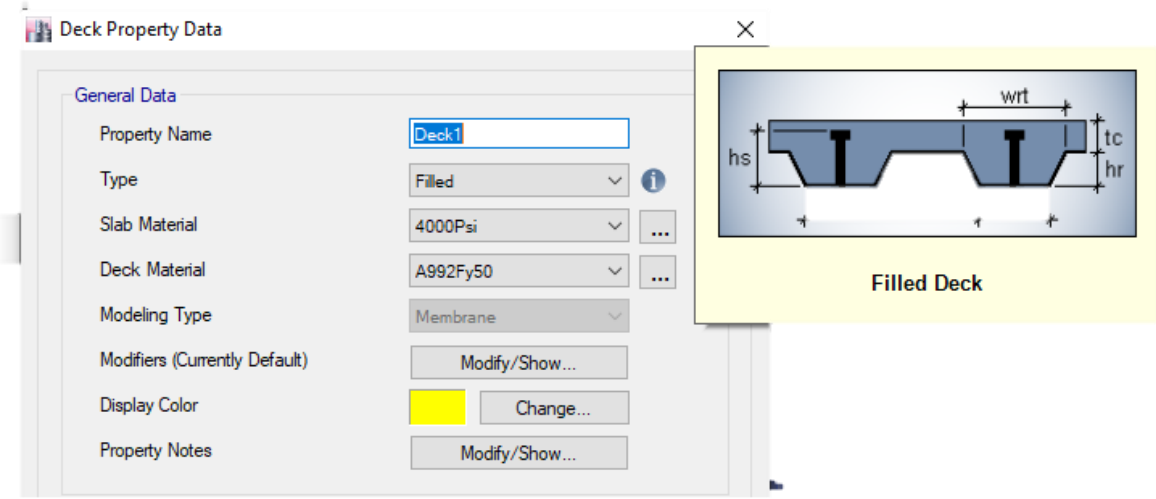

Figure 27.Example of the slim deck design in ETABs

On ETABs, the design is as follows: Define > Section Property > Deck sections > Add / modify > According to the design or calculation, it is possible to select the offered deck from program or from TATA steel. Please note that slab designed as a rigid element. Therefore, the behaviour of slab would not be very effective on total behaviour of the structure.

The slab is positioned on top of the secondary beam and joint by bolt. Slab and secondary beams are placed inside the primary beam.

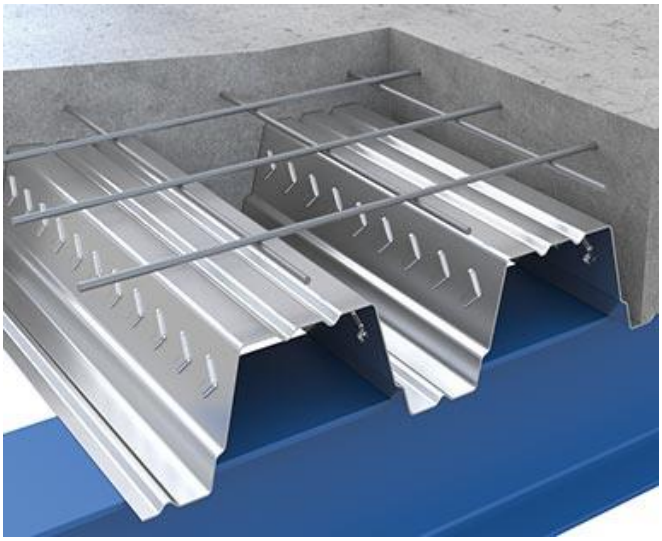

Figure 28. Example of the Slim Deck on secondary beam (credited by TATA Steel)

All the secondary beams are W14 x 30 and have been selected according to the load combination and the design criteria ComFlor 100 has been selected. Slab deck selected in this category is 160 mm.

ComFlor® 100 Composite slab - volume and weight (BS values)

Slab depth (mm)	Concrete volume (m^3/m^2)	Weight of concrete (kN/m^2)			
		Normal weight concrete		Lightweight concrete	
		Wet	Dry	Wet	Dry
150	0.090	-	-	1.69	1.60
160	0.100	2.37	2.32	1.87	1.77
170	0.110	2.60	2.55	2.06	1.95
180	0.120	2.84	2.78	2.25	2.13
190	0.130	3.07	3.01	2.43	2.30
200	0.140	3.31	3.24	2.62	2.48
210	0.150	3.54	3.47	2.80	2.66
220	0.160	3.78	3.70	2.99	2.83
230	0.170	4.01	3.93	3.18	3.01
250	0.190	4.48	4.39	3.55	3.36

Figure 29. Detail of the ComFlor 100 Deck (by TATA Steel)

4.2.2. The limitation and boundary condition of the model

Theoretically, the time history data could be applied to the foundation of the structure by the data that have been downloaded (Pacific Earthquake Engineering Research Centre). The data consist of the (Vs,30) , time interval of the seismic activities total duration and all other data required to find the exact toughness of soil on which the seismic activity occurs and the forces which go throughout the structure.

Each time history has its own data; therefore, the time interval would be different. Generally, time interval of each data was 0.005, 0.01 or 0.02.

All the damping ratio of the time history was 5% therefore exact same factor has been applied to the model to minimise any error.

The boundary condition of the soil and interaction of structure and soil is another fact, which is beyond the scope of the research. However, each factor that could lead the research to achieve a better results with more accuracy, which is not ignored in this research. In ETABs, by doing time-history analysis there is an option to apply all the details of the seismic activity and soil condition, it could simulate the interaction of the soil condition of the structure and soil and apply the force to the foundation of the structure.

Since, all three dimensions of the seismic activities have been downloaded, therefore, it was decided to apply the time-history of each axis separately to minimise the error.

Another limitation that should be taken into account is the model or structure by itself. The bottom of structure is designed as a pinned connection. The connection between the columns and the beams are pinned as well. The plastic hinge has been placed close to connection to give the slab bending condition, if required, while experiencing seismic activity.

Another factor that should be considered in the simulation is number of modes. In ETABs, the model can simulate each model up to 12 modes and as matter of fact all simulations have been pre-calculated by twelve modes, however on higher intensity most models are simulated up to three modes. More details related to the vibration mode has been provided in 4.1.1.

In the simulation, Beam-Column element and Beam element defined. And Deck and Concrete hollow section defined as shell.

4.3. Types of frames

There are three frames of structure that have been summarised below:

1. MR: Moment Resisting Frame, the original design of the structure to validate the result and figure out the deference of ASCE (American Society of Civil Engineering) and Eurocode on fragility curve
2. XB: X-Bracing Frame, additional reinforcement has been added to the current design to find the relationship between bracing system and fragility curve
3. VB: V-Bracing Frame, additional bracing system has been added to the current design to find the relationship between bracing system and fragility curve

4.3.1. Moment Resisting Frame

Table 15, summarises the simulation's results into two main regulations of Eurocode and ASCE. As the numbers show, the failure under Eurocode simulations is slightly higher after 0.7G. In the other words, the structure reacts more hazardous compared to the ASCE regulation. However, the behaviour of the building cannot be decided by the number of failures, as there are more influential factors (such as displacement, storey drift and moments).

Table 15. Data of Moment Resisting frame of Failure according to ASCE and Eurocode

PGA	NUMBER OF ANALYIS	PERCENTAGE OF TOTAL ANAYLISIS	NUMBER OF FAILURES IN ASCE REGULATION	NUMBER OF FAILURES IN EUROCODE
X>1.5	2	0.85%	2	2
1.5>X>1.3	5	2.13%	4	5
1.3>X>1.1	5	2.13%	5	5
1.1>X>1.0	2	0.85%	2	2
1.0>X>0.9	3	1.28%	3	3
0.9>X>0.8	8	3.40%	7	7
0.8>X>0.7	21	8.94%	19	20
0.7>X>0.6	25	10.64%	20	20
0.6>X>0.5	31	13.19%	22	27
0.5>X>0.25	14	5.96%	6	8
0.25>X>0.1	13	5.53%	2	4
0.1>X>0.05	14	5.96%	1	4
0.05>X>0.025	11	4.68%	0	1
0.025>X>0.0	81	34.47%	1	1

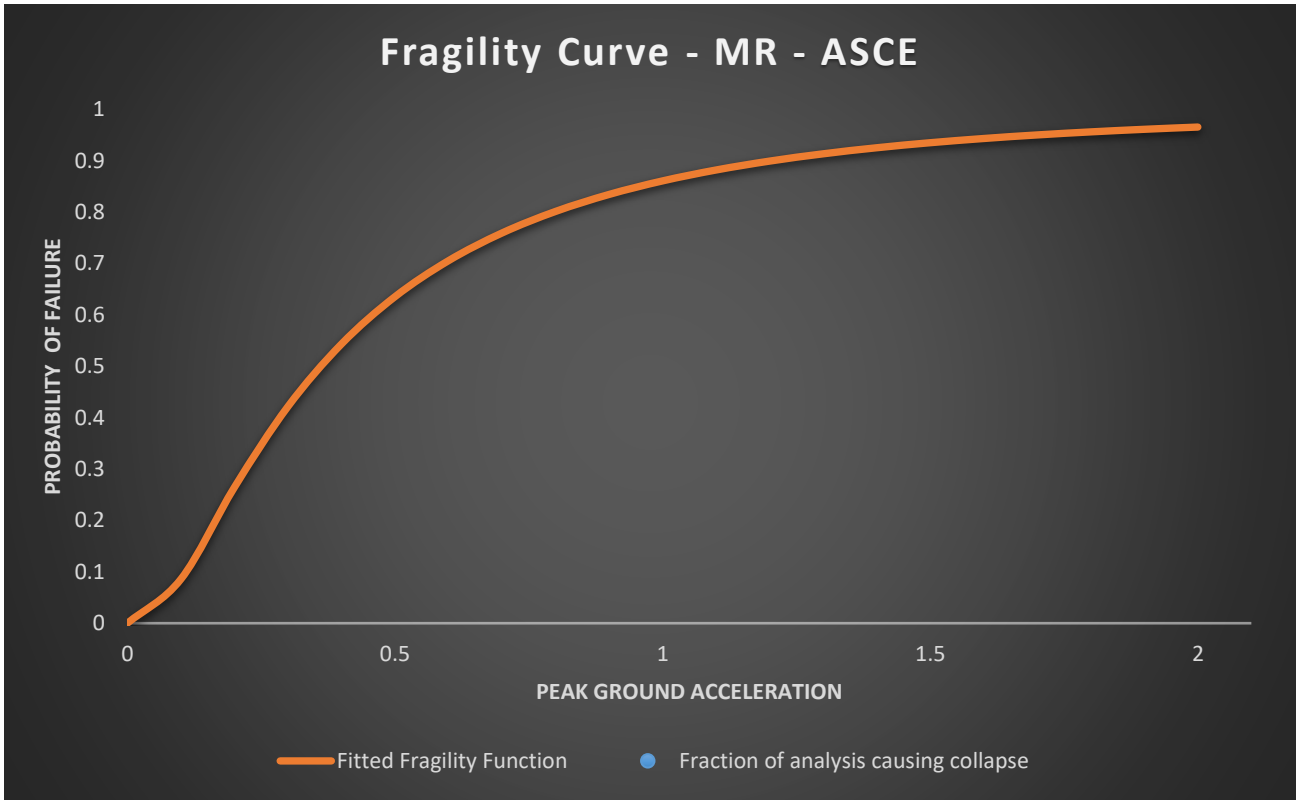

Figure 30. Fragility curve of Moment Resisting frame - ASCE Regulation

Figure 39 illustrates the fragility curve of Moment Resisting frame of the 20-storey structure under 236 seismic activities from soil condition A to E.

It summarises the probability of the failures of the structure. According to the ASCE and the choice of design limitation, any structure that exceeds the storey drift of 1.5 % it will fail. Theoretically, this fact would help to overcome the judgment of how prototype building would fail.

The simulation results show that the increase in probability in failure has a low slope up to the 0.5G ground acceleration and then the slope gradually increases.

The blue dots are representative of the fraction of analysis causing the collapse and the orange line is explaining the fitted fragility curves.

Fraction of analysis causing the collapse means the calculated and simulated results from which everything was simulated from 0-2.0g (PGA) and classified in the range of small acceleration to find the line. Therefore, the fraction can be calculated by the ratio of failures occurred on each range and the total number of the simulations on that range.

That explanation can be summarised by the formula below:

$$P(C|IM = x_j) = \frac{number\ of\ collapseswhen\ IM{=}x_j}{number\ of\ ground\ motions}$$

Which can be expressed by:

$$P(C|IM = x) = \phi\ \frac{\ln\left({}^{x}/_{\theta}\right)}{\beta}$$

Where θ and β define the fragility function. But, in order to find out the right numbers for the constants, it requires some more known factors such as theoretical fragility function and the likelihood of that.

Theoretical fragility curve can be calculated by generating normal distribution of the simulation. The probability of each range of PGA has been founded. The median and variance of this formula should be founded in order to find the fragility curve. Median is θ and β is the variance.

In order to find out the right values for these factors, the likelihood of each IM should be measured. This procedure can be done by finding the binomial distribution of (total number analysis in each range (IM), Probability of collapses (P_j) and the cumulative would the theoretical fragility curve). Then by changing the median and the variance, the product of likelihood should be maximised. To shortcut this function, it is possible to find the logarithm of each IM of likelihood and set the sum of the$\sum \log(IM) = max$.

Since the logarithm of each likelihood would be negative, the maximum for this equation would be the number near to zero.

These curves and data have been generated by the following table. (Table 16)

Table below summarises the data generated to solve the curve for MR frame by ASCE regulation.

Table 16. Details of the Moment resisting frame - Generating Fitted Fragility Curve and Fraction of Analysis Causing Collapse - ASCE

IM	NUMBER OF ANALYSES	NUMBER OF COLLAPSES	FRACTION CAUSING COLLAPSE	THEORETICAL FRAGILITY FUNCTION	LIKELIHOOD	LOG LIKELIHOOD
0.025	81	1	0.0123	0.0123	0.3702	-0.9938
0.05	11	1	0.0909	0.0589	0.3530	-1.0413
0.1	14	4	0.2857	0.1888	0.1570	-1.8517
0.25	13	4	0.3077	0.5078	0.0806	-2.5180
0.5	14	8	0.5714	0.7585	0.0652	-2.7299
0.6	31	27	0.8710	0.8109	0.1401	-1.9653
0.7	25	20	0.8000	0.8491	0.1577	-1.8471
0.8	21	20	0.9524	0.8778	0.1894	-1.6640
0.9	8	7	0.8750	0.8997	0.3829	-0.9601
1	3	3	1.0000	0.9168	0.7706	-0.2606
1.1	2	2	1.0000	0.9302	0.8653	-0.1446
1.3	5	5	1.0000	0.9497	0.7726	-0.2580
1.5	5	5	1.0000	0.9627	0.8269	-0.1901
2	2	2	1.0000	0.9806	0.9615	-0.0392

The median and the variance for this part of simulation are 0.36 and 0.94 respectively. The total logarithm of likelihood of MR is -17.61.

According to the Eurocode conditions, all the assumptions (such as dead and live loads) applied on the building would be the same. However, the design regulation will be followed by Eurocode. Although, one of the main differences between Eurocode and ASCE is the limit state of the structure. By ASCE code if theoretically a structure exceeds the storey drift of 1.50%, it can be said that the structure will be failed. But, in Eurocode this percentage is reduced to 1.00%. (It is nearly 30% less).

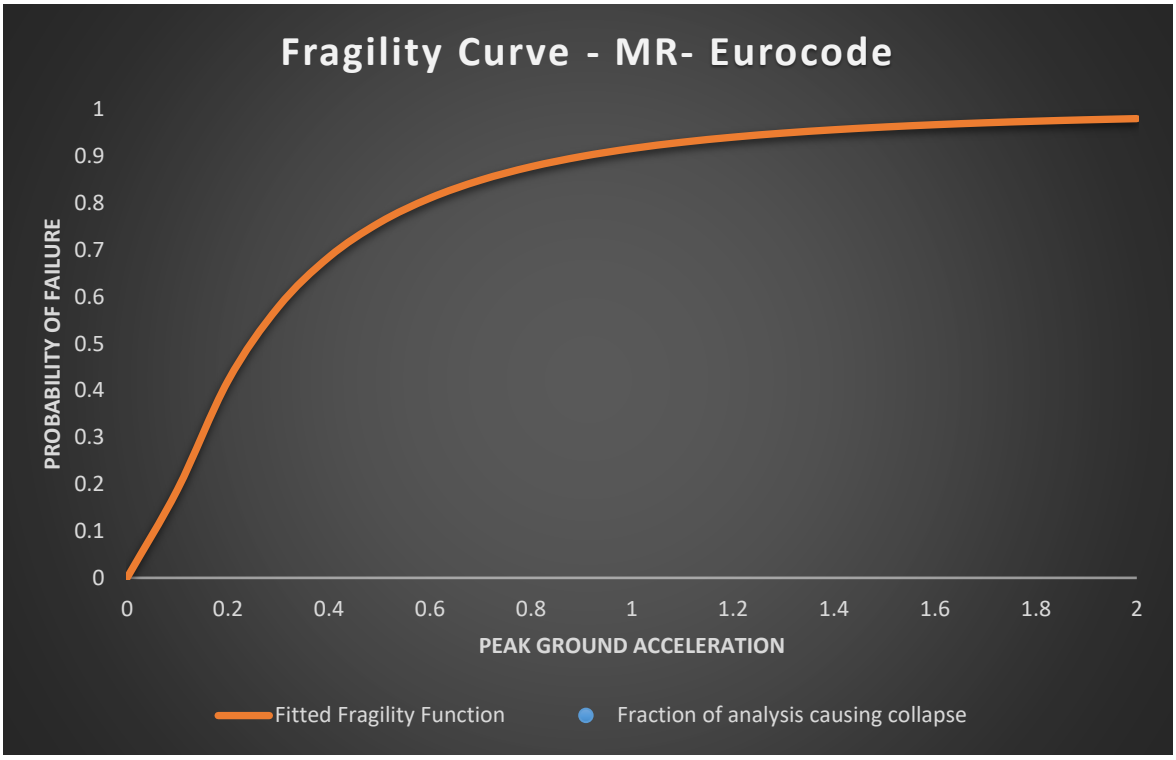

Figure 31. Fragility curve of Moment Resisting frame - Eurocode Regulation

Figure 31, shows the similar results proportionally for the same condition of the analysis. In this analysis as previously explained, the theoretical failure of structure will happen when the maximum storey drift of the structure exceeds over 1.00% , as the conditions of the Eurocode suggest.

In such circumstances, at the higher peak ground acceleration where the slope increases gradually, there are more fluctuation compared to the results have been generated under ASCE regulations. There are several factors that might lead the following results happening, which will be discussed in next chapter.

Table 17, presents the results of the Moment Resisting frame under seismic activities by Eurocode conditions.

Table 17. Data of Moment Resisting frame of Failure according to Eurocode

PGA	NUMBER OF SIMULATIONS	PERCENTAGE OF EACH SIMULATION TO TOTAL	FAILURE OF EACH GROUP IN TOTAL	E	D	C	B	A
X>1.5	2	0.85%	2	---	1	1	---	---
1.5>X>1.3	5	2.13%	5	---	---	4	---	1

1.3>X>1.1	5	2.13%	5	---	1	3	---	1
1.1>X>1.0	2	0.85%	2	---	1	1	---	---
1.0>X>0.9	3	1.28%	3	---	---	2	1	---
0.9>X>0.8	8	3.40%	7	---	2	5	1	---
0.8>X>0.7	21	8.94%	20	---	6	14	1	---
0.7>X>0.6	25	10.64%	20	2	9	14	---	---
0.6>X>0.5	31	13.19%	27	1	7	23	---	---
0.5>X>0.25	14	5.96%	8	---	5	9	---	---
0.25>X>0.1	13	5.53%	4	---	10	3	---	---
0.1>X>0.05	14	5.96%	4	---	10	3	1	---
0.05>X>0.025	11	4.68%	1	---	10	1	---	---
0.025>X>0.0	81	34.47%	1	---	36	45	---	---

Table 18 represents the step-by-step of numerical method of generating fragility curve in Eurocode.

Table 18. Details of the Moment resisting frame - Generating Fitted Fragility Curve and Fraction of Analysis Causing Collapse –Eurocode regulation

IM	NUMBER OF ANALYSES	NUMBER OF COLLAPSES	FRACTION CAUSING COLLAPSE	THEORETICAL FRAGILITY FUNCTION	LIKELIHOOD	LOG LIKELIHOOD
0.025	81	1	0.0123	0.0123	0.3702	-0.9938
0.05	11	1	0.0909	0.0589	0.3530	-1.0413
0.1	14	4	0.2857	0.1888	0.1570	-1.8517
0.25	13	4	0.3077	0.5078	0.0806	-2.5180
0.5	14	8	0.5714	0.7585	0.0652	-2.7299
0.6	31	27	0.8710	0.8109	0.1401	-1.9653
0.7	25	20	0.8000	0.8491	0.1577	-1.8471
0.8	21	20	0.9524	0.8778	0.1894	-1.6640
0.9	8	7	0.8750	0.8997	0.3829	-0.9601
1	3	3	1.0000	0.9168	0.7706	-0.2606
1.1	2	2	1.0000	0.9302	0.8653	-0.1446
1.3	5	5	1.0000	0.9497	0.7726	-0.2580
1.5	5	5	1.0000	0.9627	0.8269	-0.1901
2	2	2	1.0000	0.9806	0.9615	-0.0392

The median and the variance for this part of the simulation are 0.245 and 1.016 respectively. The total logarithm of likelihood of MR is -16.464.

The comparison of the two methods of simulating and calculating the structure reveals that there are few similarities and differences as it might be expected.

The similarities that could be mentioned are:

- The data generated are close
- Characteristics of the failures are the same

The differences are listed below:

- The scattered data generated in ASCE is more than Eurocode
- The mean and the variance of the generated data are different
- the first step of the curve (between 0 - 0.15G)

4.3.2. X-Bracing Frame

Having simulated the structure under seismic activities; all the nodes, elements and connections were analysed. As a result, most of the failures of the structure mainly occurred at the edges where the deflection, moments and the shear forces had been maximised.

As a matter of the fact, the bracing in V and X shape was added into the model to propagate the energy through more elements and impose less force on the edges in order to investigate the behaviour and the result of this action.

The following fragility curves are for the same X and V-bracing of the structure to analyse the effect of the bracing system on high-rise structure against the fragility curve.

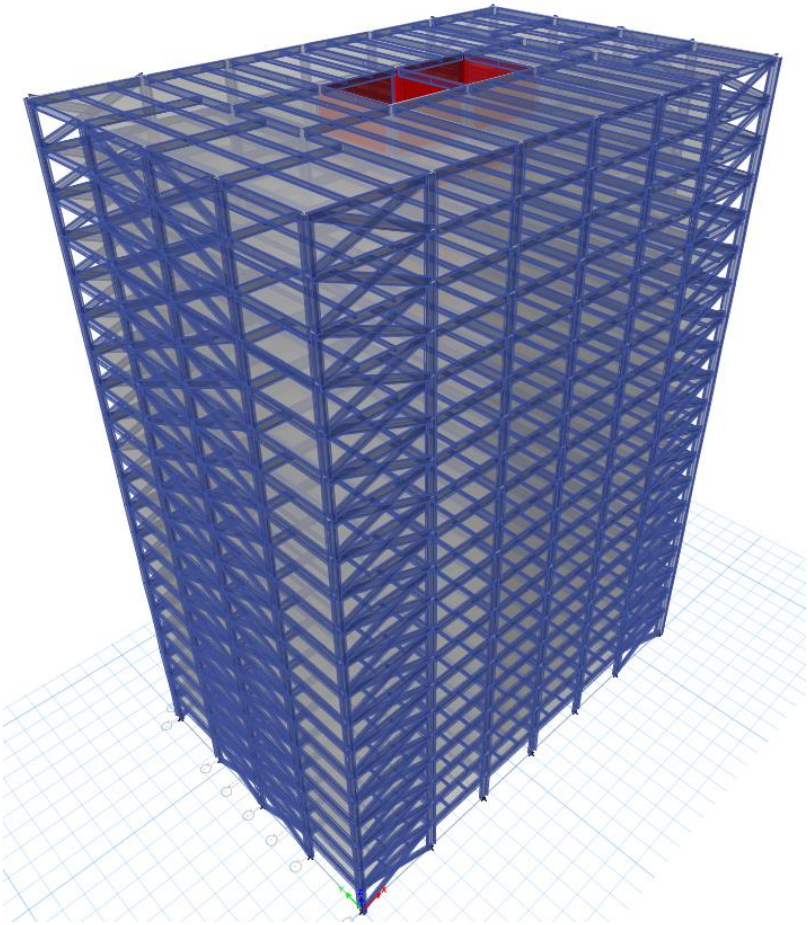

Figure 32. Overall View of the Structure in ETABS

Prior to selecting the best layout of the X-bracing for the structure, several layouts had been tested, simulated and then it was decided to place the bracing in this format as the final decision. 5 random time histories were (Two high PGA – More than 1.0g, two medium – between 1.0 and 0.25g, one low – less than 0.25g) and the best results of the layout was selected.

There are several factors which led to the selection of this type of layout. These factors are:

- Having the minimum deflection at worst case scenarios
- Better overall performance
- The lowest maximum drift storey
- Better energy dissipation

All the conditions for X-Bracing would be similar to the moment resisting frame. These factors are:

- Dead and live loads

- Layout of the structure (such as beam, column, connection, and lift shafts)
- Sizes of elements

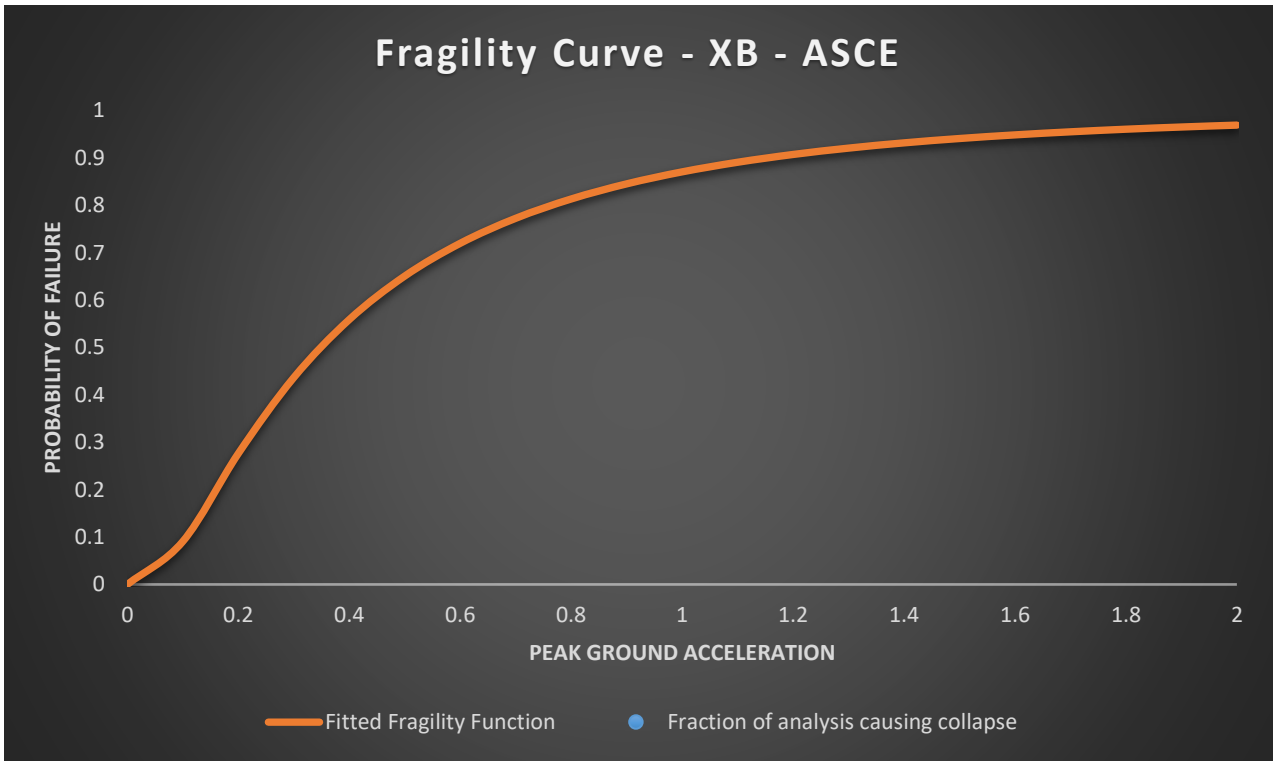

Figure 33. Fragility curve of X-Bracing frame - ASCE Regulation

As the graph above (for the same condition of structure X-bracing added) shows the slope of the curve is more inclined compared to MR (moment resisting) frame. On the other hand, as the peak ground acceleration increases, the results represent that the gradient of the curve slow down compared to the MR frame.

The following table explains the details of analysis and the numbers required to approach the fragility curve for X-Bracing in ASCE circumstances.

Table 19. Data of X-Bracing frame of Failure according to ASCE

PGA	NUMBER OF SIMULATIONS	PERCENTAGE OF EACH SIMULATION TO TOTAL	FAILURE OF EACH GROUP IN TOTAL	E	D	C	B	A
X>1.5	2	0.85%	2	---	1	1	---	---
1.5>X>1.3	5	2.13%	4	---	---	4	---	1
1.3>X>1.1	5	2.13%	5	---	1	3	---	1
1.1>X>1.0	2	0.85%	2	---	1	1	---	---
1.0>X>0.9	3	1.28%	3	---	---	2	1	---
0.9>X>0.8	8	3.40%	7	---	2	5	1	---

0.8>X>0.7	21	8.94%	19	---	6	14	1	---
0.7>X>0.6	25	10.64%	19	2	9	14	---	---
0.6>X>0.5	31	13.19%	23	1	7	23	---	---
0.5>X>0.25	14	5.96%	7	---	5	9	---	---
0.25>X>0.1	13	5.53%	2	---	10	3	---	---
0.1>X>0.05	14	5.96%	2	---	10	3	1	---
0.05>X>0.025	11	4.68%	1	---	10	1	---	---
0.025>X>0.0	81	34.47%	0	---	36	45	---	---

Table 20.Details of the X-Bracing frame - Generating Fitted Fragility Curve and Fraction of Analysis Causing Collapse - ASCE

IM	NUMBER OF ANALYSES	NUMBER OF COLLAPSES	FRACTION CAUSING COLLAPSE	THEORETICAL FRAGILITY FUNCTION	LIKELIHOOD	LOG LIKELIHOOD
0.025	81	0	0.0000	0.0024	0.8236	-0.1940
0.05	11	1	0.0909	0.0188	0.1712	-1.7649
0.1	14	2	0.1429	0.0907	0.2392	-1.4303
0.25	13	2	0.1538	0.3613	0.0734	-2.6113
0.5	14	7	0.5000	0.6508	0.1074	-2.2308
0.6	31	23	0.7419	0.7200	0.1559	-1.8584
0.7	25	19	0.7600	0.7727	0.1820	-1.7039
0.8	21	19	0.9048	0.8135	0.1447	-1.9332
0.9	8	7	0.8750	0.8454	0.3817	-0.9630
1	3	3	1.0000	0.8707	0.6602	-0.4152
1.1	2	2	1.0000	0.8910	0.7939	-0.2308
1.3	5	5	1.0000	0.9209	0.6622	-0.4122
1.5	5	4	0.8000	0.9411	0.2310	-1.4655
2.0	2	2	1.0000	0.9694	0.9398	-0.0621

The median and the variance for this part of simulation are 0.348 and 0.934 respectively. The total logarithm of likelihood of XR is -17.276.

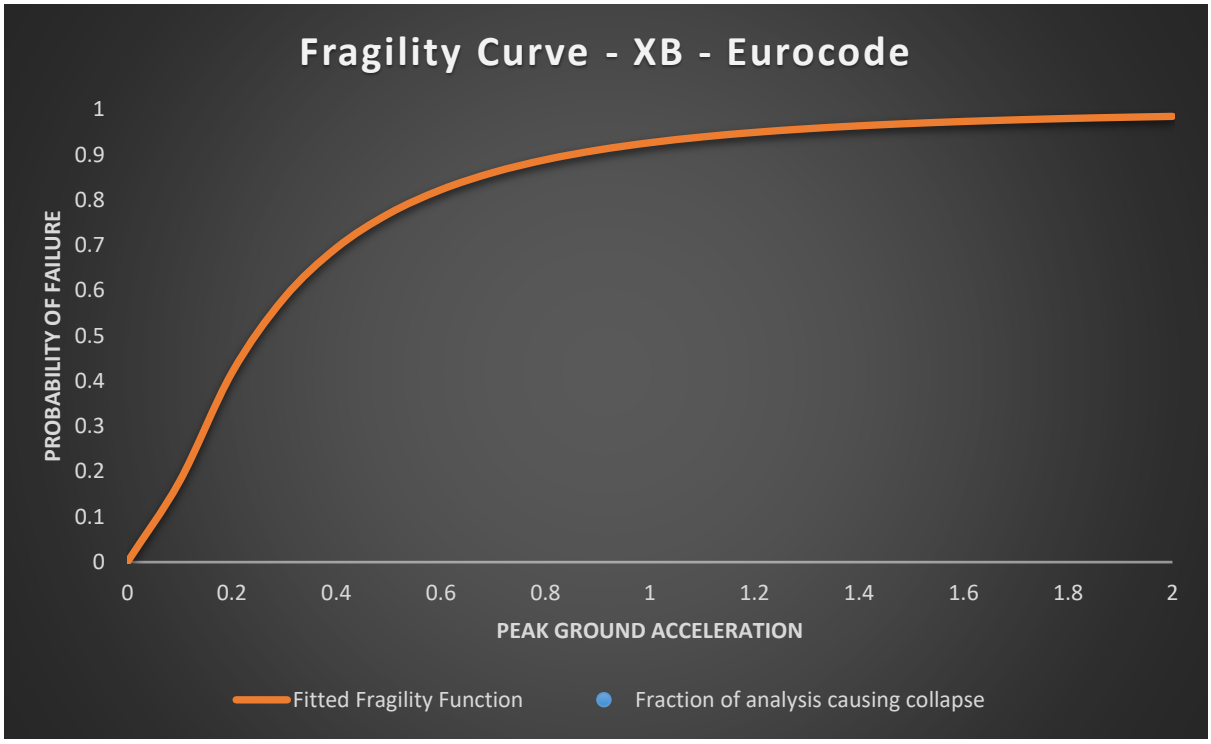

Figure 34.Fragility curve of X-Bracing frame - Eurocode Regulation

According to the graph for X-bracing with Eurocode limit, it explains that there is a sharp increase in probability of failure from the beginning and then as the peak ground acceleration increases (between 0.2 and 0.8 G – PGA), the slope increases its inclining mode and after 1.0G it decreases significantly.

The following tables are demonstrating the details of fragility curve of X-bracing for the Eurocode limitation.

Table 21. Data of X-Bracing frame of Failure according to Eurocode

PGA	NUMBER OF SIMULATIONS	PERCENTAGE OF EACH SIMULATION TO TOTAL	FAILURE OF EACH GROUP IN TOTAL	E	D	C	B	A
X>1.5	2	0.85%	2	---	1	1	---	---
1.5>X>1.3	5	2.13%	5	---	---	4	---	1
1.3>X>1.1	5	2.13%	5	---	1	3	---	1
1.1>X>1.0	2	0.85%	2	---	1	1	---	---
1.0>X>0.9	3	1.28%	3	---	---	2	1	---
0.9>X>0.8	8	3.40%	7	---	2	5	1	---
0.8>X>0.7	21	8.94%	20	---	6	14	1	---
0.7>X>0.6	25	10.64%	21	2	9	14	---	---

0.6>X>0.5	31	13.19%	27	1	7	23	---	---
0.5>X>0.25	14	5.96%	8	---	5	9	---	---
0.25>X>0.1	13	5.53%	4	---	10	3	---	---
0.1>X>0.05	14	5.96%	4	---	10	3	1	---
0.05>X>0.025	11	4.68%	2	---	10	1	---	---
0.025>X>0.0	81	34.47%	0	---	36	45	---	---

Table 22.Details of the X-Bracing frame - Generating Fitted Fragility Curve and Fraction of Analysis Causing Collapse - Eurocode

IM	NUMBER OF ANALYSES	NUMBER OF COLLAPSES	FRACTION CAUSING COLLAPSE	THEORETICAL FRAGILITY FUNCTION	LIKELIHOOD	LOG LIKELIHOOD
0.025	81	0	0.0000	0.0094	0.4654	-0.7650
0.05	11	2	0.1818	0.0510	0.0893	-2.4155
0.1	14	4	0.2857	0.1786	0.1423	-1.9495
0.25	13	4	0.3077	0.5093	0.0793	-2.5343
0.5	14	8	0.5714	0.7697	0.0552	-2.8963
0.6	31	27	0.8710	0.8227	0.1600	-1.8327
0.7	25	21	0.8400	0.8609	0.2039	-1.5902
0.8	21	20	0.9524	0.8892	0.2221	-1.5047
0.9	8	7	0.8750	0.9104	0.3715	-0.9902
1	3	3	1.0000	0.9268	0.7960	-0.2282
1.1	2	2	1.0000	0.9395	0.8826	-0.1249
1.3	5	5	1.0000	0.9575	0.8048	-0.2171
1.5	5	5	1.0000	0.9693	0.8554	-0.1562
2	2	2	1.0000	0.9849	0.9699	-0.0305

The median and the variance for this part of simulation are 0.244 and 0.970 respectively. The total logarithm of likelihood of XB is -17.205.

The similarities and the differences of the both regulations (Eurocode and ASCE) were same for the MR frame as it could be expected. On the other hand, as the data and the figures illustrated, the resistance against fragility increased slightly. The number failures in the early stages dropped trivially. Subsequently, the gradient of the slope decreased.

4.3.3. V-Bracing Frame

Another type of reinforcing the steel-frame structure is V-bracing. This type of bracing could be in different shapes. However, it has been decided to simulate V-bracing in one frame only (due to the amount of time for calculation, simulation and the hardware provided).

Same procedure for selecting layout has been taken into account. Different layouts have been examined and the one with the better performance has been selected. A proper performance means the lowest deflection in random simulations, lowest drift stories and the better energy dissipation through the structure.

All the condition for V-Bracing would be similar to the moment resisting frame. These factors are:

- Sizes of the elements
- Dead and live loads
- Layout of the structure (such as beam, column, connection and lift shafts)

The V-bracing that has been selected for this analysis is the eccentric V-bracing. Same as the other framing systems, several frames have been analysed few times and the best performance frame had been selected for applying all the available time history analysis to generate the fragility curve.

In this situation (when the structure is subjected to the seismic activities), the eccentric lateral reinforcement will have better performance compared to concentric bracing. The main reason would be the better overall performance in global energy dissipation, that would occur during seismic activities.

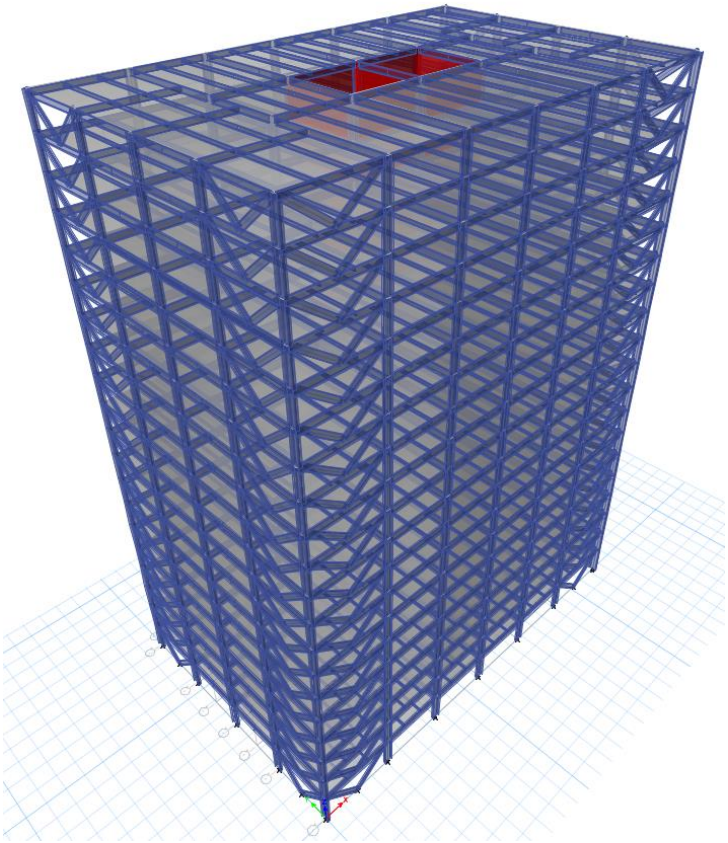

Figure 35. Overall View of V-Bracing in ETABS

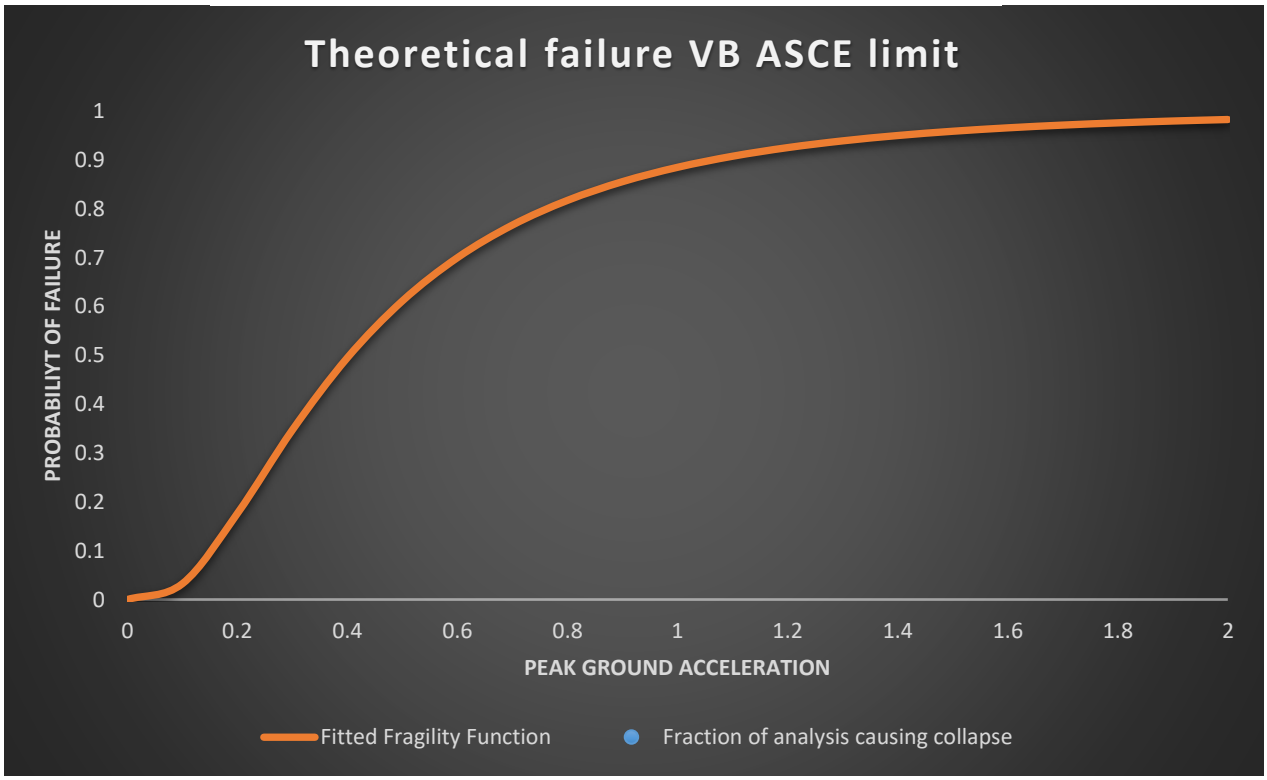

Figure 36. Fragility curve of V-Bracing frame - ASCE Regulation

The above figure (Figure 36), demonstrates the fragility curve of V-Bracing under ASCE regulation. As the graph shows the gradient of the line is considerably low up to 0.1G and then it increases rapidly till 1.2G and slows down again. The incline of curve at first stage is lower than VB and MR and in the second stage the incline is slightly slower than the other two frames.

The following tables are provided for better understanding the numbers and the detail of the simulations.

Table 23. Data of V-Bracing frame of Failure according to ASCE

PGA	NUMBER OF SIMULATIONS	PERCENTAGE OF EACH SIMULATION TO TOTAL	FAILURE OF EACH GROUP IN TOTAL	E	D	C	B	A
X>1.5	2	0.85%	2	---	1	1	---	---
1.5>X>1.3	5	2.13%	4	---	---	4	---	1
1.3>X>1.1	5	2.13%	5	---	1	3	---	1
1.1>X>1.0	2	0.85%	2	---	1	1	---	---
1.0>X>0.9	3	1.28%	3	---	---	2	1	---
0.9>X>0.8	8	3.40%	7	---	2	5	1	---
0.8>X>0.7	21	8.94%	19	---	6	14	1	---
0.7>X>0.6	25	10.64%	19	2	9	14	---	---
0.6>X>0.5	31	13.19%	22	1	7	23	---	---
0.5>X>0.25	14	5.96%	6	---	5	9	---	---
0.25>X>0.1	13	5.53%	3	---	10	3	---	---
0.1>X>0.05	14	5.96%	1	---	10	3	1	---
0.05>X>0.025	11	4.68%	0	---	10	1	---	---
0.025>X>0.0	81	34.47%	0	---	36	45	---	---

Table 24.Details of the V-Bracing frame - Generating Fitted Fragility Curve and Fraction of Analysis Causing Collapse - ASCE

IM	NUMBER OF ANALYSES	NUMBER OF COLLAPSES	FRACTION CAUSING COLLAPSE	THEORETICAL FRAGILITY FUNCTION	LIKELIHOOD	LOG LIKELIHOOD
0.025	81	0	0.0000	0.0001	0.9906	-0.0094
0.05	11	0	0.0000	0.0029	0.9690	-0.0314
0.1	14	1	0.0714	0.0324	0.2956	-1.2187
0.25	13	3	0.2308	0.2631	0.2460	-1.4026

0.5	14	6	0.4286	0.6116	0.0814	-2.5080
0.6	31	22	0.7097	0.7001	0.1552	-1.8632
0.7	25	19	0.7600	0.7669	0.1834	-1.6958
0.8	21	19	0.9048	0.8174	0.1518	-1.8849
0.9	8	7	0.8750	0.8557	0.3878	-0.9472
1	3	3	1.0000	0.8851	0.6933	-0.3662
1.1	2	2	1.0000	0.9077	0.8240	-0.1936
1.3	5	5	1.0000	0.9392	0.7307	-0.3137
1.5	5	4	0.8000	0.9588	0.1740	-1.7490
2	2	2	1.0000	0.9829	0.9661	-0.0345

The median and the variance for this part of simulation are 0.403 and 0.756 respectively. The total logarithm of likelihood of XB -14.218.

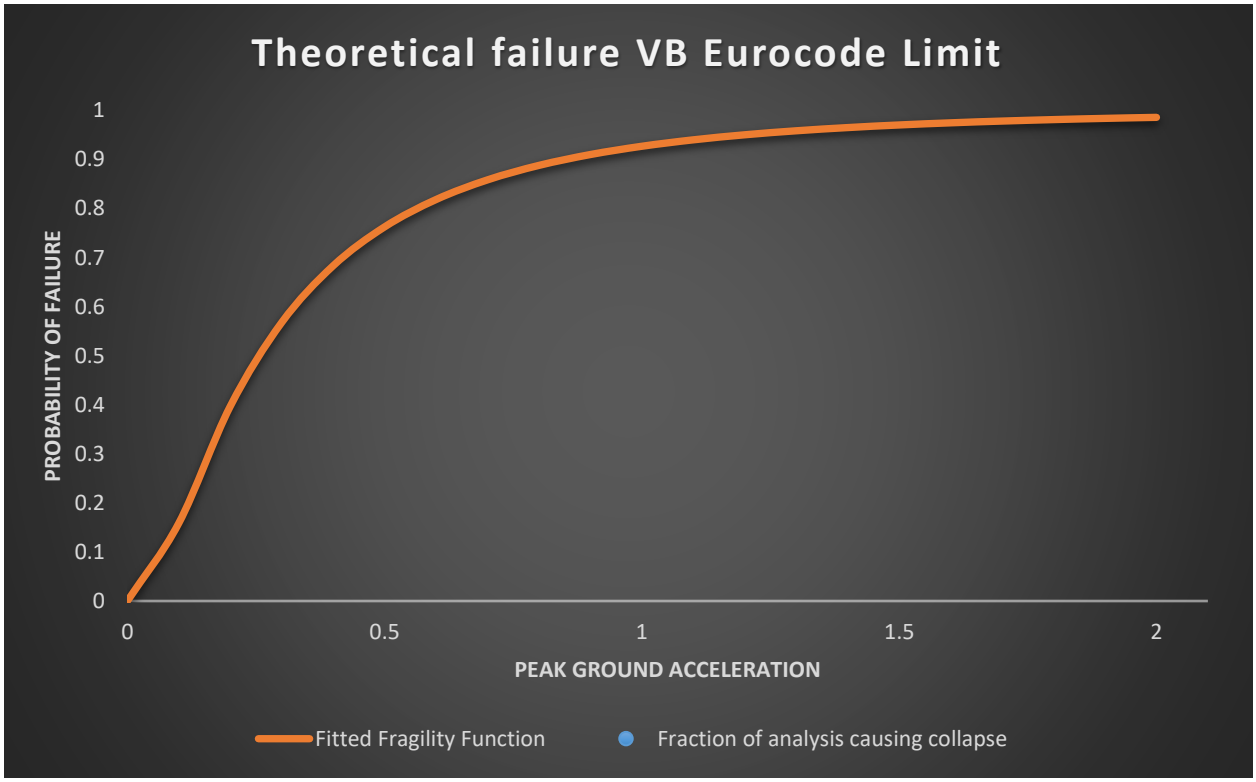

Figure 37.Fragility curve of V-Bracing frame - Eurocode Regulation

The above graph (Figure 37) represents the fragility curve of the V-bracing against all 236 seismic activities that have been applied to the structure. This graph is based on the limitations and regulations of the Eurocode.

If the curve is divided into three stages, it could be as follows:

Stage 1: nearly sharp linear early-stage incline

Stage 2: non-linear incline

Stage 3: Reach a plateau

Comparing the behaviour of V-bracing to MR and XB (X-Bracing), it can be said that the V-bracing has lower angel of inclination at the first two stages and has a longer stage three.

The comparison and the possible reason of this phenomenon will be discussed in the next chapter.

The following tables state the brief details of the number of failures in each stage of peak ground acceleration and brief explanation of generating the curve.

Table 25.Data of V-Bracing frame of Failure according to Eurocode

PGA	NUMBER OF SIMULATIONS	PERCENTAGE OF EACH SIMULATION TO TOTAL	FAILURE OF EACH GROUP IN TOTAL	E	D	C	B	A
X>1.5	2	0.85%	2	---	1	1	---	---
1.5>X>1.3	5	2.13%	5	---	---	4	---	1
1.3>X>1.1	5	2.13%	5	---	1	3	---	1
1.1>X>1.0	2	0.85%	2	---	1	1	---	---
1.0>X>0.9	3	1.28%	3	---	---	2	1	---
0.9>X>0.8	8	3.40%	7	---	2	5	1	---
0.8>X>0.7	21	8.94%	20	---	6	14	1	---
0.7>X>0.6	25	10.64%	20	2	9	14	---	---
0.6>X>0.5	31	13.19%	27	1	7	23	---	---
0.5>X>0.25	14	5.96%	8	---	5	9	---	---
0.25>X>0.1	13	5.53%	5	---	10	3	---	---
0.1>X>0.05	14	5.96%	4	---	10	3	1	---
0.05>X>0.025	11	4.68%	1	---	10	1	---	---
0.025>X>0.0	81	34.47%	0	---	36	45	---	---

Table 26.Details of the V-Bracing frame - Generating Fitted Fragility Curve and Fraction of Analysis Causing Collapse - Eurocode

IM	NUMBER OF ANALYSES	NUMBER OF COLLAPSES	FRACTION CAUSING COLLAPSE	THEORETICAL FRAGILITY FUNCTION	LIKELIHOOD	LOG LIKELIHOOD
0.025	81	0	0.0000	0.0066	0.5836	-0.5386
0.05	11	1	0.0909	0.0411	0.2970	-1.2139
0.1	14	4	0.2857	0.1587	0.1127	-2.1827
0.25	13	5	0.3846	0.4905	0.1659	-1.7963
0.5	14	8	0.5714	0.7626	0.0615	-2.7888
0.6	31	27	0.8710	0.8183	0.1527	-1.8791
0.7	25	20	0.8000	0.8584	0.1427	-1.9469
0.8	21	20	0.9524	0.8879	0.2183	-1.5219
0.9	8	7	0.8750	0.9100	0.3720	-0.9887
1	3	3	1.0000	0.9269	0.7964	-0.2277
1.1	2	2	1.0000	0.9400	0.8836	-0.1238
1.3	5	5	1.0000	0.9584	0.8087	-0.2123
1.5	5	5	1.0000	0.9703	0.8600	-0.1508
2	2	2	1.0000	0.9858	0.9718	-0.0286

The median and the variance for this part of simulation are 0.256 and 0.939 respectively. The total logarithm of likelihood of XB -15.600.

4.4. Discussion

As the details of the results show (Appendix A2, A3 and A4) most of the failure occurred in 3rd floor of the structure where the columns are changing their size. In my viewpoint, it could be happening more in a soft storey. In other words, the collapses are due to the lack of strength in the lower level of the height that leads the structure to fail completely or to cause a severe damage. There are few possibilities in this case:

1. Structure's connections are not strong enough
2. The importance of usage of structure (that makes engineers to design the structure to be sustainable and strong)
3. The lifetime of the building

According to the data that have been established regarding the maximum deflection, there are 60 (MR), 68 (XB) and 68 (VB) in Y-Direction. This type of behaviour means that the seismic activity did not affect the structure, which in turn leads to the maximum deflection occurred in Y-direction at the top floor. Average amount of maximum deflection on top floor under seismic activity is 0.002 m, which is approximately 2 mm.

By looking at the following tables and the figures, it can be said that the bracing system will help the energy dissipation throughout the structure become more fluent. In the same way, the number of failures in first stage and second stage of fragility curve will be reduced slightly.

Also, the layout of the bracing form and the position of the bracing system is important.

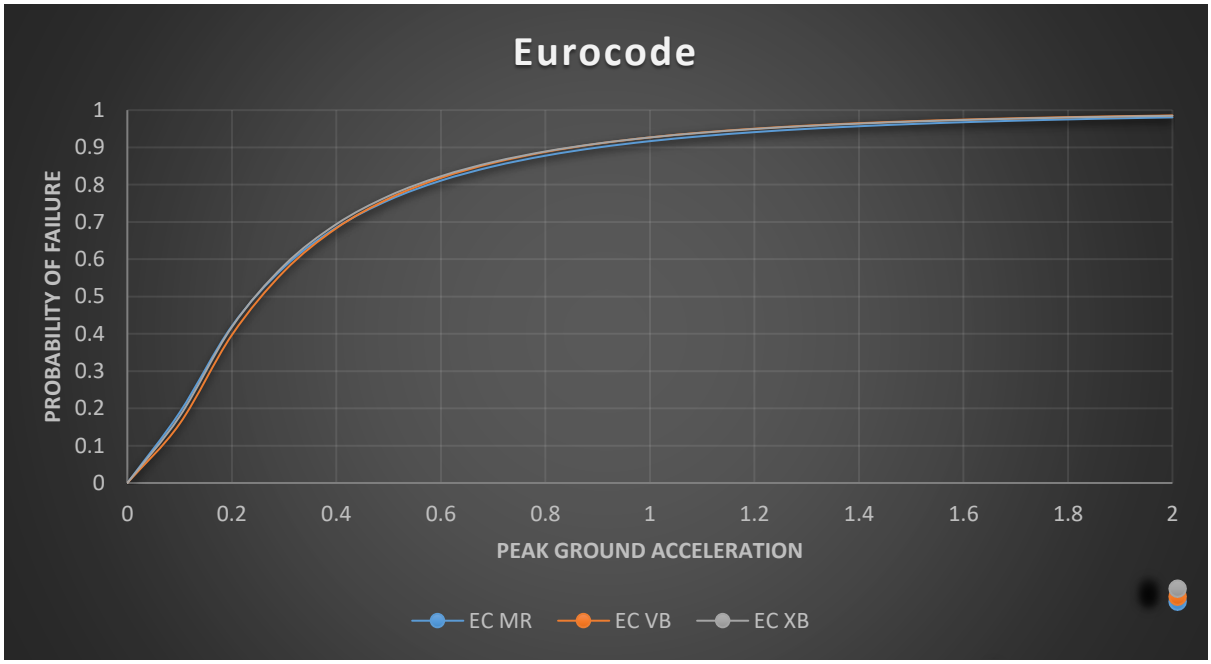

Figure 38.Comparison of fragility curves of all frames on Eurocode

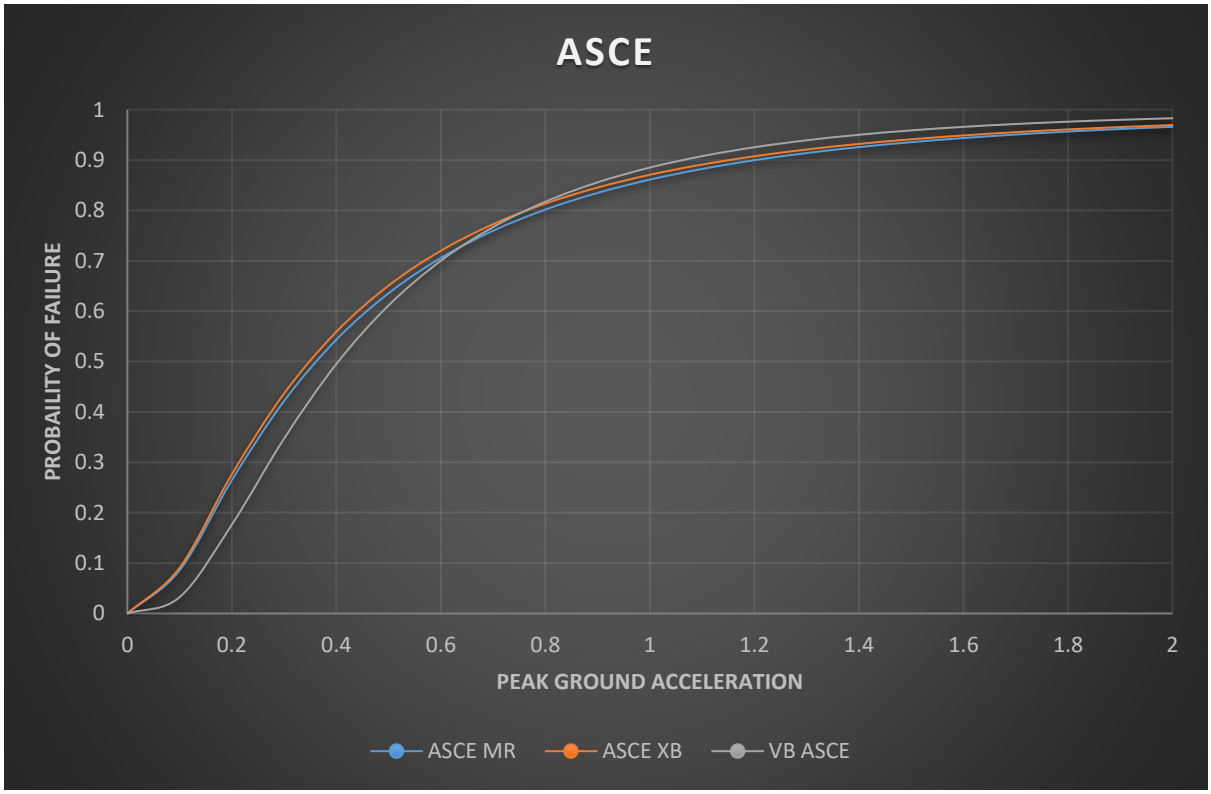

Figure 39.Comparison of fragility curves of all frames on ASCE

To summarise, based on the data collected from the simulations it is evident that the difference between regulations does not have a significant change in the results achieved..

There are slight differences that could be explained by what reaction to each regulation is, but the general behaviour would be the same.

The established data illustrates that the data from ASCE are more scattered compared to the Eurocode results. In other words, the outlier of the data in ASCE regulations are more.

On the other hand, the probability of failure in Eurocode occurring earlier and the slope (change of angle in curve) in the first step is slightly sharper. In terms of the concept, the calculation, judgement, and the approach to design are the same. But the reason that in Eurocode's results are slightly different is, the safety factors in this regulation are proportionally stricter than those in ASCE which leads the curve have a slightly sharper slope.

By adding X and V-bracing into the model, this research aimed to find out the effect of adding bracing system and to figure out how energy dissipates throughout the building. In the same way, the reduction of failure occurs. The reason that only there are few bracing applied to structure is due to the factors below:

1. Not adding considerable number of loads which will cause the change in size of columns
2. Only bracing applied to external columns due the maximum reduction by adding the minimum reinforcements
3. Having an interest in keeping the characteristic of the building with the minimum change

According to the data, VB has a better performance in the first stage by generating the least number of failures up to 0.1 G in ASCE and 0.05G in Eurocode regulation. In the next stage that is usually starts around 0.6G all three frames perform nearly the same. However, VB is performing slightly better by having 3.7% fewer number of failures in range of 0.5G to 0.6G. MR, XB and VB reaching to 95% of the failure at the range of 0.7G to 0.8G. Then, by increasing the magnitude of the ground acceleration, the failure of structure in all the three frames reaches to 100%.

There are several factors that lead the structure to fail. These factors have been discussed earlier in the literature review. One of them is resonance which occur as a result of a seismic activity, when the cycle of movement of structure becomes equal to the natural frequency of

the structure. As a result, during the oscillation, the structure experiences twice as much usual force as it should experience at the maximum displacement. Likewise, a soft storey could be another factor causing failure. This phenomenon occurs when the first or few bottom floors failed. However, the failure happens when the distance between columns is high, large doors, big windows, etc. In this situation, the height of the first floor is 4.57m that might provide the probability of this theory that most of the failure is likely to happen on the third floor.

Figure 40, represents of the summery of the results. In this figure, the median of each category has been extracted and compared to the other types. ASCE regulation has a range of 0.35 to 0.4G mean. This number means that on average of 236 simulations in each section in ASCE, building tends to fail at 0.36G (MR), 0.4G (VB) and 0.35G (XB). However, these numbers reduce to 0.24G to 0.26G in Eurocode. There is approximately 30% reduction in resistance or strength against acceptable limitations stated in Eurocode to compared to those in ASCE.

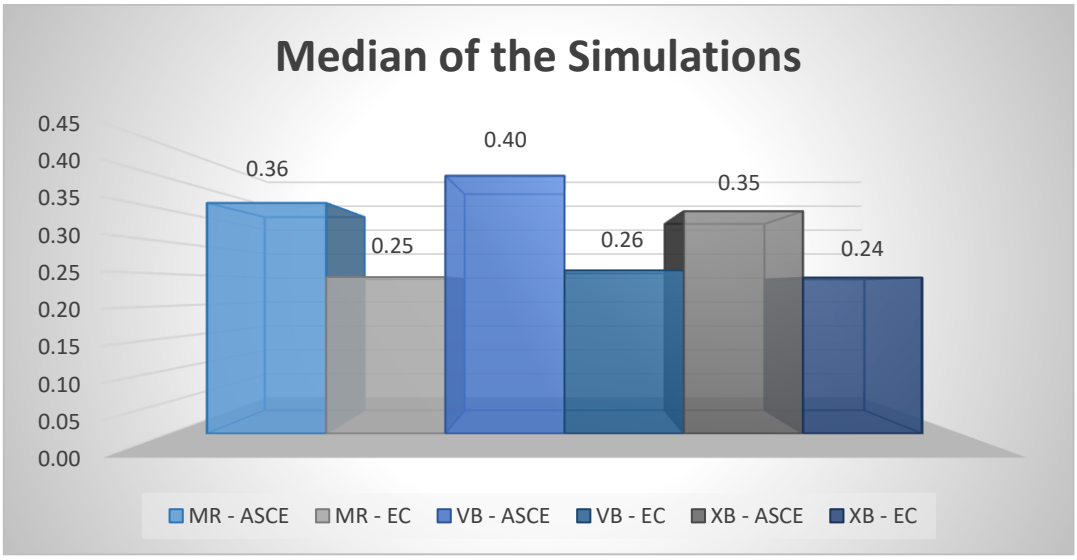

Figure 40. Median of the Simulations

Figure 41, demonstrates the variance of the data. As the number approaches to zero, the accuracy of the data gets closer to fragility curve. The accuracy of the both regulations are very close, however, ASCE is slightly better. The V-Bracing has the largest gap between the variance of both design codes.

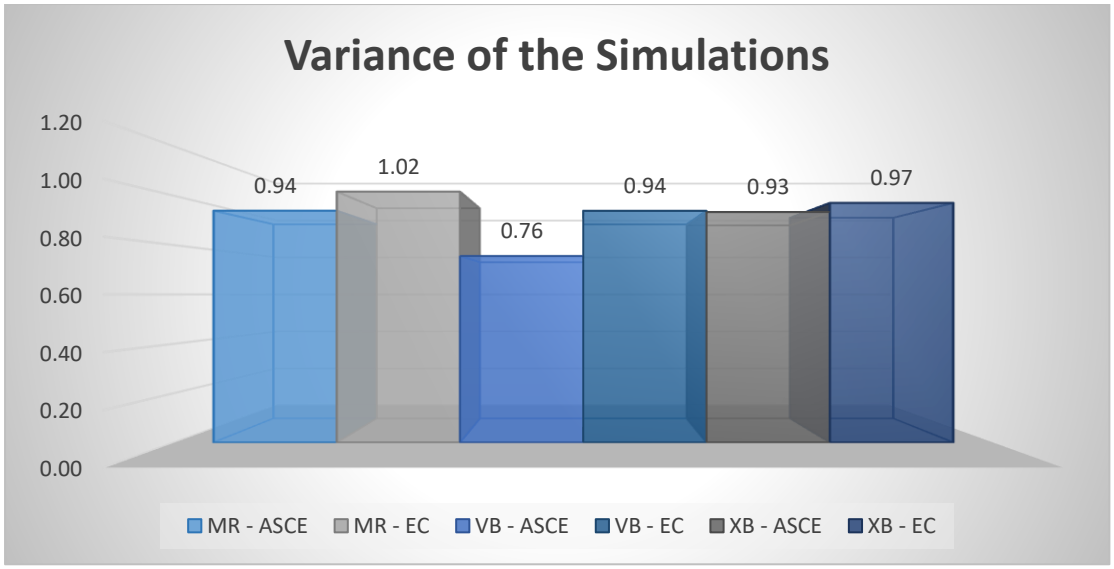

Figure 41. Variance of the Simulations

4.4.1. Vibrational modes

The simulation was run into 12 modes and the results were nearly same. The first mode was translational mode in X-direction, and the second mode was translational in Y direction and the third was representing the torsional mode.

The second series of translational mode in X and Y direction, and torsional modes were summarised in the modes 4, 5 and 6.

As a result, it can be said that the modes 1, 4, 7 and were the 1st, 2nd, 3rd and 4th vibration mode of the structure in X-direction. By the same approach, modes 2, 5, 8 and 11th summarising the modes in Y-direction and torsional mode are represented in modes 3, 6, 9 and 12.

The fundamental period of the structure was 2.958 second for MR. Due to loss of data at the end of the simulation, it was not possible to recover the data with regard to mode shape and each frame.

Chapter 5: The Effect of the Soil Conditions on Developing Fragility Curves

5.1. Detailed statistical analysis of the database

Considering the behaviour of the structure in the moment resisting frame and the bracing system, different factors were put to analysis in this chapter. Another main important element regarding this research is the type of the soil (Vs30). The factor that is not taken into account in the majority of researches and studies.

In order to generate the high resolution of fragility curve, it was required that a large number of time histories be simulated and analysed. As a matter of fact, the number of time-histories available in high PGA is very low and limited. Therefore, as it can be detected from other works, they mainly use nearly same condition of soil to overcome the lack of data.

In this research, all the data has been taken from the data server PEER (Pacific Earthquake Engineering Research Centre). All the data that have collected from PEER, has the factors called "V_s30 (m/s) selected for analysis)" and "Preferred NEHRP Based on V_s30". Based on these factors, the type of soil from each time history has been calculated and classified for further studies.

As used mentioned in the previous chapter, there are several other types of soil that participated for generating the fragility curve.

In this chapter, the fragility curve of each soil type was demonstrated and compared by the data generated in previous chapter.

There are several reasons for this comparison:

- To look closely in detail at each framing system (the characteristic of fragility curve)
- To understand how the type of soil would be effective on the fragility curve
- How structure (MR, XB and VB) behaves

As the simulations have been done on both ASCE (American Society of Civil Engineering) code and Eurocode. The detailed comparison will be according to both codes.

In this chapter, soil type C and D will be analysed, and the fragility curve of each frame will be generated and compared. Alongside with the comparison of differences in soil type the bracing system effort will be taken into account.

Soil type C and D are 54.47% (128 out of 236) and 42.13% (99 out of 236) of the total simulations and the results respectively. Therefore, majority of the results were divided into these two types of soils.

The details of the earthquakes and the required outcome of the three composite frames are available in appendix. (A2, A3 and A4)

5.2. Moment Resisting Frame

At first the Moment Resisting Frame (MR Frame) will be demonstrated. Then, V-Bracing (VB) and X-Bracing will be represented and compared.

Table 27 illustrates in detail; the results have been generated for all the moment resistant frames that were subjected to the seismic activities in type C soil.

This type of soil is over half of the total simulations in every category (i.e., MR, XB and VB), therefore analysing the behaviour in detail would lead the research to find out the relationship between soils and probability of the failure.

Table 27. MR-Type C

PGA	NUMBER OF SIMULATIONS	PERCENTAGE OF SIMULATIONS TO TOTAL	NUMBER OF FAILURES IN ASCE	NUMBER OF FAILURES IN EUROCODE
X>1.5	1	0.78%	1	1
1.5>X>1.3	4	3.13%	3	4
1.3>X>1.1	3	2.34%	3	3
1.1>X>1.0	1	0.78%	1	1
1.0>X>0.9	2	1.56%	2	2
0.9>X>0.8	5	3.91%	4	4
0.8>X>0.7	14	10.94%	13	14
0.7>X>0.6	14	10.94%	7	9
0.6>X>0.5	23	17.97%	17	21
0.5>X>0.25	9	7.03%	3	5
0.25>X>0.1	3	2.34%	0	1

0.1>X>0.05	3	2.34%	0	1
0.05>X>0.025	1	0.78%	0	0
0.025>X>0.0	45	35.16%	0	0

As the table 28 shows the vast majority of the seismic activities (Peak Ground Acceleration) are between 0.00 to 0.025 G. Then, the highest number of seismic activities simulated are in the range of 0.5 to 0.6 (23), 0.6 to 0.7 (14) and 0.7 to 0.8 (14) respectively.

Table 28. MR-Type C-ASCE

IM	NUMBER OF ANALYSES	NUMBER OF COLLAPSES	FRACTION CAUSING COLLAPSE	THEORETICAL FRAGILITY FUNCTION	LIKELIHOOD	LOG LIKELIHOOD
0.025	45	0	0.000	0.000	1.000	0.000
0.05	1	0	0.000	0.000	1.000	0.000
0.1	3	0	0.000	0.002	0.993	-0.007
0.25	3	0	0.000	0.106	0.714	-0.337
0.5	9	3	0.333	0.480	0.184	-1.693
0.6	23	17	0.739	0.604	0.074	-2.607
0.7	14	7	0.500	0.702	0.060	-2.807
0.8	14	13	0.929	0.776	0.116	-2.150
0.9	5	4	0.800	0.832	0.402	-0.910
1	2	2	1.000	0.874	0.763	-0.270
1.1	1	1	1.000	0.905	0.905	-0.100
1.3	3	3	1.000	0.945	0.844	-0.170
1.5	4	3	0.750	0.967	0.118	-2.136
2	1	1	1.000	0.990	0.990	-0.010

The median and the variance of the normal distribution of the above data are 0.515 and 0.580 with the total $log_{Likelihood}$= 13.199

The simulations and calculations leading to fragility curve have been summarised in the figure below. The figure shows the fragility curve for Moment Resisting frame under seismic activity with the soil condition of Type C and the theoretical failure of ASCE regulation.

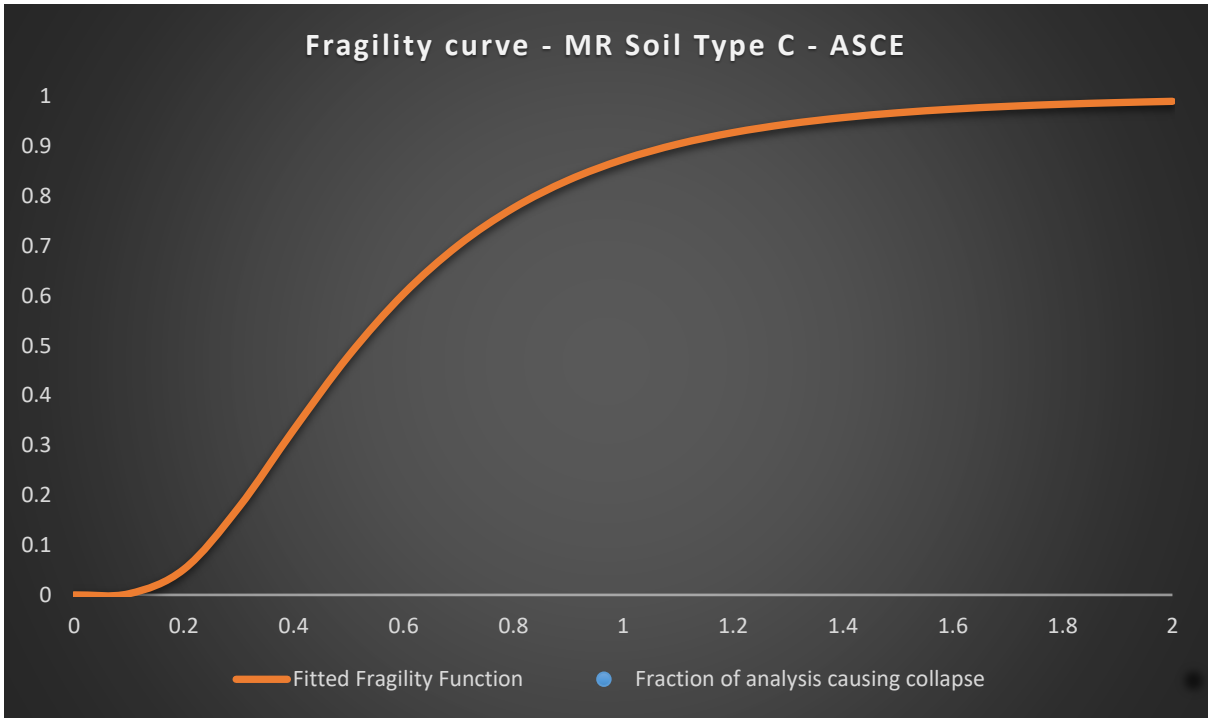

Figure 42. MR Frame - Type C soil - ASCE Regulation

As the figure 42 shows, at the very first stage, there is strong sustainability against the seismic activity up to nearly 0.15G, then the probability starts rising. Even though, the slope of increase is low.

Table 29 illustrates the summary of calculation of the same type of structure and soil condition followed by Eurocode regulation for theoretical failure.

Table 29. MR -Type C- Eurocode

IM	NUMBER OF ANALYSES	NUMBER OF COLLAPSES	FRACTION CAUSING COLLAPSE	THEORETICAL FRAGILITY FUNCTION	LIKELIHOOD	LOG LIKELIHOOD
0.025	45	0	0.0000	0.0021	0.9106	-0.0937
0.05	1	0	0.0000	0.0199	0.9801	-0.0201
0.1	3	1	0.3333	0.1066	0.2552	-1.3657
0.25	3	1	0.3333	0.4311	0.4186	-0.8709
0.5	9	5	0.5556	0.7379	0.1301	-2.0394
0.6	23	21	0.9130	0.8023	0.0969	-2.3338
0.7	14	9	0.6429	0.8485	0.0364	-3.3136
0.8	14	14	1.0000	0.8823	0.1731	-1.7538
0.9	5	4	0.8000	0.9073	0.3142	-1.1578

1	2	2	1.0000	0.9261	0.8576	-0.1536
1.1	1	1	1.0000	0.9405	0.9405	-0.0614
1.3	3	3	1.0000	0.9603	0.8855	-0.1216
1.5	4	4	1.0000	0.9727	0.8950	-0.1109
2	1	1	1.0000	0.9880	0.9880	-0.0121

The median and the variance of the normal distribution of the above data are 0.290 and 0.856 with the total $log_{Likelihood}$= 13.408.

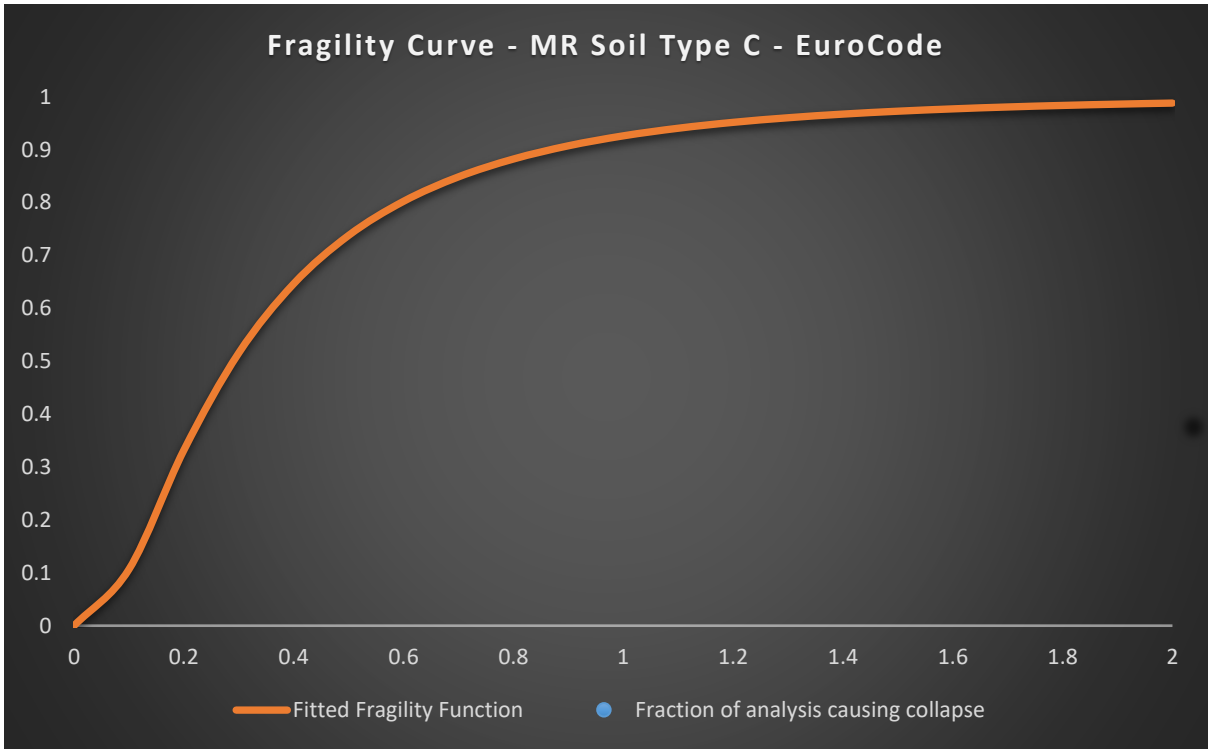

Figure 43. MR Frame - Soil Type C – Eurocode Regulation

The fragility curve for ASCE is different from that in Eurocode. The rise in first stage starts earlier and the curve at second stage is sharper compared to the curve in the ASCE. However, the last stage is more likely to reach to its limit.

Another most used soil type that have been used in the simulations and analysis is soil type D. Over 40% of the data consist of this type of soil.

Table 30 represents the distribution of the time history of the soil type D. As it shows the most data provided is for Peak Ground Acceleration (PGA) between 0.0 to 0.025G and 0.025 to 0.1G with 36 and 30 seismic activities respectively.

Table 30. MR-Type D

PGA	NUMBER OF SIMULATIONS	PERCENTAGE OF SIMULATIONS TO TOTAL	NUMBER OF FAILURES IN ASCE	NUMBER OF FAILURES IN EUROCODE
X>1.5	1	1.02%	1	1
1.5>X>1.3	0	0.00%	0	0
1.3>X>1.1	1	1.02%	1	1
1.1>X>1.0	1	1.02%	1	1
1.0>X>0.9	0	0.00%	0	0
0.9>X>0.8	2	2.04%	2	2
0.8>X>0.7	6	6.12%	6	6
0.7>X>0.6	9	9.18%	9	9
0.6>X>0.5	7	7.14%	4	5
0.5>X>0.25	5	5.10%	3	4
0.25>X>0.1	10	10.20%	2	3
0.1>X>0.05	10	10.20%	1	4
0.05>X>0.025	10	10.20%	0	1
0.025>X>0.0	36	36.73%	0	0

Table 31 demonstrates the main steps of calculation in the fragility curve from the simulation done under some specified conditions. The moment resisting frame under seismic activities with soil type D is under Eurocode and ASCE regulations.

Table 31. MR-Type D- ASCE

IM	NUMBER OF ANALYSES	NUMBER OF COLLAPSES	FRACTION CAUSING COLLAPSE	THEORETICAL FRAGILITY FUNCTION	LIKELIHOOD	LOG LIKELIHOOD
0.025	36	0	0.00E+00	3.65E-05	9.99E-01	-1.31E-03
0.05	10	0	0.00E+00	1.76E-03	9.83E-01	-1.76E-02
0.1	10	1	1.00E-01	3.06E-02	2.31E-01	-1.46E+00
0.25	10	2	2.00E-01	3.13E-01	2.19E-01	-1.52E+00
0.5	5	3	6.00E-01	7.12E-01	2.99E-01	-1.21E+00
0.6	7	4	5.71E-01	7.98E-01	1.17E-01	-2.15E+00
0.7	9	9	1.00E+00	8.57E-01	2.50E-01	-1.39E+00
0.8	6	6	1.00E+00	8.98E-01	5.24E-01	-6.46E-01

0.9	2	2	1.00E+00	9.26E-01	8.58E-01	-1.53E-01
1	0	0	---	9.46E-01	1.00E+00	0.00E+00
1.1	1	1	1.00E+00	9.60E-01	9.60E-01	-4.08E-02
1.3	1	1	1.00E+00	9.77E-01	9.77E-01	-2.28E-02
1.5	0	0	---	9.87E-01	1.00E+00	0.00E+00
2	1	1	1.00E+00	9.96E-01	9.96E-01	-3.98E-03

The median of this table is 0.345 and variance of 0.662 and the total $log_{Likelihood}$ of -8.609.

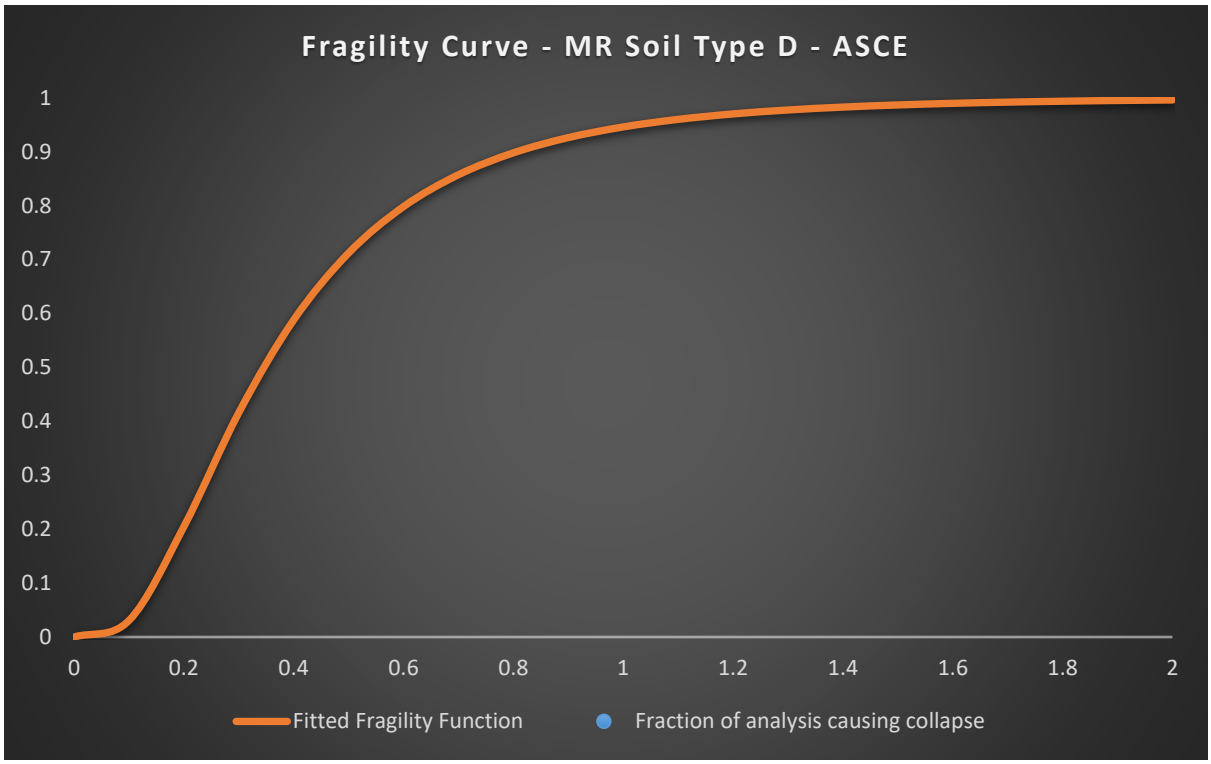

Figure 44. MR-Type D-ASCE Regulation

For the same condition of structure and regulation of design, soil type D is showing to have a higher probability of failure as the probability starts to grow from earlier stage (approximately around 0.1G) and the slope of increase in the second stage is slightly higher as well. However, it reaches its plateau earlier than type C.

Table 32 summarises the simulation and calculation of generating fragility curve for MR frame with soil type D , following Eurocode's regulations.

Table 32. MR- Type D- Eurocode

IM	NUMBER OF ANALYSES	NUMBER OF COLLAPSES	FRACTION CAUSING COLLAPSE	THEORETICAL FRAGILITY FUNCTION	LIKELIHOOD	LOG LIKELIHOOD
0.025	36	0	0.000E+00	1.129E-02	6.646E-01	-4.086E-01
0.05	10	1	1.000E-01	6.119E-02	3.466E-01	-1.059E+00
0.1	10	4	4.000E-01	2.092E-01	9.837E-02	-2.319E+00
0.25	10	3	3.000E-01	5.649E-01	6.388E-02	-2.751E+00
0.5	5	4	8.000E-01	8.157E-01	4.080E-01	-8.966E-01
0.6	7	5	7.143E-01	8.627E-01	1.892E-01	-1.665E+00
0.7	9	9	1.000E+00	8.955E-01	3.702E-01	-9.937E-01
0.8	6	6	1.000E+00	9.189E-01	6.021E-01	-5.073E-01
0.9	2	2	1.000E+00	9.361E-01	8.763E-01	-1.321E-01
1	0	0	---	9.489E-01	1.000E+00	0.000
1.1	1	1	1.000E+00	9.587E-01	9.587E-01	-4.217E-02
1.3	1	1	1.000E+00	9.721E-01	9.721E-01	-2.826E-02
1.5	0	0	---	9.805E-01	1.000E+00	0.000
2	1	1	1.000E+00	9.911E-01	9.911E-01	-8.924E-03

The median of this table is 0.214 and variance of 0.942 and the total $log_{Likelihood}$ of -10.812.

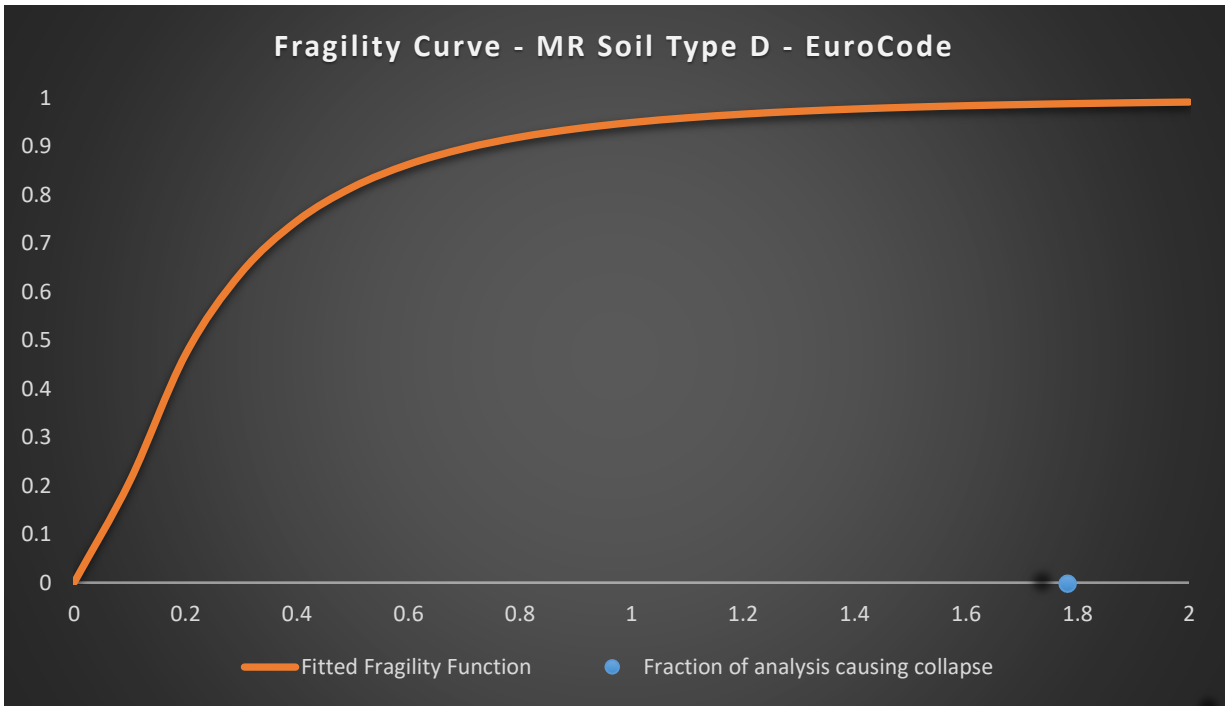

Figure 45. MR Frame - Type D soil- Eurocode Regulation

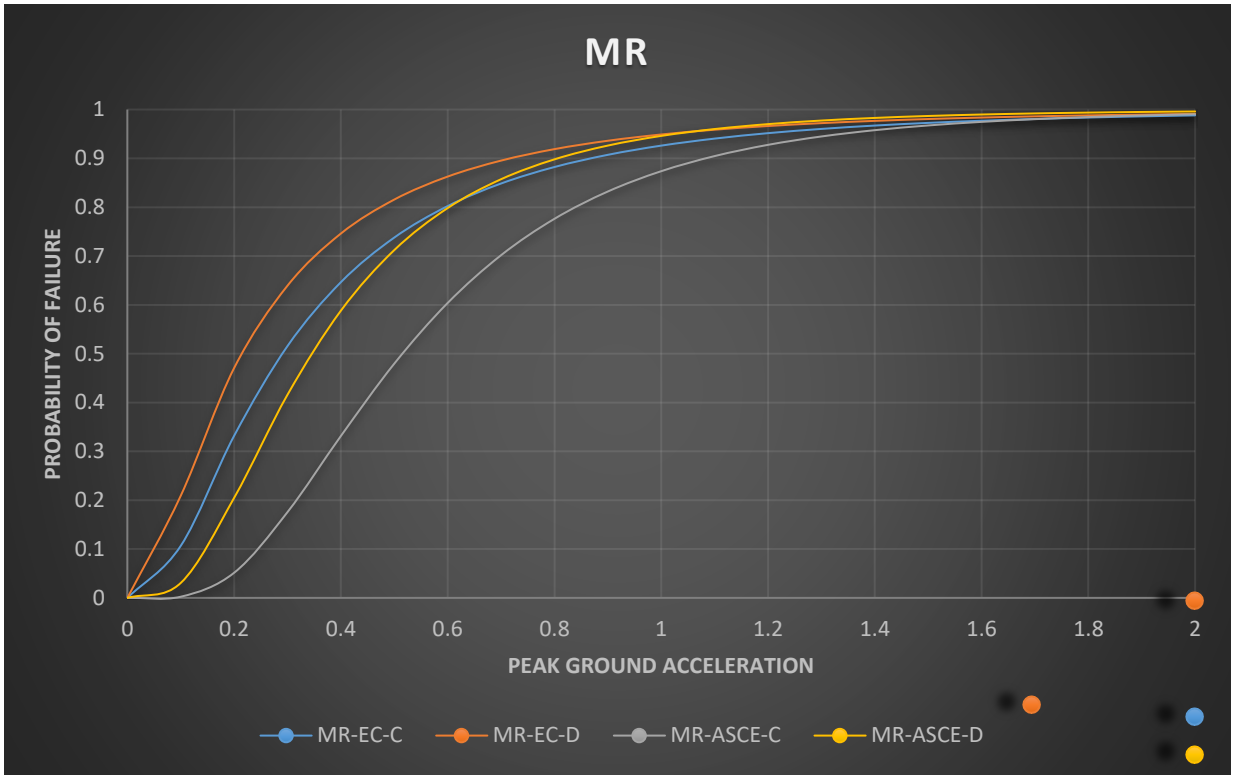

Figure 46. Fragility Curve of Moment Resisting Frame for soil type C & D in Eurocode and ASCE

As it would be expected, the first and second stage of the curve have a sharper degree of incline and the last stage is slightly longer.

5.3. X-Bracing Frame

Table 33 consists of the summarised results of simulation for the X-Bracing frame subjected to soil type C.

Table 33. XB Frame - Soil Type C - Overall Results

PGA	NUMBER OF SIMULATIONS	PERCENTAGE OF SIMULATIONS TO TOTAL	NUMBER OF FAILURES IN ASCE	NUMBER OF FAILURES IN EUROCODE
X>1.5	1	0.78%	1	1
1.5>X>1.3	4	3.13%	3	4
1.3>X>1.1	3	2.34%	3	3
1.1>X>1.0	1	0.78%	1	1
1.0>X>0.9	2	1.56%	2	2
0.9>X>0.8	5	3.91%	4	4
0.8>X>0.7	14	10.94%	12	14
0.7>X>0.6	14	10.94%	8	10

0.6>X>0.5	23	17.97%	17	21
0.5>X>0.25	9	7.03%	3	4
0.25>X>0.1	3	2.34%	0	1
0.1>X>0.05	3	2.34%	0	0
0.05>X>0.025	1	0.78%	0	0
0.025>X>0.0	45	35.16%	0	0

Table 34. XB Frame - Soil Type C - ASCE regulation

IM	NUMBER OF ANALYSES	NUMBER OF COLLAPSES	FRACTION CAUSING COLLAPSE	THEORETICAL FRAGILITY FUNCTION	LIKELIHOOD	LOG LIKELIHOOD
0.025	45	0	0.000E+00	2.744E-07	1.000E+00	-1.235E-05
0.05	1	0	0.000E+00	5.731E-05	9.999E-01	-5.731E-05
0.1	3	0	0.000E+00	3.402E-03	9.898E-01	-1.022E-02
0.25	3	0	0.000E+00	1.181E-01	6.860E-01	-3.769E-01
0.5	9	3	3.333E-01	4.866E-01	1.773E-01	-1.730E+00
0.6	23	17	7.391E-01	6.061E-01	7.576E-02	-2.580E+00
0.7	14	8	5.714E-01	7.002E-01	1.260E-01	-2.072E+00
0.8	14	12	8.571E-01	7.724E-01	2.126E-01	-1.548E+00
0.9	5	4	8.000E-01	8.270E-01	4.046E-01	-9.048E-01
1	2	2	1.000E+00	8.681E-01	7.536E-01	-2.830E-01
1.1	1	1	1.000E+00	8.990E-01	8.990E-01	-1.065E-01
1.3	3	3	1.000E+00	9.398E-01	8.300E-01	-1.863E-01
1.5	4	3	7.500E-01	9.633E-01	1.311E-01	-2.031E+00
2	1	1	1.000E+00	9.883E-01	9.883E-01	-1.172E-02

The median and the variance of the XB frame in type soil C followed by ASCE regulations are 0.510 and 0.602 respectively. Also, the total log of likelihood is -11.842.

Figure 53 is demonstrating the summary of the results and the fragility curve.

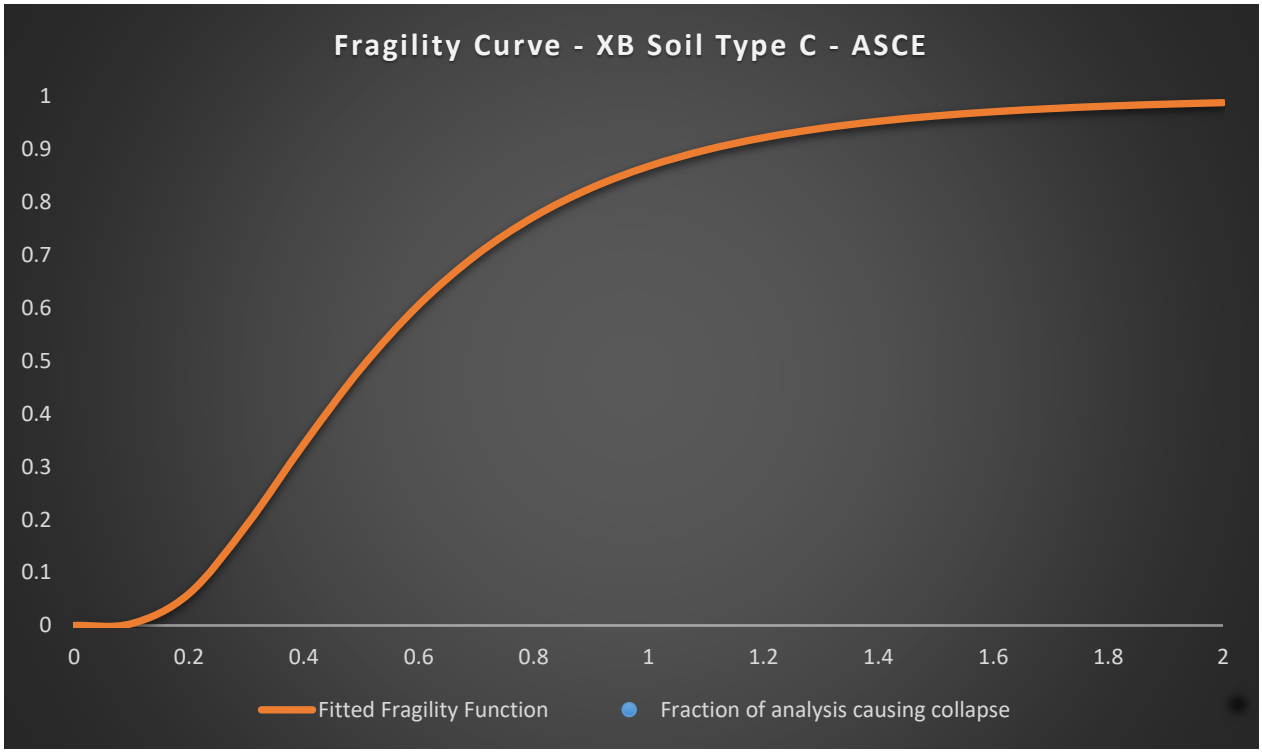

Figure 47. XB Frame - Soil Type C –ASCE Regulation

As the figure shows the overall characteristic of the curve is the same compared to the MR frame – soil type C. The first stage has a very low increase up to 0.15 G, then a slight incline. The second stage at X-Bracing is slightly more reacting stronger and also the results are closer to the fragility curve generated.

Table 35 presents the summary results of X-Bracing frame subjected to soil type C following Eurocode regulations.

Table 35. XB Frame - Type Soil C - Eurocode Regulation

IM	NUMBER OF ANALYSES	NUMBER OF COLLAPSES	FRACTION CAUSING COLLAPSE	THEORETICAL FRAGILITY FUNCTION	LIKELIHOOD	LOG LIKELIHOOD
0.025	45	0	0.000	0.000	1.000	0.000
0.05	1	0	0.000	0.000	1.000	0.000
0.1	3	0	0.000	0.006	0.982	-0.019
0.25	3	1	0.333	0.207	0.391	-0.940
0.5	9	4	0.444	0.677	0.093	-2.373
0.6	23	21	0.913	0.787	0.074	-2.598
0.7	14	10	0.714	0.860	0.086	-2.456

0.8	14	14	1.000	0.907	0.256	-1.363
0.9	5	4	0.800	0.938	0.239	-1.431
1	2	2	1.000	0.959	0.919	-0.085
1.1	1	1	1.000	0.972	0.972	-0.028
1.3	3	3	1.000	0.987	0.961	-0.040
1.5	4	4	1.000	0.993	0.974	-0.026
2	1	1	1.000	0.999	0.999	-0.001

The median and the variance of the above data are 0.389 and 0.543 respectively. Also, the total log of likelihood is -11.359

Figure 54 is the summary of the results of the X-Bracing simulation and the fragility curve generated from the data provided.

As it shows, there is a significant difference at first stage. There is a resistance up to 0.1G and slight increase. At the second stage, there is a high incline and it reaches the stage three at the point of 1.4G (reach its plateau).

There is a similarity between the results in X-bracing in soil type C that is the numbers from simulation are closer to the fragility curve. In the other words, the range values generated from simulated have less range of fluctuation.

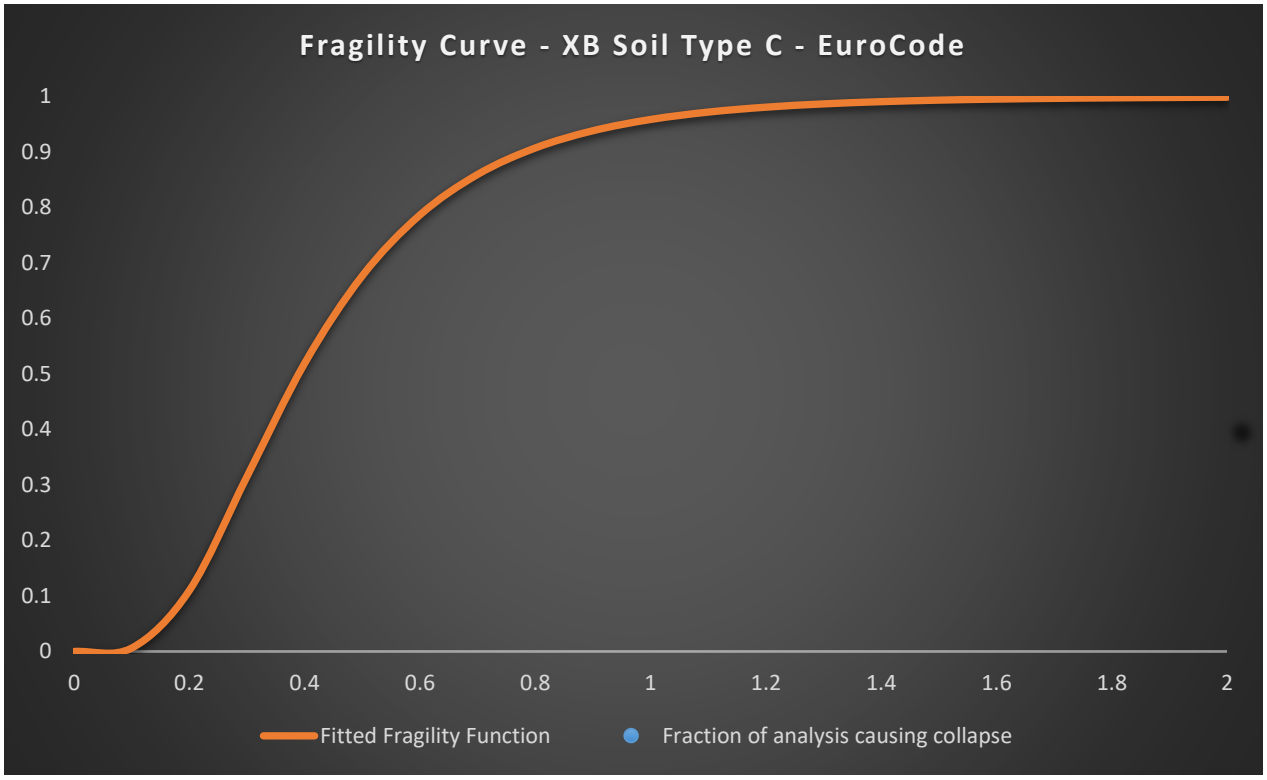

Figure 48. XB Frame - Soil Type C - Eurocode Regulation

Table 36 is the general results of the analysis that have been taken into account for soil type D in X-Bracing frame of the structure.

Table 36. XB Frame - Type Soil D - Overall Results

PGA	NUMBER OF SIMULATIONS	PERCENTAGE OF SIMULATIONS TO TOTAL	NUMBER OF FAILURES IN ASCE	NUMBER OF FAILURES IN EUROCODE
X>1.5	1	1.02%	1	1
1.5>X>1.3	0	0.00%	0	0
1.3>X>1.1	1	1.02%	1	1
1.1>X>1.0	1	1.02%	1	1
1.0>X>0.9	0	0.00%	0	0
0.9>X>0.8	2	2.04%	2	2
0.8>X>0.7	6	6.12%	6	6
0.7>X>0.6	9	9.18%	9	9
0.6>X>0.5	7	7.14%	4	5
0.5>X>0.25	5	5.10%	3	4
0.25>X>0.1	10	10.20%	2	4

0.1>X>0.05	10	10.20%	1	4
0.05>X>0.025	10	10.20%	0	1
0.025>X>0.0	36	36.73%	0	0

Table 37 and 38 are the break down calculation of fragility curves from X-Bracing for soil type D according to the Eurocode and American Society of Civil Engineering's code.

Table 37. XB Frame - Type Soil D - ASCE Regulation

IM	NUMBER OF ANALYSES	NUMBER OF COLLAPSES	FRACTION CAUSING COLLAPSE	THEORETICAL FRAGILITY FUNCTION	LIKELIHOOD	LOG LIKELIHOOD
0.025	36	0	0.000	0.000	0.999	-0.001
0.05	10	0	0.000	0.002	0.983	-0.018
0.1	10	1	0.100	0.031	0.231	-1.463
0.25	10	2	0.200	0.313	0.219	-1.520
0.5	5	3	0.600	0.712	0.299	-1.207
0.6	7	4	0.571	0.798	0.117	-2.148
0.7	9	9	1.000	0.857	0.250	-1.385
0.8	6	6	1.000	0.898	0.524	-0.646
0.9	2	2	1.000	0.926	0.858	-0.153
1.0	0	0	---	0.946	1.000	0.000
1.1	1	1	1.000	0.960	0.960	-0.041
1.3	1	1	1.000	0.977	0.977	-0.023
1.5	0	0	---	0.987	1.000	0.000
2.0	1	1	1.000	0.996	0.996	-0.004

The above data has a median of 0.345 and the variance of 0.662. The total log of likelihood is -8.609.

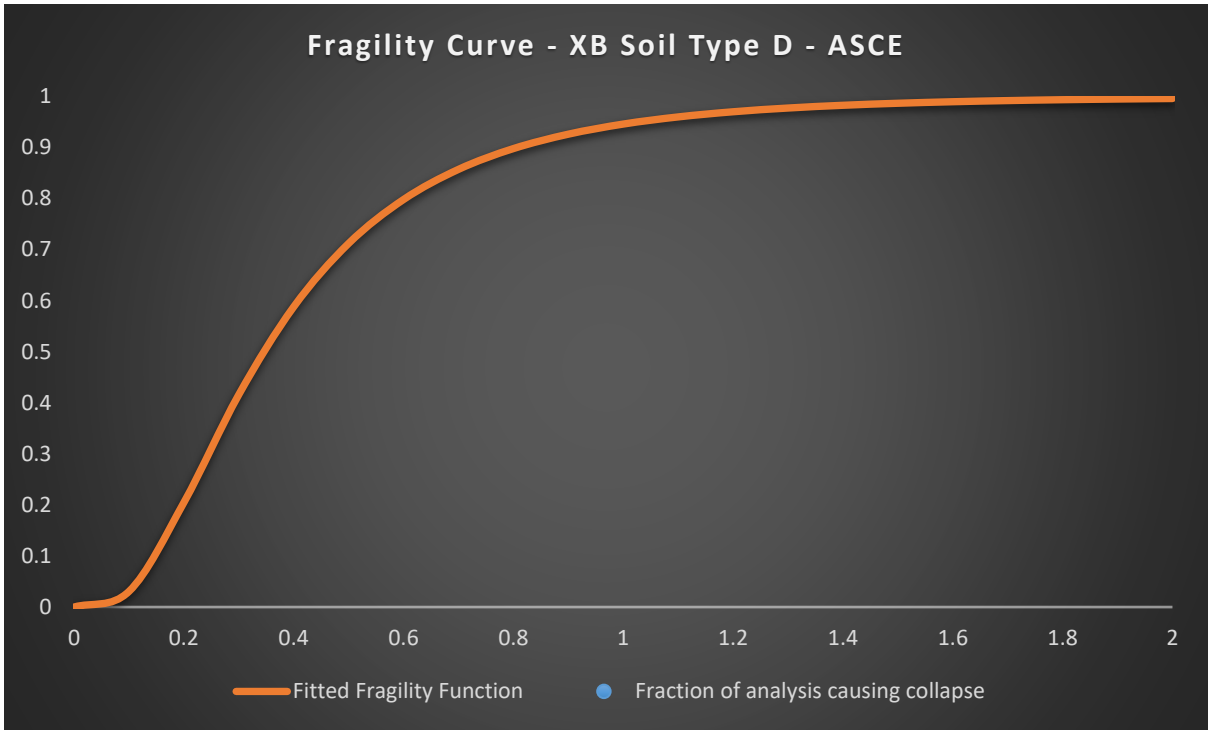

Figure 49.Fragility Curve - XB Frame - Soil Type D –ASCE Regulation

As the data generated from the simulations show the numbers are nearly the same. It can be said that the X-Bracing in soil type D following ASCE regulation has nearly no effect as the results represents (Compared to MR). The median and the variance of the data also are close to each other.

Table 38. XB Frame - Type Soil D - Eurocode Regulation

IM	NUMBER OF ANALYSES	NUMBER OF COLLAPSES	FRACTION CAUSING COLLAPSE	THEORETICAL FRAGILITY FUNCTION	LIKELIHOOD	LOG LIKELIHOOD
0.025	36	0	0.000	0.012	0.637	-0.451
0.05	10	1	0.100	0.067	0.358	-1.026
0.1	10	4	0.400	0.224	0.115	-2.159
0.25	10	4	0.400	0.588	0.123	-2.098
0.5	5	4	0.800	0.833	0.402	-0.911
0.6	7	5	0.714	0.877	0.165	-1.803
0.7	9	9	1.000	0.907	0.417	-0.874
0.8	6	6	1.000	0.929	0.643	-0.442
0.9	2	2	1.000	0.945	0.892	-0.114
1	0	0	---	0.956	1.000	0.000

1.1	1	1	1.000	0.965	0.965	-0.036
1.3	1	1	1.000	0.977	0.977	-0.024
1.5	0	0	---	0.984	1.000	0.000
2	1	1	1.000	0.993	0.993	-0.007

The median and variance of the X-bracing simulation for soil type D following ASCE regulation are 0.203 and 0.934. The total likelihood of these data is -9.944.

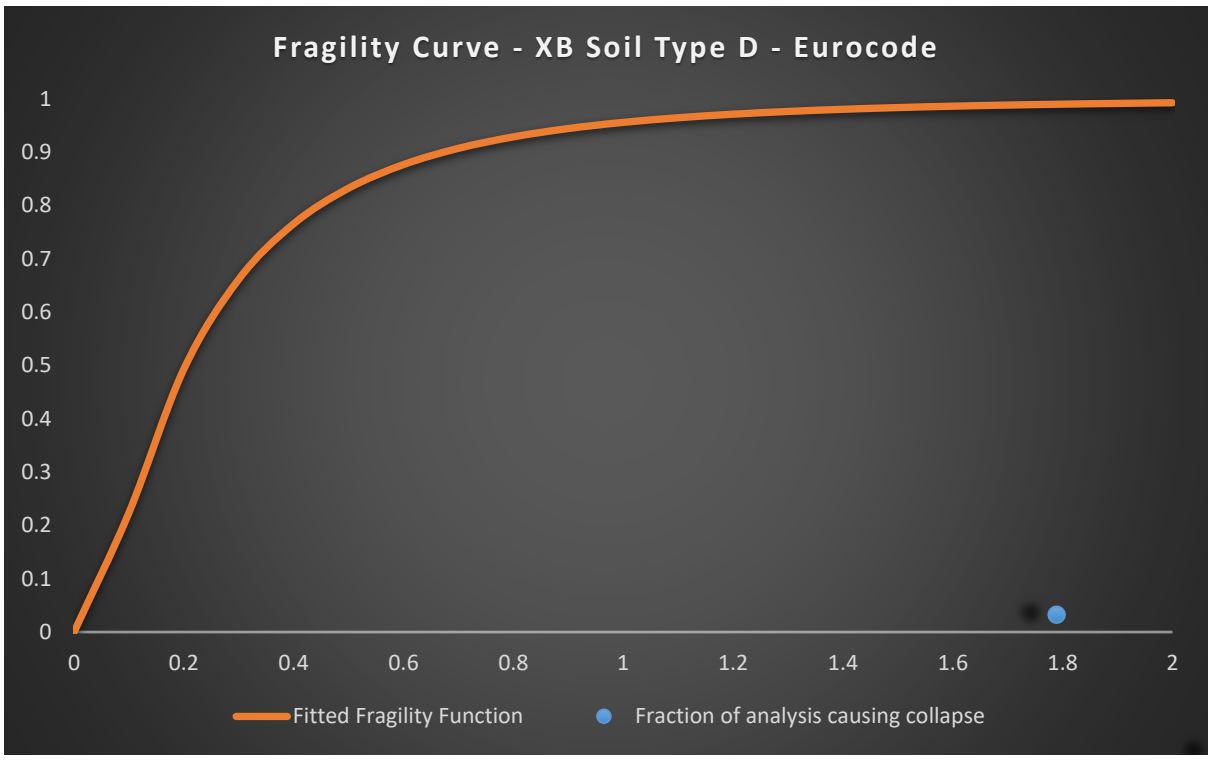

Figure 50. Fragility Curve - XB Frame - Soil Type D - Eurocode Regulation

Figure 50 is the summarised data from the analysis of structure under seismic activity with the soil type D under Eurocode regulation. As it is expected from MR-Frame, it shows a very sharp incline angle at first stage, then a small decrease in slope in the second stage and finally a long and steady slope in the third stage. The X-Bracing has a stronger reaction against seismic activity; however, it is not considerable. The first two stages are taking more energy and the third stage is shorter compared to MR-Frame.

Furthermore, the range of the data that have been established are closer compared to the MR-Frame.

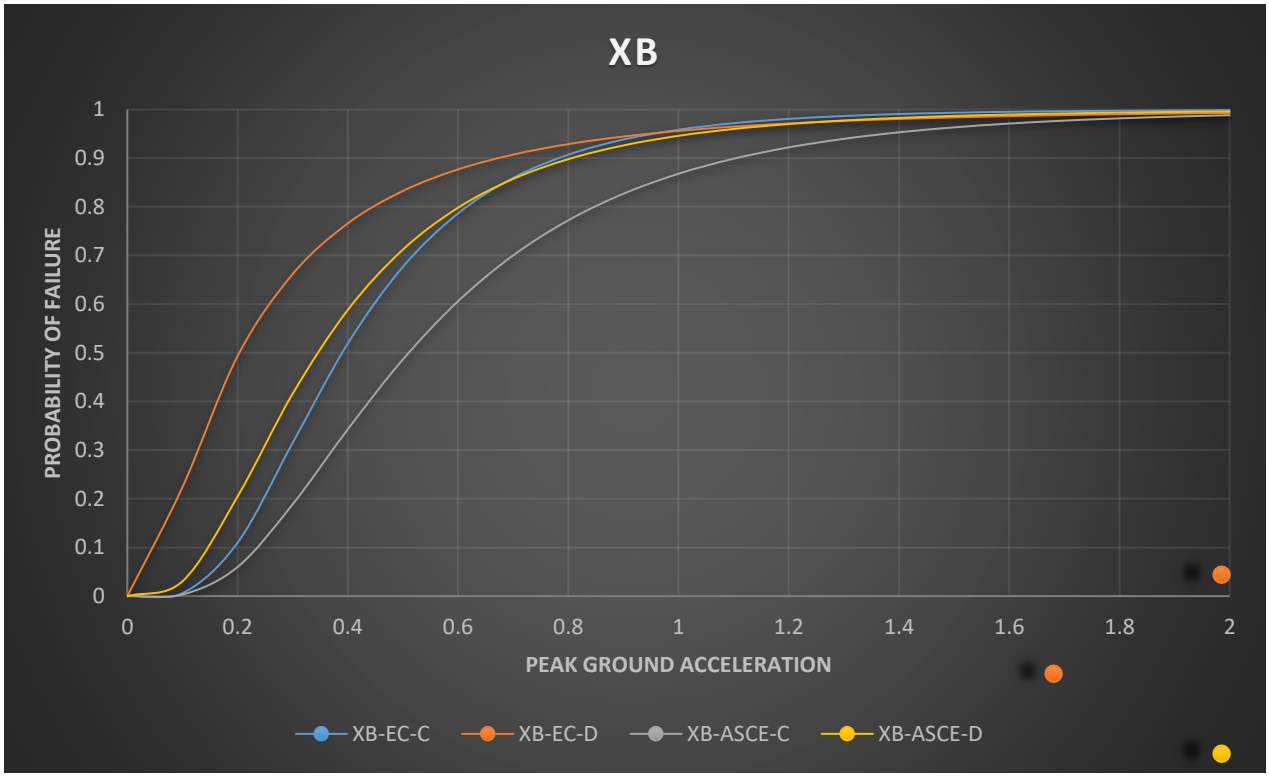

Figure 51. Fragility Curve of X-Bracing Frame for soil type C & D in Eurocode and ASCE

5.4. V-Bracing Frame

The below tables and figure are related to the results that have been generated regarding the V-Bracing (VB- Frame) in soil types of C and D under ASCE and Eurocode regulations.

Table 39. VB Frame - Type Soil C - Overall Result

PGA	NUMBER OF SIMULATIONS	PERCENTAGE OF SIMULATIONS TO TOTAL	NUMBER OF FAILURES IN ASCE	NUMBER OF FAILURES IN EUROCODE
X>1.5	1	0.78%	1	1
1.5>X>1.3	4	3.13%	3	4
1.3>X>1.1	3	2.34%	3	3
1.1>X>1.0	1	0.78%	1	1
1.0>X>0.9	2	1.56%	2	2
0.9>X>0.8	5	3.91%	4	4
0.8>X>0.7	14	10.94%	13	14
0.7>X>0.6	14	10.94%	8	9
0.6>X>0.5	23	17.97%	14	19

0.5>X>0.25	9	7.03%	3	4
0.25>X>0.1	3	2.34%	0	1
0.1>X>0.05	3	2.34%	0	0
0.05>X>0.025	1	0.78%	0	0
0.025>X>0.0	45	35.16%	0	0

Table 40 is generated data related to the soil type C under ASCE regulation.

Table 40. VB Frame - Type Soil C - ASCE Regulation

IM	NUMBER OF ANALYSES	NUMBER OF COLLAPSES	FRACTION CAUSING COLLAPSE	THEORETICAL FRAGILITY FUNCTION	LIKELIHOOD	LOG LIKELIHOOD
0.025	45	0	0.000	0.000	1.000	0.000
0.05	1	0	0.000	0.000	1.000	0.000
0.1	3	0	0.000	0.001	0.998	-0.002
0.25	3	0	0.000	0.066	0.814	-0.206
0.5	9	3	0.333	0.428	0.231	-1.466
0.6	23	14	0.609	0.566	0.155	-1.867
0.7	14	8	0.571	0.677	0.150	-1.896
0.8	14	13	0.929	0.763	0.098	-2.322
0.9	5	4	0.800	0.826	0.405	-0.904
1.0	2	2	1.000	0.873	0.762	-0.272
1.1	1	1	1.000	0.907	0.907	-0.098
1.3	3	3	1.000	0.950	0.856	-0.155
1.5	4	3	0.750	0.972	0.102	-2.280
2.0	1	1	1.000	0.993	0.993	-0.007

The above data has a median of 0.550 and the variance of 0.524. The total log of likelihood is -11.475.

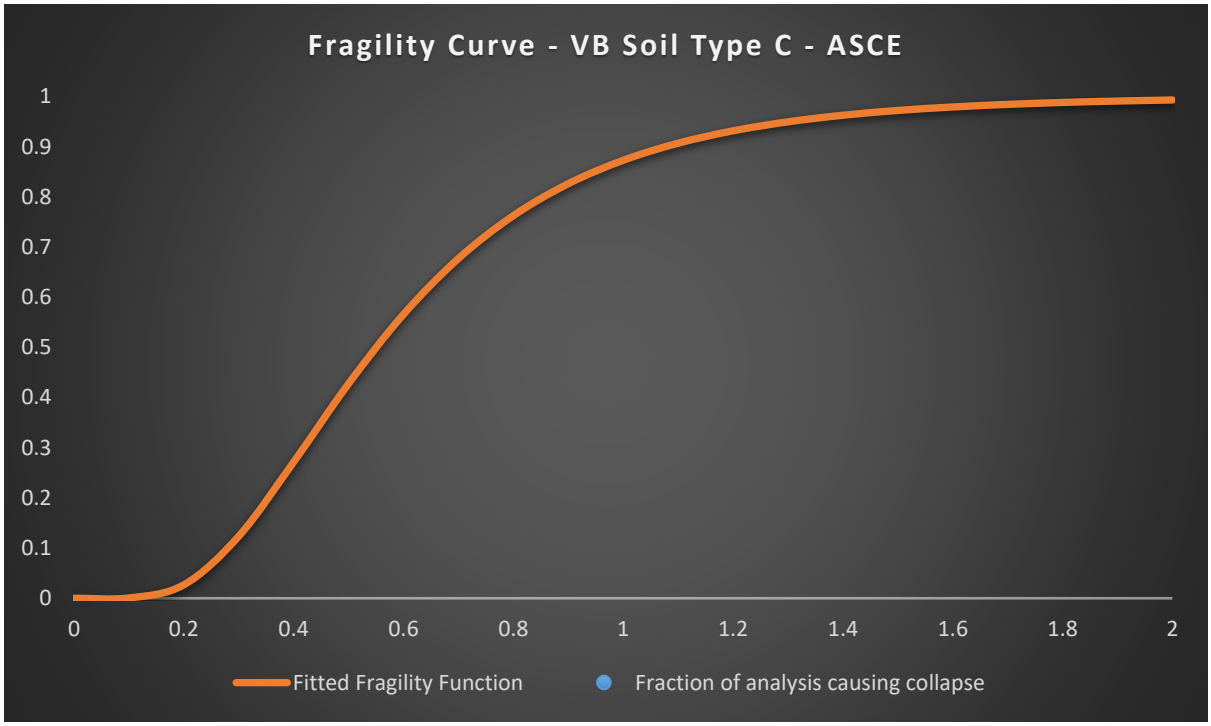

Figure 52.Fragility Curve - VB Frame - Soil Type C - ASCE Regulation

According to the numbers and the data from table and the figure regarding the V-Bracing, and comparing the results in simulations and generation of the fragility curve, it is revealed that the V-bracing has a slightly better impact on the structure and decreases the probability of the structure failure. The first stage has a longer phase compared to X-Bracing and MR and even the slope for the second phase is less steep than the other two scenarios.

Table 41. VB Frame - Soil Type C - Eurocode Regulation

IM	NUMBER OF ANALYSES	NUMBER OF COLLAPSES	FRACTION CAUSING COLLAPSE	THEORETICAL FRAGILITY FUNCTION	LIKELIHOOD	LOG LIKELIHOOD
0.025	45	0	0.000	0.000	1.000	0.000
0.05	1	0	0.000	0.000	1.000	0.000
0.1	3	0	0.000	0.005	0.986	-0.014
0.25	3	1	0.333	0.172	0.354	-1.038
0.5	9	4	0.444	0.621	0.147	-1.919
0.6	23	19	0.826	0.738	0.130	-2.042
0.7	14	9	0.643	0.820	0.063	-2.759
0.8	14	14	1.000	0.876	0.158	-1.848

0.9	5	4	0.800	0.915	0.299	-1.208
1.0	2	2	1.000	0.941	0.885	-0.122
1.1	1	1	1.000	0.958	0.958	-0.043
1.3	3	3	1.000	0.979	0.938	-0.064
1.5	4	4	1.000	0.989	0.957	-0.044
2.0	1	1	1.000	0.998	0.998	-0.002

The above data has a median of 0.422 and the variance of 0.553. The total log of likelihood is -11.103.

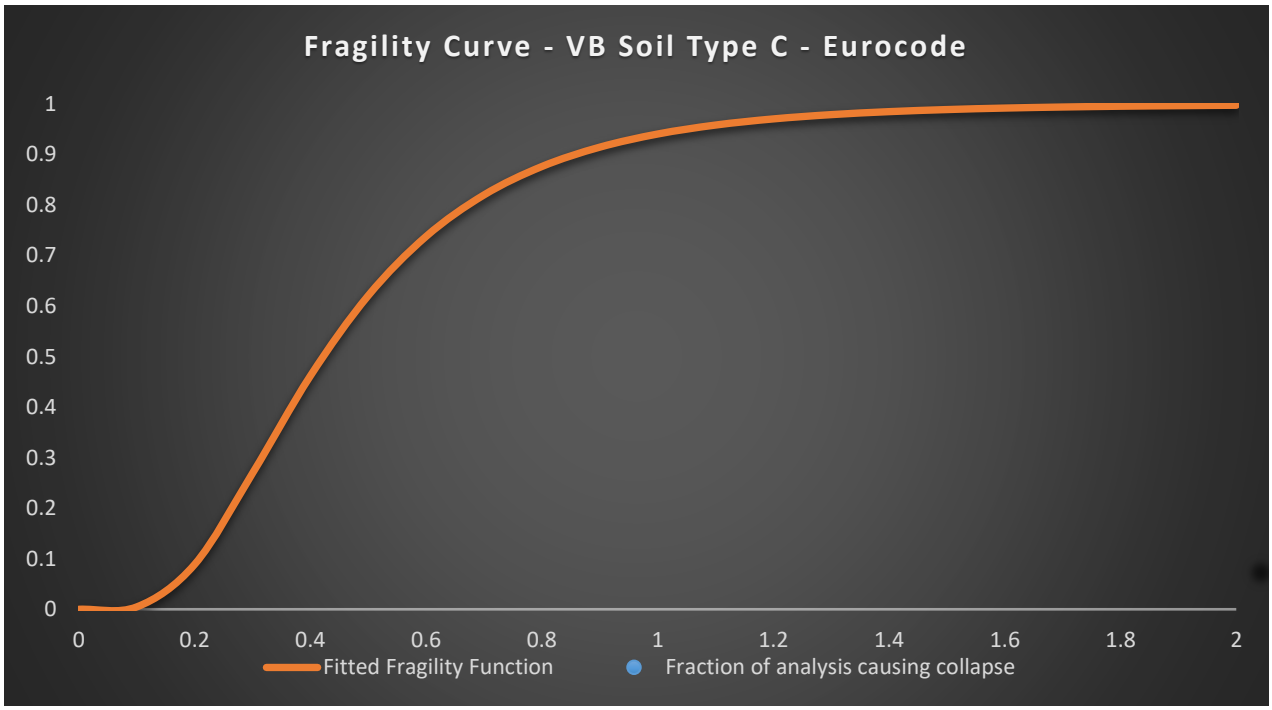

Figure 53. Fragility Curve - VB Frame - Soil Type C - Eurocode Regulation

As it expected, the Eurocode regulation's results have a sharper incline in the first and second stages generally. Through the comparison of the results with other two types framing. The results demonstrate that the VB frame has better performance against the results from XB and MR frame. However, the impact of increase in performance between XB to VB is not considerable as the same result occurred on ASCE in soil type C.

Table 42. VB Frame - Soil Type D - Overall Results

PGA	NUMBER OF SIMULATIONS	PERCENTAGE OF SIMULATIONS TO TOTAL	NUMBER OF FAILURES IN ASCE	NUMBER OF FAILURES IN EUROCODE
X>1.5	1	1.02%	1	1
1.5>X>1.3	0	0.00%	0	0
1.3>X>1.1	1	1.02%	1	1
1.1>X>1.0	1	1.02%	1	1
1.0>X>0.9	0	0.00%	0	0
0.9>X>0.8	2	2.04%	2	2
0.8>X>0.7	6	6.12%	6	6
0.7>X>0.6	9	9.18%	9	9
0.6>X>0.5	7	7.14%	4	5
0.5>X>0.25	5	5.10%	3	4
0.25>X>0.1	10	10.20%	2	3
0.1>X>0.05	10	10.20%	1	4
0.05>X>0.025	10	10.20%	0	1
0.025>X>0.0	36	36.73%	0	0

Table 43.XB Frame - Soil Type D - ASCE Regulation

IM	NUMBER OF ANALYSES	NUMBER OF COLLAPSES	FRACTION CAUSING COLLAPSE	THEORETICAL FRAGILITY FUNCTION	LIKELIHOOD	LOG LIKELIHOOD
0.025	36	0	0.000	3.648E-05	9.987E-01	-1.313E-03
0.05	10	0	0.000	1.755E-03	9.826E-01	-1.757E-02
0.10	10	1	0.100	3.062E-02	2.314E-01	-1.463E+00
0.25	10	2	0.200	3.130E-01	2.187E-01	-1.520E+00
0.50	5	3	0.600	7.123E-01	2.992E-01	-1.207E+00
0.6	7	4	0.571	7.983E-01	1.167E-01	-2.148E+00
0.7	9	9	1.000	8.573E-01	2.502E-01	-1.385E+00
0.8	6	6	1.000	8.980E-01	5.243E-01	-6.457E-01
0.9	2	2	1.000	9.262E-01	8.579E-01	-1.533E-01
1.0	0	0	---	9.460E-01	1.000E+00	0.000E+00
1.1	1	1	1.000	9.601E-01	9.601E-01	-4.077E-02

1.3	1	1	1.000	9.774E-01	9.774E-01	-2.281E-02
1.5	0	0	---	9.868E-01	1.000E+00	0.000E+00
2.0	1	1	1.000	9.960E-01	9.960E-01	-3.978E-03

The above data has a median of 0.345 and the variance of 0.662. The total log of likelihood is -8.609.

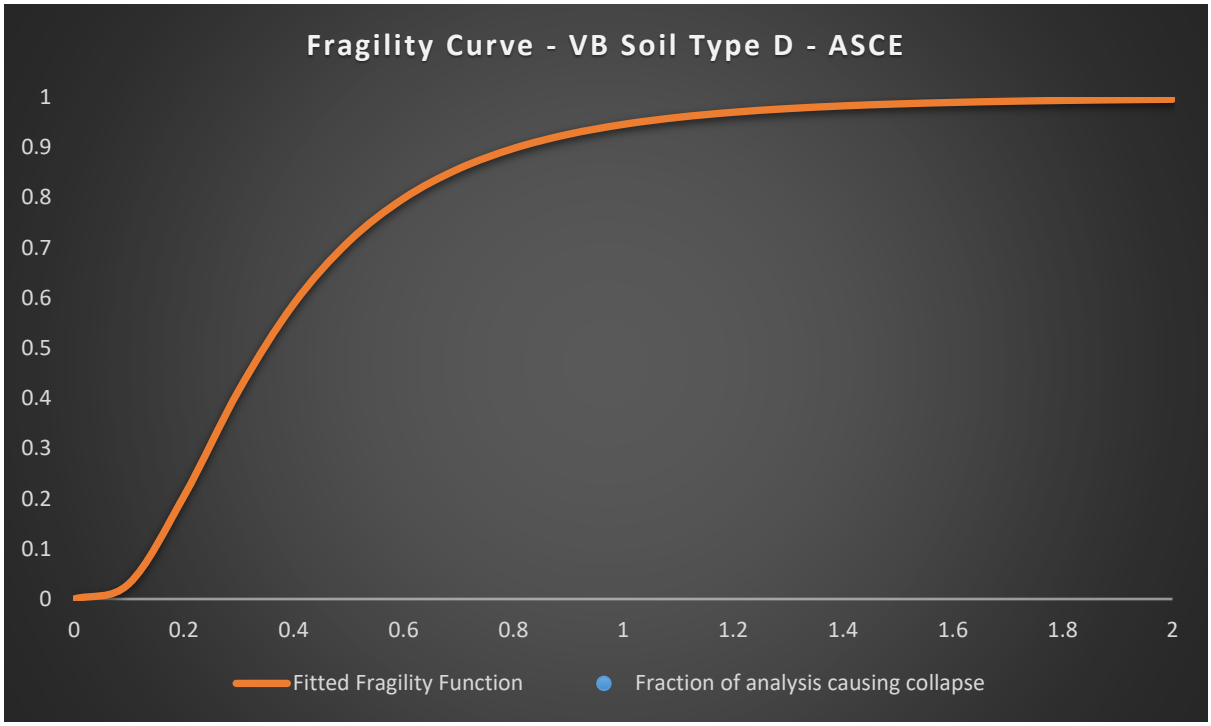

Figure 54. Fragility Curve - VB Frame - Soil Type C - Eurocode Regulation

As the graph and the data show in the soil type D in all the three frame modes the overall outcome is identical (Overall picture). Based on this fact, it could be said that, all the three stages of fragility curve and the slope are approximately similar.

According to the data, it can be said that the bracing system does not have a significant effect on the fragility curve. In other words, the effect would be negligible in ASCE regulation in soil type D.

Table 44. VB Frame - Soil Type D - Eurocode Regulation

IM	NUMBER OF ANALYSES	NUMBER OF COLLAPSES	FRACTION CAUSING COLLAPSE	THEORETICAL FRAGILITY FUNCTION	LIKELIHOOD	LOG LIKELIHOOD
0.025	36	0	0.000	0.011	0.665	-0.409
0.05	10	1	0.100	0.061	0.347	-1.059
0.1	10	4	0.400	0.209	0.098	-2.319
0.25	10	3	0.300	0.565	0.064	-2.751
0.5	5	4	0.800	0.816	0.408	-0.897
0.6	7	5	0.714	0.863	0.189	-1.665
0.7	9	9	1.000	0.895	0.370	-0.994
0.8	6	6	1.000	0.919	0.602	-0.507
0.9	2	2	1.000	0.936	0.876	-0.132
1	0	0	---	0.949	1.000	0.000
1.1	1	1	1.000	0.959	0.959	-0.042
1.3	1	1	1.000	0.972	0.972	-0.028
1.5	0	0	---	0.981	1.000	0.000
2	1	1	1.000	0.991	0.991	-0.009

The above data has a median of 0.214 and the variance of 0.942. The total log of likelihood is -10.812.

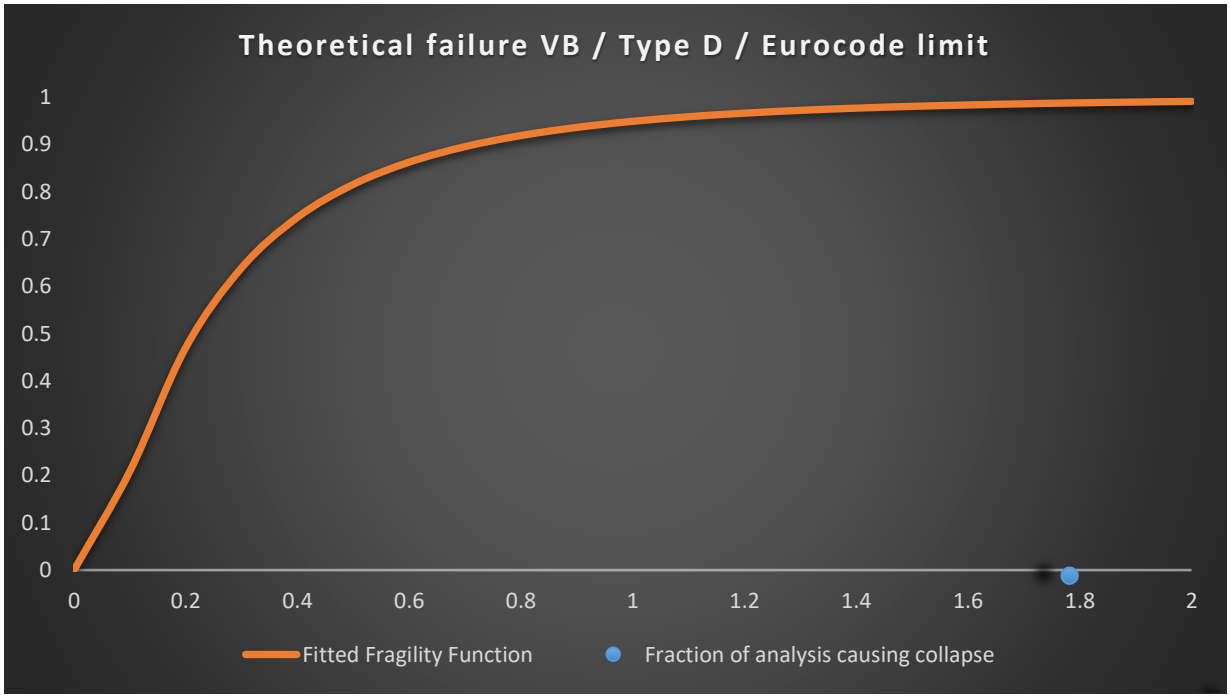

Figure 55. Fragility Curve - V-Bracing - Soil Type D – Eurocode Regulation

The same outcome occurred for the Eurocode regulation as well. The number of failure in the each range of peak ground acceleration is the same and has caused the results to have the identical outcome. Therefore, the overall outcome of fragility curves for both Eurocode and ASCE regulations are the same. However, this conclusion does not mean that there is no influence in the energy dissipation throughout the structure. As the full data in appendix show, the numbers are different but the change is not significant to represent itself in the tables and graphs that have been provided.

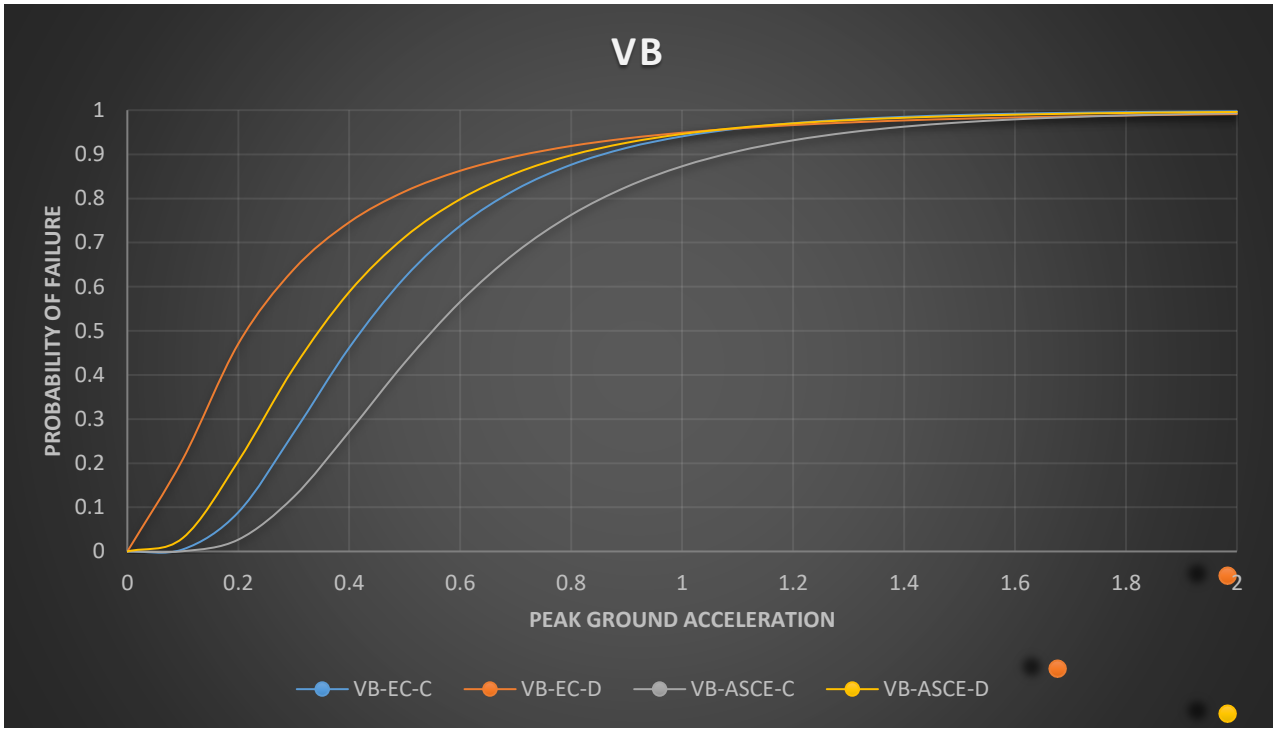

Figure 56.Fragility Curve of V-Bracing Frame for soil type C & D in Eurocode and ASCE

5.5. Discussion

To summarise, all the data that have been gathered in both Eurocode and American Society of Civil Engineering regulations for the most repeated types of soil in the simulation. The results show that the bracing system will help the structure to withstand against the seismic activities in the first two stages. In the first stage it helps the structure to absorb more energy in order to increase the chance against failure. In the same way, the second stage of progression, it experiences lower gradient of increase in the fragility curve. However, the third and final stage all have the same characteristics of the behaviour.

By comparing the European and American regulations in seismic design, the results show that the European regulation is slightly stricter than American regulation. As it was revealed, with the same condition of the structure, the slope of failure of the structure will be higher.

Another fact that these comparisons represent that the change in the type of soil could have an effect on the probability of the failure.

Type C soil shows more effects when the frame of structure changes the reason for this phenomenon is that type C soil is softer than type D. Therefore, the energy dissipation from soil to foundation is more. in this type of soil, as a result of which the structure will be taking more forces and reaction to withstand with it.

In Type D soil, due to its characteristics, the, results demonstrate less change when the additional bracing is added to the structure. According to the generated results, the fragility curve has an indirect relationship with the type of frame and the bracing; and the types of soil have a great impact on the results.

Another conclusion that can be drawn from the generated data is that even when the fragility curves in soil type D are nearly identical in all the three types of frames, however, the median and the variance of the results are not very close.

In addition, there are several external facts that need to be considered.

As the amount of peak ground acceleration increase the probability of the failure also increases gradually and proportionally. But, at some points, for instance, at the late of the second stage of the curve, the data shows 100% of models fail at the certain range of PGA. By

applying the time-history into the models, the generated time histories could be divided into two categories:

1. The seismic activity with small period of sudden shock / shocks.
2. The seismic activity with the constant range of PGA.

In the first types, the starting point is usually with small acceleration which then increases significantly and after a short period of time, the acceleration will be reduced considerable. These types of behaviour are common in higher PGA (once or several times).

To compare it with the second type, the period of earthquake is in highest or near to peak of PGA (or any other factors such as PGV and PGD)

The following categories can be explained in the better way in the figures 57 and 58.

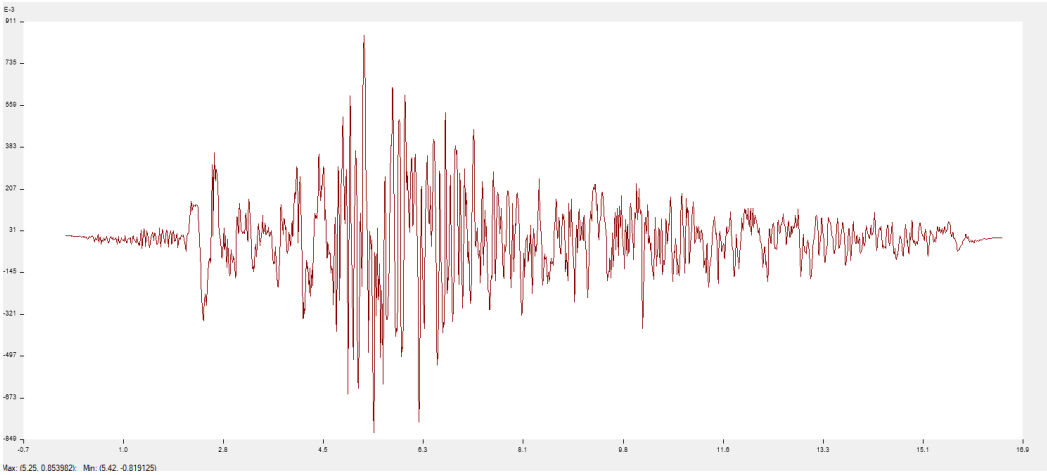

Figure 57. Example of the Time history - Sudden Shock - High PGA

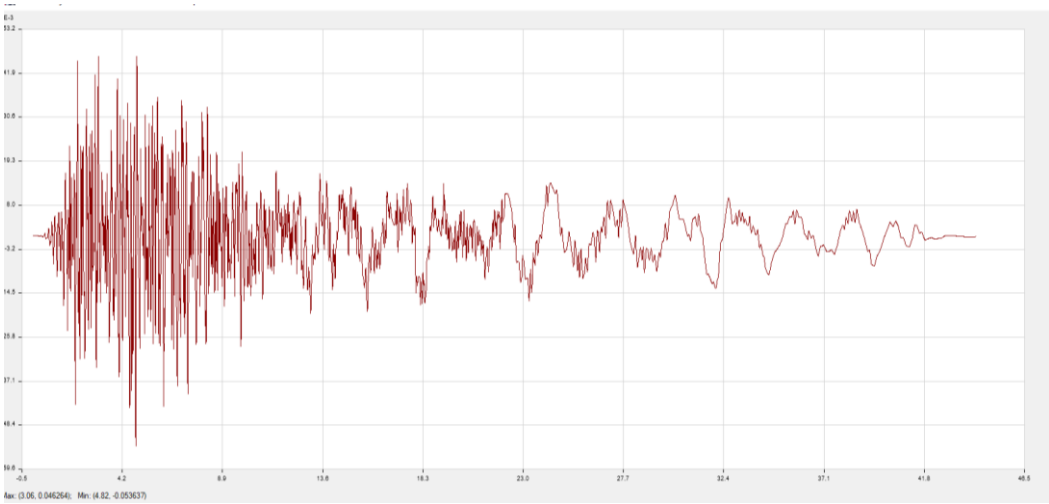

Figure 58. Example of the Time history - Few Shocks - Low PGA

Another fact that can be counted is that by the increase in PGA, the number of time-histories provided and collected falls. This fact might have an impact on the transparency and the accuracy of the curve, specifically in the third stage. To summarise the mentioned factor the table below illustrates that.

Table 45. The number of time history in each range of peak ground acceleration

PGA	Number of simulations	Percentage of simulations
X>1.5	2	0.85%
1.5>X>1.3	5	2.13%
1.3>X>1.1	5	2.13%
1.1>X>1.0	2	0.85%
1.0>X>0.9	3	1.28%
0.9>X>0.8	8	3.40%
0.8>X>0.7	21	8.94%
0.7>X>0.6	25	10.64%
0.6>X>0.5	31	13.19%
0.5>X>0.25	14	5.96%
0.25>X>0.1	13	5.53%
0.1>X>0.05	14	5.96%
0.05>X>0.025	11	4.68%
0.025>X>0.0	81	34.47%

The results on the graphs show that the change of frame in soil type D is nearly negligible. In the same way according to the results that generated by simulation confirm the above mentioned fact. However, by reviewing the facts in detail, it can be said that, there is a slight change as the mean and standard deviation are not close. In other word, the propagation of generated data in each frame is different.

In addition, the percentage of storey drift in structure for each frame with the same condition of the soil, shows the same fact. Therefore, soil condition affect the behaviour of the structure and it is as important as the type of the frame of the structure.

As a bigger picture, the number of failures in each range of ground acceleration, the simulation was experiencing the same results (in most cases) but the numbers (how strong they failed) are different.

In the appendices that have been provided, tables represent the following details:

A1. Detail of time histories: such as Year, location, Vs30 (m/s) and many other factors represented

A2 – A4. Represent the results that include the maximum displacement, storey drift, the location and direction of maximum displacement, magnitude of the seismic activity

Therefore, it is easy to track all the information required to know more about the time-history details of each ground motion. Also, from A2 to A4 the data required to extract the information to generate the fragility curve have been added in all Moment resisting frame, X-bracing, and the V-Bracing. The location of maximum displacement occurred, at which level and direction is also illustrated.

Chapter 6: The effect of Slimdeck on the performance of the structures against seismic activities

Following the additional suggestion from examiners, the difference between normal slab has been considered to compare the result of the behaviour of the structure against the seismic activity and its performance by judging them in fragility curve system.

The normal slab means that, in the simulation the slabs with same thickness were used. However, the slab would be on top of the beam. The dead load would be approximately 15% heavier than the slim deck slab. As a results, the fragility curve leads to be slightly different.

All the boundary conditions of the structure would be the same However, the change in the slab causes the dead load to increase and might lead a small change in the characteristics of the model that would behave under the same situation.

Due to the large number of time histories, it has been decided to reduce the number of simulations in only Moment resisting frame and only in ASCE regulation code as the main purpose of this section of the research is to have better understanding of normal slab versus slim deck slab, in terms of functionality and the performance.

Indeed the number of simulations has been decreased by forty, in order to have enough time for checking the results and comparing the current data with generated data.

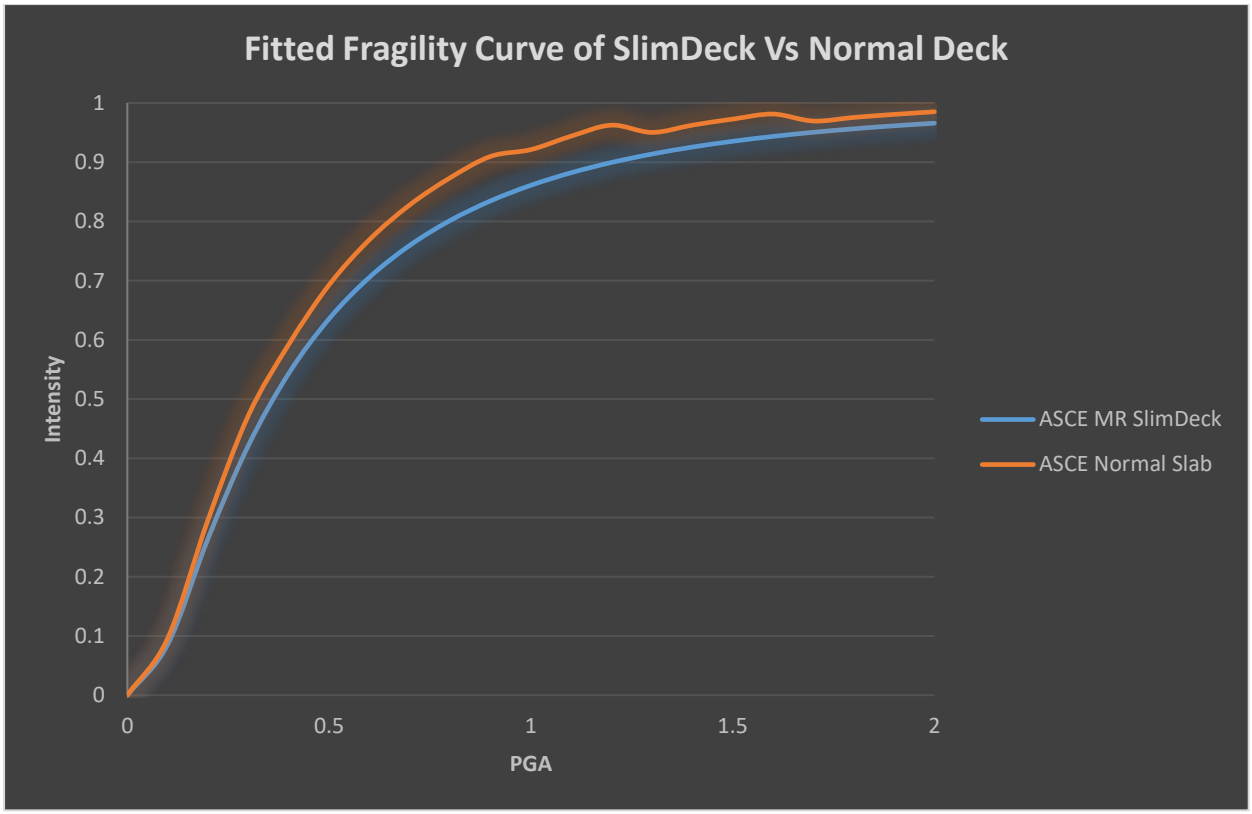

Figure 59. Comparison of the normal deck and slim deck in fragility curve

The number of failures from the beginning is slightly different compare to the slim deck but the gap is negligible. By the PGA reaching to 0.3 (m/s^2) the gap starts increasing. It means that the structure becomes more fragile against the seismic activities compared to normal slab.

Due to the lack of time and enough computational power, number of simulations decreased and as a result a less good quality resolution of the curve has been generated compared to the previous data, that could explain the wave or the dump occurred on the.

Generally, by changing the slabs, theoretically more dead load is added that might cause more failures to the connection. Therefore, as a result, it could be completely presented in the figure that the failure performance become worse.

The other fact that is represented in this comparison is by making the structure heavy in all stages, the building will become more fragile against the seismic activity. As the force applying by seismic activity increases, the possibility of having local / global failure increases proportionally.

This comparison gave us, a clear image about how effective it could be to have the balance between weight or dead load, which leads to a sustainable structure..

In the last two chapters, the focus was on finding the effect of the bracing system on steel structure upon fragility curve and in this chapter; the focus was about the difference between the behaviour of slim deck and normal deck.

Comparing the previous data with the data generated in the present study,, it can be said that the weight of slabs in general makes the structure heavier and it might change the behaviour of building against the series of the tests applied to it.

Chapter 7: Conclusion, Recommendation, and the Future Works

7.1. Conclusion and future work

This research developed a fragility curve for composite buildings using the slim deck flooring system. It also conducted relative investigation for a better understanding of the expected outcome and to discover the reasons which might lead to the failure of a building. All these simulations, research and analysis lead us to have better understanding of the situation and of the limitation there is in fragility curve for steel high rise buildings.

There have been no detailed three-dimensional simulations have been done in concrete and steel frame for high-rise structures. Therefore, having a detailed and verified research would lead us to have a better understanding of circumstances of the simulation. The simulation detailed three-dimensional time history analysis, into a 20 storey building that has been designed in real life. The structure was approved in terms of design and was constructed under ASCE code. The new flooring system was implemented into the design alongside with the other details.

In the very first stage, the structure was generally compared and analysed according to the Eurocode regulation and American Society of Civil Engineering regulation in MR (Moment Resisting), VB (V-Bracing) and XB (X-Bracing) frame separately. The results show (236 simulations in each frame, 1416 in total.

1. Eurocode regulations are stricter than ASCE ones and as a result, with the same condition of the simulations, the probability of failure in all three frames were slightly higher in Eurocode. The difference started showing itself from the beginning of the second stage of the curve.
2. Bracing system helped the structure to deal the lateral loads better. However, the changes were not very relative and remarkable. The change started from the beginning of the first stage of the curve where the PGA (Peak Ground Acceleration) start from zero to 0.5g.
3. The last stage of fragility curve in all frames were same However, MR reached to that stage earlier than other frames. In the same way, Eurocode design shows that the curves reaching to the third stage earlier compare to the ASCE regulation.

In the next chapter of thesis, the outcome of the simulations was analysed into more detail. The effect of soil types has been considered to the effect of fragility in each frame in each regulation. five types of soils have been reviewed during simulation (A to E). However, the majority of the simulations were under soil type C (54.47%) and D (41.70%). The comparison and analysis show that:

1. The general concept for comparison of both codes (Eurocode and ASCE) reveals the similar results. In other word, Eurocode simulation in both type C and D of the analysis having slightly higher rate of failure compared to the ASCE regulation.
2. In terms of the performance of the frame in soil type C, XB has a slightly better performance compared to MR ;and VB has the best performance in soil type C in both design codes.
3. Soil type C has better performance compared to the soil type D generally. It has longer resistance to start rising the probability against increasing the PGA and reaching the last stage at the higher PGA.

This research summarised the behaviour of high-rise steel structure with concrete core and slim deck flooring system under seismic activity. Generating fragility curve was the main purpose of the research. Details of simulation has been taken into account. These details are the types of soils, reinforcement system and design codes.

Displacement was one of the main aspects of judgment in this investigation, which could be summarised into three sections:

1. When structure is under very low PGA most of maximum deflection occurs in Y-Direction and it is negligible. It happens at the top floor (20th). The range of the PGA is approximately from zero to 0.005G.
2. As the ground acceleration increases, the vibration and complexity of load distribution goes up and the movement in horizontal direction becomes greater than vertical reactions. At the beginning of this range most of the maximum displacements are in top floor but in X-direction. As the ground acceleration rises, the reactions become stronger.

3. Last type of reactions, they came from peak ground accelerations that are constantly forcing structure or have very high PGA. It challenges the structure's strength and ability to leads the structure to fail, with most of the failures, happening in 3rd floor. There are two scenarios. One could the connection of the 3rd floor to higher part of the structure, as it is exactly where the columns are changing the size. The other fact could be the soft story phenomenon. It would be expected the resonance happening but in nearly most of the cases the natural frequency of the structure was nearly the same.

Another fact that can be extracted from the data in both codes is that the mean, in ASCE is slightly lower in each case. It means that the probability of the failure in ASCE required more energy and higher PGA. The other important fact revealed by the results is the variance of the outcome. Overall, the variance of ASCE was less than the variance in Eurocode's simulations. This fact indicates that the data generated from ASCE has more accuracy.

It should be stated that, this research is not comparing the accuracy of the two regulations. The aim was to compare the approach of these two codes and expanding the data in this section. It could be said that because the structure was mainly designed by ASCE code , the comparison of the data might not be fair, Nevertheless, due to the lack of information on this subject, it was decided to perform a comparison between them.

7.2. Future works and Recommendation

For the future work of this research, I would strongly recommend the simulation of the structures with different number of floors and similar limitations to this design. It could be a great idea to compare the following results with the current analysis and simulations to realise the effect of height and the bracing system under same circumstances of seismic activity.

In addition, the research could focus on other dimensions such as the economic loss. It would be highly insightful to investigate the relationship between the possibility of failure in buildings and the estimation of economic loss.

The recommendation that I believe would be very helpful for the research regarding this subject, would be doing a more detailed analysis, to be more specific, in high PGA with very limited number of time histories would be very limited.

There are several facts that caused this research to take longer than it had been initially expected. The major obstacle to this research was the availability and provision of the computational hardware and the loss of data during compilation and writing which led to a considerable delay in the process of the research. On average each simulation would take between 18 hours to 5 days (depending on the frames analysed). Had a better performance PC or external computational machine been provided this research could have covered all the other aspects in the larger scale (such as more variety in soils conditions, reinforcements, and floors of building).

References

1. Suresh (2015). Structural systems in high-rise buildings. [Online] Slideshare.net. Available at: https://www.slideshare.net/reachkarthiksuresh/structural-systems-in-high-rise-buildings [Accessed 30 Jun. 2017].
2. Designingbuildings.co.uk. (2017). High-rise building - Designing Buildings Wiki. [Online] Available at: https://www.designingbuildings.co.uk/wiki/High-rise_building [Accessed 30 Jun. 2017].
3. Vona, M. (2014). Fragility Curves of Existing RC Buildings Based on Specific Structural Performance Levels. Open Journal of Civil Engineering, 04(02), pp.120-134.
4. Padgett, J.E. and DesRoches, R. (2006) Bridge Damage-Functionality Using Expert Opinion Survey. 8th National Conference on Earthquake Engineering, Earthquake Engineering Research Institute, San Francisco.
5. Rossetto, T. and Elnashai, A. (2003) Derivation of Vulnerability Functions for European-Type RC Structures Based on Observational Data. Engineering Structures, 25, 1241-1263. http://dx.doi.org/10.1016/S0141-0296(03)00060-9 [Citation Time(s):2]
6. Huang, Q., Gardoni, P. and Hurlebaus, S. (2009) Probabilistic Capacity Models and Fragility Estimates for Reinforced Concrete Columns Incorporating NDT Data. Journal of Engineering Mechanics, 135, 1384-1392. http://dx.doi.org/10.1061/(ASCE)0733-9399(2009)135:12(1384)
7. Banerjee, S. and Shinozuka, M. (2008) Experimental Verification of Bridge Seismic Damage States Quantified by Calibrating Analytical Models with Empirical Field Data. Earthquake Engineering and Engineering Vibration, 7, 383-393.
8. Roser, M., Ritchie, H. and Ortiz-Ospina, E. (2019). World Population Growth. [Online] Our World in Data. Available at: https://ourworldindata.org/world-population-growth [Accessed 8 Dec. 2019].
9. Gulvanessian, H., Formichi, P., Calgaro, J. and Harding, G. (2009). *Designers' guide to Eurocode 1*. London: Thomas Telford.
10. FEMA-454, Designing for earthquakes: A manual for architects, Washington, Dc: Federal Emergency Management Agency, 2006
11. Designing for earthquakes. (2006). [Washington, D.C.]: U.S. Dept. of Homeland Security, FEMA, pp.142-146.
12. Structural Engineers Association of California (SEAOC) Blue Book International Code Council,
13. International Building Code, Birmingham AL, 2003
14. Lebbeus Woods: Radical Reconstruction, Princeton Architectural Press, New York, NY, 1997
15. Andrew Charleson and Mark Taylor: Earthquake Architecture Explorations, Proceedings, 13thWorld Conference on Earthquake Engineering, Vancouver, BC 2004
16. Mark Taylor, Julieanna Preston and Andrew Charleson, Moments of Resistance, Archadia Press, Sydney, Australia, 2002
17. Taranath, B. (n.d.). Tall building design. CRC Press, pp.91-93.

18. Adithya. M, Swathi rani K.S, Shruthi H K, Dr. Ramesh B.R4 Study On Effective Bracing Systems for High-rise Steel Structures. (2015). SSRG International Journal of Civil Engineering, 2(2), pp.19-21.
19. Leet, K., Uang, C. M., and Gilbert, A. 2011. “Fundamentals of Structural Analysis,” 4th ed. New York: McGraw-Hill.
20. Bruneau, M., Uang, C. and Whittaker, A. (1998). Ductile design of steel structures. New York, N.Y.: McGraw-Hill, p.347.
21. Burdekin, F. (1981). The investigation of structural failures in steel buildings, cranes and bridges. Journal of Occupational Accidents, [online] 3(3), pp.163-175. Available at: http://www.sciencedirect.com/science/article/pii/0376634981900109.
22. Luco, N.; Ellingwood, B.R.; Hamburger, R.O.; Hooper, J.D.; Kimball, J.K.; Kircher, C.A. Risk-Targeted versus Current Seismic Design Maps for the Conterminous United States. In Proceedings of the Structural Engineers Association of California 2007 Convention, Squaw Creek, CA, USA, 26–29 September 2007.
23. FEDERAL EMERGENCY MANAGEMENT AGENCY. (2017). NEHRP GUIDELINES FOR THE SEISMIC REHABILITATION OF BUILDINGS. [Online] Available at: http://www.scinc.co.jp/nanken/pdf/fema273.pdf [Accessed 5 Oct. 2017].
24. Ibrahim, Y.E.; El-Shami, M.M.: Seismic fragility curves for midrise reinforced concrete frames in Kingdom of Saudi Arabia. IES J. Part A Civil Struct. Eng. 4(4), 213–223 (2011)
25. Silva, V. et al.: Evaluation of analytical methodologies used to derive vulnerability functions. Earthq. Eng. Struct. Dyn. 43(2), 181– 204 (2014)
26. American Society of Civil Engineers. (2010). Minimum Design Loads for Buildings and Other Structures (ASCE Standard). American Society of Civil Engineers.
27. Mathiasson, A. and Medina, R. (2014). Seismic Collapse Assessment of a 20-Story Steel Moment-Resisting Frame Structure. Buildings, 4(4), pp.806-822.
28. Resilience.abag.ca.gov. (2017). Loma Prieta 25 Policy Actions « ABAG Resilience Program. [Online] Available at: http://resilience.abag.ca.gov/projects/loma-prieta-25-symposium/ [Accessed 11 Oct. 2017].
29. Prestandard and commentary for the seismic rehabilitation of buildings. (2000). Reston, Va.: American Society of Civil Engineers, pp.1-9 Table C1-1.
30. Taranath, B. (2011). Structural Analysis and Design of Tall Buildings: Steel and Composite Construction. New York: CRC Press, pp.452-455.
31. Reducing the Risks of Nonstructural Earthquake Damage – A Practical Guide. (2012). [ebook] Available at: https://www.fema.gov/media-library-data/1398197749343-db3ae43ef771e639c16636a48209926e/FEMA_E-74_Reducing_the_Risks_of_Nonstructural_Earthquake_Damage.pdf [Accessed 14 Nov. 2017].
32. Gatscher, J. and Bachman, R. (2015). Elements of 2012 IBC / ASCE 7-10 Nonstructural Seismic Provisions: Bridging the Implementation Gap. 15 WCEE, [online] pp.1-10. Available at: http://www.iitk.ac.in/nicee/wcee/article/WCEE2012_2385.pdf [Accessed 2 Oct. 2017].

33. Gillengerten, J. (2001). Design of Nonstructural Systems and Components. [online] SpringerLink. Available at: https://link.springer.com/chapter/10.1007/978-1-4615-1693-4_13 [Accessed 14 Nov. 2017].
34. Researchgate. (2017). https://www.researchgate.net/publication/269397558_Slimdek_residential_pattern_book. [online] Available at: https://www.researchgate.net/publication/269397558_Slimdek_residential_pattern_book [Accessed 14 Nov. 2017].
35. Tatasteelconstruction.com. (2019). Composite Floor Decks, Composite Decking | Tata Steel. [Online] Available at: https://www.tatasteelconstruction.com/en_GB/Products/structural-buildings-and-bridges/Composite-floor-deck [Accessed 15 Dec. 2019].
36. Majd, M., Hosseini, M. and Moein Amini, A. (2012). Developing Fragility Curves for Steel Building with X-Bracing by Nonlinear Time History Analyses. 15 WCEE, pp.1-9.
37. Prestandard and commentary for the seismic rehabilitation of buildings. (2000). Reston, Va.: American Society of Civil Engineers, pp.2-15.
38. Nazri, F. and Saruddin, S. (2015). Seismic Fragility Curves for Steel and Reinforced Concrete Frames Based on Near-Field and Far-Field Ground Motion Records. Arabian Journal for Science and Engineering, 40(8), pp.2301-2307.
39. FEMA-273: 73: NEHRP guidelines for the seismic rehabilitation of buildings. Federal Emergency Management Agency (1997)
40. Yang, L., Wang, Y. and Shi, Y. (2015). Full-Scale Test of Two-Storey Composite Slim Floor under Pseudo-Dynamic and Pseudo-Static Loadings. Advances in Structural Engineering, 18(2), pp.173-187.
41. Nielson, B.G., 2005. Analytical Fragility curves for highway bridges in moderate seismic zones. A Thesis presented for PhD degree
42. Jacob, K. H. (1992). “Seismic Hazards in the Eastern U.S. and the Impact on Transportation Lifelines.” Lifeline Earthquake Engineering in the Central and Eastern U.S., Monograph No. 5, New York, NY. ASCE
43. ÖZER AY, B. (2017). FRAGILITY BASED ASSESSMENT OF LOW–RISE AND MID–RISE REINFORCED CONCRETE FRAME BUILDINGS IN TURKEY. [Online] Available at http://users.metu.edu.tr/ozer/documents/publications/T2.pdf [Accessed 28 Mar. 2017].
44. Kumar, A. (2016). Investigation of Expected Seismic Performance on Existing Buildings: A Case Study. IOSR Journal of Mechanical and Civil Engineering, [online] 01(01), pp.88-93. Available at: http://www.iosrjournals.org/iosr-jmce/papers/Conf15010/Vol-1/15.%2088-93.pdf [Accessed 27 Mar. 2017].
45. Özcebe, G., Yücemen, M.S., Aydoğan, V., and Yakut, A. (2003). Preliminary Seismic Vulnerability Assessment of Existing Reinforced Concrete Buildings in Turkey – Part I: Statistical Model Based on Structural Characteristics, Seismic Assessment and Rehabilitation of Existing Buildings, NATO Science Series IV/29, pp. 29–42

46. Kwon O.S. and Elnashai A.S., 2006, “The Effect of Material and Ground Motion Uncertainty on the Seismic Vulnerability Curves of RC Structure”, Engineering Structures, Volume 28, pp. 289–303.
47. Elnashai, A. and Sarno, L. (2015). Fundamentals of Earthquake Engineering: From Source to Fragility, 2nd Editi. 1st ed. John Wiley & Sons, p.312.
48. Kalantari, A. (2012). Seismic Risk of Structures and the Economic Issues of Earthquakes. Earthquake Engineering, [online] pp.1-24. Available at: https://cdn.intechopen.com/pdfs-wm/38202.pdf [Accessed 12 Jul. 2017].
49. Avsar, O. and Yakut, A. (2012). Seismic vulnerability assessment criteria for RC ordinary highway bridges in Turkey. Structural Engineering and Mechanics, 43(1), pp.127-145.
50. Whitman, R.V., Reed, J.W. and Hong, S.T. (1973). “Earthquake Damage Probability Matrices”, Proceedings of the Fifth World Conference on Earthquake Engineering, Rome, Italy, Vol. 2, pp. 2531-2540
51. Ibarra, L. F., and Krawinkler, H. (2005). Global collapse of frame structures under seismic excitations. John A. Blume Earthquake Engineering Center, Stanford, CA, 324
52. Porter, K., Kennedy, R., and Bachman, R. (2007). “Creating Fragility Functions for Performance-Based Earthquake Engineering.” Earthquake Spectra, 23(2), 471–489.c
53. Bradley, B. A., and Dhakal, R. P. (2008). “Error estimation of closed-form solution for annual rate of structural collapse.” Earthquake Engineering & Structural Dynamics, 37(15)
54. Ghafory-Ashtiany, M., Mousavi, M., and Azarbakht, A. (2010). “Strong ground motion record selection for the reliable prediction of the mean seismic collapse capacity of a structure group.” Earthquake Engineering & Structural Dynamics
55. Eads, L., Miranda, E., Krawinkler, H., and Lignos, D. G. (2013). “An efficient method for estimating the collapse risk of structures in seismic regions.” Earthquake Engineering & Structural Dynamics, 42(1), 25–41
56. Csiamerica.com. (2017). Structural Software for Building Analysis and Design | ETABS. [online] Available at: https://www.csiamerica.com/products/etabs [Accessed 12 Jul. 2017].
57. Gsi-eng.eu. (2017). ETABS. [online] Available at: http://www.gsieng.eu/index.asp?mod=articles&id=81 [Accessed 12 Jul. 2017].
58. Earthquake-Resistant Design Concepts. (2010). [ebook] Federal Emergency Management Agency of the U. S. Department of Homeland Security By the National Institute of Building Sciences Building Seismic Safety Council. Available at: https://www.fema.gov/media-library-data/20130726-1759-25045-5477/fema_p_749.pdf [Accessed 14 Nov. 2017].
59. Baker, J. (2015). Efficient Analytical Fragility Function Fitting Using Dynamic Structural Analysis. Earthquake Spectra, 31(1), pp.579-599.
60. Wilkinson S, Hiley R. A non-linear response history model for the seismic analysis of high-rise framed buildings. Computers & Structures. 2006;84(5-6):318-329.

61. Ahmed, I. and Tsavdaridis, K., 2019. The evolution of composite flooring systems: applications, testing, modelling and eurocode design approaches. Journal of Constructional Steel Research, 155, pp.286-300.
62. R.M. Lawson, H. Bode, J.W.P.M. Brekelmans, P.J. Wright, D.L. Mullett, 'Slimflor' and 'Slimdek' construction: European developments, J. Struct. Eng. V77 (n8) (1999) 22–30 (ISSN: 00392553).
63. Wiki.csiamerica.com. 2021. Time-history analysis - Technical Knowledge Base - Computers and Structures, Inc. - Technical Knowledge Base. [online] Available at: <https://wiki.csiamerica.com/display/kb/Time-history+analysis>
64. Shome N, Cornell CA. Probabilistic seismic demand analysis of nonlinear structures. Report No. RMS-35, RMS Program, Stanford University, Stanford, 1999. (accessed: May 1st , 2021). URL https://stacks.stanford.edu/file/druid:tx062fx6721/RMS41.pdf
65. Vamvatsikos D, Cornell CA. Tracing and post-processing of IDA curves: Theory and software implementation. Report No. RMS-44, RMS Program, Stanford University, Stanford, 2001
66. Kappos A and Dymiotis C (2000) DRAIN-2000: a program for the inelastic time-history and seismic reliability analysis of 2-D structures. Edinburgh, UK: Department of Civil and Offshore Engineering, Heriot Watt University, Report no. STR/00/CD/01
67. Kappos A and Panagopoulos G (2009) Fragility curves for reinforced concrete buildings in Greece. Structure and Infrastructure Engineering, 6(1-2):39-53. doi: 10.1080/15732470802663771

Additional references

Taranath, B. (2017). Tall building design: steel, concrete, and composite systems. Boca Raton: CRC press.

Elghazouli, A. (2017). Seismic design of buildings to Eurocode 8. Boca Raton: CRC Press/Taylor & Francis Group.

Minimum design loads and associated criteria for buildings and other structures. (2017). Reston, Va.: American society of civil engineers.

Chew, M. (n.d.). Construction technology for tall buildings. 5th ed. New Jersey: World Scientific.

Viswanath, H., Tolloczko, J. and Clarke, J. (1997). Multi-purpose high-rise towers and tall buildings. London: New York.

Other language

Evaluation of the Fragility Curve of Steel Buildings with Crucible Brackets with Incremental Dynamic Analysis by Leila Kian and Hadi Faghih Maleki from Eighth National Congress of Civil Engineering in Iran (2015)

Evaluation of seismic fragility curve of special steel bending frames with mass irregularity in height by Amir hossein Fakhmi and Kiachehr Behfarnia from Seventh National Congress of Civil Engineering in Iran (2014)

Conventional flexural frame fragility curve by incremental nonlinear analysis under near-field earthquakes by from 3rd International Conference on Applied Research in Civil Engineering, Architecture and Urban Management in Tehran – Iran (2016)

Development of seismic fragility curves of high-rise buildings (Concrete reinforcement) by Mojtaba Ansari from Sanati Sharif University (2014)

Appendix

This section consists of the tables that are related to the results of the simulations.

The purpose of this section is to have more detail about the data that have been selected and

A1. List of the earthquakes

Table 46.list of the earthquakes selected in the analysis to develop the fragility curves

Record Sequence Number	Earthquake Name	YEAR	Station Name	Earthquake Magnitude	Magnitude Type	Magnitude Uncertainty: Study Class	Preferred NEHRP Based on Vs30	Vs30 (m/s) selected for analysis	PGA (g)	T0.2S	T1.0S
5482	Iwate	2008	AKTH04	6.90	Mw	-999	C	458.73	1.768300	5.099009	5.6877E-01
1087	Northridge-01	1994	Tarzana - Cedar Hill A	6.69	Mw	0.1	D	257.21	1.644000	5.112298	7.2338E-01
4211	Niigata, Japan	2004	NIG021	6.63	Mw	-999	C	418.5	1.476200	6.760079	2.0466E-01
825	Cape Mendocino	1992	Cape Mendocino	7.01	Mw	0.1	C	567.78	1.396300	2.589101	7.5745E-01
8157	Christchurch, New Zealand	2011	Heathcote Valley Primary School	6.2	Mw	-999	C	422	1.391400	4.37977	8.8022E-01
1051	Northridge-01	1994	Pacoima Dam (upper left)	6.69	Mw	0.1	A	2016.13	1.3889E+00	3.5855E+00	1.4839E+00
5657	Iwate	2008	IWTH25	6.90	Mw	-999	C	506.44	1.3542E+00	5.9898E+00	1.0180E+00

4209	Niigata, Japan	2004	NIG019	6.63	Mw	-999	C	372.33	1.2551E+00	2.9543E+00	1.9718E+00
77	San Fernando	1971	Pacoima Dam (upper left abut)	6.61	Mw	0.2	A	2016.13	1.2217E+00	4.5840E+00	1.5054E+00
495	Nahanni, Canada	1985	Site 1	6.76	Mw	0.1	C	605.04	1.160100	3.543714	7.3710E-01
4895	Chuetsu-oki	2007	Kashiwazaki NPP, Unit 5: ground surface	6.80	Mw	-999	D	265.5	1.153700	5.448425	1.9870E+00
585	Baja California	1987	Cerro Prieto	5.50	Mw	0.2	C	471.53	1.139400	1.774266	6.6504E-01
4116	Parkfield-02, CA	2004	Parkfield - Fault Zone 14	6.00	Mw	-999	D	246.07	1.037800	2.99187	7.4063E-01
5658	Iwate	2008	IWTH26	6.90	Mw	-999	C	371.06	1.0326E+00	7.0897E+00	7.7619E-01
8165	Duzce, Turkey	1999	IRIGM 496	7.14	Mw	0.2	B	760.0	0.996190	6.980657	3.3795E-01
451	Morgan Hill	1984	Coyote Lake Dam - Southwest Abutment	6.19	Mw	0.1	C	561.43	0.939390	2.768239	1.0892E+00
8158	Christchurch, New Zealand	2011	LPCC	6.2	Mw	-999	C	649.67	9.3132E-01	5.7579E+00	4.7306E-01
4894	Chuetsu-oki	2007	Kashiwazaki NPP, Unit 1: ground surface	6.80	Mw	-999	D	329	8.8823E-01	3.4918E+00	2.5436E+00
4816	Wenchuan, China	2008	Mianzuqingping	7.90	Mw	-999	C	551.3	8.8437E-01	2.2347E+00	8.7323E-01
4876	Chuetsu-oki	2007	Kashiwazaki Nishiyamacho Ikeura	6.80	Mw	-999	C	655.45	8.6274E-01	1.9424E+00	1.3034E+00

415	Coalinga-05	1983	Transmitter Hill	5.77	Mw	0.2	C	477.25	8.4463E-01	1.4810E+00	6.5865E-01
3968	Tottori, Japan	2000	TTRH02	6.61	Mw	-999	D	310.21	0.841610	2.3507	1.7820E+00
1231	Chi-Chi, Taiwan	1999	CHY080	7.62	Mw	0.1	C	496.21	0.832360	1.966015	3.0958E+00
4114	Parkfield-02, CA	2004	Parkfield - Fault Zone 11	6.00	Mw	-999	C	541.73	8.2618E-01	2.0742E+00	2.6131E-01
143	Tabas, Iran	1978	Tabas	7.35	Mw	0.1	B	766.77	0.812450	5.896253	9.2903E-01
1602	Duzce, Turkey	1999	Bolu	7.14	Mw	0.2	D	293.57	7.7559E-01	1.9749E+00	1.2977E+00
1106	Kobe, Japan	1995	KJMA	6.90	Mw	0.1	D	312	0.775250	1.452205	2.0577E+00
4820	Wenchuan, China	2008	Wenchuanwolong	7.90	Mw	-999	C	511.16	7.7356E-01	4.3991E+00	3.9246E-01
1197	Chi-Chi, Taiwan	1999	CHY028	7.62	Mw	0.1	C	542.61	7.6760E-01	2.1245E+00	1.3425E+00
983	Northridge-01	1994	Jensen Filter Plant Generator Building	6.69	Mw	0.1	C	525.79	7.6045E-01	2.6962E+00	1.6521E+00
1004	Northridge-01	1994	LA - Sepulveda VA Hospital	6.69	Mw	0.1	C	380.06	7.5323E-01	4.2656E+00	1.2550E+00
1549	Chi-Chi, Taiwan	1999	TCU129	7.62	Mw	0.1	C	511.18	7.5149E-01	3.6898E+00	9.0290E-01
3964	Tottori, Japan	2000	TTR007	6.61	Mw	-999	C	469.79	7.4266E-01	4.3439E+00	2.3628E-01
4219	Niigata, Japan	2004	NIGH01	6.63	Mw	-999	C	480.4	7.4056E-01	4.8609E+00	1.0722E+00
1517	Chi-Chi, Taiwan	1999	TCU084	7.62	Mw	0.1	C	665.2	7.3785E-01	1.2417E+00	2.9916E+00

4040	Bam, Iran	2003	Bam	6.6	Mw	-999	C	487.4	0.737680	6.049529	1.1387E+00
6906	Darfield, New Zealand	2010	GDLC	7.00	Mw	-999	D	344.02	0.731130	2.683416	1.3414E+00
727	Superstition Hills-02	1987	Superstition Mtn Camera	6.54	Mw	0.1	C	362.38	0.728780	3.09876	7.9182E-01
879	Landers	1992	Lucerne	7.28	Mw	0.1	B	1369	0.727240	2.490905	5.1712E-01
5663	Iwate	2008	MYG004	6.90	Mw	-999	C	479.37	7.2576E-01	5.0959E+00	6.5222E-01
3947	Tottori, Japan	2000	SMNH01	6.61	Mw	-999	C	446.34	7.1988E-01	3.0932E+00	3.3510E-01
250	Mammoth Lakes-06	1980	Long Valley Dam (Upr L Abut)	5.94	Mw	0.1	C	537.16	0.719280	1.785696	4.9250E-01
4126	Parkfield-02, CA	2004	Parkfield - Stone Corral 1E	6.00	Mw	-999	D	260.63	0.716670	2.253726	3.5496E-01
1063	Northridge-01	1994	Rinaldi Receiving Sta	6.69	Mw	0.1	D	282.25	7.0785E-01	2.1781E+00	2.0466E+00
3474	Chi-Chi, Taiwan-06	1999	TCU079	6.30	Mw	0.2	C	363.99	0.704450	3.425689	5.0941E-01
126	Gazli, USSR	1976	Karakyr	6.80	Mw	0.1	D	259.59	0.701780	2.709331	1.0696E+00
1084	Northridge-01	1994	Sylmar - Converter Sta	6.69	Mw	0.1	D	251.24	6.9753E-01	2.0780E+00	2.0718E+00
1503	Chi-Chi, Taiwan	1999	TCU065	7.62	Mw	0.1	D	305.85	6.8938E-01	1.2922E+00	2.0269E+00
2658	Chi-Chi, Taiwan-03	1999	TCU129	6.20	Mw	0.2	C	511.18	0.688770	3.110141	4.0072E-01
160	Imperial Valley-06	1979	Bonds Corner	6.53	Mw	0.1	D	223.03	0.686610	3.906185	6.0008E-01

1085	Northridge-01	1994	Sylmar - Converter Sta East	6.69	Mw	0.1	C	370.52	6.8610E-01	2.3406E+00	1.0483E+00
407	Coalinga-05	1983	Oil City	5.77	Mw	0.2	C	398.49	6.8604E-01	4.2171E+00	3.9607E-01
529	N. Palm Springs	1986	North Palm Springs	6.06	Mw	0.1	D	344.67	0.684340	2.420713	9.5764E-01
1617	Duzce, Turkey	1999	Lamont 375	7.14	Mw	0.2	C	454.2	6.8064E-01	3.0695E+00	2.2417E-01
1120	Kobe, Japan	1995	Takatori	6.90	Mw	0.1	D	256	6.7218E-01	3.7514E+00	1.7951E+00
3907	Tottori, Japan	2000	OKY004	6.61	Mw	-999	C	475.8	6.5993E-01	4.5185E+00	1.9566E-01
1044	Northridge-01	1994	Newhall - Fire Sta	6.69	Mw	0.1	D	269.14	6.5430E-01	2.2558E+00	1.2058E+00
1119	Kobe, Japan	1995	Takarazuka	6.90	Mw	0.1	D	312	6.5400E-01	2.2303E+00	1.1006E+00
4101	Parkfield-02, CA	2004	Parkfield - Cholame 3E	6.00	Mw	-999	C	397.36	6.5141E-01	1.4844E+00	2.3846E-01
4218	Niigata, Japan	2004	NIG028	6.63	Mw	-999	C	430.71	6.4783E-01	2.9734E+00	6.9641E-01
8119	Christchurch, New Zealand	2011	Pages Road Pumping Station	6.2	Mw	-999	E	206	6.4750E-01	2.2820E+00	5.8412E-01
4107	Parkfield-02, CA	2004	Parkfield - Fault Zone 1	6.00	Mw	-999	E	178.27	6.4455E-01	1.3149E+00	1.3576E+00
1080	Northridge-01	1994	Simi Valley - Katherine Rd	6.69	Mw	0.1	C	557.42	6.4410E-01	1.4728E+00	1.1224E+00

1086	Northridge-01	1994	Sylmar - Olive View Med FF	6.69	Mw	0.1	C	440.54	6.4005E-01	1.5090E+00	9.0665E-01
5264	Chuetsu-oki	2007	NIG018	6.80	Mw	-999	D	198.26	6.2519E-01	1.8796E+00	1.4834E+00
1077	Northridge-01	1994	Santa Monica City Hall	6.69	Mw	0.1	D	336.2	6.2478E-01	2.8258E+00	4.4931E-01
828	Cape Mendocino	1992	Petrolia	7.01	Mw	0.1	C	422.17	6.2397E-01	1.3196E+00	1.0022E+00
3966	Tottori, Japan	2000	TTR009	6.61	Mw	-999	C	420.2	6.2177E-01	2.8464E+00	2.4102E-01
4845	Chuetsu-oki	2007	Joetsu Oshimaku Oka	6.80	Mw	-999	C	610.05	6.2016E-01	5.0224E+00	2.6479E-01
265	Victoria, Mexico	1980	Cerro Prieto	6.33	Mw	0.2	C	471.53	0.614510	1.305754	9.7687E-01
4122	Parkfield-02, CA	2004	Parkfield - Gold Hill 3W	6.00	Mw	-999	C	510.92	6.0451E-01	2.2661E+00	1.8493E-01
540	N. Palm Springs	1986	Whitewater Trout Farm	6.06	Mw	0.1	C	425.02	0.596650	2.462142	3.8022E-01
1507	Chi-Chi, Taiwan	1999	TCU071	7.62	Mw	0.1	C	624.85	5.9346E-01	3.5170E+00	1.4749E+00
4744	Wenchuan, China	2008	Shifangbajiao	7.90	Mw	-999	C	379.28	5.9285E-01	4.9892E+00	9.8687E-01
4375	Umbria Marche (aftershock 7), Italy	1997	Nocera Umbra	4.3	ML	-999	C	428	0.592170	0.9413573	1.3074E-02
779	Loma Prieta	1989	LGPC	6.93	Mw	0.1	C	594.83	0.590120	1.461074	1.0903E+00

700	Whittier Narrows-01	1987	Tarzana - Cedar Hill	5.99	Mw	0.1	D	257.21	5.8926E-01	1.2743E+00	9.6557E-02
5818	Iwate	2008	Kurihara City	6.90	Mw	-999	C	512.26	5.8540E-01	3.3313E+00	6.5855E-01
568	San Salvador	1986	Geotech Investig Center	5.80	Mw	0.2	C	489.34	5.7610E-01		7.6835E-01
6915	Darfield, New Zealand	2010	Heathcote Valley Primary School	7.00	Mw	-999	C	422	5.7386E-01	3.8035E+00	2.7712E-01
4856	Chuetsu-oki	2007	Kashiwazaki City Center	6.80	Mw	-999	D	294.38	5.7362E-01	1.8511E+00	1.2865E+00
4874	Chuetsu-oki	2007	Oguni Nagaoka	6.80	Mw	-999	C	561.59	5.6615E-01	7.5743E-01	6.4244E-01
4891	Chuetsu-oki	2007	Iizuna Imokawa	6.80	Mw	-999	C	591.2	5.6511E-01	9.5598E-01	1.4836E+00
4070	Parkfield-02, CA	2004	PARKFIELD - JOAQUIN CANYON	6.00	Mw	-999	C	378.99	5.5980E-01	2.2705E+00	3.1039E-01
418	Coalinga-07	1983	Coalinga-14th & Elm (Old CHP)	5.21	Mw	0.2	D	286.41	5.5960E-01	1.869041	2.3000E-01
4103	Parkfield-02, CA	2004	Parkfield - Cholame 4W	6.00	Mw	-999	C	410.4	5.5915E-01	1.3453E+00	3.0886E-01
1524	Chi-Chi, Taiwan	1999	TCU095	7.62	Mw	0.1	C	446.63	5.5847E-01	1.8591E+00	5.5666E-01
4480	L'Aquila, Italy	2009	L'Aquila - V. Aterno - Centro Valle	6.30	Mw	-999	C	475	0.558440	2.018341	4.7999E-01
372	Coalinga-02	1983	Anticline Ridge Free-Field	5.09	Mw	0.2	C	478.63	0.557720	2.065164	6.6741E-02

4873	Chuetsu-oki	2007	Kashiwazaki City Takayanagicho	6.80	Mw	-999	C	561.59	5.5485E-01	1.3921E+00	4.8773E-01
3475	Chi-Chi, Taiwan-06	1999	TCU080	6.30	Mw	0.2	C	489.32	5.4809E-01	2.3433E+00	4.1965E-01
811	Loma Prieta	1989	WAHO	6.93	Mw	0.1	C	388.33	0.537300	2.579113	7.8945E-01
952	Northridge-01	1994	Beverly Hills - 12520 Mulhol	6.69	Mw	0.1	C	545.66	5.3527E-01	2.6076E+00	3.8230E-01
1728	Northridge-06	1994	Rinaldi Receiving Sta	5.28	Mw	0.2	D	282.25	0.528200	1.986786	2.3544E-01
183	Imperial Valley-06	1979	El Centro Array #8	6.53	Mw	0.1	D	206.08	5.2691E-01	1.5696E+00	3.6356E-01
901	Big Bear-01	1992	Big Bear Lake - Civic Center	6.46	Mw	0.1	C	430.36	0.524580	1.780659	2.3922E-01
982	Northridge-01	1994	Jensen Filter Plant Administrative Building	6.69	Mw	0.1	C	373.07	5.2425E-01	1.0160E+00	2.4984E+00
1633	Manjil, Iran	1990	Abbar	7.37	Mw	0.1	C	723.95	0.523480	2.491516	5.5453E-01
8123	Christchurch, New Zealand	2011	Christchurch Resthaven	6.2	Mw	-999	E	141	5.2141E-01	9.5049E-01	2.1201E+00
1520	Chi-Chi, Taiwan	1999	TCU088	7.62	Mw	0.1	C	665.2	5.2104E-01	8.8519E-01	1.5147E-01
368	Coalinga-01	1983	Pleasant Valley P.P. - yard	6.36	Mw	0.1	D	257.38	5.2073E-01		1.3088E+00
5985	El Mayor-Cucapah	2010	El Centro Differential Array	7.20	Mw	-999	D	202.26	0.507370	2.923453	9.6176E-01
1623	Stone Canyon	1972	Melendy Ranch	4.81	Mw	0.3	C	425.11	0.495510	2.031298	9.7418E-02

240	Mammoth Lakes-04	1980	Convict Creek	5.70	Mw	0.2	C	382.12	0.484200	1.780932	1.6981E-01
4352	Umbria Marche, Italy	1997	Nocera Umbra	6	Mw	-999	C	428	0.472550	3.705207	3.8337E-01
4352	Umbria Marche, Italy	1997	Nocera Umbra	6	Mw	-999	C	428	4.7255E-01		3.8337E-01
1853	Yountville	2000	Napa Fire Station #3	5.00	Mw	0.2	D	328.57	0.459710	1.764094	4.4896E-01
4260	Ancona-09, Italy	1972	Ancona-Rocca	4.7	ML	-999	C	549	0.450270	1.307453	3.4344E-02
821	Erzican, Turkey	1992	Erzincan	6.69	Mw	0.1	D	352.05	0.444990	1.27038	1.0038E+00
230	Mammoth Lakes-01	1980	Convict Creek	6.06	Mw	0.1	C	382.12	0.439150	2.236028	2.5217E-01
619	Whittier Narrows-01	1987	Garvey Res. - Control Bldg	5.99	Mw	0.1	C	468.18	0.436460	2.298856	4.1565E-01
406	Coalinga-05	1983	Coalinga-14th & Elm (Old CHP)	5.77	Mw	0.2	D	286.41	0.424860	1.494151	2.7013E-01
3733	Whittier Narrows-02	1987	Pasadena - Old House Rd	5.27	Mw	0.1	C	397.27	3.8617E-01	0.8603626	7.3351E-02
5836	El Mayor-Cucapah	2010	El Centro - Meloland Geot. Array	7.20	Mw	-999	D	264.57	3.7814E-01	1.843042	6.5062E-01
3748	Cape Mendocino	1992	Ferndale Fire Station	7.01	Mw	0.1	C	387.95	2.9416E-01	1.042291	7.8242E-01
721	Superstition Hills-02	1987	El Centro Imp. Co. Cent	6.54	Mw	0.1	D	192.05	2.6118E-01	1.251765	4.8369E-01
	Loma Prieta	1989	Hollister City Hall	6.93	Mw	0.1	D	198.77	2.3371E-01	5.1555E-01	8.0520E-01

6	Imperial Valley-02	1940	El Centro Array #9	6.95	Mw	0.2	D	213.44	2.3349E-01	1.097344	5.2348E-01
4081	Parkfield-02, CA	2004	Parkfield - Cholame 5W	6.00	Mw	-999	D	236.59	2.3324E-01	1.507901	2.2699E-01
1646	Sierra Madre	1991	Pasadena - USGS/NSMP Office	5.61	Mw	0.1	D	340	2.3178E-01	0.7172835	1.6549E-01
1055	Northridge-01	1994	Pasadena - N Sierra Madre	6.69	Mw	0.1	C	397.27	2.3087E-01	1.300332	1.2729E-01
20	Northern Calif-03	1954	Ferndale City Hall	6.50	U	0.3	D	219.31	1.8616E-01	0.4965819	3.6117E-01
34	Northern Calif-05	1967	Ferndale City Hall	5.60	Mw	0.3	D	219.31	1.8406E-01	0.541451	1.6599E-01
416	Coalinga-06	1983	Coalinga-14th & Elm (Old CHP)	4.89	Mw	0.2	D	286.41	0.151090	0.5377462	4.5711E-02
172	Imperial Valley-06	1979	El Centro Array #1	6.53	Mw	0.1	D	237.33	1.4458E-01	0.5046254	1.9838E-01
675	Whittier Narrows-01	1987	Pasadena - CIT Athenaeum	5.99	Mw	0.1	C	415.13	1.4147E-01	0.832487	1.9582E-01
99	Hollister-03	1974	Hollister City Hall	5.14	Mw	0.3	D	198.77	1.4070E-01	0.5253324	7.4889E-02
5	Northwest Calif-01	1938	Ferndale City Hall	5.50	Mw	0.3	D	219.31	1.2218E-01	0.5178267	1.7845E-01
11	Northwest Calif-03	1951	Ferndale City Hall	5.80	Mw	0.3	D	219.31	1.0709E-01	0.4312204	1.5387E-01
79	San Fernando	1971	Pasadena - CIT Athenaeum	6.61	Mw	0.2	C	415.13	1.0575E-01	0.338944	2.7584E-01

36	Borrego Mtn	1968	El Centro Array #9	6.63	Mw	0.3	D	213.44	9.4018E-02	0.345929	3.1009E-01
63	San Fernando	1971	Fairmont Dam	6.61	Mw	0.2	C	634.33	0.093858	2.0485E+00	0.09850626
102	Northern Calif-07	1975	Ferndale City Hall	5.20	Mw	0.2	D	219.31	9.0045E-02	0.5997488	1.6250E-01
23	San Francisco	1957	Golden Gate Park	5.28	Mw	0.3	B	874.72	8.6274E-02	0.3382213	3.3051E-02
26	Hollister-01	1961	Hollister City Hall	5.60	U	0.3	D	198.77	8.4991E-02	0.2676472	3.0237E-01
462	Morgan Hill	1984	Hollister City Hall	6.19	Mw	0.1	D	198.77	7.0129E-02	0.3425829	2.2726E-01
16	Northern Calif-02	1952	Ferndale City Hall	5.20	Mw	0.3	D	219.31	6.8432E-02	0.3444465	1.1856E-01
25	Northern Calif-04	1960	Ferndale City Hall	5.70	Mw	0.3	D	219.31	6.7086E-02	0.2942229	4.9824E-02
27	Hollister-02	1961	Hollister City Hall	5.50	U	0.3	D	198.77	6.2349E-02	0.2093196	2.6188E-01
2006	CA/Baja Border Area	2002	El Centro Array #10	5.31	Mw	0.2	D	202.85	6.0458E-02	0.3604261	3.8417E-02
28	Parkfield	1966	Cholame - Shandon Array #12	6.19	Mw	0.2	C	408.93	5.8666E-02	0.2772484	1.2496E-01
198	Imperial Valley-07	1979	El Centro Array #10	5.01	Mw	0.1	D	202.85	5.2531E-02	0.258163	3.4568E-02
9	Borrego	1942	El Centro Array #9	6.50	U	0.3	D	213.44	5.2247E-02	0.352805	1.2136E-01
13	Kern County	1952	Pasadena - CIT Athenaeum	7.36	Mw	0.2	C	415.13	5.1003E-02	0.1329975	2.2594E-01

7	Northwest Calif-02	1941	Ferndale City Hall	6.60	U	0.3	D	219.31	4.9416E-02	0.2088445	3.9125E-02
19	Central Calif-01	1954	Hollister City Hall	5.30	U	0.3	D	198.77	4.7679E-02	0.2426652	9.2895E-02
22	El Alamo	1956	El Centro Array #9	6.80	U	0.3	D	213.44	4.4953E-02	0.2455053	2.0996E-01
323	Coalinga-01	1983	Parkfield - Cholame 12W	6.36	Mw	0.1	D	359.03	4.4950E-02	0.3056838	1.1136E-01
21	Imperial Valley-05	1955	El Centro Array #9	5.40	U	0.3	D	213.44	4.4240E-02	0.2310494	6.3051E-02
1726	Northridge-06	1994	Pasadena - USGS/NSMP Office	5.28	Mw	0.2	D	340	4.1761E-02	0.1886488	1.9336E-02
3	Humbolt Bay	1937	Ferndale City Hall	5.80	Mw	0.3	D	219.31	4.0961E-02	0.1480843	5.2926E-02
1820	Hector Mine	1999	Pasadena - Fair Oaks & Walnut	7.13	Mw	0.1	C	430.69	3.5278E-02	0.1440745	9.2860E-02
255	Mammoth Lakes-07	1980	USC Cash Baugh Ranch	4.73	Mw	0.2	D	323.54	0.029900	0.149817	1.0193E-01
10	Imperial Valley-03	1951	El Centro Array #9	5.60	U	0.3	D	213.44	2.9364E-02	0.1091667	6.1475E-02
18	Imperial Valley-04	1953	El Centro Array #9	5.50	U	0.3	D	213.44	2.7932E-02	0.1472623	4.5482E-02
11280	40238431	2009	Parkfield - Cholame 5W	4.39	Mw	-999	D	236.6	2.0278E-02	0.0584212	7.3348E-03
4	Imperial Valley-01	1938	El Centro Array #9	5.00	U	0.3	D	213.44	1.8449E-02	0.07997533	1.7968E-02

18496	51182151	2007	Parkfield - Cholame 5W	4.01	Mw	-999	D	236.6	1.8393E-02	0.06412105	2.6527E-03
1997	Gulf of California	2001	El Centro Array #9	5.70	Mw	0.2	D	213.44	1.8280E-02	0.04383693	3.9859E-02
35	Northern Calif-06	1967	Hollister City Hall	5.20	U	0.3	D	198.77	1.5276E-02	0.05020315	3.7697E-02
1779	Hector Mine	1999	El Centro Array #10	7.13	Mw	0.1	D	202.85	1.4538E-02	0.02443579	8.9639E-02
8617	40204628	2007	San Francisco; Fire Station 22 Golden Gate Park; 16th Ave; 2-story; ground level	5.45	Mw	-999	D	338.41	1.2085E-02	0.07487677	9.6467E-03
12980	21305648	2003	San Francisco; Fire Station 22 Golden Gate Park; 16th Ave; 2-story; ground level	4.00	Mw	-999	D	338.4	1.1427E-02	0.07446805	3.5762E-03
19898	21530368	2006	San Francisco; Fire Station 22 Golden Gate Park; 16th Ave; 2-story; ground level	4.5	Mw	-999	D	338.41	1.1412E-02	0.07356783	6.4207E-03
1931	Anza-02	2001	El Centro Array #10	4.92	Mw	0.2	D	202.85	1.0910E-02	0.04825057	1.2332E-02
18435	21423530	2004	Parkfield - Cholame 5W	4.17	Mw	-999	D	236.6	9.8585E-03	0.04928151	2.7854E-03
76	San Fernando	1971	Maricopa Array #3	6.61	Mw	0.2	C	441.25	0.008986	0.04305249	2.1553E-02
39	Borrego Mtn	1968	Pasadena - CIT Athenaeum	6.63	Mw	0.3	C	415.13	8.2481E-03	0.02304938	3.2231E-02

2135	Big Bear City	2003	Pasadena - USGS/NSMP Office	4.92	Mw	0.2	D	340	7.4202E-03	0.02472001	7.0249E-03
12192	40199209	2007	San Francisco; Fire Station 22 Golden Gate Park; 16th Ave; 2-story; ground level	4.20	Mw	-999	D	338.4	6.5591E-03	0.0390688	4.1462E-03
12334	40194055	2007	San Francisco; Fire Station 22 Golden Gate Park; 16th Ave; 2-story; ground level	4.23	Mw	-999	D	338.4	6.1986E-03	0.01870343	4.2121E-03
21418	51207740	2008	San Francisco; Fire Station 22 Golden Gate Park; 16th Ave; 2-story; ground level	4.1	Mw	-999	D	338.41	5.7295E-03	0.03609781	1.2712E-03
9385	14155260	2005	Pasadena (PASA)	4.88	ML	-999	C	639.7	4.7638E-03	0.02700788	2.0173E-03
21504	51177103	2006	San Francisco; Fire Station 22 Golden Gate Park; 16th Ave; 2-story; ground level	3.6	Mw	-999	D	338.41	4.6635E-03	0.03608573	1.1138E-03
60	San Fernando	1971	Cholame - Shandon Array #2	6.61	Mw	0.2	D	184.75	4.3448E-03	0.01162891	1.7489E-02
20947	21522424	2006	San Francisco; Fire Station 22 Golden Gate Park; 16th Ave; 2-story; ground level	4.3	Mw	-999	D	338.41	3.7740E-03	0.01311636	1.4216E-03

19978	40193843	2007	San Francisco; Fire Station 22 Golden Gate Park; 16th Ave; 2-story; ground level	3.41	ML	-999	D	338.41	3.2067E-03	0.02128124	5.1807E-04
8343	Yorba Linda	2002	Pasadena (PASA)	4.27	Mw	0.2	C	639.74	2.2374E-03	0.008372696	7.3631E-04
19457	21261124	2002	San Francisco; Fire Station 22 Golden Gate Park; 16th Ave; 2-story; ground level	3.6	ML	-999	D	338.41	2.1947E-03	0.01292893	2.0595E-04
20372	30225889	2003	San Francisco; Fire Station 22 Golden Gate Park; 16th Ave; 2-story; ground level	4.12	Mw	-999	D	338.41	1.9516E-03	0.00849217	1.9267E-03
9066	14151344	2005	Pasadena (PASA)	5.20	Mw	-999	C	639.7	1.6920E-03	0.007754528	2.5389E-03
21064	51177644	2007	San Francisco; Fire Station 22 Golden Gate Park; 16th Ave; 2-story; ground level	3.7	Mw	-999	D	338.41	1.4441E-03	0.006286189	6.0103E-04
19427	30225187	2002	San Francisco; Fire Station 22 Golden Gate Park; 16th Ave; 2-story; ground level	3.9	Mw	-999	D	338.41	1.2464E-03	0.07446805	6.1778E-04
20891	21510121	2006	San Francisco; Fire Station 22 Golden	3.7	Mw	-999	D	338.41	1.2442E-03	0.006394793	3.1664E-04

			Gate Park; 16th Ave; 2-story; ground level								
9948	14138080	2005	Pasadena (PASA)	4.59	ML	-999	C	639.7	1.1067E-03	0.004163573	8.8493E-04
13735	9735129	2001	Pasadena (PASA)	3.97	ML	-999	C	639.7	1.1023E-03	0.005707753	1.2484E-04
11428	10275733	2007	Pasadena Art Center, College Of Design	4.73	ML	-999	C	714.0	1.0591E-03	0.002935982	3.7956E-04
21381	51203888	2008	San Francisco; Fire Station 22 Golden Gate Park; 16th Ave; 2-story; ground level	3.5	Mw	-999	D	338.41	9.9741E-04	0.01155717	2.7770E-04
20541	21414391	2004	San Francisco; Fire Station 22 Golden Gate Park; 16th Ave; 2-story; ground level	3.68	Mw	-999	D	338.41	9.9567E-04	0.004726523	3.4306E-04
19640	21339029	2004	San Francisco; Fire Station 22 Golden Gate Park; 16th Ave; 2-story; ground level	3.58	Mw	-999	D	338.41	8.8449E-04	0.003700601	2.1396E-04
20421	30226452	2003	San Francisco; Fire Station 22 Golden Gate Park; 16th Ave; 2-story; ground level	3.5	Mw	-999	D	338.41	7.7876E-04	0.005123554	7.4204E-04
11836	9173365	2001	Pasadena (PASA)	4.26	ML	-999	C	639.7	7.7497E-04	0.004801505	7.8688E-04

19537	30226086	2003	San Francisco; Fire Station 22 Golden Gate Park; 16th Ave; 2-story; ground level	4	Mw	-999	D	338.41	7.0533E-04	0.00417174	5.4133E-04
20710	21437727	2005	San Francisco; Fire Station 22 Golden Gate Park; 16th Ave; 2-story; ground level	4.18	Mw	-999	D	338.41	6.4725E-04	0.003268309	8.7494E-04
19488	21262721	2003	San Francisco; Fire Station 22 Golden Gate Park; 16th Ave; 2-story; ground level	4.3	Mw	-999	D	338.41	6.0343E-04	0.003666785	1.2927E-03
10108	9753485	2002	Pasadena (PASA)	4.18	ML	-999	C	639.7	5.8550E-04	0.002960831	3.8883E-04
20478	21335949	2004	San Francisco; Fire Station 22 Golden Gate Park; 16th Ave; 2-story; ground level	3.71	Mw	-999	D	338.41	5.7851E-04	0.002420711	2.1577E-04
19703	21350824	2004	San Francisco; Fire Station 22 Golden Gate Park; 16th Ave; 2-story; ground level	4.25	Mw	-999	D	338.41	5.6170E-04	0.00334994	1.0631E-03
11738	9069997	1998	Pasadena (PASA)	4.50	-999	-999	C	639.7	5.6152E-04	0.003879517	5.7180E-04
9756	14186612	2005	Pasadena (PASA)	4.69	ML	-999	C	639.7	4.6805E-04	0.002430831	9.8540E-04

19813	21502994	2006	San Francisco; Fire Station 22 Golden Gate Park; 16th Ave; 2-story; ground level	3.6	Mw	-999	D	338.41	4.2217E-04	0.003420092	1.4609E-04
11318	9064093	1998	Pasadena (PASA)	4.78	ML	-999	C	639.7	4.0512E-04	0.00306106	2.5143E-04
8253	Anza-02	2001	Pasadena (PASA)	4.92	Mw	0.2	C	639.74	3.6446E-04	0.004441565	8.7168E-04
14159	3321584	1999	Pasadena (PASA)	3.81	ML	-999	C	639.7	3.5403E-04	0.001572869	3.0285E-05
13431	9941081	2003	Pasadena (PASA)	3.90	ML	-999	C	639.7	3.2399E-04	0.001228838	1.8417E-04
19863	21508102	2006	San Francisco; Fire Station 22 Golden Gate Park; 16th Ave; 2-story; ground level	3.69	ML	-999	D	338.41	3.1662E-04	0.000413862	1.3852E-04
9242	14095628	2004	Pasadena (PASA)	5.03	Mw	-999	C	639.7	2.9899E-04	0.001389978	8.1152E-04
13763	9096960	1999	Pasadena (PASA)	3.88	ML	-999	C	639.7	2.8311E-04	0.00164069	9.2575E-05
14747	9652545	2001	Pasadena (PASA)	3.84	ML	-999	C	639.7	2.1126E-04	0.001596572	7.5098E-05
13963	10972299	2001	Pasadena (PASA)	3.79	ML	-999	C	639.7	1.6578E-04	0.000910549	7.1129E-05
10766	14312160	2007	Pasadena Art Center, College Of Design	4.66	ML	-999	C	714.0	1.4713E-04	0.000735552	7.4225E-05

15004	13692644	2002	Pasadena (PASA)	3.74	ML	-999	C	639.7	1.3598E-04	0.000304873	3.4462E-05
13335	10285533	2007	Pasadena Art Center, College Of Design	4.20	ML	-999	C	714.0	1.3594E-04	0.000470937	2.1073E-05
10256	9983429	2004	Pasadena (PASA)	4.34	ML	-999	C	639.7	1.3391E-04	0.000690208	1.6051E-04
11952	14077668	2004	Pasadena (PASA)	4.27	ML	-999	C	639.7	1.2710E-04	0.000437164	1.0174E-04
14004	9096656	1999	Pasadena (PASA)	4.15	ML	-999	C	639.7	1.2126E-04	0.000811189	5.2105E-05
20509	21397674	2004	San Francisco; Fire Station 22 Golden Gate Park; 16th Ave; 2-story; ground level	3.67	Mw	-999	D	338.41	1.1105E-04	0.000741419	9.3933E-05
13272	10059745	2004	Pasadena (PASA)	4.19	ML	-999	C	639.7	1.1037E-04	0.000486273	6.2851E-05
15120	14079184	2004	Pasadena (PASA)	3.78	ML	-999	C	639.7	1.0275E-04	0.000823788	2.3636E-05
13870	14201764	2005	Pasadena (PASA)	4.17	ML	-999	C	639.7	1.0055E-04	0.00075227	7.9664E-05
12774	14118096	2005	Pasadena (PASA)	4.26	ML	-999	C	639.7	8.6369E-05	0.000554499	9.0381E-05
14557	9655209	2001	Pasadena (PASA)	3.78	ML	-999	C	639.7	7.5117E-05	0.000289544	5.9247E-05
14603	14219360	2006	Pasadena (PASA)	4.11	ML	-999	C	639.7	5.6335E-05	0.000518312	3.2522E-05

13150	14146956	2005	Pasadena (PASA)	4.06	ML	-999	C	639.7	4.3736E-05	0.000326682	2.8133E-05
20141	40204628	2007	Capetown, Ferndale	5.45	Mw	-999	C	560.63	3.9162E-05	8.37814E-05	1.3282E-04
20846	21465580	2005	Capetown, Ferndale	4.77	Mw	-999	C	560.63	3.9062E-05	5.10815E-05	2.7562E-04
14251	14137160	2005	Pasadena (PASA)	3.94	ML	-999	C	639.7	3.3755E-05	0.000229894	3.2552E-05
12707	14330056	2007	Pasadena Art Center, College Of Design	4.34	ML	-999	C	714.0	2.3316E-05	0.000113871	3.8531E-05
13545	10276197	2007	Pasadena Art Center, College Of Design	4.06	ML	-999	C	714.0	2.1540E-05	9.00024E-05	2.6710E-05
15072	10065241	2004	Pasadena (PASA)	3.52	ML	-999	C	639.7	1.6238E-05	0.000105047	1.5447E-05
14463	10207681	2006	Pasadena (PASA)	4.05	ML	-999	C	639.7	1.4115E-05	0.000114962	1.5576E-05
19904	21530368	2006	Capetown, Ferndale	4.5	Mw	-999	C	560.63	8.4983E-06	2.19653E-05	4.2829E-05
20382	30225889	2003	Capetown, Ferndale	4.12	Mw	-999	C	560.63	7.4723E-06	1.47706E-05	4.1589E-05
19576	30226086	2003	Capetown, Ferndale	4	Mw	-999	C	560.63	7.1419E-06	1.28475E-05	3.9185E-05
21029	21526081	2006	Capetown, Ferndale	3.7	Mw	-999	C	560.63	4.0209E-06	2.15926E-05	1.6124E-05

20104	40199209	2007	Capetown, Ferndale	4.2	Mw	-999	C	560.63	3.0947E-06	1.67403E-05	2.0947E-05

A2. Summary of results in MR

Table 47. Summary of results in MR

Event Name/ Station	Station Name	Year	Magnitude	Unit	Max Story Drift	%	Story Max Avg Drift (mm)	Avg Drift	Ratio	Direction	PGA (g)	Preferred NEHRP Based on Vs30	Floor
Iwate	AKTH04	2008	6.90	Mw	0.016438	1.644%	65.095	32.625	1.995	X	1.76830	C	3rd Floor
Northridge-01	Tarzana - Cedar Hill A	1994	6.69	Mw	0.071	7.100%	281.161	141.085	1.993	X	1.64400	D	3rd Floor
Niigata, Japan	NIG021	2004	6.63	Mw	0.013353	1.335%	52.876	26.503	1.995	X	1.47620	C	3rd Floor
Cape Mendocino	Cape Mendocino	1992	7.01	Mw	0.061811	6.181%	244.772	122.772	1.994	X	1.39630	C	3rd Floor
Christchurch, New Zealand	Heathcote Valley Primary School	2011	6.2	Mw	0.038911	3.891%	154.087	77.251	1.995	X	1.39140	C	3rd Floor
Northridge-01	Pacoima Dam (upper left)	1994	6.69	Mw	0.034054	3.41%	134.854	67.632	1.994	X	1.38890	A	3rd Floor
Iwate	IWTH25	2008	6.9	Mw	0.090582	9.06%	358.706	179.847	1.995	X	1.35420	C	3rd Floor
Niigata, Japan	NIG019	2004	6.63	Mw	0.077818	7.78%	308.161	154.458	1.995	X	1.25510	C	3rd Floor
San Fernando	Pacoima Dam (upper left abut)	1971	6.61	Mw	0.029292	2.93%	115.996	58.172	1.994	X	1.22170	A	3rd Floor
Nahanni, Canada	Site 1	1985	6.76	Mw	0.019101	1.910%	75.638	38.06	1.987	X	1.16010	C	3rd Floor
Chuetsu-oki	Kashiwazaki NPP, Unit 5: ground surface	2007	6.80	Mw	0.076881	7.688%	304.448	152.772	1.993	X	1.15370	D	3rd Floor
Baja California	Cerro Prieto	1987	5.50	Mw	0.04471	4.471%	177.053	88.801	1.994	X	1.13940	C	3rd Floor
Parkfield-02, CA	Parkfield - Fault Zone 14	2004	6.00	Mw	0.044416	4.442%	175.887	88.23	1.994	X	1.03780	D	3rd Floor

Iwate	IWTH26	2008	6.9	Mw	0.043764	4.38%	173.304	86.921	1.994	X	1.03260	C	3rd Floor
Duzce, Turkey	IRIGM 496	1999	7.14	Mw	0.01721	1.721%	68.15	34.167	1.995	X	0.99619	B	3rd Floor
Morgan Hill	Coyote Lake Dam - Southwest Abutment	1984	6.19	Mw	0.038495	3.850%	152.44	76.504	1.993	X	0.93939	C	3rd Floor
Christchurch, New Zealand	LPCC	2011	6.2	Mw	0.031944	3.19%	126.499	63.455	1.994	X	0.93132	C	3rd Floor
Chuetsu-oki	Kashiwazaki NPP, Unit 1: ground surface	2007	6.8	Mw	0.103482	10.35%	409.788	205.604	1.993	X	0.88823	D	3rd Floor
Chuetsu-oki	Kashiwazaki Nishiyamacho Ikeura	2007	6.8	Mw	0.053598	5.36%	212.25	106.505	1.993	X	0.86274	C	3rd Floor
Coalinga-05	Transmitter Hill	1983	5.77	Mw	0.028938	2.89%	114.595	57.467	1.994	X	0.84463	C	3rd Floor
Tottori, Japan	TTRH02	2000	6.61	Mw	0.057855	5.786%	229.108	114.981	1.993	X	0.84161	D	3rd Floor
Chi-Chi, Taiwan	CHY080	1999	7.62	Mw	0.154656	15.466%	612.437	307.309	1.993	X	0.83236	C	3rd Floor
Parkfield-02, CA	Parkfield - Fault Zone 11	2004	6	Mw	0.007892	0.79%	31.252	15.672	1.994	X	0.82618	C	3rd Floor
Tabas, Iran	Tabas	1978	7.35	Mw	0.082347	8.235%	326.093	163.659	1.993	X	0.81245	B	3rd Floor
Duzce, Turkey	Bolu	1999	7.14	Mw	0.046038	4.60%	182.312	91.384	1.995	X	0.77559	D	3rd Floor
Kobe, Japan	KJMA	1995	6.90	Mw	0.118129	11.813%	467.792	234.626	1.994	X	0.77525	D	3rd Floor
Chi-Chi, Taiwan	CHY028	1999	7.62	Mw	0.057032	5.70%	225.847	113.307	1.993	X	0.76760	C	3rd Floor
Northridge-01	Jensen Filter Plant Generator Building	1994	6.69	Mw	0.052074	5.21%	206.211	103.484	1.993	X	0.76045	C	3rd Floor
Northridge-01	LA - Sepulveda VA Hospital	1994	6.69	Mw	0.070757	7.08%	280.197	140.484	1.995	X	0.75323	C	3rd Floor
Chi-Chi, Taiwan	TCU129	1999	7.62	Mw	0.063744	6.37%	252.428	126.621	1.994	X	0.75149	C	3rd Floor
Tottori, Japan	TTR007	2000	6.61	Mw	0.016889	1.69%	66.882	33.494	1.997	X	0.74266	C	3rd Floor
Niigata, Japan	NIGH01	2004	6.63	Mw	0.057364	5.74%	227.16	114.001	1.993	X	0.74056	C	3rd Floor

Chi-Chi, Taiwan	TCU084	1999	7.62	Mw	0.194484	19.45%	770.155	386.361	1.993	X	0.73785	C	3rd Floor
Bam, Iran	Bam	2003	6.6	Mw	0.127084	12.708%	503.253	252.526	1.993	X	0.73768	C	3rd Floor
Darfield, New Zealand	GDLC	2010	7.00	Mw	0.100566	10.057%	398.241	199.866	1.993	X	0.73113	D	3rd Floor
Superstition Hills-02	Superstition Mtn Camera	1987	6.54	Mw	0.048592	4.859%	192.424	96.457	1.995	X	0.72878	C	3rd Floor
Landers	Lucerne	1992	7.28	Mw	0.001931	0.193%	7.647	3.81	2.007	X	0.72724	B	3rd Floor
Iwate	MYG004	2008	6.9	Mw	0.031518	3.15%	124.811	62.617	1.993	X	0.72576	C	3rd Floor
Tottori, Japan	SMNH01	2000	6.61	Mw	0.012097	1.21%	47.902	24.035	1.993	X	0.71988	C	3rd Floor
Mammoth Lakes-06	Long Valley Dam (Upr L Abut)	1980	5.94	Mw	0.016852	1.685%	66.734	33.465	1.994	X	0.71928	C	3rd Floor
Parkfield-02, CA	Parkfield - Stone Corral 1E	2004	6.00	Mw	0.021926	2.193%	86.826	43.544	1.994	X	0.71667	D	20th Floor
Northridge-01	Rinaldi Receiving Sta	1994	6.69	Mw	0.145852	14.59%	577.573	289.838	1.993	X	0.70785	D	3rd Floor
Chi-Chi, Taiwan-06	TCU079	1999	6.30	Mw	0.015911	1.591%	63.008	31.584	1.995	X	0.70445	C	3rd Floor
Gazli, USSR	Karakyr	1976	6.80	Mw	0.056844	5.684%	225.1	112.96	1.993	X	0.70178	D	3rd Floor
Northridge-01	Sylmar - Converter Sta	1994	6.69	Mw	0.097633	9.76%	386.626	193.862	1.994	X	0.69753	D	3rd Floor
Chi-Chi, Taiwan	TCU065	1999	7.62	Mw	0.089879	8.99%	355.923	178.534	1.994	X	0.68938	D	3rd Floor
Chi-Chi, Taiwan-03	TCU129	1999	6.20	Mw	0.007934	0.793%	31.419	15.739	1.996	X	0.68877	C	3rd Floor
Imperial Valley-06	Bonds Corner	1979	6.53	Mw	0.023468	2.347%	92.935	46.62	1.993	X	0.68661	D	3rd Floor
Northridge-01	Sylmar - Converter Sta East	1994	6.69	Mw	0.065826	6.58%	260.67	130.787	1.993	X	0.68610	C	3rd Floor

Coalinga-05	Oil City	1983	5.77	Mw	0.027453	2.75%	108.712	54.48	1.995	X	0.68604	C	3rd Floor
N. Palm Springs	North Palm Springs	1986	6.06	Mw	0.065246	6.525%	258.375	129.651	1.993	X	0.68434	D	3rd Floor
Duzce, Turkey	Lamont 375	1999	7.14	Mw	0.009142	0.91%	36.202	18.143	1.995	X	0.68064	C	3rd Floor
Kobe, Japan	Takatori	1995	6.9	Mw	0.218854	21.89%	866.662	434.839	1.993	X	0.67218	D	3rd Floor
Tottori, Japan	OKY004	2000	6.61	Mw	0.005796	0.58%	22.954	11.519	1.993	X	0.65993	C	3rd Floor
Northridge-01	Newhall - Fire Sta	1994	6.69	Mw	0.081835	8.18%	324.068	162.636	1.993	X	0.65430	D	3rd Floor
Kobe, Japan	Takarazuka	1995	6.9	Mw	0.090485	9.05%	358.319	179.691	1.994	X	0.65400	D	3rd Floor
Parkfield-02, CA	Parkfield - Cholame 3E	2004	6	Mw	0.009237	0.92%	36.58	18.342	1.994	X	0.65141	C	3rd Floor
Niigata, Japan	NIG028	2004	6.63	Mw	0.02191	2.19%	86.764	43.531	1.993	X	0.64783	C	3rd Floor
Christchurch, New Zealand	Pages Road Pumping Station	2011	6.2	Mw	0.108423	10.84%	429.357	215.295	1.994	X	0.64750	E	3rd Floor
Parkfield-02, CA	Parkfield - Fault Zone 1	2004	6	Mw	0.07024	7.02%	278.149	139.589	1.993	X	0.64455	E	3rd Floor
Northridge-01	Simi Valley - Katherine Rd	1994	6.69	Mw	0.048872	4.89%	193.535	97.113	1.993	X	0.64410	C	3rd Floor
Northridge-01	Sylmar - Olive View Med FF	1994	6.69	Mw	0.065687	6.57%	260.12	130.554	1.992	X	0.64005	C	3rd Floor
Chuetsu-oki	NIG018	2007	6.8	Mw	0.110835	11.08%	438.905	220.184	1.993	X	0.62519	D	3rd Floor
Northridge-01	Santa Monica City Hall	1994	6.69	Mw	0.03414	3.41%	135.193	67.845	1.993	X	0.62478	D	3rd Floor
Cape Mendocino	Petrolia	1992	7.01	Mw	2.9665E-02	2.97%	117.472	58.937	1.993	X	0.62397	C	3rd Floor
Tottori, Japan	TTR009	2000	6.61	Mw	0.013807	1.38%	54.677	27.397	1.996	X	0.62177	C	3rd Floor
Chuetsu-oki	Joetsu Oshimaku Oka	2007	6.8	Mw	0.015134	1.51%	59.931	30.045	1.995	X	0.62016	C	3rd Floor
Victoria, Mexico	Cerro Prieto	1980	6.33	Mw	0.048261	4.826%	191.112	95.861	1.994	X	0.61451	C	3rd Floor
Parkfield-02, CA	Parkfield - Gold Hill 3W	2004	6	Mw	0.007909	0.79%	31.32	15.692	1.996	X	0.60451	C	3rd Floor
N. Palm Springs	Whitewater Trout Farm	1986	6.06	Mw	0.019315	1.932%	76.488	38.338	1.995	X	0.59665	C	3rd Floor

Chi-Chi, Taiwan	TCU071	1999	7.62	Mw	0.056601	5.66%	224.14	112.43	1.994	X	0.59346	C	3rd Floor
Umbria Marche (aftershock 7), Italy	Nocera Umbra	1997	4.3	ML	0.001027	0.103%	4.068	2.013	2.021	X	0.59217	C	3rd Floor
Loma Prieta	LGPC	1989	6.93	Mw	0.107531	10.753%	425.823	213.557	1.994	X	0.59012	C	3rd Floor
Whittier Narrows-01	Tarzana - Cedar Hill	1987	5.99	Mw	0.005672	0.57%	22.462	11.246	1.997	X	0.58926	D	3rd Floor
Iwate	Kurihara City	2008	6.9	Mw	0.033796	3.38%	133.833	67.118	1.994	X	0.58540	C	3rd Floor
San Salvador	Geotech Investig Center	1986	5.80	Mw	0.057227	5.723%	226.618	113.7	1.993	X	0.57610	C	3rd Floor
Darfield, New Zealand	Heathcote Valley Primary School	2010	7	Mw	0.011037	1.10%	43.707	21.883	1.997	X	0.57386	C	3rd Floor
Chuetsu-oki	Kashiwazaki City Center	2007	6.8	Mw	0.09185	9.19%	363.725	182.452	1.994	X	0.57362	D	3rd Floor
Chuetsu-oki	Oguni Nagaoka	2007	6.8	Mw	0.02783	2.78%	110.206	55.277	1.994	X	0.56615	C	3rd Floor
Chuetsu-oki	Iizuna Imokawa	2007	6.8	Mw	0.049416	4.94%	195.687	98.174	1.993	X	0.56511	C	3rd Floor
Parkfield-02, CA	PARKFIELD - JOAQUIN CANYON	2004	6	Mw	0.011672	1.17%	46.219	23.185	1.993	X	0.55980	C	3rd Floor
Coalinga-07	Coalinga-14th & Elm (Old CHP)	1983	5.21	Mw	0.007571	0.757%	29.98	15.019	1.996	X	0.55960	D	3rd Floor
Parkfield-02, CA	Parkfield - Cholame 4W	2004	6	Mw	0.01588	1.59%	62.884	31.55	1.993	X	0.55915	C	3rd Floor
Chi-Chi, Taiwan	TCU095	1999	7.62	Mw	0.016661	1.67%	65.978	33.087	1.994	X	0.55847	C	3rd Floor
L'Aquila, Italy	L'Aquila - V. Aterno - Centro Valle	2009	6.30	Mw	0.028786	2.879%	113.994	57.183	1.993	X	0.55844	C	3rd Floor
Coalinga-02	Anticline Ridge Free-Field	1983	5.09	Mw	0.003657	0.366%	14.483	7.242	2	X	0.55772	C	3rd Floor

Chuetsu-oki	Kashiwazaki City Takayanagicho	2007	6.8	Mw	0.040528	4.05%	160.489	80.524	1.993	X	0.55485	C	3rd Floor
Chi-Chi, Taiwan-06	TCU080	1999	6.3	Mw	0.027047	2.70%	107.106	53.736	1.993	X	0.54809	C	3rd Floor
Loma Prieta	WAHO	1989	6.93	Mw	0.03039	3.039%	120.346	60.376	1.993	X	0.53730	C	3rd Floor
Northridge-01	Beverly Hills - 12520 Mulhol	1994	6.69	Mw	0.02856	2.86%	113.098	56.731	1.994	X	0.53527	C	3rd Floor
Northridge-06	Rinaldi Receiving Sta	1994	5.28	Mw	0.011446	1.145%	45.326	22.707	1.996	X	0.52820	D	3rd Floor
Imperial Valley-06	El Centro Array #8	1979	6.53	Mw	0.071959	7.20%	284.956	142.931	1.994	X	0.52691	D	3rd Floor
Big Bear-01	Big Bear Lake - Civic Center	1992	6.46	Mw	0.010008	1.001%	39.632	19.863	1.995	X	0.52458	C	3rd Floor
Northridge-01	Jensen Filter Plant Administrative Building	1994	6.69	Mw	0.086494	8.65%	342.517	171.632	1.996	X	0.52425	C	3rd Floor
Manjil, Iran	Abbar	1990	7.37	Mw	0.027375	2.738%	108.406	54.368	1.994	X	0.52348	C	3rd Floor
Christchurch, New Zealand	Christchurch Resthaven	2011	6.2	Mw	0.087064	8.71%	344.775	173.034	1.993	X	0.52141	E	3rd Floor
Chi-Chi, Taiwan	TCU088	1999	7.62	Mw	0.01428	1.43%	56.548	28.313	1.997	X	0.52104	C	3rd Floor
Coalinga-01	Pleasant Valley P.P. - yard	1983	6.36	Mw	0.053238	5.324%	210.821	105.762	1.993	X	0.52073	D	3rd Floor
El Mayor-Cucapah	El Centro Differential Array	2010	7.20	Mw	0.018717	1.872%	74.121	37.16	1.995	X	0.50737	D	3rd Floor
Stone Canyon	Melendy Ranch	1972	4.81	Mw	0.002426	0.243%	9.606	4.795	2.003	X	0.49551	C	3rd Floor
Mammoth Lakes-04	Convict Creek	1980	5.70	Mw	0.00795	0.795%	31.482	15.775	1.996	X	0.48420	C	3rd Floor

Umbria Marche, Italy	Nocera Umbra	1997	6	Mw	0.014769	1.477%	58.484	29.335	1.994	X	0.47255	C	3rd Floor
Yountville	Napa Fire Station #3	2000	5.00	Mw	0.019788	1.979%	78.359	39.295	1.994	X	0.45971	D	3rd Floor
Ancona-09, Italy	Ancona-Rocca	1972	4.7	ML	0.00011	0.011%	0.436	0.032	13.613	Y	0.45027	C	20th Floor
Erzican, Turkey	Erzincan	1992	6.69	Mw	0.087659	8.766%	347.131	174.168	1.993	X	0.44499	D	3rd Floor
Mammoth Lakes-01	Convict Creek	1980	6.06	Mw	0.033063	3.306%	130.931	65.652	1.994	X	0.43915	C	3rd Floor
Whittier Narrows-01	Garvey Res. - Control Bldg	1987	5.99	Mw	0.008403	0.840%	33.275	16.665	1.997	X	0.43646	C	3rd Floor
Coalinga-05	Coalinga-14th & Elm (Old CHP)	1983	5.77	Mw	0.005457	0.546%	21.609	10.819	1.997	X	0.42486	D	3rd Floor
Whittier Narrows-02	Pasadena - Old House Rd	1987	5.27	Mw	0.004235	0.424%	16.771	8.403	1.996	X	0.38617	C	3rd Floor
El Mayor-Cucapah	El Centro - Meloland Geot. Array	2010	7.20	Mw	0.014041	1.404%	55.602	27.873	1.995	X	0.37814	D	3rd Floor
Cape Mendocino	Ferndale Fire Station	1992	7.01	Mw	0.080362	8.036%	318.235	159.624	1.994	X	0.29416	C	4th Floor
Superstition Hills-02	El Centro Imp. Co. Cent	1987	6.54	Mw	0.047101	4.710%	186.521	93.505	1.995	X	0.26118	D	3rd Floor
Imperial Valley-02	El Centro Array #9	1940	6.95	Mw	0.026847	2.685%	106.316	53.319	1.994	X	0.23349	D	3rd Floor
Parkfield-02, CA	Parkfield - Cholame 5W	2004	6.00	Mw	0.01028	1.028%	40.709	20.396	1.996	X	0.23324	D	3rd Floor
Sierra Madre	Pasadena - USGS/NSMP Office	1991	5.61	Mw	0.007852	0.785%	31.092	15.576	1.996	X	0.23178	D	3rd Floor

Northridge-01	Pasadena - N Sierra Madre	1994	6.69	Mw	0.006964	0.696%	27.576	13.815	1.996	X	0.23087	C	3rd Floor
Northern Calif-03	Ferndale City Hall	1954	6.50	U	0.046884	4.688%	185.659	93.177	1.993	X	0.18616	D	3rd Floor
Northern Calif-05	Ferndale City Hall	1967	5.60	Mw	0.005251	0.525%	20.794	10.407	1.998	X	0.18406	D	3rd Floor
Coalinga-06	Coalinga-14th & Elm (Old CHP)	1983	4.89	Mw	0.001762	0.176%	6.979	3.475	2.008	X	0.15109	D	3rd Floor
Imperial Valley-06	El Centro Array #1	1979	6.53	Mw	0.008588	0.859%	34.01	17.042	1.996	X	0.14458	D	3rd Floor
Whittier Narrows-01	Pasadena - CIT Athenaeum	1987	5.99	Mw	0.01024	1.024%	40.549	20.321	1.995	X	0.14147	C	3rd Floor
Hollister-03	Hollister City Hall	1974	5.14	Mw	0.002318	0.232%	9.18	4.581	2.004	X	0.14070	D	3rd Floor
Northwest Calif-01	Ferndale City Hall	1938	5.50	Mw	0.003456	0.346%	13.688	6.841	2.001	X	0.12218	D	3rd Floor
Northwest Calif-03	Ferndale City Hall	1951	5.80	Mw	0.004778	0.478%	18.921	9.465	1.999	X	0.10709	D	3rd Floor
San Fernando	Pasadena - CIT Athenaeum	1971	6.61	Mw	0.006388	0.639%	25.296	12.669	1.997	X	0.10575	C	3rd Floor
Borrego Mtn	El Centro Array #9	1968	6.63	Mw	0.030022	3.002%	118.887	59.636	1.994	X	0.09402	D	3rd Floor
San Fernando	Fairmont Dam	1971	6.61	Mw	0.001379	0.138%	5.46	2.715	2.011	X	0.09386	C	3rd Floor
Northern Calif-07	Ferndale City Hall	1975	5.20	Mw	0.003339	0.334%	13.223	6.61	2.001	X	0.09005	D	3rd Floor
San Francisco	Golden Gate Park	1957	5.28	Mw	0.000717	0.072%	2.839	1.415	2.007	X	0.08627	B	3rd Floor
Hollister-01	Hollister City Hall	1961	5.60	U	0.010755	1.076%	42.591	21.339	1.996	X	0.08499	D	3rd Floor

Morgan Hill	Hollister City Hall	1984	6.19	Mw	0.011488	1.149%	45.491	22.83	1.993	X	0.07013	D	3rd Floor
Northern Calif-02	Ferndale City Hall	1952	5.20	Mw	0.005958	0.596%	23.593	11.817	1.997	X	0.06843	D	3rd Floor
Northern Calif-04	Ferndale City Hall	1960	5.70	Mw	0.00341	0.341%	13.505	6.751	2.001	X	0.06709	D	3rd Floor
Hollister-02	Hollister City Hall	1961	5.50	U	0.006229	0.623%	24.665	12.353	1.997	X	0.06235	D	3rd Floor
CA/Baja Border Area	El Centro Array #10	2002	5.31	Mw	0.00166	0.166%	6.573	3.273	2.008	X	0.06046	D	3rd Floor
Parkfield	Cholame - Shandon Array #12	1966	6.19	Mw	0.00749	0.749%	29.661	14.883	1.993	X	0.05867	C	3rd Floor
Imperial Valley-07	El Centro Array #10	1979	5.01	Mw	0.000929	0.093%	3.68	1.837	2.003	X	0.05253	D	3rd Floor
Borrego	El Centro Array #9	1942	6.50	U	0.010441	1.044%	41.348	20.724	1.995	X	0.05225	D	3rd Floor
Kern County	Pasadena - CIT Athenaeum	1952	7.36	Mw	0.00814	0.814%	32.233	16.146	1.996	X	0.05100	C	3rd Floor
Northwest Calif-02	Ferndale City Hall	1941	6.60	U	0.00381	0.381%	38.2	22.82	12.49	X	0.04942	D	3rd Floor
Central Calif-01	Hollister City Hall	1954	5.30	U	0.002959	0.296%	11.716	5.853	2.002	X	0.04768	D	3rd Floor
El Alamo	El Centro Array #9	1956	6.80	U	0.003909	0.391%	15.481	7.743	1.999	X	0.04495	D	3rd Floor
Coalinga-01	Parkfield - Cholame 12W	1983	6.36	Mw	0.011774	1.177%	46.626	23.382	1.994	X	0.04495	D	3rd Floor
Imperial Valley-05	El Centro Array #9	1955	5.40	U	0.00395	0.395%	15.642	7.825	1.999	X	0.04424	D	3rd Floor
Northridge-06	Pasadena - USGS/NSMP Office	1994	5.28	Mw	0.001153	0.115%	4.565	2.264	2.016	X	0.04176	D	3rd Floor

Humbolt Bay	Ferndale City Hall	1937	5.80	Mw	0.002442	0.244%	9.67	4.827	2.003	X	0.04096	D	3rd Floor
Hector Mine	Pasadena - Fair Oaks & Walnut	1999	7.13	Mw	0.004255	0.426%	16.849	8.428	1.999	X	0.03528	C	3rd Floor
Mammoth Lakes-07	USC Cash Baugh Ranch	1980	4.73	Mw	0.004653	0.465%	18.425	9.221	1.998	X	0.02990	D	3rd Floor
Imperial Valley-03	El Centro Array #9	1951	5.60	U	0.001738	0.174%	6.881	3.428	2.007	X	0.02936	D	3rd Floor
Imperial Valley-04	El Centro Array #9	1953	5.50	U	0.000315	0.032%	1.246	0.6	2.077	X	0.02793	D	3rd Floor
40238431	Parkfield - Cholame 5W	2009	4.39	Mw		0.000%	0.909	0.004	217.13		0.02028	D	
Imperial Valley-01	El Centro Array #9	1938	5.00	U	0.000359	0.036%	1.42	0.687	2.067	X	0.01845	D	3rd Floor
51182151	Parkfield - Cholame 5W	2007	4.01	Mw	0.00011	0.011%	0.445	0.001	541.045	X	0.01839	D	3rd Floor
Gulf of California	El Centro Array #9	2001	5.70	Mw	0.002446	0.245%	8.998	4.492	2.003	X	0.01828	D	3rd Floor
Northern Calif-06	Hollister City Hall	1967	5.20	U	0.001752	0.175%	6.937	3.456	2.007	X	0.01528	D	3rd Floor
Hector Mine	El Centro Array #10	1999	7.13	Mw	0.004758	0.476%	18.842	9.427	1.999	X	0.01454	D	3rd Floor
40204628	San Francisco; Fire Station 22 Golden Gate Park; 16th Ave; 2-story; ground level	2007	5.45	Mw	0.000307	0.031%	1.214	0.584	2.08	X	0.01209	D	3rd Floor
21305648	San Francisco; Fire Station 22 Golden Gate	2003	4.00	Mw	0.00011	0.011%	0.445	0.001	362.584	X	0.01143	D	1st Floor

	Park; 16th Ave; 2-story; ground level												
21530368	San Francisco; Fire Station 22 Golden Gate Park; 16th Ave; 2-story; ground level	2006	4.5	Mw	0.00011	0.011%	0.445	0.001	395.012	X	0.01141	D	1st Floor
Anza-02	El Centro Array #10	2001	4.92	Mw	0.000572	0.057%	2.265	1.111	2.038	X	0.01091	D	3rd Floor
21423530	Parkfield - Cholame 5W	2004	4.17	Mw	0.00011	0.011%	0.445	0.001	440.766	X	0.00986	D	3rd Floor
San Fernando	Maricopa Array #3	1971	6.61	Mw	0.00392	0.392%	15.525	7.757	2.001	X	0.00899	C	3rd Floor
Borrego Mtn	Pasadena - CIT Athenaeum	1968	6.63	Mw	0.002313	0.231%	9.159	4.572	2.003	X	0.00825	C	3rd Floor
Big Bear City	Pasadena - USGS/NSMP Office	2003	4.92	Mw	0.000247	0.025%	0.979	0.466	2.101	X	0.00742	D	3rd Floor
40199209	San Francisco; Fire Station 22 Golden Gate Park; 16th Ave; 2-story; ground level	2007	4.20	Mw	0.000119	0.012%	0.47	0.21	2.236	X	0.00656	D	20th Floor
40194055	San Francisco; Fire Station 22 Golden Gate Park; 16th Ave; 2-story; ground level	2007	4.23	Mw	0.445	44.50%	0.445	0.001	467.471	X	0.00620	D	1st Floor
51207740	San Francisco; Fire Station 22 Golden Gate Park; 16th Ave; 2-story; ground level	2008	4.1	Mw	0.00011	0.011%	0.436	0.032	13.613	Y	0.00573	D	20th Floor

14155260	Pasadena (PASA)	2005	4.88	ML	0.00011	0.011%	0.445	0.001	514.612	X	0.00476	C	1st Floor
51177103	San Francisco; Fire Station 22 Golden Gate Park; 16th Ave; 2-story; ground level	2006	3.6	Mw	0.00011	0.011%	0.436	0.032	13.613	Y	0.00466	D	20th Floor
San Fernando	Cholame - Shandon Array #2	1971	6.61	Mw	0.001168	0.117%	4.627	2.311	2.002	X	0.00434	D	3rd Floor
21522424	San Francisco; Fire Station 22 Golden Gate Park; 16th Ave; 2-story; ground level	2006	4.3	Mw	0.00011	0.011%	0.445	0.001	591.261	X	0.00377	D	1st Floor
40193843	San Francisco; Fire Station 22 Golden Gate Park; 16th Ave; 2-story; ground level	2007	3.41	ML	0.00011	0.011%	0.436	0.032	13.613	Y	0.00321	D	20th Floor
Yorba Linda	Pasadena (PASA)	2002	4.27	Mw	0.00011	0.011%	0.444	0.001	727.451	X	0.00224	C	1st Floor
21261124	San Francisco; Fire Station 22 Golden Gate Park; 16th Ave; 2-story; ground level	2002	3.6	ML	0.00011	0.011%	0.436	0.032	13.613	Y	0.00219	D	20th Floor
30225889	San Francisco; Fire Station 22 Golden Gate Park; 16th Ave; 2-story; ground level	2003	4.12	Mw	0.00011	0.011%	0.436	0.032	13.613	Y	0.00195	D	20th Floor
14151344	Pasadena (PASA)	2005	5.20	Mw	0.00011	0.011%	0.445	0.001	545.884	X	0.00169	C	1st Floor

51177644	San Francisco; Fire Station 22 Golden Gate Park; 16th Ave; 2-story; ground level	2007	3.7	Mw	0.00011	0.011%	0.436	0.032	13.613	Y	0.00144	D	20th Floor
30225187	San Francisco; Fire Station 22 Golden Gate Park; 16th Ave; 2-story; ground level	2002	3.9	Mw	0.00011	0.011%	0.436	0.032	13.613	Y	0.00125	D	20th Floor
21510121	San Francisco; Fire Station 22 Golden Gate Park; 16th Ave; 2-story; ground level	2006	3.7	Mw	0.00011	0.011%	0.436	0.032	13.613	Y	0.00124	D	20th Floor
14138080	Pasadena (PASA)	2005	4.59	ML	0.00011	0.011%	0.436	0.032	13.613	Y	0.00111	C	20th Floor
9735129	Pasadena (PASA)	2001	3.97	ML	0.00011	0.011%	0.436	0.032	13.613	Y	0.00110	C	20th Floor
10275733	Pasadena Art Center, College Of Design	2007	4.73	ML	0.00011	0.011%	0.436	0.032	13.613	Y	0.00106	C	20th Floor
51203888	San Francisco; Fire Station 22 Golden Gate Park; 16th Ave; 2-story; ground level	2008	3.5	Mw	0.00011	0.011%	0.436	0.032	13.613	Y	0.00100	D	20th Floor
21414391	San Francisco; Fire Station 22 Golden Gate	2004	3.68	Mw	0.00011	0.011%	0.436	0.032	13.613	Y	0.00100	D	20th Floor

	Park; 16th Ave; 2-story; ground level												
21339029	San Francisco; Fire Station 22 Golden Gate Park; 16th Ave; 2-story; ground level	2004	3.58	Mw	0.00011	0.011%	0.436	0.032	13.613	Y	0.00088	D	20th Floor
30226452	San Francisco; Fire Station 22 Golden Gate Park; 16th Ave; 2-story; ground level	2003	3.5	Mw	0.00011	0.011%	0.436	0.032	13.613	Y	0.00078	D	20th Floor
9173365	Pasadena (PASA)	2001	4.26	ML	0.00011	0.011%	0.436	0.032	13.613	Y	0.00077	C	20th Floor
30226086	San Francisco; Fire Station 22 Golden Gate Park; 16th Ave; 2-story; ground level	2003	4	Mw	0.00011	0.011%	0.436	0.032	13.613	Y	0.00071	D	20th Floor
21437727	San Francisco; Fire Station 22 Golden Gate Park; 16th Ave; 2-story; ground level	2005	4.18	Mw	0.00011	0.011%	0.436	0.032	13.613	Y	0.00065	D	20th Floor
21262721	San Francisco; Fire Station 22 Golden Gate Park; 16th Ave; 2-story; ground level	2003	4.3	Mw	0.00011	0.011%	0.436	0.032	13.613	Y	0.00060	D	20th Floor

9753485	Pasadena (PASA)	2002	4.18	ML	0.00011	0.011%	0.436	0.032	13.613	Y	0.00059	C	20th Floor
21335949	San Francisco; Fire Station 22 Golden Gate Park; 16th Ave; 2-story; ground level	2004	3.71	Mw	0.00011	0.011%	0.436	0.032	13.613	Y	0.00058	D	20th Floor
21350824	San Francisco; Fire Station 22 Golden Gate Park; 16th Ave; 2-story; ground level	2004	4.25	Mw	0.00011	0.011%	0.436	0.032	13.613	Y	0.00056	D	20th Floor
9069997	Pasadena (PASA)	1998	4.50	-999	0.00011	0.011%	0.436	0.032	13.613	Y	0.00056	C	20th Floor
14186612	Pasadena (PASA)	2005	4.69	ML	0.00011	0.011%	0.436	0.032	13.613	Y	0.00047	C	20th Floor
21502994	San Francisco; Fire Station 22 Golden Gate Park; 16th Ave; 2-story; ground level	2006	3.6	Mw	0.00011	0.011%	0.436	0.032	13.613	Y	0.00042	D	20th Floor
9064093	Pasadena (PASA)	1998	4.78	ML	0.00011	0.011%	0.436	0.032	13.613	Y	0.00041	C	20th Floor
Anza-02	Pasadena (PASA)	2001	4.92	Mw	0.00011	0.011%	0.444	0.001	650.589	X	0.00036	C	1st Floor
3321584	Pasadena (PASA)	1999	3.81	ML	0.00011	0.011%	0.436	0.032	13.613	Y	0.00035	C	20th Floor
9941081	Pasadena (PASA)	2003	3.90	ML	0.00011	0.011%	0.436	0.032	13.613	Y	0.00032	C	20th Floor

21508102	San Francisco; Fire Station 22 Golden Gate Park; 16th Ave; 2-story; ground level	2006	3.69	ML	0.00011	0.011%	0.436	0.032	13.613	Y	0.00032	D	20th Floor
14095628	Pasadena (PASA)	2004	5.03	Mw	0.00011	0.011%	0.436	0.032	13.613	Y	0.00030	C	20th Floor
9096960	Pasadena (PASA)	1999	3.88	ML	0.00011	0.011%	0.436	0.032	13.613	Y	0.00028	C	20th Floor
9652545	Pasadena (PASA)	2001	3.84	ML	0.00011	0.011%	0.436	0.032	13.613	Y	0.00021	C	20th Floor
10972299	Pasadena (PASA)	2001	3.79	ML	0.00011	0.011%	0.436	0.032	13.613	Y	0.00017	C	20th Floor
14312160	Pasadena Art Center, College Of Design	2007	4.66	ML	0.00011	0.011%	0.436	0.032	13.613	Y	0.00015	C	20th Floor
13692644	Pasadena (PASA)	2002	3.74	ML	0.00011	0.011%	0.436	0.032	13.613	Y	0.00014	C	20th Floor
10285533	Pasadena Art Center, College Of Design	2007	4.20	ML	0.00011	0.011%	0.436	0.032	13.613	Y	0.00014	C	20th Floor
9983429	Pasadena (PASA)	2004	4.34	ML	0.00011	0.011%	0.436	0.032	13.613	Y	0.00013	C	20th Floor
14077668	Pasadena (PASA)	2004	4.27	ML	0.00011	0.011%	0.436	0.032	13.613	Y	0.00013	C	20th Floor
9096656	Pasadena (PASA)	1999	4.15	ML	0.00011	0.011%	0.436	0.032	13.613	Y	0.00012	C	20th Floor

21397674	San Francisco; Fire Station 22 Golden Gate Park; 16th Ave; 2-story; ground level	2004	3.67	Mw	0.00011	0.011%	0.436	0.032	13.613	Y	0.00011	D	20th Floor
10059745	Pasadena (PASA)	2004	4.19	ML	0.00011	0.011%	0.436	0.032	13.613	Y	0.00011	C	20th Floor
14079184	Pasadena (PASA)	2004	3.78	ML	0.00011	0.011%	0.436	0.032	13.613	Y	0.00010	C	20th Floor
14201764	Pasadena (PASA)	2005	4.17	ML	0.00011	0.011%	0.436	0.032	13.613	Y	0.00010	C	20th Floor
14118096	Pasadena (PASA)	2005	4.26	ML	0.00011	0.011%	0.436	0.032	13.613	Y	0.00009	C	20th Floor
9655209	Pasadena (PASA)	2001	3.78	ML	0.00011	0.011%	0.436	0.032	13.613	Y	0.00008	C	20th Floor
14219360	Pasadena (PASA)	2006	4.11	ML	0.00011	0.011%	0.436	0.032	13.613	Y	0.00006	C	20th Floor
14146956	Pasadena (PASA)	2005	4.06	ML	0.00011	0.011%	0.436	0.032	13.613	Y	0.00004	C	20th Floor
40204628	Capetown, Ferndale	2007	5.45	Mw	0.00011	0.011%	0.436	0.032	13.613	Y	0.00004	C	20th Floor
21465580	Capetown, Ferndale	2005	4.77	Mw	0.00011	0.011%	0.436	0.032	13.613	Y	0.00004	C	20th Floor
14137160	Pasadena (PASA)	2005	3.94	ML	0.00011	0.011%	0.436	0.032	13.613	Y	0.00003	C	20th Floor

14330056	Pasadena Art Center, College Of Design	2007	4.34	ML	0.00011	0.011%	0.436	0.032	13.613	Y	0.00002	C	20th Floor
10276197	Pasadena Art Center, College Of Design	2007	4.06	ML	0.00011	0.011%	0.436	0.032	13.613	Y	0.00002	C	20th Floor
10065241	Pasadena (PASA)	2004	3.52	ML	0.00011	0.011%	0.436	0.032	13.613	Y	0.00002	C	20th Floor
10207681	Pasadena (PASA)	2006	4.05	ML	0.00011	0.011%	0.436	0.032	13.613	Y	0.00001	C	20th Floor
21530368	Capetown, Ferndale	2006	4.5	Mw	0.00011	0.011%	0.436	0.032	13.613	Y	0.00001	C	20th Floor
30225889	Capetown, Ferndale	2003	4.12	Mw	0.00011	0.011%	0.436	0.032	13.613	Y	0.00001	C	20th Floor
30226086	Capetown, Ferndale	2003	4	Mw	0.00011	0.011%	0.436	0.032	13.613	Y	0.00001	C	20th Floor
21526081	Capetown, Ferndale	2006	3.7	Mw	0.00011	0.011%	0.436	0.032	13.613	Y	0.000004	C	20th Floor
40199209	Capetown, Ferndale	2007	4.2	Mw	0.00011	0.011%	0.436	0.032	13.613	Y	0.000003	C	20th Floor

A3. Summary of results in XB

Table 48. Summary of results in XB

Event Name/ Station	Station Name	Year	Magnitude	Unit	Max Story Drift	%	Story Max Avg Drift (mm)	Avg Drift	Ratio	Direction	PGA (g)	Preferred NEHRP Based on Vs30	Floor
Iwate	AKTH04	2008	6.90	Mw	0.01766	1.766%	69.934	35.045	1.996	X	1.768300	C	3rd Floor
Northridge-01	Tarzana - Cedar Hill A	1994	6.69	Mw	0.072524	7.252%	287.197	144.04	1.994	X	1.644000	D	3rd Floor
Niigata, Japan	NIG021	2004	6.63	Mw	0.013538	1.354%	53.609	26.876	1.995	X	1.476200	C	3rd Floor
Cape Mendocino	Cape Mendocino	1992	7.01	Mw	0.063567	6.357%	251.726	126.233	1.994	X	1.396300	C	3rd Floor
Christchurch, New Zealand	Heathcote Valley Primary School	2011	6.2	Mw	0.043149	4.315%	170.869	85.654	1.995	X	1.391400	C	3rd Floor
Northridge-01	Pacoima Dam (upper left)	1994	6.69	Mw	0.036012	3.601%	142.606	71.497	1.995	X	1.38890	A	3rd Floor
Iwate	IWTH25	2008	6.9	Mw	0.095429	9.543%	377.897	189.424	1.995	X	1.35420	C	3rd Floor
Niigata, Japan	NIG019	2004	6.63	Mw	0.080759	8.08%	319.804	160.259	1.996	X	1.25510	C	3rd Floor
San Fernando	Pacoima Dam (upper left abut)	1971	6.61	Mw	0.122741	12.27%	486.053	243.817	1.994	X	1.22170	A	3rd Floor

Nahanni, Canada	Site 1	1985	6.76	Mw	0.018081	1.808%	71.603	35.985	1.99	Y	1.160100	C	3rd Floor
Chuetsu-oki	Kashiwazaki NPP, Unit 5: ground surface	2007	6.80	Mw	0.078043	7.804%	309.05	154.989	1.994	X	1.153700	D	3rd Floor
Baja California	Cerro Prieto	1987	5.50	Mw	0.043462	4.346%	172.108	86.301	1.994	X	1.139400	C	3rd Floor
Parkfield-02, CA	Parkfield - Fault Zone 14	2004	6.00	Mw	0.023148	2.315%	91.668	45.978	1.994	X	1.037800	D	3rd Floor
Iwate	IWTH26	2008	6.9	Mw	0.043965	4.40%	174.102	87.299	1.994	X	1.03260	C	3rd Floor
Duzce, Turkey	IRIGM 496	1999	7.14	Mw	0.016871	1.687%	66.811	33.504	1.994	X	0.996190	B	3rd Floor
Morgan Hill	Coyote Lake Dam - Southwest Abutment	1984	6.19	Mw	0.040984	4.098%	162.296	81.406	1.994	X	0.939390	C	3rd Floor
Christchurch, New Zealand	LPCC	2011	6.2	Mw	0.032608	3.26%	129.128	64.747	1.994	X	0.93132	C	3rd Floor
Chuetsu-oki	Kashiwazaki NPP, Unit 1: ground surface	2007	6.8	Mw	0.121211	12.12%	479.997	240.658	1.995	X	0.88823	D	3rd Floor
Chuetsu-oki	Kashiwazaki Nishiyamacho Ikeura	2007	6.8	Mw	0.058214	5.82%	230.529	115.639	1.994	X	0.86274	C	3rd Floor
Coalinga-05	Transmitter Hill	1983	5.77	Mw	0.029719	2.97%	117.687	59.022	1.994	X	0.84463	C	3rd Floor
Tottori, Japan	TTRH02	2000	6.61	Mw	0.058548	5.855%	231.85	116.322	1.993	X	0.841610	D	3rd Floor

Chi-Chi, Taiwan	CHY080	1999	7.62	Mw	0.165692	16.569%	656.142	329.034	1.994	X	0.832360	C	3rd Floor
Parkfield-02, CA	Parkfield - Fault Zone 11	2004	6	Mw	0.008329	0.83%	32.981	16.534	1.995	X	0.82618	C	3rd Floor
Tabas, Iran	Tabas	1978	7.35	Mw	0.090122	9.012%	356.884	179.021	1.994	X	0.812450	B	3rd Floor
Duzce, Turkey	Bolu	1999	7.14	Mw	0.04725	4.73%	187.111	93.781	1.995	X	0.77559	D	3rd Floor
Kobe, Japan	KJMA	1995	6.90	Mw	0.117057	11.706%	463.547	232.419	1.994	X	0.775250	D	3rd Floor
Chi-Chi, Taiwan	CHY028	1999	7.62	Mw	0.061988	6.20%	245.473	123.127	1.994	X	0.76760	C	3rd Floor
Northridge-01	Jensen Filter Plant Generator Building	1994	6.69	Mw	0.05114	5.11%	202.514	101.585	1.994	X	0.76045	C	3rd Floor
Northridge-01	LA - Sepulveda VA Hospital	1994	6.69	Mw	0.073665	7.37%	291.713	146.251	1.995	X	0.75323	C	3rd Floor
Chi-Chi, Taiwan	TCU129	1999	7.62	Mw	0.064559	6.46%	255.652	128.21	1.994	X	0.75149	C	3rd Floor
Tottori, Japan	TTR007	2000	6.61	Mw	0.017037	1.70%	67.467	33.803	1.996	X	0.74266	C	3rd Floor
Niigata, Japan	NIGH01	2004	6.63	Mw	0.0571	5.71%	226.115	113.422	1.994	X	0.74056	C	3rd Floor
Chi-Chi, Taiwan	TCU084	1999	7.62	Mw	0.202111	20.21%	800.361	401.436	1.994	X	0.73785	C	3rd Floor

Bam, Iran	Bam	2003	6.6	Mw	0.128726	12.873%	509.754	255.671	1.994	X	0.737680	C	3rd Floor
Darfield, New Zealand	GDLC	2010	7.00	Mw	0.107089	10.709%	424.072	212.762	1.993	X	0.731130	D	3rd Floor
Superstition Hills-02	Superstition Mtn Camera	1987	6.54	Mw	0.030362	3.036%	120.234	60.388	1.991	X	0.728780	C	3rd Floor
Landers	Lucerne	1992	7.28	Mw	0.001832	0.183%	7.253	3.619	2.004	X	0.727240	B	3rd Floor
Iwate	MYG004	2008	6.9	Mw	0.028716	2.87%	113.715	57.032	1.994	X	0.72576	C	3rd Floor
Tottori, Japan	SMNH01	2000	6.61	Mw	0.012295	1.23%	48.687	24.417	1.994	X	0.71988	C	3rd Floor
Mammoth Lakes-06	Long Valley Dam (Upr L Abut)	1980	5.94	Mw	0.017741	1.774%	70.252	35.233	1.994	X	0.719280	C	3rd Floor
Parkfield-02, CA	Parkfield - Stone Corral 1E	2004	6.00	Mw	0.04584	4.584%	181.525	91.055	1.994	X	0.716670	D	3rd Floor
Northridge-01	Rinaldi Receiving Sta	1994	6.69	Mw	0.15434	15.43%	611.187	306.571	1.994	X	0.70785	D	3rd Floor
Chi-Chi, Taiwan-06	TCU079	1999	6.30	Mw	0.015959	1.596%	63.197	31.697	1.994	X	0.704450	C	3rd Floor
Gazli, USSR	Karakyr	1976	6.80	Mw	0.05415	5.415%	214.436	107.559	1.994	X	0.701780	D	3rd Floor
Northridge-01	Sylmar - Converter Sta	1994	6.69	Mw	0.101684	10.17%	402.669	201.873	1.995	X	0.69753	D	3rd Floor

Chi-Chi, Taiwan	TCU065	1999	7.62	Mw	0.093738	9.37%	371.203	186.121	1.994	X	0.68938	D	3rd Floor
Chi-Chi, Taiwan-03	TCU129	1999	6.20	Mw	0.007843	0.784%	31.058	15.564	1.996	X	0.688770	C	3rd Floor
Imperial Valley-06	Bonds Corner	1979	6.53	Mw	0.024141	2.414%	95.6	47.948	1.994	X	0.686610	D	3rd Floor
Northridge-01	Sylmar - Converter Sta East	1994	6.69	Mw	0.067	6.70%	265.322	133.073	1.994	X	0.68610	C	3rd Floor
Coalinga-05	Coalinga (Oil City)	1983	5.77	Mw	0.028179	2.82%	111.59	55.891	1.997	X	0.68604	C	3rd Floor
N. Palm Springs	North Palm Springs	1986	6.06	Mw	0.066943	6.694%	265.095	132.975	1.994	X	0.684340	D	3rd Floor
Duzce, Turkey	Lamont 375	1999	7.14	Mw	0.010264	1.03%	40.644	20.373	1.995	X	0.68064	C	3rd Floor
Kobe, Japan	Takatori	1995	6.9	Mw	0.234437	23.44%	928.372	465.604	1.994	X	0.67218	D	3rd Floor
Tottori, Japan	OKY004	2000	6.61	Mw	0.005852	0.59%	23.172	11.626	1.993	X	0.65993	C	3rd Floor
Northridge-01	Newhall - Fire Sta	1994	6.69	Mw	0.086632	8.66%	343.061	172.07	1.994	X	0.65430	D	3rd Floor
Kobe, Japan	Takarazuka	1995	6.9	Mw	0.092332	9.23%	365.633	183.315	1.995	X	0.65400	D	3rd Floor
Parkfield-02, CA	Parkfield - Cholame 3E	2004	6	Mw	0.009449	0.94%	37.416	18.76	1.994	X	0.65141	C	3rd Floor

Niigata, Japan	NIG028	2004	6.63	Mw	0.022523	2.25%	89.193	44.74	1.994	X	0.64783	C	3rd Floor
Christchurch, New Zealand	Pages Road Pumping Station	2011	6.2	Mw	0.10693	10.69%	423.444	212.28	1.995	X	0.64750	E	3rd Floor
Parkfield-02, CA	Parkfield - Fault Zone 1	2004	6	Mw	0.07106	7.11%	281.397	141.151	1.994	X	0.64455	E	3rd Floor
Northridge-01	Simi Valley - Katherine Rd	1994	6.69	Mw	0.048564	4.86%	192.312	96.459	1.994	X	0.64410	C	3rd Floor
Northridge-01	Sylmar - Olive View Med FF	1994	6.69	Mw	0.066441	6.64%	263.107	132.002	1.993	X	0.64005	C	3rd Floor
Chuetsu-oki	NIG018	2007	6.8	Mw	0.11319	11.32%	448.23	224.744	1.994	X	0.62519	D	3rd Floor
Northridge-01	Santa Monica City Hall	1994	6.69	Mw	0.03572	3.57%	141.453	70.912	1.995	X	0.62478	D	3rd Floor
Cape Mendocino	Petrolia	1992	7.01	Mw	0.031632	3.16%	125.262	62.821	1.994	X	0.62397	C	3rd Floor
Tottori, Japan	TTR009	2000	6.61	Mw	0.014038	1.40%	55.591	27.869	1.995	X	0.62177	C	3rd Floor
Chuetsu-oki	Joetsu Oshimaku Oka	2007	6.8	Mw	0.017232	1.72%	68.239	34.203	1.995	X	0.62016	C	3rd Floor
Victoria, Mexico	Cerro Prieto	1980	6.33	Mw	0.051368	5.137%	203.418	102.012	1.994	X	0.614510	C	3rd Floor
Parkfield-02, CA	Parkfield - Gold Hill 3W	2004	6	Mw	0.008187	0.82%	32.42	16.243	1.996	X	0.60451	C	3rd Floor

N. Palm Springs	Whitewater Trout Farm	1986	6.06	Mw	0.019754	1.975%	78.224	39.215	1.995	X	0.596650	C	3rd Floor
Chi-Chi, Taiwan	TCU071	1999	7.62	Mw	0.052201	5.22%	206.717	103.673	1.994	X	0.59346	C	3rd Floor
Umbria Marche (aftershock 7), Italy	Nocera Umbra	1997	4.3	ML	0.001078	0.108%	4.268	2.119	2.014	X	0.592170	C	3rd Floor
Loma Prieta	LGPC	1989	6.93	Mw	0.032834	3.283%	130.022	65.22	1.994	X	0.590120	C	3rd Floor
Whittier Narrows-01	Tarzana - Cedar Hill	1987	5.99	Mw	0.005895	0.59%	23.346	11.709	1.994	X	0.58926	D	3rd Floor
Iwate	Kurihara City	2008	6.9	Mw	0.033692	3.37%	133.421	66.883	1.995	X	0.58540	C	3rd Floor
San Salvador	Geotech Investig Center	1986	5.80	Mw	0.059034	5.903%	233.774	117.241	1.994	X	5.7610E-01	C	3rd Floor
Darfield, New Zealand	Heathcote Valley Primary School	2010	7	Mw	0.01212	1.21%	47.996	24.031	1.997	X	0.57386	C	3rd Floor
Chuetsu-oki	Kashiwazaki City Center	2007	6.8	Mw	0.092712	9.27%	367.138	184.068	1.995	X	0.57362	D	3rd Floor
Chuetsu-oki	Oguni Nagaoka	2007	6.8	Mw	0.028537	2.85%	113.007	56.648	1.995	X	0.56615	C	3rd Floor
Chuetsu-oki	Iizuna Imokawa	2007	6.8	Mw	0.053565	5.36%	212.116	106.375	1.994	X	0.56511	C	3rd Floor

Parkfield-02, CA	PARKFIELD - JOAQUIN CANYON	2004	6	Mw	0.01111	1.11%	43.994	22.067	1.994	X	0.55980	C	3rd Floor
Coalinga-07	Coalinga-14th & Elm (Old CHP)	1983	5.21	Mw	0.008109	0.811%	32.113	16.09	1.996	X	5.5960E-01	D	3rd Floor
Parkfield-02, CA	Parkfield - Cholame 4W	2004	6	Mw	0.016745	1.67%	66.309	33.252	1.994	X	0.55915	C	3rd Floor
Chi-Chi, Taiwan	TCU095	1999	7.62	Mw	0.018654	1.87%	73.868	37.034	1.995	X	0.55847	C	3rd Floor
L'Aquila, Italy	L'Aquila - V. Aterno - Centro Valle	2009	6.30	Mw	0.03027	3.027%	119.871	60.111	1.994	X	0.558440	C	3rd Floor
Coalinga-02	Anticline Ridge Free-Field	1983	5.09	Mw	0.00389	0.389%	15.404	7.707	1.999	X	0.557720	C	3rd Floor
Chuetsu-oki	Kashiwazaki City Takayanagicho	2007	6.8	Mw	0.03671	3.67%	145.372	72.909	1.994	X	0.55485	C	3rd Floor
Chi-Chi, Taiwan-06	TCU080	1999	6.3	Mw	0.028051	2.81%	111.083	55.692	1.995	X	0.54809	C	3rd Floor
Loma Prieta	WAHO	1989	6.93	Mw	0.031331	3.133%	124.072	62.227	1.994	X	0.537300	C	3rd Floor
Northridge-01	Beverly Hills - 12520 Mulhol	1994	6.69	Mw	0.029873	2.99%	118.297	59.327	1.994	X	0.53527	C	3rd Floor
Northridge-06	Rinaldi Receiving Sta	1994	5.28	Mw	0.012011	1.201%	47.562	23.82	1.997	X	0.528200	D	3rd Floor
Imperial Valley-06	El Centro Array #8	1979	6.53	Mw	0.071725	7.17%	284.033	142.438	1.994	X	0.52691	D	3rd Floor

Big Bear-01	Big Bear Lake - Civic Center	1992	6.46	Mw	0.015382	1.538%	60.912	30.538	1.995	X	0.524580	C	3rd Floor
Northridge-01	Jensen Filter Plant Administrative Building	1994	6.69	Mw	0.088513	8.85%	350.512	175.616	1.996	X	0.52425	C	3rd Floor
Manjil, Iran	Abbar	1990	7.37	Mw	0.026925	2.693%	106.624	53.485	1.994	X	0.523480	C	3rd Floor
Christchurch, New Zealand	Christchurch Resthaven	2011	6.2	Mw	0.089817	8.98%	355.675	178.411	1.994	X	0.52141	E	3rd Floor
Chi-Chi, Taiwan	TCU088	1999	7.62	Mw	0.014702	1.47%	58.222	29.144	1.998	X	0.52104	C	3rd Floor
Coalinga-01	Pleasant Valley P.P. - yard	1983	6.36	Mw	0.055276	5.528%	218.892	109.792	1.994	X	5.2073E-01	D	3rd Floor
El Mayor-Cucapah	El Centro Differential Array	2010	7.20	Mw	0.018801	1.880%	74.454	37.339	1.994	X	0.507370	D	3rd Floor
Stone Canyon	Melendy Ranch	1972	4.81	Mw	0.002492	0.249%	9.868	4.932	2.001	X	0.495510	C	3rd Floor
Mammoth Lakes-04	Convict Creek	1980	5.70	Mw	0.00822	0.822%	32.55	16.31	1.996	X	0.484200	C	3rd Floor
Umbria Marche, Italy	Nocera Umbra	1997	6	Mw	0.015916	1.592%	63.028	31.597	1.995	X	0.472550	C	3rd Floor
Umbria Marche, Italy	Nocera Umbra	1997	6	Mw	0.015916	1.592%	63.028	31.597	1.995	X	4.7255E-01	C	3rd Floor

Yountville	Napa Fire Station #3	2000	5.00	Mw	0.021838	2.184%	86.478	43.357	1.995	X	0.459710	D	3rd Floor
Ancona-09, Italy	Ancona-Rocca	1972	4.7	ML	0.002308	0.231%	9.139	4.561	2.004	X	0.450270	C	3rd Floor
Erzican, Turkey	Erzincan	1992	6.69	Mw	0.091167	9.117%	361.023	181.051	1.994	X	0.444990	D	3rd Floor
Mammoth Lakes-01	Convict Creek	1980	6.06	Mw	0.033937	3.394%	134.389	67.372	1.995	X	0.439150	C	3rd Floor
Whittier Narrows-01	Garvey Res. - Control Bldg	1987	5.99	Mw	0.008634	0.863%	34.19	17.124	1.997	X	0.436460	C	3rd Floor
Coalinga-05	Coalinga-14th & Elm (Old CHP)	1983	5.77	Mw	0.006607	0.661%	26.164	13.103	1.997	X	0.424860	D	3rd Floor
Whittier Narrows-02	Pasadena - Old House Rd	1987	5.27	Mw	0.004495	0.450%	17.802	8.911	1.998	X	3.8617E-01	C	3rd Floor
El Mayor-Cucapah	El Centro - Meloland Geot. Array	2010	7.20	Mw	0.013028	1.303%	51.591	25.863	1.995	X	3.7814E-01	D	3rd Floor
Cape Mendocino	Ferndale Fire Station	1992	7.01	Mw	0.0821	8.210%	325.118	163.033	1.994	X	2.9416E-01	C	3rd Floor
Superstition Hills-02	El Centro Imp. Co. Cent	1987	6.54	Mw	0.048622	4.862%	192.544	96.514	1.995	X	2.6118E-01	D	3rd Floor
	Hollister City Hall	1989	6.93	Mw	0.031171	3.117%	123.439	61.919	1.994	X	2.3371E-01	D	3rd Floor
Imperial Valley-02	El Centro Array #9	1940	6.95	Mw	0.029843	2.984%	118.18	59.273	1.994	X	2.3349E-01	D	3rd Floor

Parkfield-02, CA	Parkfield - Cholame 5W	2004	6.00	Mw	0.010908	1.091%	43.194	21.645	1.996	X	2.3324E-01	D	3rd Floor
Sierra Madre	Pasadena - USGS/NSMP Office	1991	5.61	Mw	0.006217	0.622%	24.621	12.311	2	X	2.3178E-01	D	3rd Floor
Northridge-01	Pasadena - N Sierra Madre	1994	6.69	Mw	0.006657	0.666%	26.363	13.208	1.996	X	2.3087E-01	C	3rd Floor
Northern Calif-03	Ferndale City Hall	1954	6.50	U	0.045966	4.597%	182.027	91.31	1.994	X	1.8616E-01	D	3rd Floor
Northern Calif-05	Ferndale City Hall	1967	5.60	Mw	0.005254	0.525%	20.804	10.413	1.998	X	1.8406E-01	D	3rd Floor
Coalinga-06	Coalinga-14th & Elm (Old CHP)	1983	4.89	Mw	0.001817	0.182%	7.197	3.59	2.005	Y	0.151090	D	3rd Floor
Imperial Valley-06	El Centro Array #1	1979	6.53	Mw	0.008572	0.857%	33.946	17.008	1.996	X	1.4458E-01	D	3rd Floor
Whittier Narrows-01	Pasadena - CIT Athenaeum	1987	5.99	Mw	0.010432	1.043%	41.312	20.71	1.995	X	1.4147E-01	C	3rd Floor
Hollister-03	Hollister City Hall	1974	5.14	Mw	0.002508	0.251%	9.932	4.962	2.002	X	1.4070E-01	D	3rd Floor
Northwest Calif-01	Ferndale City Hall	1938	5.50	Mw	0.003601	0.360%	14.261	7.133	1.999	X	1.2218E-01	D	3rd Floor
Northwest Calif-03	Ferndale City Hall	1951	5.80	Mw	0.004249	0.425%	16.825	8.417	1.999	X	1.0709E-01	D	3rd Floor
San Fernando	Pasadena - CIT Athenaeum	1971	6.61	Mw	0.006799	0.680%	26.926	13.487	1.996	X	1.0575E-01	C	3rd Floor

Borrego Mtn	El Centro Array #9	1968	6.63	Mw	0.030367	3.037%	120.253	60.287	1.995	X	9.4018E-02	D	3rd Floor
San Fernando	Fairmont Dam	1971	6.61	Mw	0.001301	0.130%	5.153	2.585	1.994	X	0.093858	C	3rd Floor
Northern Calif-07	Ferndale City Hall	1975	5.20	Mw	0.003286	0.329%	13.011	6.509	1.999	X	9.0045E-02	D	3rd Floor
San Francisco	Golden Gate Park	1957	5.28	Mw	0.000692	0.069%	2.74	1.355	2.022	X	8.6274E-02	B	20th Floor
Hollister-01	Hollister City Hall	1961	5.60	U	0.010628	1.063%	42.087	21.1	1.995	X	8.4991E-02	D	3rd Floor
Morgan Hill	Hollister City Hall	1984	6.19	Mw	0.011551	1.155%	45.743	22.926	1.995	X	7.0129E-02	D	3rd Floor
Northern Calif-02	Ferndale City Hall	1952	5.20	Mw	0.006412	0.641%	25.39	12.718	1.996	X	6.8432E-02	D	3rd Floor
Northern Calif-04	Ferndale City Hall	1960	5.70	Mw	0.003539	0.354%	14.013	7.009	1.999	X	6.7086E-02	D	3rd Floor
Hollister-02	Hollister City Hall	1961	5.50	U	0.007262	0.726%	28.756	14.401	1.997	X	6.2349E-02	D	3rd Floor
CA/Baja Border Area	El Centro Array #10	2002	5.31	Mw	0.001825	0.183%	7.228	3.607	2.004	X	6.0458E-02	D	3rd Floor
Parkfield	Cholame - Shandon Array #12	1966	6.19	Mw	0.007274	0.727%	28.806	14.431	1.996	X	5.8666E-02	C	3rd Floor
Imperial Valley-07	El Centro Array #10	1979	5.01	Mw	0.000922	0.092%	3.65	1.817	2.008	X	5.2531E-02	D	3rd Floor

Borrego	El Centro Array #9	1942	6.50	U	0.010296	1.030%	40.772	20.434	1.995	X	5.2247E-02	D	3rd Floor
Kern County	Pasadena - CIT Athenaeum	1952	7.36	Mw	0.00856	0.856%	33.896	16.983	1.996	X	5.1003E-02	C	3rd Floor
Northwest Calif-02	Ferndale City Hall	1941	6.60	U	0.003884	0.388%	15.38	7.706	1.996	X	4.9416E-02	D	3rd Floor
Central Calif-01	Hollister City Hall	1954	5.30	U	0.003037	0.304%	12.028	6.015	2	X	4.7679E-02	D	3rd Floor
El Alamo	El Centro Array #9	1956	6.80	U	0.006715	0.672%	26.591	13.321	1.996	X	4.4953E-02	D	3rd Floor
Coalinga-01	Parkfield - Cholame 12W	1983	6.36	Mw	0.011233	1.123%	44.482	22.297	1.995	X	4.4950E-02	D	3rd Floor
Imperial Valley-05	El Centro Array #9	1955	5.40	U	0.004124	0.412%	16.329	8.173	1.998	X	4.4240E-02	D	3rd Floor
Northridge-06	Pasadena - USGS/NSMP Office	1994	5.28	Mw	0.001249	0.125%	4.947	2.467	2.005	X	4.1761E-02	D	3rd Floor
Humbolt Bay	Ferndale City Hall	1937	5.80	Mw	0.002525	0.253%	9.998	4.996	2.001	X	4.0961E-02	D	3rd Floor
Hector Mine	Pasadena - Fair Oaks & Walnut	1999	7.13	Mw	0.004587	0.459%	18.164	9.093	1.998	X	3.5278E-02	C	3rd Floor
Mammoth Lakes-07	USC Cash Baugh Ranch	1980	4.73	Mw	0.005133	0.513%	20.326	10.178	1.997	X	0.029900	D	3rd Floor
Imperial Valley-03	El Centro Array #9	1951	5.60	U	0.001882	0.188%	7.451	3.718	2.004	X	2.9364E-02	D	3rd Floor

Imperial Valley-04	El Centro Array #9	1953	5.50	U	0.000375	0.038%	1.485	0.725	2.047	X	2.7932E-02	D	3rd Floor
40238431	Parkfield - Cholame 5W	2009	4.39	Mw	0.000197	0.020%	0.778	0.371	2.097	X	2.0278E-02	D	3rd Floor
Imperial Valley-01	El Centro Array #9	1938	5.00	U	0.000396	0.040%	1.57	0.768	2.045	X	1.8449E-02	D	3rd Floor
51182151	Parkfield - Cholame 5W	2007	4.01	Mw	0.000171	0.017%	0.679	0.082	8.242	Y	1.8393E-02	D	20th Floor
Gulf of California	El Centro Array #9	2001	5.70	Mw	0.002497	0.250%	9.889	4.941	2.001	X	1.8280E-02	D	3rd Floor
Northern Calif-06	Hollister City Hall	1967	5.20	U	0.001824	0.182%	7.223	3.605	2.004	X	1.5276E-02	D	3rd Floor
Hector Mine	El Centro Array #10	1999	7.13	Mw	0.0043	0.430%	17.029	8.523	1.998	X	1.4538E-02	D	3rd Floor
40204628	San Francisco; Fire Station 22 Golden Gate Park; 16th Ave; 2-story; ground level	2007	5.45	Mw	0.00032	0.032%	1.266	0.616	2.056	X	1.2085E-02	D	20th Floor
21305648	San Francisco; Fire Station 22 Golden Gate Park; 16th Ave; 2-story; ground level	2003	4.00	Mw	0.000106	0.011%	0.418	0.21	1.993	X	1.1427E-02	D	3rd Floor
21530368	San Francisco; Fire Station 22 Golden Gate Park; 16th Ave; 2-story; ground level	2006	4.5	Mw	0.000171	0.017%	0.679	0.082	8.242	Y	1.1412E-02	D	20th Floor
Anza-02	El Centro Array #10	2001	4.92	Mw	0.000524	0.052%	2.075	1.022	2.031	X	1.0910E-02	D	3rd Floor

21423530	Parkfield - Cholame 5W	2004	4.17	Mw	0.000171	0.017%	0.679	0.082	8.242	Y	9.8585E-03	D	20th Floor
San Fernando	Maricopa Array #3	1971	6.61	Mw	0.004121	0.412%	16.32	8.16	2	X	0.008986	C	3rd Floor
Borrego Mtn	Pasadena - CIT Athenaeum	1968	6.63	Mw	0.002285	0.229%	9.048	4.52	2.002	X	8.2481E-03	C	3rd Floor
Big Bear City	Pasadena - USGS/NSMP Office	2003	4.92	Mw	0.000255	0.026%	1.009	0.487	2.072	X	7.4202E-03	D	3rd Floor
40199209	San Francisco; Fire Station 22 Golden Gate Park; 16th Ave; 2-story; ground level	2007	4.20	Mw	0.000171	0.017%	0.679	0.082	8.242	Y	6.5591E-03	D	20th Floor
40194055	San Francisco; Fire Station 22 Golden Gate Park; 16th Ave; 2-story; ground level	2007	4.23	Mw	0.000171	0.017%	0.679	0.082	8.242	Y	6.1986E-03	D	20th Floor
51207740	San Francisco; Fire Station 22 Golden Gate Park; 16th Ave; 2-story; ground level	2008	4.1	Mw	0.000171	0.017%	0.679	0.082	8.242	Y	5.7295E-03	D	20th Floor
14155260	Pasadena (PASA)	2005	4.88	ML	0.000171	0.017%	0.679	0.082	8.242	Y	4.7638E-03	C	20th Floor
51177103	San Francisco; Fire Station 22 Golden Gate Park; 16th Ave; 2-story; ground level	2006	3.6	Mw	0.000171	0.017%	0.679	0.082	8.242	Y	4.6635E-03	D	20th Floor
San Fernando	Cholame - Shandon Array #2	1971	6.61	Mw	0.001045	0.105%	4.137	2.056	2.012	X	4.3448E-03	D	3rd Floor

21522424	San Francisco; Fire Station 22 Golden Gate Park; 16th Ave; 2-story; ground level	2006	4.3	Mw	0.000171	0.017%	0.679	0.082	8.242	Y	3.7740E-03	D	20th Floor
40193843	San Francisco; Fire Station 22 Golden Gate Park; 16th Ave; 2-story; ground level	2007	3.41	ML	0.000171	0.017%	0.679	0.082	8.242	Y	3.2067E-03	D	20th Floor
Yorba Linda	Pasadena (PASA)	2002	4.27	Mw	0.000083	0.008%	0.327	0.071	4.594	Y	2.2374E-03	C	20th Floor
21261124	San Francisco; Fire Station 22 Golden Gate Park; 16th Ave; 2-story; ground level	2002	3.6	ML	0.000171	0.017%	0.679	0.082	8.242	Y	2.1947E-03	D	20th Floor
30225889	San Francisco; Fire Station 22 Golden Gate Park; 16th Ave; 2-story; ground level	2003	4.12	Mw	0.000083	0.008%	0.327	0.071	4.594	Y	1.9516E-03	D	20th Floor
14151344	Pasadena (PASA)	2005	5.20	Mw	0.000171	0.017%	0.679	0.082	8.242	Y	1.6920E-03	C	20th Floor
51177644	San Francisco; Fire Station 22 Golden Gate Park; 16th Ave; 2-story; ground level	2007	3.7	Mw	0.000171	0.017%	0.679	0.082	8.242	Y	1.4441E-03	D	20th Floor
30225187	San Francisco; Fire Station 22 Golden Gate Park; 16th Ave; 2-story; ground level	2002	3.9	Mw	0.000171	0.017%	0.679	0.082	8.242	Y	1.2464E-03	D	20th Floor
21510121	San Francisco; Fire Station 22 Golden Gate Park; 16th Ave; 2-story; ground level	2006	3.7	Mw	0.000171	0.017%	0.679	0.082	8.242	Y	1.2442E-03	D	20th Floor

14138080	Pasadena (PASA)	2005	4.59	ML	0.000171	0.017%	0.679	0.082	8.242	Y	1.1067E-03	C	20th Floor
9735129	Pasadena (PASA)	2001	3.97	ML	0.000171	0.017%	0.679	0.082	8.242	Y	1.1023E-03	C	20th Floor
10275733	Pasadena Art Center, College Of Design	2007	4.73	ML	0.000171	0.017%	0.679	0.082	8.242	Y	1.0591E-03	C	20th Floor
51203888	San Francisco; Fire Station 22 Golden Gate Park; 16th Ave; 2-story; ground level	2008	3.5	Mw	0.000171	0.017%	0.679	0.082	8.242	Y	9.9741E-04	D	20th Floor
21414391	San Francisco; Fire Station 22 Golden Gate Park; 16th Ave; 2-story; ground level	2004	3.68	Mw	0.000171	0.017%	0.679	0.082	8.242	Y	9.9567E-04	D	20th Floor
30226452	San Francisco; Fire Station 22 Golden Gate Park; 16th Ave; 2-story; ground level	2003	3.5	Mw	0.000171	0.017%	0.679	0.082	8.242	Y	7.7876E-04	D	20th Floor
9173365	Pasadena (PASA)	2001	4.26	ML	0.000171	0.017%	0.679	0.082	8.242	Y	7.7497E-04	C	20th Floor
30226086	San Francisco; Fire Station 22 Golden Gate Park; 16th Ave; 2-story; ground level	2003	4	Mw	0.000171	0.017%	0.679	0.082	8.242	Y	7.0533E-04	D	20th Floor
21437727	San Francisco; Fire Station 22 Golden Gate Park; 16th Ave; 2-story; ground level	2005	4.18	Mw	0.000171	0.017%	0.679	0.082	8.242	Y	6.4725E-04	D	20th Floor
9753485	Pasadena (PASA)	2002	4.18	ML	0.000171	0.017%	0.679	0.082	8.242	Y	5.8550E-04	C	20th Floor

21335949	San Francisco; Fire Station 22 Golden Gate Park; 16th Ave; 2-story; ground level	2004	3.71	Mw	0.000171	0.017%	0.679	0.082	8.242	Y	5.7851E-04	D	20th Floor
21350824	San Francisco; Fire Station 22 Golden Gate Park; 16th Ave; 2-story; ground level	2004	4.25	Mw	0.000171	0.017%	0.679	0.082	8.242	Y	5.6170E-04	D	20th Floor
9069997	Pasadena (PASA)	1998	4.50	-999	0.000171	0.017%	0.679	0.082	8.242	Y	5.6152E-04	C	20th Floor
14186612	Pasadena (PASA)	2005	4.69	ML	0.000171	0.017%	0.679	0.082	8.242	Y	4.6805E-04	C	20th Floor
21502994	San Francisco; Fire Station 22 Golden Gate Park; 16th Ave; 2-story; ground level	2006	3.6	Mw	0.000171	0.017%	0.679	0.082	8.242	Y	4.2217E-04	D	20th Floor
9064093	Pasadena (PASA)	1998	4.78	ML	0.000171	0.017%	0.679	0.082	8.242	Y	4.0512E-04	C	20th Floor
Anza-02	Pasadena (PASA)	2001	4.92	Mw	0.000171	0.017%	0.679	0.082	8.242	Y	3.6446E-04	C	20th Floor
3321584	Pasadena (PASA)	1999	3.81	ML	0.000171	0.017%	0.679	0.082	8.242	Y	3.5403E-04	C	20th Floor
9941081	Pasadena (PASA)	2003	3.90	ML	0.000171	0.017%	0.679	0.082	8.242	Y	3.2399E-04	C	20th Floor
21508102	San Francisco; Fire Station 22 Golden Gate Park; 16th Ave; 2-story; ground level	2006	3.69	ML	0.000171	0.017%	0.679	0.082	8.242	Y	3.1662E-04	D	20th Floor

14095628	Pasadena (PASA)	2004	5.03	Mw	0.000171	0.017%	0.679	0.082	8.242	Y	2.9899E-04	C	20th Floor
9096960	Pasadena (PASA)	1999	3.88	ML	0.000171	0.017%	0.679	0.082	8.242	Y	2.8311E-04	C	20th Floor
9652545	Pasadena (PASA)	2001	3.84	ML	0.000171	0.017%	0.679	0.082	8.242	Y	2.1126E-04	C	20th Floor
10972299	Pasadena (PASA)	2001	3.79	ML	0.000171	0.017%	0.679	0.082	8.242	Y	1.6578E-04	C	20th Floor
14312160	Pasadena Art Center, College Of Design	2007	4.66	ML	0.000171	0.017%	0.679	0.082	8.242	Y	1.4713E-04	C	20th Floor
13692644	Pasadena (PASA)	2002	3.74	ML	0.000171	0.017%	0.679	0.082	8.242	Y	1.3598E-04	C	20th Floor
10285533	Pasadena Art Center, College Of Design	2007	4.20	ML	0.000171	0.017%	0.679	0.082	8.242	Y	1.3594E-04	C	20th Floor
9983429	Pasadena (PASA)	2004	4.34	ML	0.000171	0.017%	0.679	0.082	8.242	Y	1.3391E-04	C	20th Floor
14077668	Pasadena (PASA)	2004	4.27	ML	0.000171	0.017%	0.679	0.082	8.242	Y	1.2710E-04	C	20th Floor
9096656	Pasadena (PASA)	1999	4.15	ML	0.000171	0.017%	0.679	0.082	8.242	Y	1.2126E-04	C	20th Floor
10059745	Pasadena (PASA)	2004	4.19	ML	0.000171	0.017%	0.679	0.082	8.242	Y	1.1037E-04	C	20th Floor
14079184	Pasadena (PASA)	2004	3.78	ML	0.000171	0.017%	0.679	0.082	8.242	Y	1.0275E-04	C	20th Floor

14201764	Pasadena (PASA)	2005	4.17	ML	0.000171	0.017%	0.679	0.082	8.242	Y	1.0055E-04	C	20th Floor
14118096	Pasadena (PASA)	2005	4.26	ML	0.000171	0.017%	0.679	0.082	8.242	Y	8.6369E-05	C	20th Floor
9655209	Pasadena (PASA)	2001	3.78	ML	0.000171	0.017%	0.679	0.082	8.242	Y	7.5117E-05	C	20th Floor
14219360	Pasadena (PASA)	2006	4.11	ML	0.000171	0.017%	0.679	0.082	8.242	Y	5.6335E-05	C	20th Floor
14146956	Pasadena (PASA)	2005	4.06	ML	0.000171	0.017%	0.679	0.082	8.242	Y	4.3736E-05	C	20th Floor
40204628	Capetown, Ferndale	2007	5.45	Mw	0.000171	0.017%	0.679	0.082	8.242	Y	3.9162E-05	C	20th Floor
21465580	Capetown, Ferndale	2005	4.77	Mw	0.000171	0.017%	0.679	0.082	8.242	Y	3.9062E-05	C	20th Floor
14137160	Pasadena (PASA)	2005	3.94	ML	0.000171	0.017%	0.679	0.082	8.242	Y	3.3755E-05	C	20th Floor
14330056	Pasadena Art Center, College Of Design	2007	4.34	ML	0.000171	0.017%	0.679	0.082	8.242	Y	2.3316E-05	C	20th Floor
10276197	Pasadena Art Center, College Of Design	2007	4.06	ML	0.000171	0.017%	0.679	0.082	8.242	Y	2.1540E-05	C	20th Floor
10065241	Pasadena (PASA)	2004	3.52	ML	0.000171	0.017%	0.679	0.082	8.242	Y	1.6238E-05	C	20th Floor
10207681	Pasadena (PASA)	2006	4.05	ML	0.000171	0.017%	0.679	0.082	8.242	Y	1.4115E-05	C	20th Floor

21530368	Capetown, Ferndale	2006	4.5	Mw	0.000171	0.017%	0.679	0.082	8.242	Y	8.4983E-06	C	20th Floor
30225889	Capetown, Ferndale	2003	4.12	Mw	0.000171	0.017%	0.679	0.082	8.242	Y	7.4723E-06	C	20th Floor
30226086	Capetown, Ferndale	2003	4	Mw	0.000171	0.017%	0.679	0.082	8.242	Y	7.1419E-06	C	20th Floor
21526081	Capetown, Ferndale	2006	3.7	Mw	0.000171	0.017%	0.679	0.082	8.242	Y	4.0209E-06	C	20th Floor
40199209	Capetown, Ferndale	2007	4.2	Mw	0.000171	0.017%	0.679	0.082	8.242	Y	3.0947E-06	C	20th Floor

A4. Summary of the VB results

Table 49. VB Summary of the results

Event Name/ Station	Station Name	Year	Magnitude	Unit	Max Story Drift	%	Story Max Avg Drift (mm)	Avg Drift	Ratio	Direction	PGA (g)	Preferred NEHRP Based on Vs30	Floor
Iwate	AKTH04	2008	6.90	Mw	0.017002	1.700%	67.328	33.754	1.995	X	1.7683	C	3rd Floor
Northridge-01	Tarzana - Cedar Hill A	1994	6.69	Mw	0.071835	7.184%	284.468	142.676	1.994	X	1.644	D	3rd Floor
Niigata, Japan	NIG021	2004	6.63	Mw	0.01344	1.344%	53.222	26.678	1.995	X	1.4762	C	3rd Floor
Cape Mendocino	Cape Mendocino	1992	7.01	Mw	0.062858	6.286%	248.918	124.821	1.994	X	1.3963	C	3rd Floor
Christchurch, New Zealand	Heathcote Valley Primary School	2011	6.2	Mw	0.042264	4.226%	167.365	83.896	1.995	X	1.3914	C	3rd Floor
Northridge-01	Pacoima Dam (upper left)	1994	6.69	Mw	0.034914	3.491%	138.261	69.307	1.995	X	1.38890	A	3rd Floor
Iwate	IWTH25	2008	6.9	Mw	0.093302	9.33%	369.478	185.181	1.995	X	1.35420	C	3rd Floor
Niigata, Japan	NIG019	2004	6.63	Mw	0.079258	7.93%	313.863	157.284	1.996	X	1.25510	C	3rd Floor
San Fernando	Pacoima Dam (upper left abut)	1971	6.61	Mw	0.029762	2.98%	117.859	59.106	1.994	X	1.22170	A	3rd Floor
Nahanni, Canada	Site 1	1985	6.76	Mw	0.018505	1.851%	73.279	36.835	1.989	Y	1.1601	C	3rd Floor
Chuetsu-oki	Kashiwazaki NPP, Unit 5: ground surface	2007	6.80	Mw	0.078079	7.808%	309.194	155.067	1.994	X	1.1537	D	3rd Floor
Baja California	Cerro Prieto	1987	5.50	Mw	0.043524	4.352%	172.356	86.43	1.994	X	1.1394	C	3rd Floor
Parkfield-02, CA	Parkfield - Fault Zone 14	2004	6.00	Mw	0.045305	4.531%	179.409	89.982	1.994	X	1.0378	D	3rd Floor
Iwate	IWTH26	2008	6.9	Mw	0.044229	4.42%	175.149	87.818	1.994	X	1.03260	C	3rd Floor
Duzce, Turkey	IRIGM 496	1999	7.14	Mw	0.017306	1.731%	68.532	34.374	1.994	X	0.99619	B	3rd Floor

Morgan Hill	Coyote Lake Dam - Southwest Abutment	1984	6.19	Mw	0.039617	3.962%	156.884	78.697	1.994	X	0.93939	C	3rd Floor
Christchurch, New Zealand	LPCC	2011	6.2	Mw	0.03206	3.21%	126.957	63.649	1.995	X	0.93132	C	3rd Floor
Chuetsu-oki	Kashiwazaki NPP, Unit 1: ground surface	2007	6.8	Mw	0.11094	11.09%	439.322	220.286	1.994	X	0.88823	D	3rd Floor
Wenchuan, China	Mianzuqingping	2008	7.9	Mw							0.88437	C	
Chuetsu-oki	Kashiwazaki Nishiyamacho Ikeura	2007	6.8	Mw	0.055417	5.54%	219.452	110.084	1.993	X	0.86274	C	3rd Floor
Coalinga-05	Transmitter Hill	1983	5.77	Mw	0.029312	2.93%	116.077	58.207	1.994	X	0.84463	C	3rd Floor
Tottori, Japan	TTRH02	2000	6.61	Mw	0.058114	5.811%	230.132	115.448	1.993	X	0.84161	D	3rd Floor
Chi-Chi, Taiwan	CHY080	1999	7.62	Mw	0.160469	16.047%	635.458	318.679	1.994	X	0.83236	C	3rd Floor
Parkfield-02, CA	Parkfield - Fault Zone 11	2004	6	Mw	0.008092	0.81%	32.045	16.05	1.997	X	0.82618	C	3rd Floor
Tabas, Iran	Tabas	1978	7.35	Mw	0.084017	8.402%	332.706	166.904	1.993	X	0.81245	B	3rd Floor
Duzce, Turkey	Bolu	1999	7.14	Mw	0.046588	4.66%	184.487	92.458	1.995	X	0.77559	D	3rd Floor
Kobe, Japan	KJMA	1995	6.90	Mw	0.118168	11.817%	467.944	234.611	1.995	X	0.77525	D	3rd Floor
Chi-Chi, Taiwan	CHY028	1999	7.62	Mw	0.05946	5.95%	235.463	118.096	1.994	X	0.76760	C	3rd Floor
Northridge-01	Jensen Filter Plant Generator Building	1994	6.69	Mw	0.051199	5.12%	202.749	101.709	1.993	X	0.76045	C	3rd Floor
Northridge-01	LA - Sepulveda VA Hospital	1994	6.69	Mw	0.072104	7.21%	285.533	143.132	1.995	X	0.75323	C	3rd Floor
Chi-Chi, Taiwan	TCU129	1999	7.62	Mw	0.064209	6.42%	254.267	127.507	1.994	X	0.75149	C	3rd Floor
Tottori, Japan	TTR007	2000	6.61	Mw	0.016962	1.70%	67.171	33.653	1.996	X	0.74266	C	3rd Floor
Niigata, Japan	NIGH01	2004	6.63	Mw	0.057217	5.72%	226.579	113.654	1.994	X	0.74056	C	3rd Floor
Chi-Chi, Taiwan	TCU084	1999	7.62	Mw	0.197815	19.78%	783.349	392.846	1.994	X	0.73785	C	3rd Floor

Bam, Iran	Bam	2003	6.6	Mw	0.127963	12.796%	506.734	254.156	1.994	X	0.73768	C	3rd Floor
Darfield, New Zealand	GDLC	2010	7.00	Mw	0.103801	10.380%	411.052	206.21	1.993	X	0.73113	D	3rd Floor
Superstition Hills-02	Superstition Mtn Camera	1987	6.54	Mw	0.047825	4.783%	189.385	94.928	1.995	X	0.72878	C	3rd Floor
Landers	Lucerne	1992	7.28	Mw	0.001898	0.190%	7.518	3.753	2.003	X	0.72724	B	3rd Floor
Iwate	MYG004	2008	6.9	Mw	0.030325	3.03%	120.088	60.235	1.994	X	0.72576	C	3rd Floor
Tottori, Japan	SMNH01	2000	6.61	Mw	0.01219	1.22%	48.271	24.208	1.994	X	0.71988	C	3rd Floor
Mammoth Lakes-06	Long Valley Dam (Upr L Abut)	1980	5.94	Mw	0.01716	1.716%	67.955	34.088	1.994	X	0.71928	C	3rd Floor
Parkfield-02, CA	Parkfield - Stone Corral 1E	2004	6.00	Mw	0.022598	2.260%	89.488	44.882	1.994	X	0.71667	D	3rd Floor
Northridge-01	Rinaldi Receiving Sta	1994	6.69	Mw	0.149851	14.99%	593.409	297.639	1.994	X	0.70785	D	3rd Floor
Chi-Chi, Taiwan-06	TCU079	1999	6.30	Mw	0.016006	1.601%	63.385	31.775	1.995	X	0.70445	C	3rd Floor
Gazli, USSR	Karakyr	1976	6.80	Mw	0.055888	5.589%	221.315	111.009	1.994	X	0.70178	D	3rd Floor
Northridge-01	Sylmar - Converter Sta	1994	6.69	Mw	0.099531	9.95%	394.144	197.578	1.995	X	0.69753	D	3rd Floor
Chi-Chi, Taiwan	TCU065	1999	7.62	Mw	0.092342	9.23%	365.676	183.351	1.994	X	0.68938	D	3rd Floor
Chi-Chi, Taiwan-03	TCU129	1999	6.20	Mw	0.064209	6.421%	254.267	127.511	1.994	X	0.68877	C	3rd Floor
Imperial Valley-06	Bonds Corner	1979	6.53	Mw	0.02343	2.343%	92.783	46.544	1.993	X	0.68661	D	3rd Floor
Northridge-01	Sylmar - Converter Sta East	1994	6.69	Mw	0.066411	6.64%	262.99	131.893	1.994	X	0.68610	C	3rd Floor
Coalinga-05	Oil City	1983	5.77	Mw	0.027793	2.78%	110.061	55.128	1.996	X	0.68604	C	3rd Floor
N. Palm Springs	North Palm Springs	1986	6.06	Mw	0.03297	3.297%	130.561	65.459	1.995	X	0.68434	D	3rd Floor
Duzce, Turkey	Lamont 375	1999	7.14	Mw	0.009689	0.97%	38.369	19.234	1.995	X	0.68064	C	3rd Floor

Kobe, Japan	Takatori	1995	6.9	Mw	0.225778	22.58%	894.082	448.391	1.994	X	0.67218	D	3rd Floor
Tottori, Japan	OKY004	2000	6.61	Mw	0.005829	0.58%	23.081	11.579	1.993	X	0.65993	C	3rd Floor
Northridge-01	Newhall - Fire Sta	1994	6.69	Mw	0.084314	8.43%	333.885	167.464	1.994	X	0.65430	D	3rd Floor
Kobe, Japan	Takarazuka	1995	6.9	Mw	0.091466	9.15%	362.205	181.59	1.995	X	0.65400	D	3rd Floor
Parkfield-02, CA	Parkfield - Cholame 3E	2004	6	Mw	0.009313	0.93%	36.88	18.474	1.996	X	0.65141	C	3rd Floor
Niigata, Japan	NIG028	2004	6.63	Mw	0.022216	2.22%	87.975	44.113	1.994	X	0.64783	C	3rd Floor
Christchurch, New Zealand	Pages Road Pumping Station	2011	6.2	Mw	0.107985	10.80%	427.622	214.36	1.995	X	0.64750	E	3rd Floor
Parkfield-02, CA	Parkfield - Fault Zone 1	2004	6	Mw	0.00006	0.01%	275.814	138.355	1.994	x	0.64455	E	3rd Floor
Northridge-01	Simi Valley - Katherine Rd	1994	6.69	Mw	0.048902	4.89%	193.653	97.127	1.994	X	0.64410	C	3rd Floor
Northridge-01	Sylmar - Olive View Med FF	1994	6.69	Mw	0.065982	6.60%	261.289	131.081	1.993	X	0.64005	C	3rd Floor
Chuetsu-oki	NIG018	2007	6.8	Mw	0.112076	11.21%	443.823	222.541	1.994	X	0.62519	D	3rd Floor
Northridge-01	Santa Monica City Hall	1994	6.69	Mw	0.034946	3.49%	138.385	69.404	1.994	X	0.62478	D	3rd Floor
Cape Mendocino	Petrolia	1992	7.01	Mw	0.03057	3.06%	121.059	60.722	1.994	X	0.62397	C	3rd Floor
Tottori, Japan	TTR009	2000	6.61	Mw	0.013907	1.39%	55.074	27.596	1.996	X	0.62177	C	3rd Floor
Chuetsu-oki	Joetsu Oshimaku Oka	2007	6.8	Mw	0.016173	1.62%	64.044	32.106	1.995	X	0.62016	C	3rd Floor
Victoria, Mexico	Cerro Prieto	1980	6.33	Mw	0.049693	4.969%	196.785	98.669	1.994	X	0.61451	C	3rd Floor
Parkfield-02, CA	Parkfield - Gold Hill 3W	2004	6	Mw	0.008036	0.80%	31.824	15.948	1.995	X	0.60451	C	3rd Floor
N. Palm Springs	Whitewater Trout Farm	1986	6.06	Mw	0.066046	6.605%	261.542	131.189	1.994	X	0.59665	C	3rd Floor
Chi-Chi, Taiwan	TCU071	1999	7.62	Mw	0.054999	5.50%	217.796	109.209	1.994	X	0.59346	C	3rd Floor

Umbria Marche (aftershock 7), Italy	Nocera Umbra	1997	4.3	ML	0.001049	0.105%	4.153	2.063	2.013	X	0.59217	C	3rd Floor
Loma Prieta	LGPC	1989	6.93	Mw	0.104347	10.435%	413.213	207.204	1.994	X	0.59012	C	3rd Floor
Whittier Narrows-01	Tarzana - Cedar Hill	1987	5.99	Mw	0.005791	0.58%	22.931	11.486	1.996	X	0.58926	D	3rd Floor
Iwate	Kurihara City	2008	6.9	Mw	0.033831	3.38%	133.972	67.166	1.995	X	0.58540	C	3rd Floor
San Salvador	Geotech Investig Center	1986	5.80	Mw	0.058102	5.810%	230.085	115.382	1.994	X	0.5761	C	3rd Floor
Darfield, New Zealand	Heathcote Valley Primary School	2010	7	Mw	0.011533	1.15%	45.672	22.871	1.997	X	0.57386	C	3rd Floor
Chuetsu-oki	Kashiwazaki City Center	2007	6.8	Mw	0.092373	9.24%	365.797	183.398	1.995	X	0.57362	D	3rd Floor
Chuetsu-oki	Oguni Nagaoka	2007	6.8	Mw	0.028553	2.86%	113.07	56.686	1.995	X	0.56615	C	3rd Floor
Chuetsu-oki	Iizuna Imokawa	2007	6.8	Mw	0.05133	5.13%	203.267	101.942	1.994	X	0.56511	C	3rd Floor
Parkfield-02, CA	PARKFIELD - JOAQUIN CANYON	2004	6	Mw	0.011344	1.13%	44.923	22.516	1.995	X	0.55980	C	3rd Floor
Coalinga-07	Coalinga-14th & Elm (Old CHP)	1983	5.21	Mw	0.007836	0.784%	31.029	15.549	1.996	X	0.5596	D	3rd Floor
Parkfield-02, CA	Parkfield - Cholame 4W	2004	6	Mw	0.016275	1.63%	64.45	32.308	1.995	X	0.55915	C	3rd Floor
Chi-Chi, Taiwan	TCU095	1999	7.62	Mw	0.017635	1.76%	69.834	35.014	1.994	X	0.55847	C	3rd Floor
L'Aquila, Italy	L'Aquila - V. Aterno - Centro Valle	2009	6.30	Mw	0.029476	2.948%	116.726	58.546	1.994	X	0.55844	C	3rd Floor
Coalinga-02	Anticline Ridge Free-Field	1983	5.09	Mw	0.003763	0.376%	14.901	7.459	1.998	X	0.55772	C	3rd Floor
Chuetsu-oki	Kashiwazaki City Takayanagicho	2007	6.8	Mw	0.038214	3.82%	151.327	75.904	1.994	X	0.55485	C	3rd Floor
Chi-Chi, Taiwan-06	TCU080	1999	6.3	Mw	0.027528	2.75%	109.01	54.668	1.994	X	0.54809	C	3rd Floor
Loma Prieta	WAHO	1989	6.93	Mw	0.029986	2.999%	118.744	59.562	1.994	X	0.5373	C	3rd Floor

Northridge-01	Beverly Hills - 12520 Mulhol	1994	6.69	Mw	0.02912	2.91%	115.315	57.834	1.994	X	0.53527	C	3rd Floor
Northridge-06	Rinaldi Receiving Sta	1994	5.28	Mw	0.011704	1.170%	46.346	23.208	1.997	X	0.5282	D	3rd Floor
Imperial Valley-06	El Centro Array #8	1979	6.53	Mw	0.072086	7.21%	285.461	143.146	1.994	X	0.52691	D	3rd Floor
Big Bear-01	Big Bear Lake - Civic Center	1992	6.46	Mw	0.01502	1.502%	59.478	29.834	1.994	X	0.52458	C	3rd Floor
Northridge-01	Jensen Filter Plant Administrative Building	1994	6.69	Mw	0.087465	8.75%	346.361	173.528	1.996	X	0.52425	C	3rd Floor
Manjil, Iran	Abbar	1990	7.37	Mw	0.027278	2.728%	108.022	54.172	1.994	X	0.52348	C	3rd Floor
Christchurch, New Zealand	Christchurch Resthaven	2011	6.2	Mw	0.088695	8.87%	351.232	176.184	1.994	X	0.52141	E	3rd Floor
Chi-Chi, Taiwan	TCU088	1999	7.62	Mw	0.014535	1.45%	57.559	28.827	1.997	X	0.52104	C	3rd Floor
Coalinga-01	Pleasant Valley P.P. - yard	1983	6.36	Mw	0.053816	5.382%	213.111	106.887	1.994	X	0.52073	D	3rd Floor
El Mayor-Cucapah	El Centro Differential Array	2010	7.20	Mw	0.018876	1.888%	74.749	37.488	1.994	X	0.50737	D	3rd Floor
Stone Canyon	Melendy Ranch	1972	4.81	Mw	0.00246	0.246%	9.74	4.871	2	X	0.49551	C	3rd Floor
Mammoth Lakes-04	Convict Creek	1980	5.70	Mw	0.007983	0.798%	31.614	15.845	1.995	X	0.4842	C	3rd Floor
Umbria Marche, Italy	Nocera Umbra	1997	6	Mw	0.015292	1.529%	60.557	30.358	1.995	X	0.47255	C	3rd Floor
Umbria Marche, Italy	Nocera Umbra	1992	6	Mw	0.014467	1.447%	57.288	28.73	1.994	X	0.47255	C	3rd Floor
Yountville	Napa Fire Station #3	2000	5.00	Mw	0.020581	2.058%	81.503	40.875	1.994	X	0.45971	D	3rd Floor
Ancona-09, Italy	Ancona-Rocca	1972	4.7	ML	0.00225	0.225%	8.909	4.448	2.003	X	0.45027	C	3rd Floor
Erzican, Turkey	Erzincan	1992	6.69	Mw	0.090449	9.045%	358.179	179.616	1.994	X	0.44499	D	3rd Floor
Mammoth Lakes-01	Convict Creek	1980	6.06	Mw	0.019583	1.958%	77.548	38.879	1.995	X	0.43915	C	3rd Floor

Whittier Narrows-01	Garvey Res. - Control Bldg	1987	5.99	Mw	0.008517	0.852%	33.727	16.893	1.996	X	0.43646	C	3rd Floor
Coalinga-05	Coalinga-14th & Elm (Old CHP)	1983	5.77	Mw	0.005608	0.561%	22.207	11.125	1.996	X	0.42486	D	3rd Floor
Whittier Narrows-02	Pasadena - Old House Rd	1987	5.27	Mw	0.004355	0.436%	17.245	8.633	1.998	X	0.38617	C	3rd Floor
El Mayor-Cucapah	El Centro - Meloland Geot. Array	2010	7.20	Mw	0.01359	1.359%	53.815	26.977	1.995	X	0.37814	D	3rd Floor
Cape Mendocino	Ferndale Fire Station	1992	7.01	Mw	0.081299	8.130%	321.943	161.435	1.994	X	0.29416	C	3rd Floor
Superstition Hills-02	El Centro Imp. Co. Cent	1987	6.54	Mw	0.047825	4.783%	189.385	94.926	1.995	X	0.26118	D	3rd Floor
	Hollister City Hall	1989	6.93	Mw	0.030971	3.097%	122.647	61.515	1.994	X	0.23371	D	3rd Floor
Imperial Valley-02	El Centro Array #9	1940	6.95	Mw	0.030348	3.035%	120.178	60.277	1.994	X	0.23349	D	3rd Floor
Parkfield-02, CA	Parkfield - Cholame 5W	2004	6.00	Mw	0.010547	1.055%	41.766	20.944	1.994	X	0.23324	D	3rd Floor
Sierra Madre	Pasadena - USGS/NSMP Office	1991	5.61	Mw	0.007538	0.754%	29.852	14.958	1.996	X	0.23178	D	3rd Floor
Northridge-01	Pasadena - N Sierra Madre	1994	6.69	Mw	0.006867	0.687%	27.195	13.627	1.996	X	0.23087	C	3rd Floor
Northern Calif-03	Ferndale City Hall	1954	6.50	U	0.046357	4.636%	183.574	92.094	1.993	X	0.18616	D	3rd Floor
Northern Calif-05	Ferndale City Hall	1967	5.60	Mw	0.00525	0.525%	20.789	10.41	1.997	X	0.18406	D	3rd Floor
Coalinga-06	Coalinga-14th & Elm (Old CHP)	1983	4.89	Mw	0.001792	0.179%	7.095	3.541	2.004	X	0.15109	D	3rd Floor
Imperial Valley-06	El Centro Array #1	1979	6.53	Mw	0.008582	0.858%	33.985	17.032	1.995		0.14458	D	3rd Floor
Whittier Narrows-01	Pasadena - CIT Athenaeum	1987	5.99	Mw	0.010124	1.012%	40.09	20.095	1.995	X	0.14147	C	3rd Floor
Hollister-03	Hollister City Hall	1974	5.14	Mw	0.002414	0.241%	9.558	4.778	2	X	0.1407	D	3rd Floor
Northwest Calif-01	Ferndale City Hall	1938	5.50	Mw	0.003524	0.352%	13.956	6.983	1.999	X	0.12218	D	3rd Floor
Northwest Calif-03	Ferndale City Hall	1951	5.80	Mw	0.004549	0.455%	18.016	9.017	1.998	X	0.10709	D	3rd Floor

San Fernando	Pasadena - CIT Athenaeum	1971	6.61	Mw	0.006636	0.664%	26.279	13.18	1.994	X	0.10575	C	3rd Floor
Borrego Mtn	El Centro Array #9	1968	6.63	Mw	0.030214	3.021%	119.648	59.989	1.995	X	0.094018	D	3rd Floor
San Fernando	Fairmont Dam	1971	6.61	Mw	0.001345	0.135%	5.326	2.655	2.006	X	0.093858	C	3rd Floor
Northern Calif-07	Ferndale City Hall	1975	5.20	Mw	0.003345	0.335%	13.247	6.631	1.998	X	0.090045	D	3rd Floor
San Francisco	Golden Gate Park	1957	5.28	Mw	0.000717	0.072%	2.838	1.406	2.018	X	0.086274	B	3rd Floor
Hollister-01	Hollister City Hall	1961	5.60	U	0.010738	1.074%	42.523	21.313	1.995	X	0.084991	D	3rd Floor
Morgan Hill	Hollister City Hall	1984	6.19	Mw	0.011528	1.153%	45.651	22.898	1.994	X	0.070129	D	3rd Floor
Northern Calif-02	Ferndale City Hall	1952	5.20	Mw	0.00619	0.619%	24.512	12.283	1.996	X	0.068432	D	3rd Floor
Northern Calif-04	Ferndale City Hall	1960	5.70	Mw	0.003473	0.347%	13.752	6.881	1.998	X	0.067086	D	3rd Floor
Hollister-02	Hollister City Hall	1961	5.50	U	0.006845	0.685%	27.106	13.58	1.996	X	0.062349	D	3rd Floor
CA/Baja Border Area	El Centro Array #10	2002	5.31	Mw	0.001699	0.170%	6.73	3.36	2.003	X	0.060458	D	3rd Floor
Parkfield	Cholame - Shandon Array #12	1966	6.19	Mw	0.007232	0.723%	28.638	14.352	1.995	X	0.058666	C	3rd Floor
Imperial Valley-07	El Centro Array #10	1979	5.01	Mw	0.000926	0.093%	3.667	1.823	2.012	X	0.052531	D	3rd Floor
Borrego	El Centro Array #9	1942	6.50	U	0.010415	1.042%	41.241	20.672	1.995	X	0.052247	D	3rd Floor
Kern County	Pasadena - CIT Athenaeum	1952	7.36	Mw	0.008372	0.837%	33.154	16.611	1.996	X	0.051003	C	3rd Floor
Northwest Calif-02	Ferndale City Hall	1941	6.60	U	0.003848	0.385%	15.239	7.636	1.996	X	0.049416	D	3rd Floor
Central Calif-01	Hollister City Hall	1954	5.30	U	0.003012	0.301%	11.926	5.966	1.999	X	0.047679	D	3rd Floor
El Alamo	El Centro Array #9	1956	6.80	U	0.006753	0.675%	26.743	13.407	1.995	X	0.044953	D	3rd Floor
Coalinga-01	Parkfield - Cholame 12W	1983	6.36	Mw	0.01167	1.167%	46.214	23.175	1.994	X	0.04495	D	3rd Floor

Imperial Valley-05	El Centro Array #9	1955	5.40	U	0.004078	0.408%	16.149	8.086	1.997	X	0.04424	D	3rd Floor
Northridge-06	Pasadena - USGS/NSMP Office	1994	5.28	Mw	0.001216	0.122%	4.816	2.398	2.008	X	0.041761	D	3rd Floor
Humbolt Bay	Ferndale City Hall	1937	5.80	Mw	0.002486	0.249%	9.843	4.921	2	X	0.040961	D	3rd Floor
Hector Mine	Pasadena - Fair Oaks & Walnut	1999	7.13	Mw	0.004418	0.442%	17.497	8.76	1.997	X	0.035278	C	3rd Floor
Mammoth Lakes-07	USC Cash Baugh Ranch	1980	4.73	Mw	0.004838	0.484%	19.16	9.597	1.996	X	0.0299	D	3rd Floor
Imperial Valley-03	El Centro Array #9	1951	5.60	U	0.001783	0.178%	7.061	3.526	2.003	X	0.029364	D	3rd Floor
Imperial Valley-04	El Centro Array #9	1953	5.50	U	0.00034	0.034%	1.348	0.659	2.045	X	0.027932	D	3rd Floor
40238431	Parkfield - Cholame 5W	2009	4.39	Mw	0.000171	0.017%	0.676	0.322	2.1	X	0.020278	D	3rd Floor
Imperial Valley-01	El Centro Array #9	1938	5.00	U	0.00038	0.038%	1.503	0.737	2.041	X	0.018449	D	3rd Floor
51182151	Parkfield - Cholame 5W	2007	4.01	Mw	0.000147	0.015%	0.581	0.216	2.688	Y	0.018393	D	20th Floor
Gulf of California	El Centro Array #9	2001	5.70	Mw	0.002461	0.246%	9.747	4.873	2	X	0.01828	D	3rd Floor
Northern Calif-06	Hollister City Hall	1967	5.20	U	0.001834	0.183%	7.263	3.627	2.002	X	0.015276	D	3rd Floor
Hector Mine	El Centro Array #10	1999	7.13	Mw	0.004586	0.459%	18.16	9.092	1.997	X	0.014538	D	3rd Floor
40204628	San Francisco; Fire Station 22 Golden Gate Park; 16th Ave; 2-story; ground level	2007	5.45	Mw	0.000313	0.031%	1.241	0.605	2.05	X	0.012085	D	3rd Floor
21305648	San Francisco; Fire Station 22 Golden Gate Park; 16th Ave; 2-story; ground level	2003	4.00	Mw	0.000147	0.015%	0.581	0.216	2.688	Y	0.011427	D	20th Floor
21530368	San Francisco; Fire Station 22 Golden Gate Park; 16th Ave; 2-story; ground level	2006	4.5	Mw	0.000147	0.015%	0.581	0.216	2.688	Y	0.011412	D	20th Floor
Anza-02	El Centro Array #10	2001	4.92	Mw	0.000549	0.055%	2.174	1.074	2.025	X	0.01091	D	3rd Floor

21423530	Parkfield - Cholame 5W	2004	4.17	Mw	0.000147	0.015%	0.581	0.216	2.688	Y	0.0098585	D	20th Floor
San Fernando	Maricopa Array #3	1971	6.61	Mw	0.004018	0.402%	15.913	7.959	1.999	X	0.0089858	C	3rd Floor
Borrego Mtn	Pasadena - CIT Athenaeum	1968	6.63	Mw	0.002298	0.230%	9.102	4.566	1.993	X	0.0082481	C	3rd Floor
Big Bear City	Pasadena - USGS/NSMP Office	2003	4.92	Mw	0.000249	0.025%	0.985	0.477	2.065	X	0.0074202	D	3rd Floor
40199209	San Francisco; Fire Station 22 Golden Gate Park; 16th Ave; 2-story; ground level	2007	4.20	Mw	0.000717	0.072%	2.838	1.406	2.018	X	0.0065591	D	20th Floor
40194055	San Francisco; Fire Station 22 Golden Gate Park; 16th Ave; 2-story; ground level	2007	4.23	Mw	0.000717	0.072%	2.838	1.406	2.018	X	0.0061986	D	20th Floor
51207740	San Francisco; Fire Station 22 Golden Gate Park; 16th Ave; 2-story; ground level	2008	4.1	Mw	0.000147	0.015%	0.581	0.216	2.688	Y	0.0057295	D	20th Floor
14155260	Pasadena (PASA)	2005	4.88	ML	0.000147	0.015%	0.581	0.216	2.688	Y	0.0047638	C	20th Floor
51177103	San Francisco; Fire Station 22 Golden Gate Park; 16th Ave; 2-story; ground level	2006	3.6	Mw	0.000147	0.015%	0.581	0.216	2.688	Y	0.0046635	D	20th Floor
San Fernando	Cholame - Shandon Array #2	1971	6.61	Mw	0.001114	0.111%	4.412	2.196	2.009	X	0.0043448	D	3rd Floor
21522424	San Francisco; Fire Station 22 Golden Gate Park; 16th Ave; 2-story; ground level	2006	4.3	Mw	0.000147	0.015%	0.581	0.216	2.688	Y	0.003774	D	20th Floor
40193843	San Francisco; Fire Station 22 Golden Gate Park; 16th Ave; 2-story; ground level	2007	3.41	ML	0.000147	0.015%	0.581	0.216	2.688	Y	0.0032067	D	20th Floor
Yorba Linda	Pasadena (PASA)	2002	4.27	Mw	0.000147	0.015%	0.581	0.216	2.688	Y	0.0022374	C	20th Floor
21261124	San Francisco; Fire Station 22 Golden Gate Park; 16th Ave; 2-story; ground level	2002	3.6	ML	0.000147	0.015%	0.581	0.216	2.688	Y	0.0021947	D	20th Floor
30225889	San Francisco; Fire Station 22 Golden Gate Park; 16th Ave; 2-story; ground level	2003	4.12	Mw	0.000147	0.015%	0.581	0.216	2.688	Y	0.0019516	D	20th Floor

14151344	Pasadena (PASA)	2005	5.20	Mw	0.000147	0.015%	0.581	0.216	2.688	Y	0.001692	C	20th Floor
51177644	San Francisco; Fire Station 22 Golden Gate Park; 16th Ave; 2-story; ground level	2007	3.7	Mw	0.000147	0.015%	0.581	0.216	2.688	Y	0.0014441	D	20th Floor
30225187	San Francisco; Fire Station 22 Golden Gate Park; 16th Ave; 2-story; ground level	2002	3.9	Mw	0.000147	0.015%	0.581	0.216	2.688	Y	0.0012464	D	20th Floor
21510121	San Francisco; Fire Station 22 Golden Gate Park; 16th Ave; 2-story; ground level	2006	3.7	Mw	0.000147	0.015%	0.581	0.216	2.688	Y	0.0012442	D	20th Floor
14138080	Pasadena (PASA)	2005	4.59	ML	0.000147	0.015%	0.581	0.216	2.688	Y	0.0011067	C	20th Floor
9735129	Pasadena (PASA)	2001	3.97	ML	0.000147	0.015%	0.581	0.216	2.688	Y	0.0011023	C	20th Floor
10275733	Pasadena Art Center, College Of Design	2007	4.73	ML	0.000147	0.015%	0.581	0.216	2.688	Y	0.0010591	C	20th Floor
51203888	San Francisco; Fire Station 22 Golden Gate Park; 16th Ave; 2-story; ground level	2008	3.5	Mw	0.000147	0.015%	0.581	0.216	2.688	Y	0.00099741	D	20th Floor
21414391	San Francisco; Fire Station 22 Golden Gate Park; 16th Ave; 2-story; ground level	2004	3.68	Mw	0.000147	0.015%	0.581	0.216	2.688	Y	0.00099567	D	20th Floor
21339029	San Francisco; Fire Station 22 Golden Gate Park; 16th Ave; 2-story; ground level	2004	3.58	Mw	0.000147	0.015%	0.581	0.216	2.688	Y	0.00088449	D	20th Floor
30226452	San Francisco; Fire Station 22 Golden Gate Park; 16th Ave; 2-story; ground level	2003	3.5	Mw	0.000147	0.015%	0.581	0.216	2.688	Y	0.00077876	D	20th Floor
9173365	Pasadena (PASA)	2001	4.26	ML	0.000147	0.015%	0.581	0.216	2.688	Y	0.00077497	C	20th Floor
30226086	San Francisco; Fire Station 22 Golden Gate Park; 16th Ave; 2-story; ground level	2003	4	Mw	0.000147	0.015%	0.581	0.216	2.688	Y	0.00070533	D	20th Floor
21437727	San Francisco; Fire Station 22 Golden Gate Park; 16th Ave; 2-story; ground level	2005	4.18	Mw	0.000147	0.015%	0.581	0.216	2.688	Y	0.00064725	D	20th Floor

21262721	San Francisco; Fire Station 22 Golden Gate Park; 16th Ave; 2-story; ground level	2003	4.3	Mw	0.000147	0.015%	0.581	0.216	2.688	Y	0.00060343	D	20th Floor
9753485	Pasadena (PASA)	2002	4.18	ML	0.000147	0.015%	0.581	0.216	2.688	Y	0.0005855	C	20th Floor
21335949	San Francisco; Fire Station 22 Golden Gate Park; 16th Ave; 2-story; ground level	2004	3.71	Mw	0.000147	0.015%	0.581	0.216	2.688	Y	0.00057851	D	20th Floor
21350824	San Francisco; Fire Station 22 Golden Gate Park; 16th Ave; 2-story; ground level	2004	4.25	Mw	0.000147	0.015%	0.581	0.216	2.688	Y	0.0005617	D	20th Floor
9069997	Pasadena (PASA)	1998	4.50	-999	0.000147	0.015%	0.581	0.216	2.688	Y	0.00056152	C	20th Floor
14186612	Pasadena (PASA)	2005	4.69	ML	0.000147	0.015%	0.581	0.216	2.688	Y	0.00046805	C	20th Floor
21502994	San Francisco; Fire Station 22 Golden Gate Park; 16th Ave; 2-story; ground level	2006	3.6	Mw	0.000147	0.015%	0.581	0.216	2.688	Y	0.00042217	D	20th Floor
9064093	Pasadena (PASA)	1998	4.78	ML	0.000147	0.015%	0.581	0.216	2.688	Y	0.00040512	C	20th Floor
Anza-02	Pasadena (PASA)	2001	4.92	Mw	0.000147	0.015%	0.581	0.216	2.688	Y	0.00036446	C	20th Floor
3321584	Pasadena (PASA)	1999	3.81	ML	0.000147	0.015%	0.581	0.216	2.688	Y	0.00035403	C	20th Floor
9941081	Pasadena (PASA)	2003	3.90	ML	0.000147	0.015%	0.581	0.216	2.688	Y	0.00032399	C	20th Floor
21508102	San Francisco; Fire Station 22 Golden Gate Park; 16th Ave; 2-story; ground level	2006	3.69	ML	0.000147	0.015%	0.581	0.216	2.688	Y	0.00031662	D	20th Floor
14095628	Pasadena (PASA)	2004	5.03	Mw	0.000147	0.015%	0.581	0.216	2.688	Y	0.00029899	C	20th Floor
9096960	Pasadena (PASA)	1999	3.88	ML	0.000147	0.015%	0.581	0.216	2.688	Y	0.00028311	C	20th Floor
9652545	Pasadena (PASA)	2001	3.84	ML	0.000147	0.015%	0.581	0.216	2.688	Y	0.00021126	C	20th Floor
10972299	Pasadena (PASA)	2001	3.79	ML	0.000147	0.015%	0.581	0.216	2.688	Y	0.00016578	C	20th Floor

14312160	Pasadena Art Center, College Of Design	2007	4.66	ML	0.000147	0.015%	0.581	0.216	2.688	Y	0.00014713	C	20th Floor
13692644	Pasadena (PASA)	2002	3.74	ML	0.000147	0.015%	0.581	0.216	2.688	Y	0.00013598	C	20th Floor
10285533	Pasadena Art Center, College Of Design	2007	4.20	ML	0.000147	0.015%	0.581	0.216	2.688	Y	0.00013594	C	20th Floor
9983429	Pasadena (PASA)	2004	4.34	ML	0.000147	0.015%	0.581	0.216	2.688	Y	0.00013391	C	20th Floor
14077668	Pasadena (PASA)	2004	4.27	ML	0.000147	0.015%	0.581	0.216	2.688	Y	0.0001271	C	20th Floor
9096656	Pasadena (PASA)	1999	4.15	ML	0.000147	0.015%	0.581	0.216	2.688	Y	0.00012126	C	20th Floor
21397674	San Francisco; Fire Station 22 Golden Gate Park; 16th Ave; 2-story; ground level	2004	3.67	Mw	0.000147	0.015%	0.581	0.216	2.688	Y	0.00011105	D	20th Floor
10059745	Pasadena (PASA)	2004	4.19	ML	0.000147	0.015%	0.581	0.216	2.688	Y	0.00011037	C	20th Floor
14079184	Pasadena (PASA)	2004	3.78	ML	0.000147	0.015%	0.581	0.216	2.688	Y	0.00010275	C	20th Floor
14201764	Pasadena (PASA)	2005	4.17	ML	0.000147	0.015%	0.581	0.216	2.688	Y	0.00010055	C	20th Floor
14118096	Pasadena (PASA)	2005	4.26	ML	0.000147	0.015%	0.581	0.216	2.688	Y	0.000086369	C	20th Floor
9655209	Pasadena (PASA)	2001	3.78	ML	0.000147	0.015%	0.581	0.216	2.688	Y	0.000075117	C	20th Floor
14219360	Pasadena (PASA)	2006	4.11	ML	0.000147	0.015%	0.581	0.216	2.688		0.000056335	C	20th Floor
14146956	Pasadena (PASA)	2005	4.06	ML	0.000147	0.015%	0.581	0.216	2.688	Y	0.000043736	C	20th Floor
40204628	Capetown, Ferndale	2007	5.45	Mw	0.000147	0.015%	0.581	0.216	2.688	Y	0.000039162	C	20th Floor
21465580	Capetown, Ferndale	2005	4.77	Mw	0.000147	0.015%	0.581	0.216	2.688	Y	0.000039062	C	20th Floor
14137160	Pasadena (PASA)	2005	3.94	ML	0.000147	0.015%	0.581	0.216	2.688	Y	0.000033755	C	20th Floor
14330056	Pasadena Art Center, College Of Design	2007	4.34	ML	0.000147	0.015%	0.581	0.216	2.688	Y	0.000023316	C	20th Floor

10276197	Pasadena Art Center, College Of Design	2007	4.06	ML	0.000147	0.015%	0.581	0.216	2.688	Y	0.00002154	C	20th Floor
10065241	Pasadena (PASA)	2004	3.52	ML	0.000147	0.015%	0.581	0.216	2.688	Y	0.000016238	C	20th Floor
10207681	Pasadena (PASA)	2006	4.05	ML	0.000147	0.015%	0.581	0.216	2.688	Y	0.000014115	C	20th Floor
21530368	Capetown, Ferndale	2006	4.5	Mw	0.000147	0.015%	0.581	0.216	2.688	Y	8.4983E-06	C	20th Floor
30225889	Capetown, Ferndale	2003	4.12	Mw	0.000147	0.015%	0.581	0.216	2.688	Y	7.4723E-06	C	20th Floor
30226086	Capetown, Ferndale	2003	4	Mw	0.000147	0.015%	0.581	0.216	2.688	Y	7.1419E-06	C	20th Floor
21526081	Capetown, Ferndale	2006	3.7	Mw	0.000147	0.015%	0.581	0.216	2.688	Y	4.0209E-06	C	20th Floor
40199209	Capetown, Ferndale	2007	4.2	Mw	0.000147	0.015%	0.581	0.216	2.688	Y	3.0947E-06	C	20th Floor